AD-763 092

EFFECTS OF BREATHING LIQUID FLUORO-
CARBONS ON REGIONAL DIFFERENCES IN
PLEURAL PRESSURES AND OTHER PHYSIO-
LOGICAL PARAMETERS

Donald J. Sass, et al

Mayo Clinic

AD 763092

EFFECTS OF BREATHING LIQUID FLUOROCARBONS ON REGIONAL DIFFERENCES IN PLEURAL PRESSURES AND OTHER PHYSIOLOGICAL PARAMETERS

DONALD J. SASS, M.D., et al.

DDC
RECEIVED
JUL 17 1973
C

Qualified requesters may obtain copies of this report from DDC. Orders will be expedited if placed through the librarian or other person designated to request documents from DDC.

When U. S. Government drawings, specifications, or other data are used for any purpose other than a definitely related Government procurement operation, the Government thereby incurs no responsibility nor any obligation whatsoever; and the fact that the government may have formulated, furnished, or in any way supplied the said drawings, specifications, or other data is not to be regarded by implication or otherwise, as in any manner licensing the holder or any other person or corporation, or conveying any rights or permission to manufacture, use, or sell any patented invention that may in any way be related thereto.

EFFECTS OF BREATHING LIQUID FLUOROCARBONS ON REGIONAL DIFFERENCES IN PLEURAL PRESSURES AND OTHER PHYSIOLOGICAL PARAMETERS

DONALD J. SASS, M.D.
EARL H. WOOD, M.D., Ph. D.
JAMES F. GREENLEAF, Ph. D.
ERIK L. RITMAN, M.B.
HUGH C. SMITH, M.D.

ib

FOREWORD

This report has been reviewed and is approved.

EVAN R. GOLDMA, Colonel, USAF, MC
Commander

ABSTRACT

A water-immersion respirator and liquid oxygenator assembly of special design was used to control respiratory rate and tidal and residual lung volumes in dogs breathing first, air or oxygen, and then, either liquid fluorocarbon FC 80 or silicone oil DC 200. In separate studies in 30 animals: (1) Arterial hypoxemia due to dependent pulmonary arteriovenous shunting caused by transverse acceleration was not minimized by water-immersion alone, but liquid breathing combined with water immersion did prevent dependent pulmonary arteriovenous shunting and downward displacement of the heart due to transverse acceleration. (2) Blood flow velocity in the ascending aorta was recorded by a chronically implanted electromagnetic flowmeter, and the beat-to-beat stroke volume was computed by an on-line CDC 3300 digital computer. Phasic changes in left ventricular stroke volume were caused by variations in intrathoracic, airway, and other internal body pressures produced by the respirator to maintain adequate respiratory gas exchange with liquid fluorocarbon. (3) The spatial distribution of pulmonary blood flow was determined by a radioactive embolization technique. Up to 4 injections of differentially labeled microspheres were made into the right ventricle, and the distribution of microspheres from each injection, representative of pulmonary blood flow at the time of each injection, was determined throughout the entire lung by a high-resolution computer-controlled scintiscanning technique. When dogs breathed the heavier-than-blood fluorocarbon, blood flow was increased in the superior regions of the lung during exposures to transverse acceleration; blood flow decreased when they breathed the lighter-than-blood silicone oil. (4) Blood P_{CO_2} could be controlled at normal or hypocapnic levels in normothermic dogs breathing oxygenated fluorocarbon for 4 to 8 hours. The possibility is discussed that oxygen toxicity and/or escape of fluorocarbon from the airways into the circulatory system contributed to the death of these animals 24 to 30 hours after cessation of liquid breathing. On-line digital computer processing of multiple physiological variables used in these studies is described.

CONTENTS

Preceding page blank

CONTENTS (continued)

DOCUMENT CONTROL DATA - R & D

(Security classification of title, body of abstract and indexing annotation must be entered when the overall report is classified)

1. ORIGINATING ACTIVITY *(Corporate author)*	2a. REPORT SECURITY CLASSIFICATION
Mayo Clinic Mayo Foundation Rochester, Minnesota 55901	Unclassified
	2b. GROUP

3. REPORT TITLE

EFFECTS OF BREATHING LIQUID FLUOROCARBONS ON REGIONAL DIFFERENCES IN PLEURAL PRESSURES AND OTHER PHYSIOLOGICAL PARAMETERS

4. DESCRIPTIVE NOTES *(Type of report and inclusive dates)*

Final report - 23 May 1969 - 3 January 1972

5. AUTHOR(S) *(First name, middle initial, last name)*

Donald J. Sass   Erik L. Ritman
Earl H. Wood   Hugh C. Smith
James F. Greenleaf

6. REPORT DATE	7a. TOTAL NO. OF PAGES	7b. NO. OF REFS
December 1972	173	105

8a. CONTRACT OR GRANT NO. F41609-69-C-0058	9a. ORIGINATOR'S REPORT NUMBER(S)
b. PROJECT NO. 7930	SAM-TR-72-15
c. Task No. -03	9b. OTHER REPORT NO(S) *(Any other numbers that may be assigned this report)*
d. Work Unit No. -39	

10. DISTRIBUTION STATEMENT

Approved for public release; distribution unlimited.

11. SUPPLEMENTARY NOTES	12. SPONSORING MILITARY ACTIVITY
	USAF School of Aerospace Medicine Aerospace Medical Division (AFSC) Brooks Air Force Base, Texas 78235

13. ABSTRACT

A water-immersion respirator and liquid oxygenator assembly of special design was used to control respiratory rate and tidal and residual lung volumes in dogs breathing first, air or oxygen, and then, either liquid fluorocarbon FC 80 or silicone oil DC 200. In separate studies in 30 animals: (1) Arterial hypoxemia due to dependent pulmonary arteriovenous shunting caused by transverse acceleration was not minimized by water-immersion alone, but liquid breathing combined with water immersion did prevent dependent pulmonary arteriovenous shunting and downward displacement of the heart due to transverse acceleration. (2) Blood flow velocity in the ascending aorta was recorded by a chronically implanted electromagnetic flowmeter, and the beat-to-beat stroke volume was computed by an on-line CDC 3300 digital computer. Phasic changes in left ventricular stroke volume were caused by variations in intrathoracic, airway, and other internal body pressures produced by the respirator to maintain adequate respiratory gas exchange with liquid fluorocarbon. (3) The spatial distribution of pulmonary blood flow was determined by a radioactive embolization technique. Up to 4 injections of differentially labeled microspheres were made into the right ventricle, and the distribution of microspheres from each injection, representative of pulmonary blood flow at the time of each injection, was determined throughout the entire lung by a high-resolution computer-controlled scintiscanning technique. When dogs breathed the heavier-than-blood fluorocarbon, blood flow was increased in the superior regions of the lung during exposures to transverse acceleration; blood flow decreased when they breathed the lighter-than-blood silicone oil. (4) Blood P_{CO_2} could be controlled at normal or hypocapnic levels in normothermic dogs breathing oxygenated fluorocarbon for 4 to 8 hours. The possibility is discussed that oxygen toxicity and/or escape of fluorocarbon from the airways into the circulatory system contributed to the death of these animals 24 to 30 hours after cessation of liquid breathing. On-line digital computer processing of multiple physiological variables used in these studies is described.

14. KEY WORDS	LINK A		LINK B		LINK C	
	ROLE	WT	ROLE	WT	ROLE	WT
Acceleration						
Pulmonary function						
Liquid fluorocarbon						
Oxygen saturation						
Pleural pressure						
Stroke volume						
Pulmonary blood flow						
Computer processing						

ia

LIST OF ILLUSTRATIONS

Section V

Section VI

LIST OF TABLES

EFFECTS OF BREATHING LIQUID FLUOROCARBONS ON REGIONAL DIFFERENCES IN PLEURAL PRESSURES AND OTHER PHYSIOLOGICAL PARAMETERS

SECTION I

Introduction and Summary of Separate Studies

All physiological as well as injurious effects of whole-animal acceleration are produced by relative movement and deformation of the body tissues. Visceral organs and body structures move and deform in a gravitational-inertial force environment because the body parts differ in specific weight and in their mechanical properties. Theoretically, none of the physiological or injurious effects of acceleration would occur if the animal were supported or restrained in such a way that there is no relative movement or deformation of the body tissues due to inertial forces. Each method of body support will influence to some extent the mechanical response of the animal and, hence, the physiological effects produced by the acceleration. Since it is impossible to subject an experimental animal to other than a zero-G-force environment without some method of body support, the method of support is frequently an important variable in these investigations.

The method of body support is especially important in studies of the effects of the force environment on the lung. The lung is particularly vulnerable when the animal is exposed to increased force environments, irrespective of whether the forces are produced by air or water blast (1), vibration (2), impact (3) or centripetal acceleration (4). The susceptibility of the lung is principally due to the large difference in specific weights between the blood and gases on opposite sides of the very thin alveolar membrane (these differences in specific weight increase in proportion to the acceleration), but the lung is also susceptible to inertial movement of structures adjacent to the lung, particularly the relatively dense and mobile abdomen, mediastinum, and chest wall. Depending upon the magnitude and direction of the force environment, relative movement of the heart, chest wall, and abdomen may cause more important effects in the lung than those effects due to the differences in specific weights between blood and gases on opposite sides of the alveolar membrane; for example, the inward displacement of the chest wall in air blast (5), and the inertial displacement of the heart and abdomen during impact (6) and vibration (2). The importance of relative motion of the abdomen and chest wall in producing alveolar rupture, mediastinal emphysema, and other lung injuries has been recognized for hundreds of years (7,8).

The purpose of the studies detailed in this report was to investigate the physiological effects in dogs caused by increased force environments produced by the Mayo Clinic human centrifuge. As the separate studies in this report indicate, we were concerned with demonstrating effects which could be attributed to differences between the specific

1

gravity of the alveolar contents and that of the surrounding blood and pulmonary parenchyma. Thus, the method of body support or restraint was the first consideration. A method was required which would minimize inertial movements of the chest wall and abdomen and at the same time permit chest wall and diaphragm motion necessary for respiration. Immersion in water was the method of body support used to satisfy these requirements. Water-immersion supports have been used by numerous others in experimental animal studies of G-protection (9), as well as in studies of protection in human subjects against blackout due to centripetal acceleration in this laboratory (10), and in studies of human tolerance to acceleration by others (11).

The second section of this report describes the initial study in which we measured arterial blood oxygen saturation in dogs exposed to a $+6G_y$ force environment breathing room air; first, with the dogs simply lying on their left sides, and then when the dogs were supported by water immersion. The results of this study demonstrate that water immersion alone does not protect against the decrease in arterial blood oxygen saturation in dogs due to transverse acceleration at magnitudes up to $+6G_y$. Hence, we conclude that the fall in arterial blood oxygen saturation observed in these experiments (and presumably in all previous studies in this laboratory in humans, dogs and chimpanzees performed with simple body support) was due to pulmonary blood perfusing dependent regions of the lung in which the alveoli were collapsed and poorly ventilated, principally because of the increased weight of the superposed lungs and mediastinal structures and not because of inertial movements of the abdomen and chest wall.

Theoretically, dependent pulmonary atelectasis as well as other cardiopulmonary effects of acceleration could be prevented if the air in the respiratory tree were replaced by an incompressible liquid having the same specific gravity as that of the blood and pulmonary parenchyma. The availability of organic liquids which dissolve large quantities of oxygen and carbon dioxide relative to whole blood enabled us to test this concept, and the results of this study are also presented in Section II. Briefly, breathing of liquids prevented arteriovenous shunting in the dependent lung and prevented downward displacement of the heart during one-minute exposures to $+6G_y$ acceleration. Protection against adverse effects of acceleration by liquid breathing and water immersion is a well-known concept which has been tested by different methods by others (9).

Continuous measurements of mixed venous blood oxygen saturation during liquid breathing showed cyclic variations at the respiration frequency. The computer-generated plots of blood oxygen saturation shown in Section II are illustrative. Since measurements of cardiac output by the indocyanine-green dye dilution technique were appreciably different when the dye was injected at different phases of the respiration cycle, we concluded that the cyclic variations in mixed venous blood oxygen saturation were caused by changes in cardiac output consequent to the sinusoidal changes in external and internal body

2

pressures produced by the respirator. To determine whether or not this was so, an electromagnetic flowmeter was chronically implanted around the root of the aorta in one dog, and the beat-to-beat changes in left ventricular stroke volume were continuously monitored throughout the respiratory cycle, first with the dog breathing room air, and then when breathing oxygenated liquid fluorocarbon in the water-immersion respirator. Details and results of the study are given in Section III. Maximum stroke volume occurred soon after the start of inspiration when the dog breathed air, and just prior to full inspiration when the dog breathed fluorocarbon. The average stroke volume was approximately one-third greater, and the peak-to-peak changes in stroke volume were roughly twice as great, comparing measurements from liquid-breathing and air-breathing experiments, respectively. These results were thus in agreement with our earlier conclusions.

Use of a water-immersion body support in these studies offered what at first was thought to be a secondary advantage, but which over the course of all of the studies has proved to be a primary advantage; viz., that of providing accurate control of the rate and depth of respiration, and of the residual volume of the lung. Thus, the water-immersion respirator progressively developed during the course of these studies into a well-instrumented and extremely valuable whole-body water-filled plethysmograph especially suited to centrifuge studies in dogs.

As is well known, capillary blood flow, or total capillary blood flow per cubic centimeter of tissue, is not uniform throughout the lung but generally increases in successive horizontal strata through the lungs in a superior-to-dependent direction, i.e., in the direction of gravity, until near the dependent parts of the lung where the flow decreases (12, 13,14). These regional differences in blood flow become exaggerated when the force environment is increased (15,16). Various mathematical and physical models have been proposed to explain the regional differences in pulmonary blood flow (12,13,14). All of these models make two basic assumptions: 1) the blood pathways are in continuity in the lung and, thus, the capillary blood pressure in any stratum can be predicted from purely hydrostatic considerations; and, 2) the respiratory passages are also in continuity so that when there is no flow of respiratory gases, the alveolar pressure in all expanded regions of the lung is atmospheric (the specific weight of the gases is virtually zero). Theoretically, blood flow would be uniform throughout the lungs in a zero-G environment, or if the alveoli were filled with a liquid having the same specific weight as blood and other tissues; viz., about 1.0.

In the study described in Section IV, we tested this concept by measuring the effects of the force environment on the three-dimensional distribution of pulmonary blood flow in dogs breathing first air, and then an organic liquid. Over the past five years, investigators in this

3

laboratory have performed numerous studies with the radioactive micro-sphere method of measuring pulmonary blood flow in dogs and chimpanzees, and during the course of these studies have developed the technological skills necessary for the computer measurement and display of pulmonary blood flow in three dimensions throughout the entire lung (15,16). The computer programs and other techniques for pulmonary blood flow measurement were utilized in the current study. Since no liquid was available with a specific gravity of 1.0 with suitable solubility and other necessary properties for a respirable liquid, we performed the study described in Section IV using two different liquids, each of which adequately supported respiration except that one was heavier and the other was lighter than blood. Liquid fluorocarbon (FC80) (17) which has a specific gravity of 1.76 was used in five dogs, and silicone oil (DC 200) (18) which has a specific gravity of 0.8 was used in one dog. Silicone oil was used with only one dog because the 1.0 cs. viscosity liquid has a flash point of 39° C and, thus when saturated with oxygen, the experiment was hazardous. Furthermore, the 1.0 cs. DC 200 silicone oil is toxic (19) and the duration of liquid breathing could not be as long as with the relatively nontoxic fluorocarbon. However, by using either of the two liquids with specific gravity bracketing the ideal 1.0 value, we were able to demonstrate the dominant role of the specific gravity of the alveolar contents in determining the direction of changes in the regional distribution of pulmonary blood flow due to changes in the inertial force environment.

One significant problem with liquid breathing reported in studies from other laboratories has been the accumulation of carbon dioxide in the blood (19,20,21,22). Carbon dioxide elimination was not a problem in the studies reported here, possibly because the method we used to ventilate the animals produced better exchange of the alveolar liquid than methods used by others, and possibly because of the almost complete extraction of carbon dioxide from the exhaled fluorocarbon in the oxygenator. However, acidemia was observed in all 17 liquid-breathing animals, including the dog ventilated with silicone oil. Since blood-carbon dioxide tensions could be maintained at normal values during liquid breathing, the rapid onset of acidemia (within the first fifteen minutes of liquid breathing) was apparently due to metabolic causes. We could not explain why metabolic acidosis occurred in these animals when mixed venous blood gas tensions and cardiac output were all within normal limits, and we therefore performed an additional study in two animals as described in Section V. In this study, the dogs were ventilated for 4-7 hours with oxygenated liquid fluorocarbon with the respiration rate adjusted to maintain arterial blood P_{CO_2} at 38 ± 5 mm Hg. Electrolytes, enzymes, lactic and pyruvic acid, glucose, and other metabolically related variables were determined periodically in samples of mixed venous blood to better characterize the acidemia. The results, described in Section V, indicate that the acidemia was related to decreased buffering capacity of the blood during liquid breathing and was not due to increased products of metabolism. High blood P_{O_2}

4

tensions maintained the oxygen saturation of mixed venous blood at relatively high levels (approximately 70%) and may have caused both the acidemia and the loss of blood-buffering capacity by a well-known mechanism (23).

Most of the animals in these studies had saline-filled pressure-recording catheters in the thoracic aorta, the main pulmonary artery, the right and left pleural spaces, esophagus, upper trachea, and in either a major bronchus or the lower trachea. Pressure signals from strain-gauge manometers connected to these catheters were recorded simultaneously on digital and analog magnetic tape, and on two paper photokymograph assemblies (on 30-cm-wide paper at 25 cm/sec and on 45-cm-wide paper at 5 cm/sec), along with signals from the cuvette oximeters and from numerous other instruments. Twenty channels of pressure and other data were routinely recorded on the two photokymographs alone. Analysis of these data would have been extremely laborious because of the large number of traces, the uncertainty in some instances in identifying the individual traces when the traces criss-crossed and overlapped as frequently occurred during rotation of the centrifuge, and because pressure corrections had to be applied to a number of traces. The pressure corrections were necessary because the zero baselines shift due to changes in the force environment, because the animal shifts relative to the zero-pressure reference level due to inertial forces, and because we express some of the pressures (the two pleurals and the esophageal) as catheter-tip pressure by subtracting the vertical height of each appropriate catheter tip, determined from biplane thoracic roentgenograms, from the zero-pressure reference level. Furthermore, we refer the two airway pressures (tracheal and bronchial) to the animal's midlung level, and since these pressures were measured in liquids of different specific gravity from that of the saline in the recording catheters, additional corrections to the airway pressure traces had to be made during the liquid-breathing portion of each study. The data reduction was enormously simplified by the development of several computer programs during the course of these studies. These programs were fully utilized in the analysis of the pressure data recorded during the last seven animal experiments when the programs were operational for the first time. Details concerning the use of these programs and the results of the pressure analysis in these animals are described in Section VI of this report.

All investigations concerning the physiological or pathological effects of acceleration are implicitly, if not explicitly, concerned with the same fundamental problem. The problem is one of determining the relative motion and deformation of body tissues when a known accelerative stress is applied. Tissues move in a very complex manner which is frequently difficult to measure but even more difficult to predict. Measurement by roentgenographic means is difficult because the relative displacements are often quite small, even at levels of acceleration which produce gross injury, and because usually there are not enough radiopaque parenchymal land marks to serve as motion indicators. Mathematical models are sometimes helpful, but usually are of limited

5

value unless they are based on measurements in living animals. The best understanding of tissue deformation due to inertial forces can be determined from measurements in the living animal. Perhaps the best examples are found in head injury investigations in which complex brain movements have been photographed through transparent skull caps (24) and measured in 70-nanosecond roentgenograms obtained in rapid sequence during acceleration using implanted metallic beads as motion indicators (25).

Comparable studies were not available concerning displacement and deformation of lung parenchyma due to increased force environments. We, therefore, performed special studies to develop techniques for measurement and display in three dimensions of the complex pattern of parenchymal deformation due to gravitational and inertial forces throughout the entire lung. The position of the lung parenchyma in three-dimensional space throughout the lung must be known for each force environment investigated to accurately determine, for example, the blood flow per cubic centimeter (cm^3) of lung tissue at every vertical level in the lung.

In Section VII, the technique of percutaneously tagging the lung parenchyma with 25-50, 1-2 mm radiopaque stainless steel markers is described, and biplane roentgenographic measurements in 3 dogs of lung movement with respiration and with changes in body position from the prone to the head-up and prone to head-down positions are presented. Each dog was supported in a molded half-body cast with its fore and hind limbs secured and with its abdomen partially restrained by a binder. Regional shifts in position and deformation of the lung due to changes in body position and due to respiration were strongly influenced by changes in position and shape of the respiratory diaphragm. Thus, the study demonstrates the importance of controlling inertial movement of the abdominal viscera in studies of lung movement due only to inertial forces within the lung itself.

Section VIII describes use of the parenchymal tagging technique to study movement of the lungs in left lateral decubitus dogs exposed to increased force environments when breathing air in a water-immersion respirator. A method for computing regional changes in lung volume, and hence regional ventilation, is also described, based on relative movement of the parenchymal tags with respiration.

Almost all of the animals that did not receive succinylcholine during liquid breathing, resumed spontaneous respiration on 100% oxygen at first and then room air, after completion of the liquid-breathing studies. The dogs in the initial studies were sacrificed and histological slides prepared immediately after spontaneous respiration in air was established, but we did attempt to have the last eight dogs survive. Of these eight, the dog which had breathed silicone oil died one hour after resuming spontaneous respiration on air. The arterial blood pressure in this animal progressively decreased shortly after the start of liquid

6

breathing and had declined to 25/5 mm Hg by the time the animal was switched to respiration with 100% oxygen. Arterial blood oxygen saturation and blood-gas tensions had been normal throughout the liquid-breathing period.

Each of the other 7 animals had breathed FC80 liquid fluorocarbon and fared better in the post-liquid-breathing period. Each maintained normal blood-gas tensions for approximately 20 to 24 hours while breathing an air-oxygen mixture or 100% oxygen, administered either via endotracheal catheter or animal-triggered intermittent-positive-pressure respirator. After approximately 20 to 24 hours, each animal became hypoxic and hypercapnic and died within 30 hours after resuming gaseous respiration. In those animals ventilated with intermittent positive pressure, progressively higher airway pressures were necessary to ventilate the increasingly stiff lungs. All dogs showed clearing of both lung fields in repeated fluoroscopic examination and in thoracic roentgenograms within the first hour of gaseous respiration.

At autopsy, the lungs were very congested and had a solid, liver-like appearance and texture, especially in the dorsal and diaphragmatic regions of the lower lobe. Only scattered areas of apparently normal tissue remained, largely in the apical lobes. Microscopic examinations in the last two dogs studied (See Section V) showed capillary congestion, widening of the perivascular spaces presumably due to edema, and generally normal alveolar architecture with minimal intra-alveolar hemorrhage or edema. The respiratory passages were clear. There were focal areas of dense alveolar infiltration of polymorphonuclear cells, suggestive of a chemical pneumonitis. Several sections showed thromboemboli.

The mechanism which produces acute congestive lesions of the lung is unknown (26,27). Evidently this lesion is a nonspecific response of the lung to closed-chest trauma of various kinds (26,27). Respiration with 100% oxygen administered to dogs by endotracheal catheter or intermittent-positive-pressure respiration for 60 to 30 hours has been shown by others to regularly produce pulmonary congestive lesions (28,29). Spontaneous respiration with 95-98% oxygen caused massive congestive pulmonary atelectasis and death in other dogs in 32 to 83 hours (30). Apparently, the surfactant of alveolar lining cells is eventually inactivated by high tensions of oxygen (28,29). Oxygen toxicity due to the high oxygen tensions in the liquid fluorocarbon during the 4 to 8 hours of liquid breathing, and due to the liberal administration of oxygen in the post-liquid-breathing period may have been a factor contributing to the death with congestive pulmonary lesions in the dogs we attempted to have survive.

Previously, other workers have shown that FC80 is lethal when administered in unemulsified form in dogs in quantities as small as 0.1 (31) to 0.25 ml/kg (32). Dogs lived less than 60 hours

after intravenous injection of 0.1 ml/kg (31) and about 5 hours after 0.25 ml/kg (32). In rats and mice, intravenous injection of 0.4 ml FC 80 per 100 gm body mass proved lethal within 1-2 minutes in both species (33), and in newborn puppies 1 ml of FC 75 (industrial grade, similar to medical grade FC 80) injected intravenously caused death within 30 minutes (34). In most studies, the animals died with gas distending the right side of the heart (32,33,34).

We have confirmed these findings in unanesthetized dogs, cats, rabbits, and rats. When unemulsified FC 80 was injected into a peripheral vein, pulmonary artery, aorta, or renal artery in doses of 0.1 ml FC 80/kg body mass, some of the animals died within 45 minutes with roentgenographic evidence of gas in cardiac chambers. All of the animals eventually died, one (a rabbit) as long as 5 days after the injection. Unanesthetized dogs usually died within 45 to 75 minutes after the injection. At autopsy, foamed blood was always found in the right heart and numerous gas bubbles were always present in the veins throughout the body. Usually there was little blood and no free gas in the left side of the heart. The lungs and other organs were normal to gross and microscopic examination. Neither thrombocytopenia nor platelet aggregation, nor any other hematological abnormality usually associated with gas embolism due to decompression were observed.

Gas was sampled from the right ventricle immediately after death in several dogs that had been injected intravenously with FC 80. The gas was found to consist of FC 80 at its vapor pressure along with oxygen and carbon dioxide at tensions equivalent to their respective tensions in venous blood sampled immediately before death. The balance of gas was assumed to consist of nitrogen and water vapor.

Others have reported that FC 80 fluorocarbon can escape from the respiratory passages to the circulatory system during liquid breathing (35). Assays of fluorocarbon levels in blood and other tissues indicate that a total amount of approximately 0.5 ml is absorbed by a 15 kg dog breathing this liquid for one hour and that the highest concentrations of FC 80 are found in the brain and adipose tissue (35). These investigators did not report gas embolism in their liquid-breathing animals, nor have we observed gas embolism in any of our 17 animals that breathed fluorocarbon. However, we attempted but were unable to produce gas embolism by injecting 0.1 to 1.0 ml FC 80/kg intravenously in dogs breathing this fluorocarbon.

In Section IX a possible explanation is offered as to why gas embolism occurs after dogs are injected intravenously with FC 80 while breathing air, and why gas embolism does not occur after the same dose in dogs that are breathing oxygenated FC 80. The explanation assumes that FC 80 in the circulation contributes the same vapor pressure as that of FC 80 (at 37°C) alone to the total tensions of the respiratory gases dissolved in the blood. The mechanism does not explain why animals that have breathed FC 80 in other laboratories have survived breathing air

spontaneously, without gas embolism occurring, 10 days or longer at which time FC 80 was still measurable in the blood (36). Possibly the quantity of FC 80 which was absorbed in the circulatory system of the dogs breathing liquid FC 80 in the latter study did not fully saturate the blood and thus did not contribute the vapor pressure of FC 80 alone to the total tension of gases dissolved in the blood.

Gas embolism due to intravenously administered FC 80 in dogs could be delayed but not prevented by ventilating the animals with 100% oxygen, or subjecting the dogs breathing compressed air to 3 ATA, or to 9-ATA breathing 5% oxygen, 95% helium.

Our primary interest in liquid breathing has been in its use as a physiological tool in studies of the effects of changes in the gravitational-inertial force environment on the cardiorespiratory system; and not with a view toward possible practical applications in man. Modell et al. (22) are currently investigating the possible application of liquid breathing for pulmonary lavage in humans, and these workers have demonstrated that long-term survival of animals which have breathed oxygenated fluorocarbon is possible. They report that 2 of 4 dogs are living at least nine months after breathing FC 80 for 8 hours, and 3 of 6 dogs are alive one year after breathing this liquid for 30 minutes (37).

Needless to say, practical applications of liquid breathing in man must await the development of a nontoxic respirable liquid and safe techniques for its administration. Until that time, liquid breathing should continue to prove an extremely useful physiological tool in studies of the cardiorespiratory system in animals.

9

REFERENCES

1. Bennzinger, T. H. Physiological effects of blast in air and water. In German Aviation Medicine, World War II. Department of the Air Force, Washington, D. C., pp. 1225-1259.

2. Roman, J. Effects of severe whole body vibration on mice and methods of protection from vibration injury. USAF WADC-TR 58-107, 1958.

3. Lombard, C. F., et al. Pathology and physiology of guinea pigs under selected conditions of impact and support-restraint. Aerosp Med 35:860-866 (1964).

4. Coburn, K. R., P. H. Craig, and E. L. Beckman. Effects of positive G on chimpanzees immersed in water. NADC-MA-6139, U. S. Naval Air Develop. Center, 1964.

5. Clemedson, C. J. Blast injury. Physiol. Rev. 36:336-354 (1956).

6. Hanson, P. G. Cardiac displacement and thoracic vascular trauma resulting from abrupt deceleration of dogs. Aerosp. Med. 38:1259-1263 (1967).

7. Hewson, W. The operation of the paracentesis thoracis, proposed for air in the chest, with some remarks on the emphysema, and on wounds of the lungs in general. In Medical Observations and Inquiries, by a Society of Physicians in London, Vol. III, p. 372 8VO, London, 1767. Reproduced in the Works of William Hewson, G. Gulliver (ed.), London, Sydenham Society, 1846, pp. 291-302.

8. Morgagni, J. B. The seats and causes of diseases investigated by anatomy. Printed for A. Millar, T. Cadell, London, 1769. Reproduced in the book by the same title, Vol. 3, p. 199. Hafner Co., N. Y., 1960.

9. Margaria, R., T. Gultierotti, and D. Spinelli. Protection against acceleration forces in animals by immersion in water. Aerosp. Med. 29:433-437 (1958).

10. Code, C. F., E. H. Wood, and E. J. Baldes. Hydrostatic anti-black-out protection; the protection afforded man against the effects of positive acceleration by immersion in water. Fed. Proc. 4(1):15 (1945).

11. Webb, M. G., and R. F. Gray. A new method of protection against the effects of acceleration on the cardiovascular system. Am. J. Cardiol. 6:1070-1077 (1960).

12. Permutt, S., B. Bromberger-Banner, and H. N. Bane. Alveolar pressure, pulmonary venous pressure, and the vascular water fall. Respiration 19:239-260 (1962).

13. Rodbard, S. Distribution of flow through a pulmonary manifold. Am. Heart J. 51(1):106-126 (1956).

14. West, J. B. Distribution of blood flow and ventilation in saline filled lung. J. Appl. Physiol. 20:1107-1117 (1965).

15. Greenleaf, J. F. Distribution of pulmonary blood flow: technics of measurement and display of influence of magnitude and duration of the gravitation-inertial force environment. Ph.D. dissertation, Purdue University, Feb. 1970.

16. Wood, E. H., et al. Scintiscanning system for study of regional distribution of blood flow. SAM-TR-70-6, Feb. 1970.

17. Minnesota Mining and Manufacturing Co. Technical bulletin, Fluorinert brand electronic liquids. 3M Co., St. Paul, Minn., 1965.

18. Dow-Corning Company, Midland, Mich.

19. Clark, L. C., and F. Gollan. Survival of mammals breathing organic liquids equilibrated with oxygen at atmospheric pressures. Science 152:1755-1756 (1966).

20. Kylstra, J. A. The feasibility of liquid-breathing and artificial gills. In The Physiology and Medicine of Diving and Compressed Air Work. (P. B. Bennett and D. H. Elliott, eds.) Balliere, Tindall and Lassell, London, 1969.

21. Lukin, L. Oxygenation of blood during inhalation of a liquid medium. Proc. Soc. Exp. Biol. Med. 121:703-707 (1966).

22. Modell, J. H., E. J. Newby, and B. C. Ruiz. Long-term survival of dogs after breathing oxygenated liquid fluorocarbon. Fed. Proc. 29:1731-1736 (1970).

23. Gesell, R. On the chemical regulation of respiration I. The regulation of respiration with special reference to the metabolism of the respiratory center and the coordination of the dual function of hemoglobin. Am. J. Physiol. 66: 5-49 (1923).

24. Pudenz, R. H., and C. H. Shelden. The Lucite calvarium: a method for direct observation of the brain. II. Cranial trauma and brain movement. J. Neurosurg. 3:487-505 (1946).

25. Hodgson, R. R., E. S. Gurdjian, and L. M. Thomas. Experimental skull deformation and brain displacement demonstrated by flash x-ray technique. J. Neurosurg. 25:549-552 (1966).

26. Jenkins, M. T., et al. Congestive atelectasis - a complication of the intravenous infusion of fluids. Ann. Surg. 132(3):327-347 (1950).

27. Keller, C. S., et al. The cause of acute congestive lesions of the lung. J. Thorac. Cardiovasc. Surg. 53:743 (1967).

28. Lee, C. J., et al. Effects of spontaneous and positive-pressure breathing of ambient air and pure oxygen at one atmosphere pressure on pulmonary surface characteristics. J. Thorac. Cardiovasc. Surg. 53(6) 759 (1967).

29. Lee, C. J., J. H. Lyons, and F. D. Moore. Cardiovascular and metabolic responses to spontaneous and positive-pressure breathing of 100 percent oxygen at one atmosphere pressure. J. Thorac. Cardiovasc. Surg. 53(6) 770-780 (1967).

30. Smith, C. W., P. H. Lehan, and J. J. Monks. Cardiopulmonary manifestations with high O_2 tensions at atmospheric pressure. J. Appl. Physiol. 18(5):849-853 (1963).

31. Nose, Y., et al. Physiological effects of intravascular fluorocarbon liquids. Fed. Proc. 29(5):1789-1804 (1970).

32. Beisang, A. A., et al. Damage assay of kidneys frozen by intraarterial perfusion with a fluorocarbon. Fed. Proc. 29(5):1782-1788 (1970).

33. Geyer, R. P. Whole animal perfusion with fluorocarbon dispersions. Fed. Proc. 29(5):1758-1763 (1970).

34. Gollan, F., and R. M. Clark. Experimental pathology after respiration and injection of various fluorocarbon liquids. Exp. Med. Surg. 26:249-262 (1968).

35. Holaday, D. A. Distribution of fluorocarbon liquids. Fed. Proc. 29(5):1815-1816 (1970).

36. Holaday, D. A., et al. Uptake, distribution, and excretion of fluorocarbon FX-80 (Perfluorobutyl Perfluorotetrahydrofuran) during liquid breathing in the dog. Anesthesiology 37(4):387-394, 1972.

37. Pulmonary rinse of the future. Medical World News, pp. 20-21, November 28, 1969.

SECTION II

Effects of +Gy Acceleration on Blood Oxygen Saturation and Pleural Pressure Relationships in Dogs Breathing First Air, Then Liquid Fluorocarbon in a Whole-Body Water-Immersion Respirator

Abstract

A water-immersion respirator assembly has been used with dogs on the human centrifuge to compare effects of $+1G_y$ and $+6G_y$ acceleration on cardiovascular and respiratory function under three conditions: (1) normal respiration in air; (2) breathing air or oxygen while totally immersed in a saline-filled respirator chamber which provides control of respiratory rate, and tidal and residual volumes; and (3) when respired in the same manner with oxygenated liquid fluorocarbon. Intrathoracic pressures were recorded by strain-gauge manometers connected to saline-filled catheters introduced without thoracotomy into the thoracic aorta, pulmonary artery, right and left atria, left pulmonary vein, and right and left pleural spaces. Three cuvette oximeters measured oxygen saturation of blood continuously withdrawn from the thoracic aorta, pulmonary artery, and left pulmonary vein. Oxygen saturation measurements and intrathoracic pressures were analyzed on-line by a CDC 3300 digital computer. The results indicate that: (1) arterial hypoxemia due to dependent pulmonary arteriovenous shunting caused by acceleration is not minimized by water immersion alone; (2) dogs can be respired with liquid fluorocarbon for four hours or longer, without clinical signs of respiratory distress, with arterial P_{CO_2} values maintained at will between 16 and 40 mm Hg, and with arterial blood fully oxygenated at breathing rates between 4 and 8 per minute; (3) liquid respiration prevented dependent pulmonary arteriovenous shunting at $+6G_y$; (4) vertical gradients in pleural pressure were approximately 0.7 cm H_2O/cm vertical distance between pleural catheter tips in air-breathing dogs in contrast to slightly greater than 1.0 cm H_2O/cm vertical distance in liquid-breathing experiments; (5) liquid breathing prevented inertial displacements of the heart and other mediastinal structures to dependent sites in the thorax, and roentgenographically evident pulmonary atelectasis in dependent regions. During exposures to $+6G_y$, the heart floated upward into the superior hemithorax with somewhat overexpansion of the dependent left lung. The specific gravity of the fluorocarbon was 1.76. Theoretically, liquid breathing can protect against pulmonary-arteriovenous shunting and injury due to acceleration, and injury to the thoracic contents due to transient or sustained extreme changes in environmental pressure. Liquid breathing can also minimize decompression problems associated with such changes.

13

Introduction

Previous studies in this laboratory have shown that exposure to centripetal acceleration produces in man, chimpanzees and dogs, a decrease in arterial blood oxygen saturation, and that this decrease in blood oxygen saturation is due to pulmonary blood perfusing poorly ventilated regions in the most dependent parts of the lung (1,2,3). Pleural pressure measurements along with observations from biplane roentgenograms and videotape angiograms indicate that pulmonary atelectasis in dependent regions is due to lung collapse in these regions because of the increased weight of the superposed lung and mediastinal structures, particularly the heart and great vessels. However, dependent atelectasis may also be produced by inertial displacement of the diaphragm into the thorax and by inward movement of the rib cage. If the atelectasis due to these effects of acceleration were significant, then improved restraint of the chest wall and abdomen should minimize the decrease in blood oxygen saturation during acceleration. Furthermore, if alveolar collapse due to the increased weight of the lung were the primary cause of the arterial desaturation, then filling the alveoli and conducting airways with a respirable liquid should prevent alveolar collapse, and thereby prevent decreases in oxygen saturation due to blood perfusing poorly ventilated atelectatic regions.

With these principles in mind, we exposed dogs to either $+1G_y$ and $+6G_y$, or $+1G_y$, $+3.7G_y$, and $+6.9G_y$ (inertial movements of the heart and other viscera from the right side of the body to the left) under three conditions, and measured the oxygen saturation of blood continuously withdrawn from the aorta, pulmonary artery, and from a vein draining the dependent left lung. The three conditions were: first, with the dogs immersed in air and spontaneously breathing room air (i.e., the dogs were positioned on their left side in the cockpit of the centrifuge with only pelvic and shoulder belts for restraint); second, with the dogs immersed in saline and mechanically ventilated with room air (water immersion was used to minimize inertial displacements of the chest wall and abdomen); and third, with the dogs immersed in water and ventilated with oxygenated liquid fluorocarbon at normal body temperature (37°C).

The solubility of oxygen in fluorocarbon is about 40 ml oxygen/100 ml, and solubility of carbon dioxide in fluorocarbon is about 160 ml carbon dioxide/100 ml. It is biologically inert, and the vapor pressure, viscosity, and appearance of liquid fluorocarbon are similar to those of water (4). Unlike water, the specific gravity of fluorocarbon is 1.76; 1.0 would have been ideal in these studies. In this part of the study the respiratory passages were completely filled with liquid (i.e., contained no free gas), and the dogs literally breathed liquid fluorocarbon for periods of 4 to 8 hours at normal body temperature, with ventilation rates of 4 to 6 per minute, all the while

14

maintaining normal blood P_{O_2} and P_{CO_2} values, and without signs of respiratory distress.

Methods

Seventeen dogs, 11.0 to 14.5 kg body mass, were anesthetized with sodium pentobarbital, 30 mg/kg i.v. initially, with supplemental i.v. administrations of sodium pentobarbital and morphine sulphate as required throughout the experiment. In the first 12 dogs, a straight thin-walled metal endotracheal tube was inserted through a tracheotomy and the esophagus tied through the same wound after an esophageal or gastric catheter had been positioned. A flexible Tygon endotracheal tube was inserted through a tracheotomy in the latter 5 dogs, and the esophagus was not tied.

Radiopaque Teflon or woven nylon catheters were introduced percutaneously and positioned under fluoroscopic control as follows: two were placed in the main pulmonary artery for recording pressure and blood sampling, one in the right atrium, one in the thoracic aorta, and one in the abdominal aorta for recording pressure and blood sampling, respectively, and one in the femoral vein for reinfusion of the sampled blood. Two catheters introduced via the right external jugular vein were positioned in the left atrium and a left pulmonary vein (in one dog, a right pulmonary vein was catheterized by a transseptal technique). In all but the first three dogs, two radiopaque polyethylene catheters (1.3 n o.d., 0.8 mm i.d.) were inserted without thoracotomy into the left and right pleural spaces and their tips manipulated under fluoroscopic control to the superior and dependent surfaces of the lung. All catheters were filled with heparinized Ringer's solution (2500 units heparin/100 ml). Tables I and II (See Appendix) summarize the experimental arrangement for each of the 17 animals; dogs numbered 1 through 8 in Table I, and the first 9 dogs listed in Table II.

The dog was then placed in the left lateral position within a water-immersion body-support respirator assembly (to be described), and the assembly mounted in the cockpit of a 4.4 meter radius centrifuge. During the rotation of the centrifuge, the cockpit tilted such that the resultant vector of acceleration remained in the same direction relative to the animal as the 1G gravitational vector. Using biplane roentgenograms, the tank was positioned so that the long axis of the tank and the midlung level of the dog coincided with the axis of tilt of the cockpit. All catheters were connected to Statham strain gauges mounted in the cockpit at approximately the level of its axis of tilt. This level was the zero-pressure reference and corresponded to the midlung of the animal at $+1G_y$. Details of the techniques used to measure pressure during centripetal acceleration are described elsewhere (5).

15

Figure 1 is a schematic drawing of the water-immersion body-support respirator assembly when the dogs were totally immersed in saline (37°C) and ventilated with room air.

ASSEMBLY FOR STUDY OF EFFECTS OF WATER IMMERSION
ON INTRATHORACIC PRESSURE RELATIONSHIPS

BV = Breathing Valve
▨ Saline
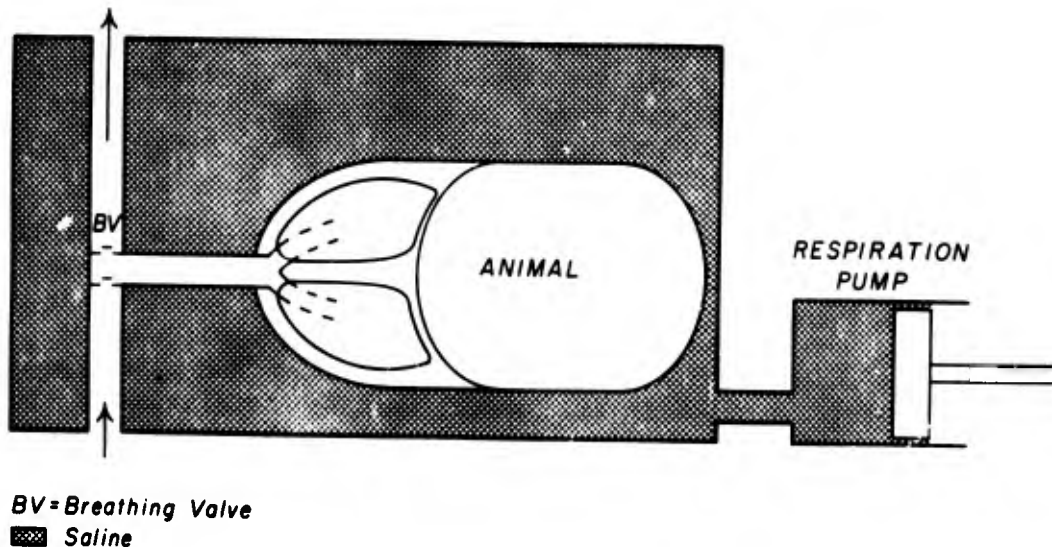
Figure 1. Assembly for study of effects of body support by water immersion on intrathoracic pressure relationships during changes in the magnitude of the gravitational-inertial force environment. The whole animal is enclosed in a rigid chamber filled with saline. Respiratory rate and tidal volume are controlled by the motor-driven respiration pump which adds and removes saline from the immersion tank in a sinusoidal manner. The functional residual lung volume is controlled by adding or withdrawing saline from the immersion chamber. The assembly is thus a whole-body plethysmograph mounted in the cockpit of the centrifuge, permitting control of many variables of respiration during centripetal acceleration.

The assembly was fabricated almost entirely of rigid transparent acrylic material. A breathing valve connected to the endotracheal tube separated inhalation and exhalation lines, which in turn were connected through large-bore, two-way valves to room air. The respiration pump

ventilated the animals in a sinusoidal manner by alternately withdrawing and returning saline from and to the immersion tank in Drinker respirator fashion. Tidal volume and frequency were continuously variable by the pump over the ranges of 0 to 480 ml and 0 to 20 per minute, respectively. Residual lung volume was varied by either adding or subtracting saline from the constant volume system. Residual lung volume was measured as in air-filled plethysmographs by application of Boyle's Law. In this measurement, the inhalation and exhalation lines were occluded by the two large outside valves, and the decrease in airway pressure was measured as the airway volume was increased in known increments by withdrawing known volumes of air from the airway into a calibrated syringe. When necessary, a small dose of succinylcholine (0.3 mg/kg, i.v.) was administered to prevent spontaneous respiratory movements which frequently occurred during the 20-30 second measurement period, especially when the residual lung volume was small.

Figure 2 illustrates the arrangement of the assembly used in the first three liquid-breathing studies.

ASSEMBLY FOR STUDY OF EFFECTS OF BREATHING LIQUID FLUOROCARBON
ON FORCE ENVIRONMENT DEPENDENT REGIONAL DIFFERENCES
IN INTRATHORACIC PRESSURES, BLOOD FLOW, AND OXYGENATION
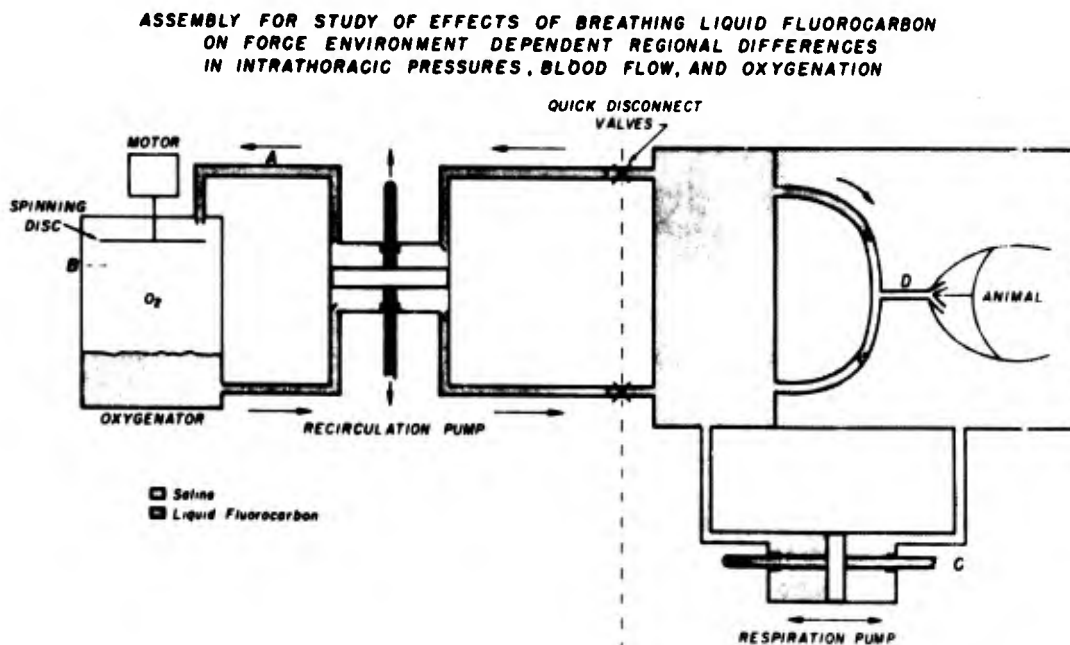
Figure 2. Representative drawing of the water-immersion respirator assembly. A) Recirculation pump. Variable displacement and frequency pump similar to respiration pump (C), transfers exhaled fluorocarbon to the oxygenator (B), and returns oxygenated fluorocarbon to the breathing compartment.

17

B) Oxygenator. Exhaled fluorocarbon is nebulized by flowing the liquid onto a rapidly spinning disc. Carbon dioxide is removed from the fluorocarbon and oxygen is replaced by nebulizing the liquid in an oxygen-rich, carbon dioxide-poor atmosphere.

C) Respiration pump. Inspires the water-immersed animal by removing a volume of saline from the immersion tank while simultaneously supplying the same volume of fluorocarbon to the animal's airway from the breathing compartment. Expires the animal by adding saline to the immersion tank while removing an equal value of fluorocarbon from the airway. Displacement and frequency of the pump are continuously variable over the ranges of 0-500 ml and 0-20 per minute, respectively.

D) Breathing valve. Separates flow of inhaled and exhaled fluorocarbon. Dead space is minimized by connecting the valve directly to the endotracheal tube.

The respiration pump withdraws saline from the immersion tank on inspiration and simultaneously supplies an equal volume of oxygenated liquid fluorocarbon from the breathing compartment to the airway. On expiration, the respiration pump reverses the flow, returning saline to the immersion tank and removing fluorocarbon from the lung. The total displacement of the system, consisting of fluorocarbon, saline, and animal, should thus remain constant throughout the respiration cycle, and as a result, the pleural, intravascular, and immersion tank pressures would be expected to vary little throughout the cycle.

The remainder of the equipment shown in Figure 2 was used to oxygenate the fluorocarbon, remove cardon dioxide from the fluorocarbon, and return freshly oxygenated fluorocarbon to the breathing compartment.

The fluorocarbon was continuously oxygenated and carbon dioxide continuously removed by circulating the fluorocarbon in the oxygenator reservoir over a rapidly spinning 8-inch aluminum disc which nebulized the liquid in a 100% oxygen atmosphere. The atmosphere was maintained by a 3-liter-per-minute flow of oxygen into the oxygenator.

Just prior to the liquid-breathing portion of the study, the animals were ventilated with 100% oxygen for about 15 minutes to denitrogenate the blood and other tissues. Gas bubbles were visible in the exhaled liquid immediately after switching the inhalation and exhalation lines to the breathing compartment filled with oxygenated fluorocarbon. The gas bubbles progressively diminished in number with each exhalation, and after 5 or 10 minutes of liquid breathing, there were no gas bubbles visible in either the exhaled or inhaled fluorocarbon.

During experiments in which the centrifuge rotated or during control, 1G experiments, the oxygenator assembly mounted on a mobile cart was disconnected, the animal inhaled and exhaled fluorocarbon from the 4-liter breathing compartment, and the oxygenator was promptly

reconnected after the 1- or 2-minute exposure to centripetal acceleration. Heaters in the oxygenator reservoir maintained the liquid at normal body temperature (37°C). A rectal thermistor probe was used to continuously monitor body temperature, and a similar thermistor probe monitored the temperature of the surrounding saline.

Figure 3 is a photograph of the apparatus used in the initial liquid-breathing studies. The oxygenator is shown connected to the respirator. For a clear view, the respirator was photographed on a small table.
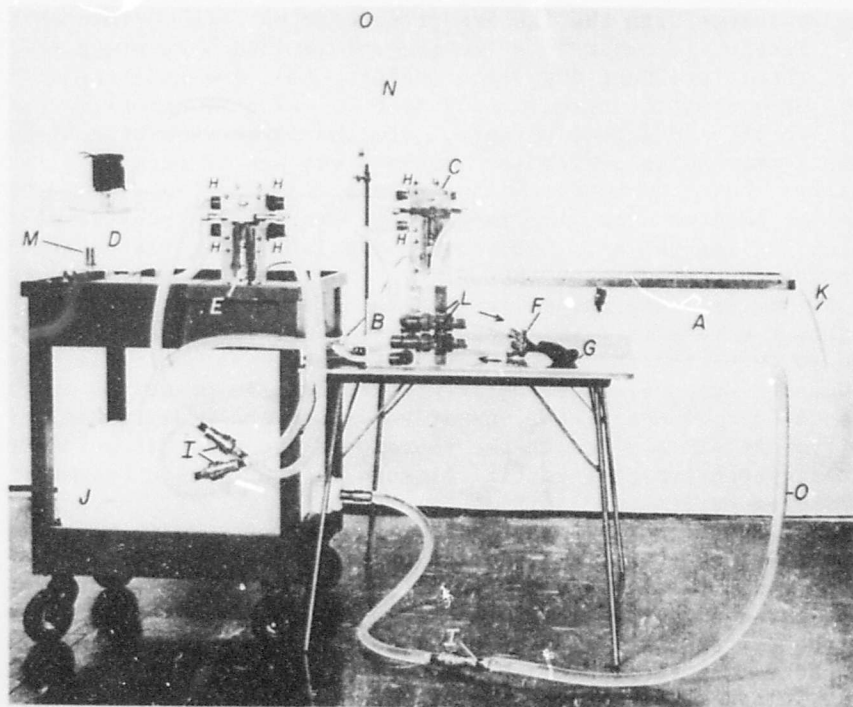
Figure 3. Photograph of the fluorocarbon oxygenator and water-immersion respirator assemblies used in the initial liquid-breathing studies. (A) Water-immersion respirator. Removable cover for access to the immersed animal. Transparent Lucite, 20 cm x 20 cm x 100 cm. (B) Breathing liquid compartment. Transparent Lucite tank holds approximately 4 liters of oxygenated fluorocarbon. (C) Respiration pump. (D) Oxygenator. (E) Recirculation pump. Transfers exhaled fluorocarbon to the oxygenator (D), and returns oxygenated fluorocarbon to the breathing compartment (B). (F) Breathing valve. (G) Balloon. Simulates the animal's

19

lungs in preliminary tests. (H) Check valves in the recirculation pump. (I) Quick-disconnect valves, separate the portable oxygenator assembly from the restraint system prior to rotation of the centrifuge, and reconnect the two assemblies after the centrifuge stops. (J) Reservoir, supplies water for filling the immersion tank (A) and drains the tank (13-gallon capacity). (K) Air supply to pneumatic seal in the cover of the immersion tank. Rapid access to the immersed animal is accomplished by deflating an air cuff in the tank cover and removing the cover. (L) 3-way valves for switching the animal's airway from room air to respirable liquid. (M) Electric heater to control the temperature of the oxygenated fluorocarbon. Body temperature is held constant by heat exchange with the inspired fluorocarbon. (N) Fluorocarbon reservoir. Used to prime the recirculation pump and to fill the interconnecting Tygon tubing. (O) The interrupted line separates the respirator assembly, which is normally mounted in the centrifuge cockpit, from the oxygenator assembly, which is pushed to or from the cockpit via mobile cart.

A major problem with this arrangement was partial closure of the airways during expiration. Due to the much larger compliance of the 40-liter immersion tank than the 4-liter breathing compartment, the immersion tank pressure lagged the breathing compartment pressure. On expiration, the rate of fluorocarbon removal was initially greater than the rate at which the thorax was compressed externally, and large pressure gradients were developed between intrathoracic pressures and the lumen of the endotracheal tube, negative within the endotracheal tube, and positive at other sites in the thorax. These pressure imbalances were large enough to cause partial closure of the trachea or major bronchi during expiration, just distal to the intrathoracic end of the endotracheal tube. During inspiration, the intratracheal and intrabronchial pressures were greater than the intrathoracic pressures, and the airways remained patent. Even with the partial airway closure problem, the first three animals were ventilated for 4 to 6 hours with liquid fluorocarbon at rates of about 4 per minute while maintaining satisfactory control of blood P_{CO_2} and P_{O_2} values. Blood pH was maintained between 7.35 and 7.45 when the animal breathed room air in the water-immersion respirator for several hours before liquid breathing commenced. Immediately after the animals were switched to liquid breathing, the blood pH progressively decresed to values near 7.0 by the end of the fourth hour of liquid breathing. Since cardiac output and the tensions of oxygen and carbon dioxide in mixed venous blood were within the range of normal, we cannot explain the abrupt onset of metabolic acidosis observed in these three dogs during the liquid-breathing part of the studies.

After the first three experiments, the apparatus was modified.

20

The last three experiments showed that large increases in resistance to flow through the trachea during expiration (i.e., partial airway closure) did not occur when the animal's airway was connected to a reservoir filled with oxygenated fluorocarbon and with the surface of the fluorocarbon maintained at approximately midlung level. The fluorocarbon side of the respiration pump was disconnected, and the animal respired by withdrawing and adding saline from and to the immersion tank, but the fluorocarbon in the modified arrangement flowed passively between oxygenator and the animal. At those times when the centrifuge rotated, or during control 1G exposures, the oxygenator was disconnected and the animal breathed fluorocarbon from the breathing compartment. The liquid level in the breathing compartment had been previously adjusted to the same level as in the oxygenator, and inhaled and exhaled fluorocarbon were partially separated by a baffle dividing the breathing compartment. Partial airway collapse would still occur when residual lung volume was small, but was promptly relieved when saline was removed from the immersion tank to increase residual lung volume. To promptly detect airway closure if it occurred, pressures in the inhalation and exhalation lines, and within the trachea and endotracheal tube, were continuously monitored and displayed on an 8-channel recording oscilloscope at the centrifuge control station.

Oxygen saturation was measured in blood continuously sampled from the pulmonary artery, pulmonary vein, and abdominal aorta by cuvette oximetry. Three roller pumps positioned between the cuvettes and a femoral vein reinfusion catheter withdrew blood through the cuvettes and reinfused this blood back into the animal during these measurements. The oximeter signals were digitized, fed on-line to a CDC 3300 digital computer, and the oxygen saturation measurements along with the calculated pulmonary and systemic arteriovenous shunt values were displayed every 2 seconds on a storage oscilloscope at the centrifuge control station. Immediately after each exposure to centripetal acceleration and after the $+1G_y$ control exposures, the oxygen saturation values measured during the exposure were graphed on a high speed computer-driven incremental plotter (Calcomp).

21
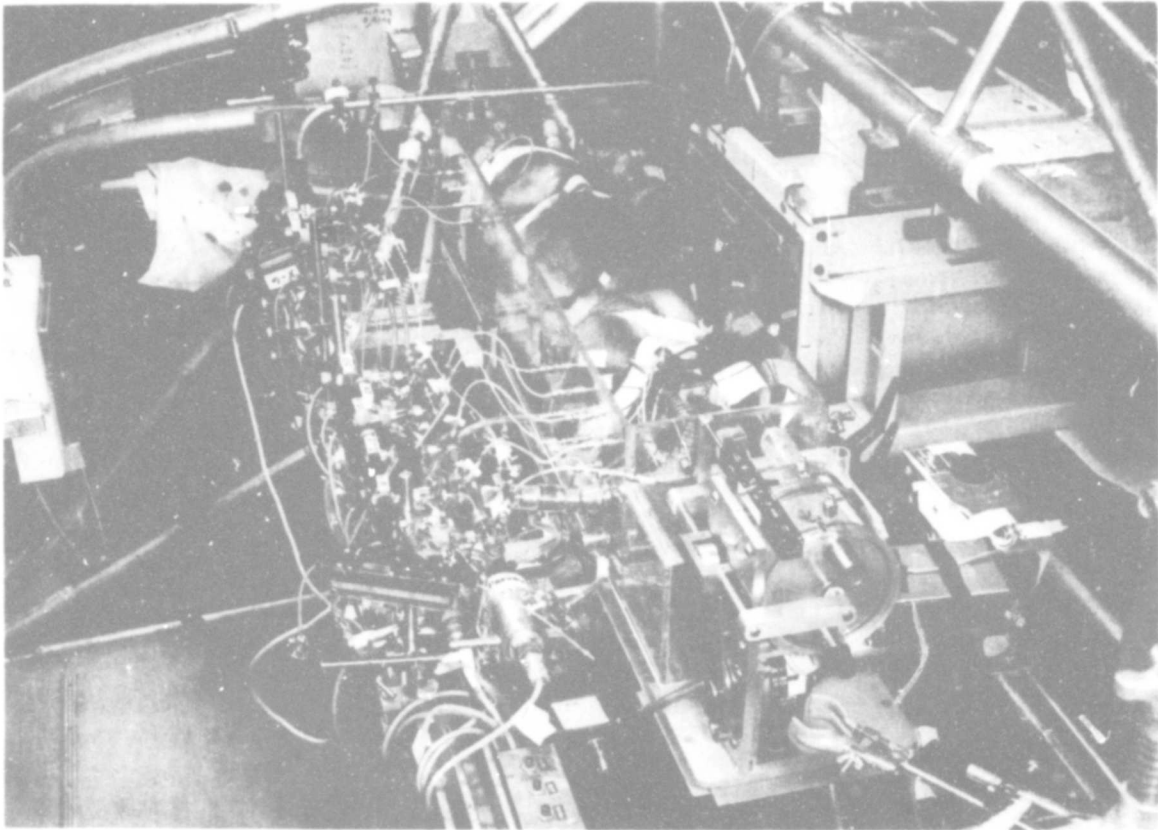
Figure 4. Water-immersion liquid-breathing apparatus mounted in the centrifuge cockpit. Dog positioned left side down in the immersion tank, with head nearest the camera. At this time, the dog was restrained only by pelvic and shoulder straps and breathed room air spontaneously. Later, the dog was immersed in saline. The respiration pump in the foreground withdraws a tidal volume of saline from the immersion tank on inspiration and returns the saline to the tank on expiration. The small Lucite tank beneath the respirator pump contains fluorocarbon during the liquid-breathing part of the experiment which followed. The row of catheters from ports along the side of the immersion tank are connected to individual strain gauges through hydraulically actuated valves. The valves permit flushing the catheters and inserting calibration pressures in the strain-gauge lines from a remote station during rotation of the centrifuge. X-ray source and image intensifier used to obtain biplane films and video images are shown in the left and right-hand margins, respectively.

22

Figures 6 and 8 are illustrative of these plots. Cardiac output was measured with the indocyanine-green dye technique. The densitometer signal was digitized and the cardiac output computed on-line and displayed along with the dye curve in real-time on another storage oscilloscope at the centrifuge control station. Techniques for the on-line, real-time display of blood oxygen saturation and cardiac output are described elsewhere (5).

Pressure and other data were recorded in parallel on two photo-kymographic assemblies, 14-channel and 7-channel magnetic tape instrumentation recorders, and on digital tape. Simultaneous events were identified in the separate records by binary coded decimal signals recorded simultaneously by each recording assembly.

Either an AP or lateral roentgenogram was obtained in almost every exposure to centripetal acceleration and during the control +1G_y exposures to determine the position of the tips of the pleural catheters relative to midlung. The vertical positions of the catheters were measured to calculate the pressure at the catheter tip as described elsewhere (5). Figures 5 and 12 are examples of AP roentgenograms obtained during control and +6G_y exposures in both air-breathing and liquid-breathing experiments, respectively, and show the number and relative position of the recording and sampling catheters.

The partial pressures of oxygen and carbon dioxide, and pH of blood sampled from the pulmonary artery, aorta, and pulmonary vein catheters were measured immediately before (in some animals) and always after each exposure, as well as periodically throughout each experiment to monitor the cardiovascular status during the course of the experiments which typically lasted 12 to 20 hours.

Procedures

Initial determinations of pressures, cardiac output, blood gases, and oxygen saturations were made in all dogs during +1G_y control periods, and during at least one +6G_y exposure in each of nine dogs, with the animal immersed in air (immersion tank dry) and breathing room air spontaneously. The immersion tank was then filled with physiologic saline, the stroke volume of the respiration pump adjusted to 480 ml, and the control and +G_y measurements were repeated under each of three conditions:

1) Saline was either added to or removed from the tank until the respiratory variations in tank pressure balanced around zero. Typically the peak tank pressures would measure + 15 cm H_2O on expiration and -15 cm H_2O on inspiration under balanced conditions. Lung volume at full expiration was typically 600-800 ml, and 1,000 to 1,300 ml at full inspiration, as measured by the

23

Boyle's Law technique.

2) Approximately 200-300 ml saline was removed from tank to increase residual lung volume by approximately this amount. Tank pressures were typically zero at full expiration.

3) Residual lung volume was then reduced by approximately 300 ml by adding this much saline to the balanced tank. Tank pressures usually varied between 0 at full inspiration, and +25 to +30 cm H_2O at full expiration under these conditions.

Eight dogs were studied under the above three conditions. Nine additional dogs were similarly studied and measurements of oxygen saturation, cardiac output, and pressures were repeated when ventilated with liquid fluorocarbon immediately after the air-breathing experiments. Only control measurements at 1G were made with the dog immersed in air and breathing air spontaneously, but the water-immersion air-breathing experiments were made under the three conditions of residual lung volume. The last dog was exposed to +1Gy, +3.7Gy, and +6.9Gy while immersed in water and first breathing air, then liquid fluorocarbon. Anesthesia was maintained in all dogs throughout the experiments by supplemental doses of intravenous sodium pentobarbital and morphine sulphate as required.

After the studies were completed, the animal was switched from liquid ventilation to ventilation with 100% oxygen. Two valves in the inhalation and exhalation lines were turned to arrange the apparatus as shown in Figure 1, and approximately 100-200 ml fluorocarbon were removed from the lung in 3 or 4 exhalations. Compression of the thoracic wall, by adding 200 to 300 ml saline to the immersion tank, resulted in removal of only small amounts of additional fluorocarbon from the lung. The saline was then drained from the immersion tank, and spontaneous respiration was resumed, first with 100% oxygen, then with room air, by all dogs that had not received repeated doses of succinylcholine (0.3 mg/kg) during the experiment.

The dogs were sacrificed with a lethal dose of sodium pentobarbital and the lungs resected en bloc. Only small amounts of additional fluorocarbon could be drained from the resected lungs, although judging by their weight, the lungs probably contained 200 to 500 ml fluorocarbon. The lungs were perfused with formalin and histological sections were prepared. The results of the histological studies will not be presented here.

Results and Conclusions

In the air-breathing experiments, water immersion minimized narrowing of the rib cage, and minimized inertial displacements and deformation of the abdomen during the exposures to centripetal acceleration, as the films shown in Figure 5 demonstrate.

A-P ROENTGENOGRAMS DURING +1G_y AND +6G_y
WITH AIR (A,C) AND WATER (B,D) IMMERSION RESTRAINT
(Dog, 12.5 kg, Morphine-Pentobarbital Anesthesia)
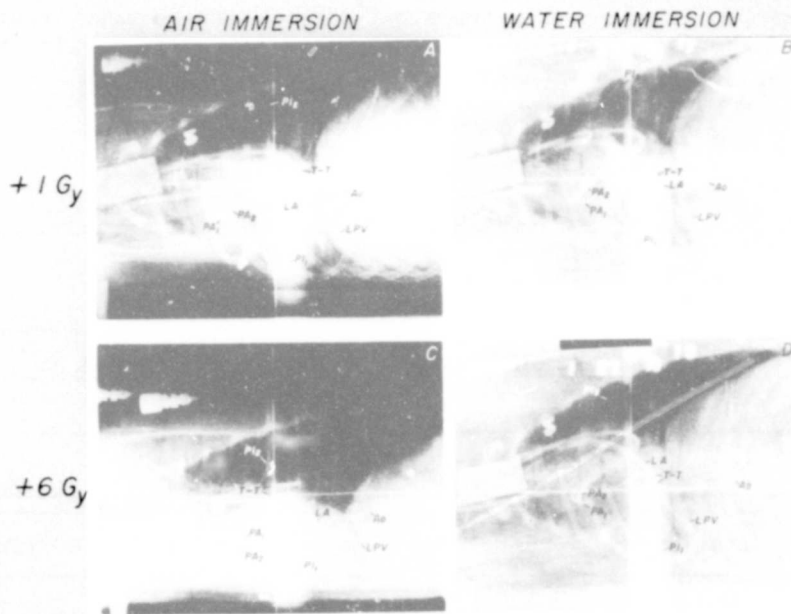
Figure 5. Thoracic roentgenograms of a dog in the left decubitus position at 1G_y and during exposures to +6G_y during spontaneous respiration in an air environment (A,C), and during controlled respiration of air in a water-immersion restraint system (B,D).

Identification of positions of the tips of the recording catheters: PA, pulmonary artery, PA_1, for pressure recording, PA_2, for injection of circulatory indicators (indocyanine green, 69% renovist); LA, left atrium; LPV, left pulmonary vein; Ao, aorta; Pl, pleural catheters, Pl_2, lateral (superior) border of right pleural space, Pl_1, lateral

(dependent) border of left pleural space. T-T indicates lead-tagged floats on the menisci of the zero-reference water-filled thistle-tube system, the vertical height of which is adjusted to coincide with midlung level (5).

However, there were no statistically significant differences in the oxygen saturation measurements, or in the computed arteriovenous shunt values when the animal was immersed in saline and when immersed in air. The table compares arterial oxygen saturation values, and computed A-V shunts in dogs at $+1G_y$ and $+6G_y$, first during air immersion, then during water immersion. Average values and standard error of the mean are shown for 7 dogs. We conclude that improved support of the abdomen and chest wall by water immersion does not protect against A-V shunting in the lower lung during transverse $+G_y$ acceleration. The Calcomp plots shown in Figure 6 show the similarity in oxygen saturation values recorded during $+6G_y$ exposures in 1 dog first immersed in air, then immersed in saline under balanced tank conditions.

Table

EFFECT OF BODY RESTRAINT ON OXYGENATION OF BLOOD IN THE LUNGS

(Average Values - 7 Dogs)		
Arterial Blood Oxygen Saturation - Per Cent		
	Air Immersion	Water Immersion
$+1G_y$	89 ± 1*	87 ± 1
$+6G_y$ **	69 ± 2	64 ± 2
Pulmonary Arteriovenous Shunt - Per Cent of Pulmonary Blood Flow		
	Air Immersion	Water Immersion
$+1G_y$	15 ± 2	20 ± 2
$+6G_y$ ***	44 ± 2	52 ± 2

* Standard error of the mean.
** Minimum values at end of 60-second exposures.
*** Maximum values.

COMPUTER (Calcomp) PLOT OF OXYGEN SATURATION
OF RIGHT PULMONARY VENOUS, MIXED VENOUS, AND ARTERIAL BLOOD
DURING 60-second EXPOSURE TO +6 Gy WITH AIR IMMERSION
(Dog. 14 kg. Morphine-Pentobarbital Anesthesia)
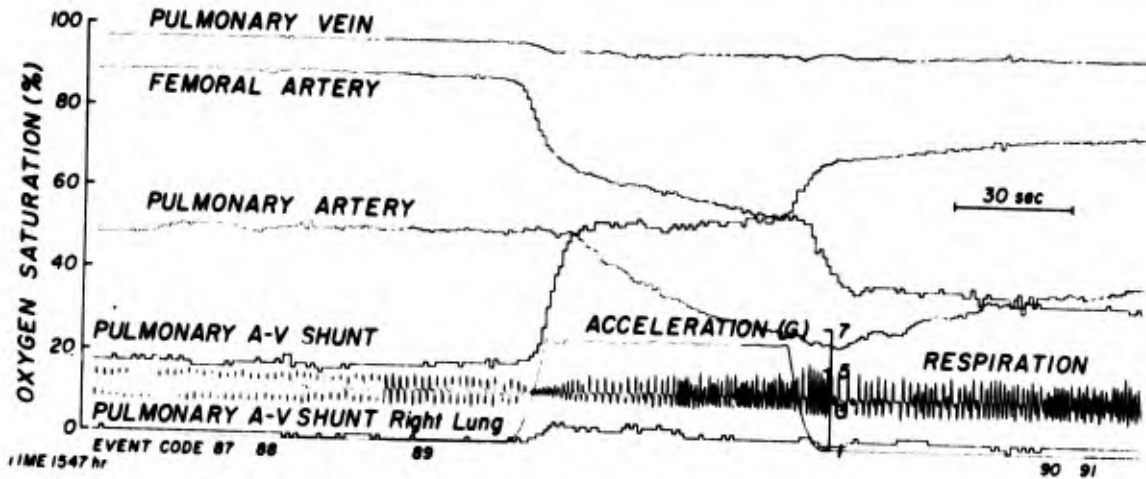
Figure 6 A

COMPUTER (Calcomp) PLOT OF OXYGEN SATURATION
OF RIGHT PULMONARY VENOUS, MIXED VENOUS, AND ARTERIAL BLOOD
DURING 60-second EXPOSURE TO +6 Gy WITH WATER IMMERSION
(Dog. 14 kg. Morphine-Pentobarbital Anesthesia)

Figure 6 B

27
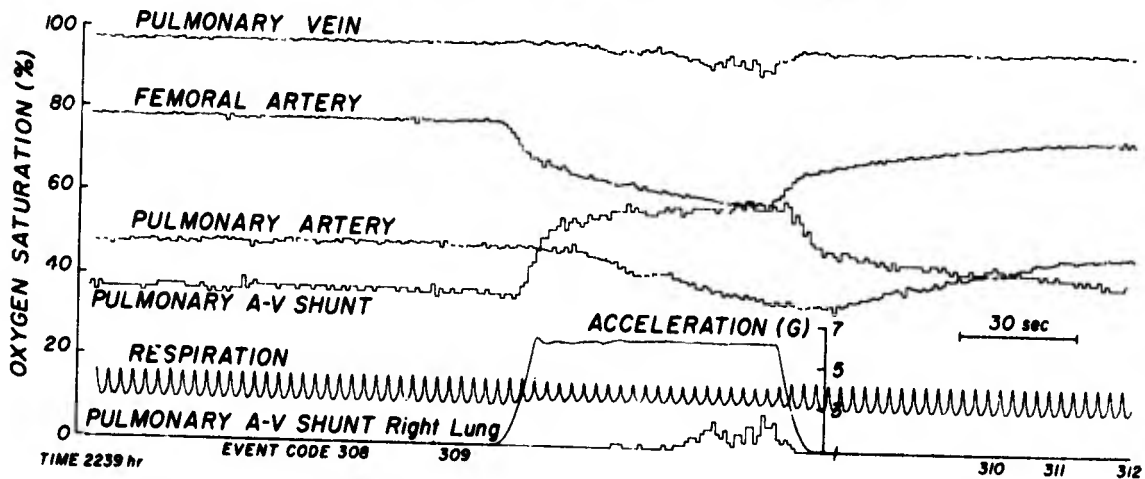
Figure 6. Computer-generated (Calcomp) plot of oxygen saturation
of right pulmonary venous, mixed venous and arterial blood
during 60-second exposures to +6G$_y$ when (A) breathing air
spontaneously, and (B) breathing air in the water-immersion
respirator. The tip of the pulmonary vein catheter was
located near the upper (medial) margin of the dependent left
lung. The decrease in the amplitude of the airway pressure
(respiration trace) during the acceleration plateau in (B)
may have been due to a decrease in compliance of the chest
wall. A smaller than normal residual lung volume could
account for the decrease in chest wall compliance and the
larger systemic shunt during the control period in (B)
compared with (A).

Figure 7 compares pleural pressure measurements at end-expiration
in 5 dogs at +1G$_y$ and +6G$_y$ when the dogs were immersed in air, and when
immersed in saline. Each of the four panels has the same set of scales,
viz., end-expiration pleural pressure at the catheter tip, in cm H$_2$O,
on the vertical scale, and catheter-tip distance above and below the
midlung in centimeters on the horizontal scale. The pleural pressure
gradient, i.e., the pressure difference between the two catheter tips,
in cm H$_2$O, divided by the vertical distance between the catheter tips,
in cm, per G acceleration, was always less than 1.0 cm H$_2$O/cm/G for
all dogs, as shown by the 1:1 line included for reference. The 1:1 rela-
tionship would have been observed if the intrathoracic contents behaved
as a simple liquid with a specific gravity of 1.0. Figure 7 was plotted
from the measurements shown for the individual dogs in Table III (See
Appendix).

28

RELATIONSHIP OF PLEURAL PRESSURES TO VERTICAL HEIGHT
IN THORAX OF 5 DOGS DURING AIR AND WATER IMMERSION
IN LEFT DECUBITUS POSITION

DISTANCE below MIDLUNG (cm)
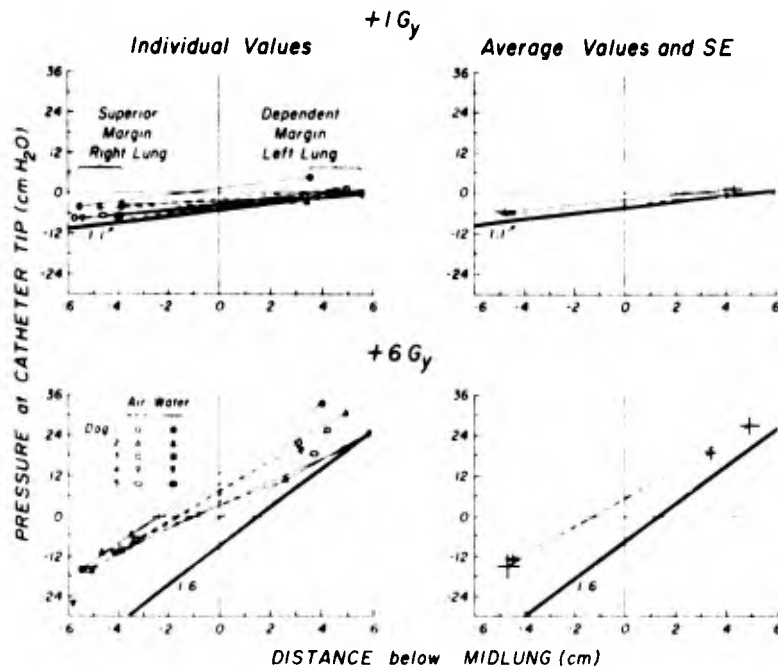
Figure 7   Effect of $+G_y$ acceleration on the difference between end-
expiratory pleural pressures at superior (right) and depen-
dent (left) surfaces of the lungs of 5 dogs. The animals
were first immersed in air and then immersed in water. The
symbols identify individual dogs. The open symbols connected
by dashed lines and the solid symbols connected by solid lines
are values measured simultaneously at superior and dependent
regions in the thorax when dogs were immersed in air and water,
respectively. The thick-hatched line indicates the gradient
in pressure between superior and dependent sites in the pleu-
ral spaces which would be expected if the thoracic contents
behaved like a system with a specific gravity of 1.0. Cath-
eter-tip positions were determined using biplane thoracic
roentgenograms obtained during expiratory phase of respira-
tion. Pleural pressures were measured in photokymographs
and adjusted to catheter-tip level (5).

The two right-hand panels of Figure 7 show that there were no sig-
nificant differences in gradient between air-immersed and water-immersed
animals. However, some measure of the improved support by water immer-
sion is shown in the right-hand panels by the minimum shift in catheter-
tip positions relative to each other and relative to midlung; i.e., the
chest wall and lung margins apparently did not move nearly as much

29

during the +6Gy exposures when the animals were immersed in water, as when immersed in air, consistent with roentgenographic observations, such as illustrated by Figure 6.

In the liquid-breathing studies, which in the last 9 dogs were performed in addition to air-breathing studies, pulmonary arterial-venous shunting due to acceleration was either prevented or greatly minimized, as the Calcomp plot of Figure 8(B) illustrates.

COMPARISON OF EFFECTS OF G$_y$ ACCELERATION ON BLOOD OXYGEN SATURATION WHEN BREATHING AIR AND LIQUID FLUOROCARBON

(DOG 10.3 kg. MORPHINE - PENTOBARBITAL ANESTHESIA)
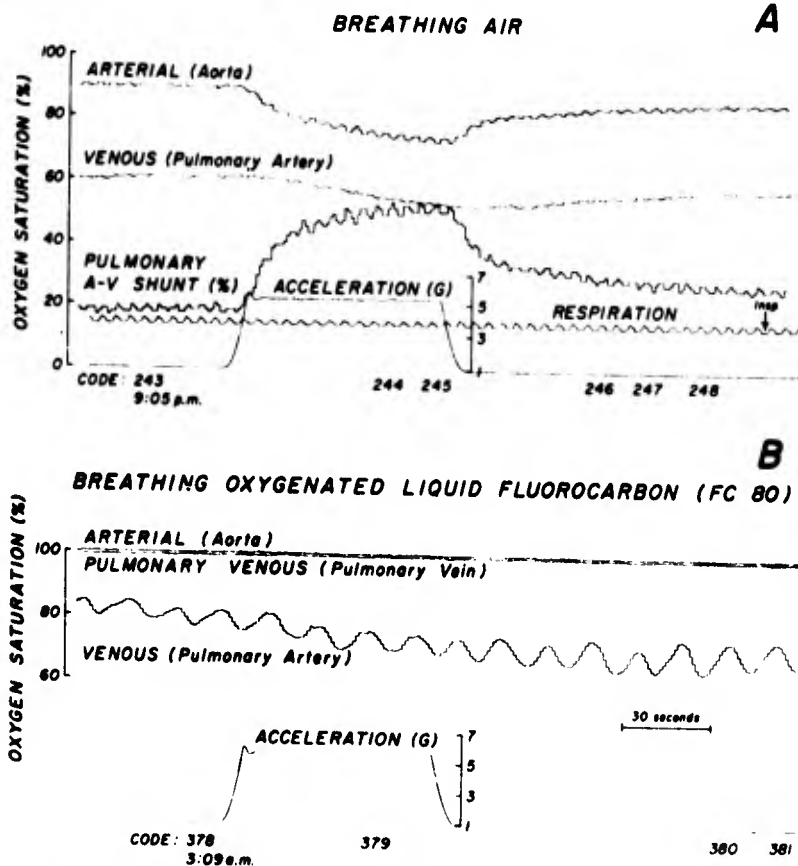
Figure 8   Computer (Calcomp) plot of oxygen saturation during 1-minute exposures to +Gy acceleration when (A) breathing air, immersed in water, and (B) breathing oxygenated liquid fluorocarbon, immersed in water. The decrease in the pulmonary artery blood oxygen saturation during the acceleration plateau in (B) was probably due to the steady decrease in oxygen content of fluorocarbon contained in the 4-liter rebreathing compartment. The oxygenator was promptly reconnected

30

to the breathing compartment after the centrifuge stopped
rotating, and the pulmonary artery saturation gradually re-
turned to the pre-acceleration value. The sinusoidal vari-
ations in the oxygen saturation of the mixed venous (pul-
monary artery) blood are at respiratory frequency and result
from the changes in cardiac output associated with the si-
nusoidal variations in pressure applied to the dogs total
surface area by the respiration pump. (See Section III).

No pulmonary arteriovenous shunt was demonstrated in this dog during
the exposure to 6Gy when breathing liquid fluorocarbon. Small pulmon-
ary shunts were, however, detected in several dogs during exposures to
4-6Gy when breathing fluorocarbon. These small shunts were presumably
due to blood perfusing poorly ventilated regions in the superior lung,
since the oxygen saturation of blood sampled from a vein draining the
dependent left lung in these dogs remained at 100% throughout the expo-
sures. The specific gravity of fluorocarbon (1.76) is greater than that
of blood and other tissues (approximately 1.0), and thus pulmonary blood
flow may have shifted to superior portions of the lung, while concomi-
tantly, the heavier fluorocarbon may have preferentially ventilated the
dependent regions.

The results of oxygen saturation measurements and computed phys-
iological shunts in a total of 14 liquid-breathing animals described in
this section and in Section IV, are presented in Figures 9,10 and 11.
The number of animals represented by each mean value in the plots is
shown above each data point and the standard error estimate of the mean
is indicated by the vertical bar at each point. No bar is shown by
points computed for one animal only. Multiple determinations were made
in each animal under each condition of ventilation and the means for
each animal were used to compute the means for the group.

When the dogs breathed room air in the respirator (Figure 9), the
arterial blood oxygen saturation decreased abruptly during the first
twenty seconds of exposure to +3, +4, +6, or +7Gy followed by a less
rapid decrease during the remainder of each exposure. Systemic shunts
of greater than 50% were computed for 20 seconds or longer exposure to
either +6 or +7Gy. The greater decrease in oxygen saturation of pul-
monary vein blood sampled from the left, dependent lungs at comparable
times indicated that the venous-to-arterial shunting occurred in the
dependent lung. Similar results have been reported in previous studies
in this laboratory (3).

31
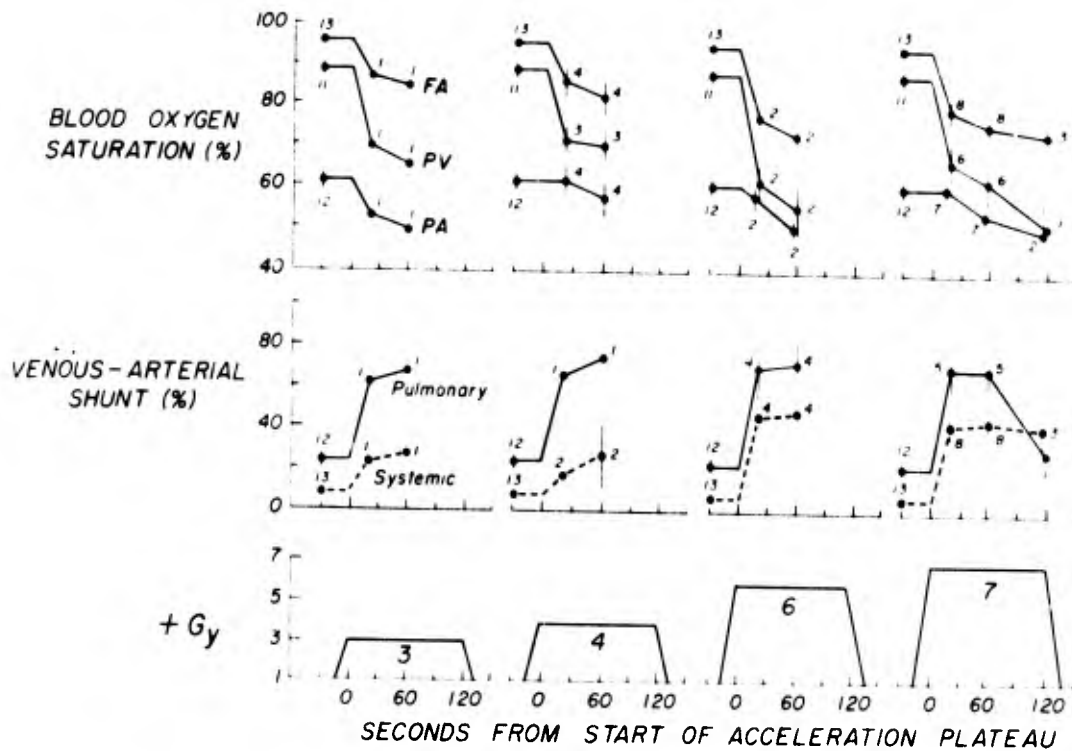
Figure 9. Blood oxygen saturation and physiological venous-arterial
shunts in dogs exposed to increased force environments
breathing air in water-immersion respirator. Left decub-
itus position; morphine-pertobarbital anesthesia. Each data
point is the mean computed for number of dogs shown at each
point. Vertical bar is standard error estimate of mean for
more than one dog. Multiple determinations were usually
made in each animal under each set of conditions, and the
mean for each dog was used to compute the means where more
than one dog is indicated. FA, PV, and PA are oxygen satur-
ation values in percent, measured by cuvette oximetry in
blood continuously withdrawn from catheters positioned in
the abdominal aorta (or femoral artery), a pulmonary vein
draining the dependent left lung and main pulmonary artery,
respectively. Values were determined from computer-generated
plots, such as illustrated in Figure 8, for the control peri-
od and at 20 to 60 seconds after the start of the acceler-
ation plateau. Most exposures lasted 60 seconds, but some
animals were exposed for 120 seconds (for pulmonary blood
flow determinations), as indicated.

Systemic venous-arterial physiological shunt is the fraction (in
percent) of systemic arterial blood which was not oxygenated after trav-
ersing the pulmonary circuit. Systemic shunt values were determined
from the relationship:

32

$$\frac{\dot{Q}_S}{\dot{Q}_T} = \frac{97.5 - FA}{97.5 - PA}$$

where $\frac{\dot{Q}_S}{\dot{Q}_T}$ is the ratio of shunt flow, $\dot{Q}_S$, to the total pulmonary flow, $\dot{Q}_T$; FA and PA are oxygen saturations in percent of systemic arterial and mixed venous blood, respectively; 97.5 is the assumed percent oxygen saturation of pulmonary blood which has perfused alveoli ventilated with room air.

Pulmonary venous-arterial physiological shunt is the fraction (in percent) of blood sampled from the pulmonary vein catheter which was not oxygenated after traversing the capillary bed. The size of the shunt depends upon the particular region of the lung from which venous blood was sampled. Pulmonary shunt values were determined from the relationship

$$\frac{\dot{Q}_S'}{\dot{Q}_T'} = \frac{97.5 - PV}{97.5 - PA}$$

where $\frac{\dot{Q}_S'}{\dot{Q}_T'}$ is the ratio of shunt flow, $\dot{Q}_S'$, to the total flow, $\dot{Q}_T'$, in the vein at the tip of the sampling catheter; PV is the percent oxygen saturation of blood sampled from the pulmonary vein; PA and 97.5 were defined earlier. Shunt values of less than 20-25 percent are probably not significant (3). Note the abrupt decrease in blood oxygen saturation during the first 20 seconds of each exposure, followed by a less rapid decrease during remainder of the exposure. The greater decrease in oxygen saturation of pulmonary vein blood sampled from the left dependent lung at comparable times indicates that most of the physiological shunting occurred in the dependent lung.

As shown in Figure 10, when the dogs breathed 100% oxygen in the respirator during exposures to similar force environments, the decrease in arterial blood oxygen saturation was less abrupt, and the computed systemic shunt was smaller than when the dogs breathed room air during these exposures.

BLOOD OXYGEN SATURATION (%)

VENOUS-ARTERIAL SHUNT (%)

+ G_y

SECONDS FROM START
OF ACCELERATION PLATEAU
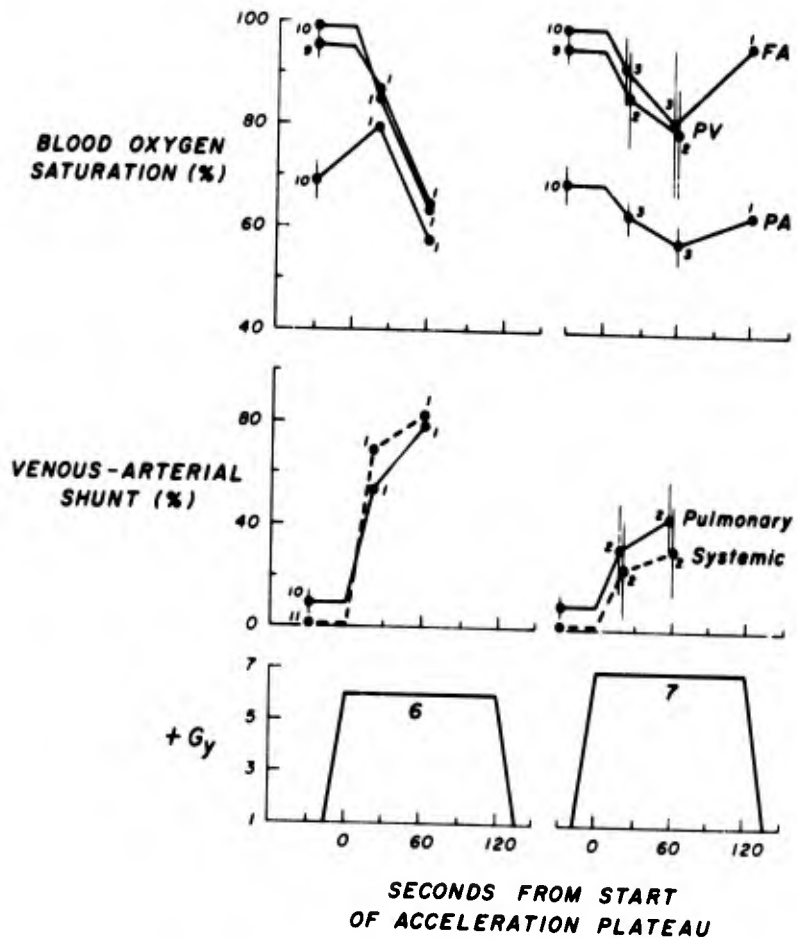
Figure 10. Blood oxygen saturation and physiological venous-arterial shunts in dogs exposed to increased force environments, breathing 99.6 percent oxygen in water-immersion respirator, left decubitus position; morphine-pentobarbital anesthesia. See legend of Figure 9 for details. When breathing oxygen, the decrease in arterial blood oxygen saturation was less abrupt and the physiological systemic shunt was smaller than in dogs breathing air during comparable exposures to increased force environments.

Ventilation with oxygenated FC 80 fluorocarbon (Figure 11) demonstrated even smaller decreases in arterial blood oxygen saturation as well as smaller decreases in saturation of mixed venous and pulmonary vein blood during exposures to comparable force environments.

34
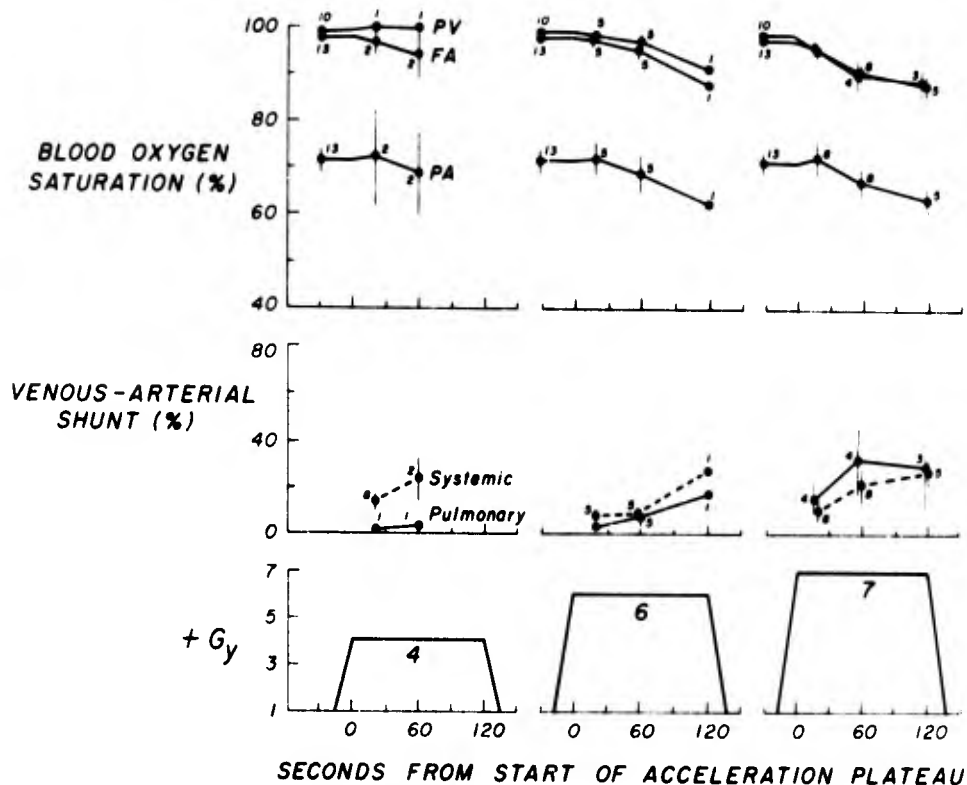
Figure 11. Blood oxygen saturation and physiological venous-arterial
shunts in dogs exposed to increased force environments and
breathing FC80 liquid fluorocarbon. Decreases in blood
oxygen saturation produced by exposure to increased force
environment were smaller than the decrease produced by com-
parable exposures when breathing air or oxygen. Pulmonary
shunt values were less than systemic shunt values at corres-
ponding times during exposures to +4Gy indicating that the
small shunts that did occur were produced by pulmonary
blood perfusing poorly ventilated regions in the upper parts
of the lung.

During the control period prior to rotation of the centrifuge, the
oxygen saturation values were higher in mixed venous blood than when
the dogs breathed 100% oxygen. Pulmonary shunt values were less than
systemic shunt values at corresponding times during exposures to +4Gy
and +6Gy, indicating that the small shunts that did occur were produced
by pulmonary blood perfusing poorly ventilated regions in the upper
parts of the lung. In the five dogs exposed to +7Gy for 120 seconds, the
pulmonary shunt was larger than the systemic. However, blood flow in
the pulmonary vein catheter blocked in two of these animals, and in one

35

of the other three dogs in this group, the pulmonary vein blood remained 100% oxygenated throughout the 120-second exposure. In the other two dogs, the pulmonary vein blood was slightly less well saturated with oxygen than the femoral artery blood, indicating venous-arterial shunting in the particular region of the lung from which venous blood was being sampled by the catheter. Variation between animals in the vertical position of the pulmonary vein-sampling catheter could account for a large part of the variability in the calculated pulmonary shunt values obtained. In each of the three plots, venous-arterial shunt values of less than 20-25% are probably not significant (3).

The data used in the plots of Figures 9,10, and 11 are shown in Table IV (See Appendix).

The inertial effects of acceleration on the chest wall, thoracic contents, and abdomen were reversed when the animal breathed fluorocarbon, compared with air, as illustrated in Figure 12.

THORACIC ROENTGENOGRAMS DURING RESPIRATION WITH AIR (A,C) AND LIQUID FLUOROCARBON (B,D)
(Dog 14.5 kg, Morphine-Pentobarbital Anesthesia, Water Immersion Restraint)
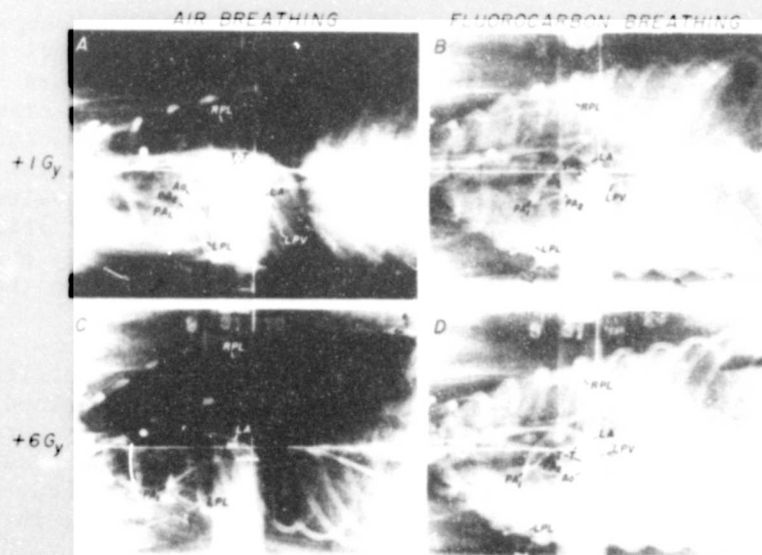
Figure 12. Comparative thoracic roentgenograms of a dog under morphine-pentobarbital anesthesia with controlled respiration in a water-immersion restraint system, breathing air at 1G and during exposure to +6Gy (left upper and lower panels,

respectively), and breathing liquid fluorocarbon under the same conditions (right panels).

Note that the heart shadow is less radiopaque than the more dense fluorocarbon liquid (specific gravity: 1.76). The heart is "floating" at about midchest level (right upper panel) at 1G instead of being displaced towards the dependent border of the thorax as normally occurs (left upper panel).

The 6-fold exaggeration of this condition during the exposure to +6G$_y$ results in severe overexpansion of the superior (right) and concomitant partial collapse of the dependent (left) lung when breathing air (left lower panel). This situation is prevented when the lungs are filled with a practically incompressible liquid. Since in this instance the liquid is more dense than the heart and blood, the heart actually "floats" upwards into the right hemithorax during the exposure to +6G$_y$ (right lower panel), so that the dependent (left) lung is somewhat overexpanded. See legend 6 for definition of symbols identifying positions of tips of recording catheters.

Due to the difference in specific gravity between fluorocarbon and blood and other tissues, the diaphragm and heart floated upward during exposures to centripetal acceleration, and the lower chest wall curved downward, as the roentgenogram illustrates.

Preliminary determinations of the pleural pressure relationships in these animals indicate that the gradients in pleural pressure in air-breathing dogs were about 0.7 cm H_2O/cm/G, and that in dogs breathing liquid fluorocarbon with a specific gravity of 1.76, the pleural pressure gradients were 1.0 cm H_2O/cm/G or slightly greater.

In summary, blood oxygen saturation measurements in dogs exposed to +1G$_y$ and +6-7G$_y$ under three conditions of restraint; viz., immersed in air and spontaneously breathing air, immersed in water and breathing air, and immersed in water and breathing oxygenated liquid fluorocarbon, indicate that decreases in oxygen saturation due to transverse acceleration cannot be significantly minimized by improved external restraint alone, but a combination of external body support and internal support of the lung by a respirable liquid can prevent significant alterations in arterial blood oxygen saturation due to acceleration. We described a technique for ventilating dogs for a number of hours with liquid fluorocarbon, at normal body temperature, at respiratory rates between 4 and 6 per minute, while maintaining normal and controllable blood P_{CO_2} and P_{O_2} tensions, with 100% saturation of systemic arterial blood without signs of respiratory distress. The capability of maintaining arterial P_{CO_2} at normal and below normal levels (16 to 40 mm Hg,

37

depending on respiration rate) with this system was somewhat surprising, since a major problem in liquid-breathing studies reported by others has been the accumulation of carbon dioxide in the blood (8,9). Partial closure of the airways during expiration was a major problem with earlier methods investigated, and probably will be a potential problem in all methods of liquid ventilation. Metabolic acidosis occurred in all dogs shortly after switching to liquid breathing for reasons which are not clear.

Theoretically, liquid respiration can protect the lung against adverse effects of extremely high acceleration (6), and may some day offer a practical solution to problems of decompression presently encountered in deep sea diving with gaseous respiration (7,8,9).

References

1. Nolan, A. C., et al. Decreases in arterial oxygen saturation and associated changes in pressures and roentgenographic appearances of the thorax during forward ($+G_y$) acceleration. Aerosp. Med. 34:797-813 (1963).

2. Banchero, N., et al. Effect of transverse acceleration on blood oxygen saturation. J. Appl. Physiol. 22:731-739 (1967).

3. Vandenberg, R. A., et al. Regional pulmonary arterial-venous shunting caused by gravitational and inertial forces. J. Appl. Physiol. 25(5):516-527 (1968).

4. Minnesota Mining and Manufacturing Co. Technical bulletin, "Fluorinert" brand electronic liquids. 3M Company, St. Paul, Minn. (1965).

5. Wood, E. H., et al. Scintiscanning system for study of regional distribution of blood flow. SAM-TR-70-6, Feb., 1970.

6. Coburn, K. R., P. H. Craig, and E. L. Beckman. Effects of positive G on chimpanzees immersed in water. Aerosp. Med. 36:233-245 (1965).

7. Gollan, F., and L. C. Clark. Prevention of bends by breathing an organic liquid. Trans. Assoc. Am. Physicians LXXX:102-110 (1967).

8. Kylstra, J. A., V. Paganelli, and E. H. Lanphier. Pulmonary gas exchange in dogs ventilated with hyperbarically oxygenated liquid. J. Appl. Physiol. 21:177-184 (1966).

9. Clark, L. C., Jr., and F. Gollan. Survival of mammals breathing organic liquids equilibrated with oxygen at atmospheric pressure. Science 152:1755-1756 (1966).

SECTION III

Respiratory Variations in Left Ventricular Stroke Volume
During Liquid Breathing

Introduction

The previous study demonstrated that when dogs breathed oxygenated
liquid fluorocarbon in a water-immersion respirator, the oxygen satura-
tion of blood continuously withdrawn from the thoracic aorta and from
a vein draining the dependent lung was maintained at 100%. However, the
oxygen saturation in mixed systemic venous blood varied in an approxi-
mately sinusoidal manner with the same frequency but not in phase with
respiration. As discussed previously, these variations were thought to
be caused by changes in cardiac output consequent to the sinusoidal
changes in external and internal body pressures produced by the respira-
tor. The purpose of the present investigation was to study the beat-
to-beat changes in left ventricular stroke volume in relation to the
phase of respiration in a dog breathing first air, then oxygenated liq-
uid fluorocarbon in a water-immersion respirator providing control of
respiration rate, tidal and residual lung volumes.

Methods

Nine weeks prior to this study, a dual-channel square-wave elec-
tromagnetic flowmeter (Carolina Medical Electronics model 322) was
implanted around the root of the aorta of a 13.5 kg dog, and eight.
weeks prior to this study, complete heart block was produced in this
animal by formaldehyde injection into the A-V bundle by a percutaneous
technique (1). On the day of the study, catheters were introduced per-
cutaneously into the main pulmonary artery, aorta, right atrium, right
ventricle and right and left pleural spaces for recording pressures and
for sampling. A catheter was placed in the inferior vena cava for rein-
fusion of blood withdrawn through the cuvette oximeters. The right
atrial and right ventricular catheters also incorporated electrodes for
electrical pacing of the heart in addition to their use for pressure
recording. The positions of most of the catheters and the flowmeter
probe are shown in the lateral roentgenogram in the left-hand panel of
Figure 2.

The dog was then positioned on its right side in the initially
dry water-immersion respirator illustrated in the schematic drawing
of Figure 1. The location on the animal's body surface of the flow-
meter electrical connector prevented us from placing the dog in the
left lateral position as in the other studies of this report. All cath-
eters were filled with heparinized Ringer's solution and were connected

Preceding page blank

via individual ports in the side of the immersion tank to strain-gauge manometers mounted outside the tank at approximately midchest level of the dog. This level, determined from P-A roentgenograms, was used as the zero-pressure reference for all manometers. The vertical distances of the pleural and esophageal catheter tips relative to the midlung level were measured from biplane roentgenograms, and these distances were used to correct the pleural and esophageal pressures to their respective catheter-tip levels (2).
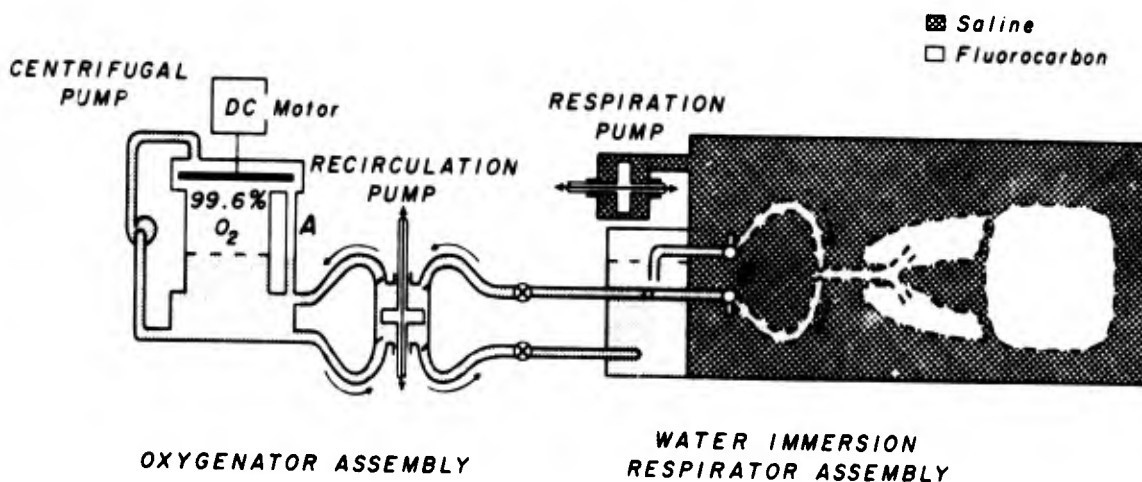
Figure 1. Diagram of water-immersion respirator and fluorocarbon oxygenator assembly used for liquid-breathing experiments.

The dog, who is completely immersed in isotonic saline, is represented by a diagrammatic sketch of fluorocarbon-filled lungs and a blank space for the remainder of his body.

The respirator-oxygenator assembly shown in Figure 1 was modified from the one described previously. The breathing compartment was divided by a vertical baffle into partially separate inhalation and exhalation chambers to minimize venous admixture in the fluorocarbon. The recirculation pump replenished the inhalation chamber with freshly oxygenated fluorocarbon and transferred exhaled fluorocarbon to the oxygenator. Before the animal was switched to liquid ventilation, a known quantity of fluorocarbon was added to the oxygenator, a shunt was opened between the inhalation and exhalation lines near the externally mounted valves (B), and oxygenated fluorocarbon was circulated by the pump to fill the system up to valves (B). Fluorocarbon was added to the system as necessary to adjust the liquid levels in the oxygenator and breathing compartment to the midthoracic level of the animal. The shunt was

then closed. After the animal was switched to liquid ventilation via valves (B), fluorocarbon was added to the oxygenator to maintain the liquid levels in the various compartments coincident with the midthoracic level of the animal. Thus, the amount added was equal to the quantity of fluorocarbon contained in the lungs and the inhalation and exhalation lines on the animal side of the valves (B). The liquid levels in the oxygenator were read on the indicator (A), a thin-walled Lucite pipe calibrated in liters of liquid contained in the oxygenator reservoir. Liquid levels were maintained at midthoracic level by periodically stopping the recirculation and respiration pumps, the latter in the full expiratory position, and allowing the levels to equilibrate by passive flow through the check valves in the recirculation pump. Tidal volume was read directly from calibrated scales attached to both chambers of the Lucite breathing compartment.

Baseline measurements of oxygen saturation, blood gas tensions, cardiac output, left ventricular stroke volume, pressures, and other data were first obtained with the dog breathing air spontaneously. The immersion tank was then filled with isotonic saline at 37°C, and the volume of saline adjusted until the variations in tank pressure produced by the respiration pump were balanced around zero, measured at midchest level. All measurements were repeated with the dog immersed and mechanically ventilated with room air at approximately ten to twelve 320-ml breaths per minute. The animal was next ventilated with 100% oxygen for 10-15 minutes to remove nitrogen from the respiratory tree and body tissues before connecting the animal's airway to the breathing compartment containing oxygenated liquid fluorocarbon at 37°C. The respiration rate was reduced to approximately three to four 480 ml breaths per minute and the liquid breathing studies performed. The water-immersed dog was also subjected when breathing first air and then fluorocarbon to 1 - minute exposures to $-4G_y$ and $-7G_y$ force environments produced by the human centrifuge, but the results of these experiments will not be reported here.

Oxygen saturation was measured in blood continuously sampled from the pulmonary artery and femoral artery by withdrawal through cuvette oximeters. Cardiac output was measured with the indocyanine-green-dye technique at different phases of respiration, and these values were used to calibrate the flowmeter when the dog breathed room air spontaneously at the start of the study. The oximeter and densitometer signals were digitized and analyzed by an on-line CDC 3300 digital computer by techniques previously described (2). The flowmeter signal, all strain-gauge data, pneumotachograph signal, ECG, respiration pump displacement, cuvette and densitometer signals, and other variables were recorded in parallel on digital tape, analog tape, and two paper photokymographic recorders. Blood and liquid fluorocarbon gas tensions were measured periodically with an Il-113 blood gas analyzer. The heart was electronically paced at 140 beats-per-minute with an A-V delay of 100 milliseconds throughout the study.

Anesthesia was maintained during all surgical and experimental procedures with sodium pentobarbital and morphine.

THORACIC ROENTGENOGRAMS SHOWING POSITION OF
SENSING DEVICES FOR BREATHING LIQUID FLUOROCARBON

(13.5 kg Dog, Right Decubitus Position,
Morphine - Pentobarbital Anesthesia)
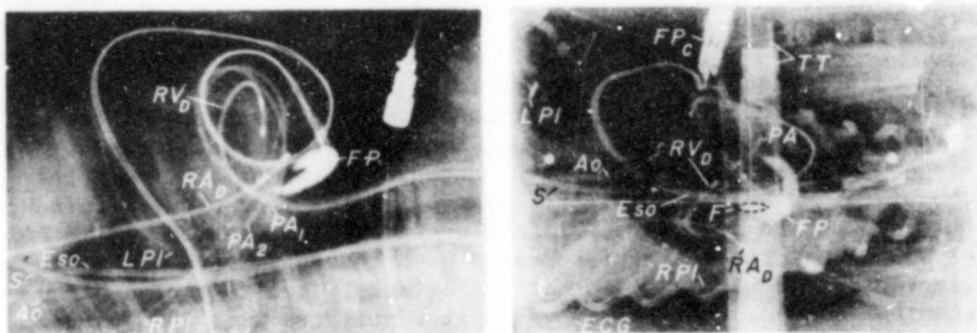
Figure 2.   Lateral roentgenogram before beginning of liquid breathing (left) and dorsal-ventral roentgenogram during liquid breathing (right). FP and FP_c; electromagnetic flow probe chronically implanted around ascending aorta, and its cutaneous connector, respectively. RV_D and RA_D; electrode catheters with tips positioned in right ventricular outflow tract and in right atrium near the superior caval orifice, respectively, for control of heart rate and atrial-ventricular systolic interval. LPl and RPl catheters with tips positioned in pleural space at left superior and right dependent margins of lungs, respectively. PA_1 and PA_2 catheters with tips positioned in pulmonary artery. ECG; electrocardiographic leads. TT; bilateral fluid-filled tubes with menisci (F) at mid-lung level for recording this zero-reference level for each strain gauge-catheter manometer system by connecting each gauge via its respective remotely controlled 3-way stopcock to this hydraulic pressure reference system. Note in the right panel that: 1) the lung fields appear as lighter areas in relation to the darker silhouette of the heart, which is less dense than the fluorocarbon-filled lungs; 2) the dark margin between the superior border of the lungs and the parietal margin of the thoracic wall caused by pleural fluid displaced upward by the heavier fluorocarbon-filled lungs.

44

The sterile pleural effusion present in this dog was a non-infectious reaction to the implanted flowmeter.

Results

Left ventricular stroke volume was calculated from the flowmeter signal by an on-line CDC 3300 digital computer and the beat-to-beat values were plotted versus time by a computer-driven incremental plotter (Calcomp) along with concomitant measurements of intrathoracic pressures and other variables.

COMPUTER-GENERATED PLOTS OF LEFT VENTRICULAR
STROKE VOLUME AND RESPIRATORY PRESSURES
DURING AIR AND LIQUID BREATHING

(13.5 kg Dog, -1 Gy, Morphine-Pentobarbital Anesthesia)
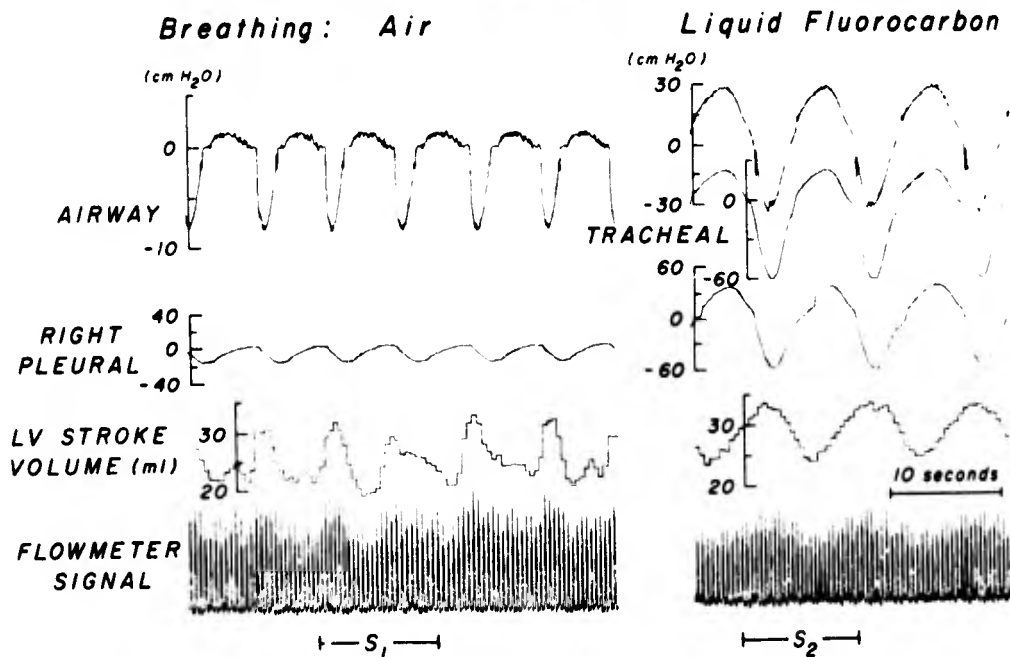
Figure 3. Computer-generated plots illustrating the phasic relationships between the respiratory cyclic changes in airway and pleural pressures generated by the water-immersion respirator and the associated variations in left ventricular stroke volume. S1 and S2 indicate the time intervals in their recordings, tracings from which are displayed on a faster time base in Figure 4.

The left-hand panel of Figure 3 is an example of one such computer-generated plot of stroke volume, right pleural pressure, and airway pressure obtained during an experiment in which the water-immersed dog was ventilated with room air. The right-hand panel of Figure 3 is a similar plot obtained during a liquid-breathing experiment.

The plots of left ventricular stroke volume versus time were approximately sinusoidal and synchronized with respiration (9-10 per minute when breathing air, and 3-4 per minute when breathing liquid fluorocarbon), as illustrated in Figure 4. Maximum stroke volume occurred soon after the start of the inspiratory phase when the dog breathed air, and just prior to full inspiration when the dog breathed fluorocarbon. The average stroke volume was approximately 1/3 greater, and the peak-to-peak changes in stroke volume were roughly twice as great, comparing plots and air-breathing experiments, respectively.

COMPUTER-GENERATED PLOTS OF
AORTIC FLOW PULSES AND RESPIRATORY PRESSURES
DURING AIR AND LIQUID BREATHING

(13.5 kg DOG, -1Gy, MORPHINE-PENTOBARBITAL ANESTHESIA)

Breathing Air

AIRWAY

RIGHT
PLEURAL

AORTIC FLOW
PULSES

LV STROKE
VOLUME (ml)

Breathing Liquid Fluorocarbon

AIRWAY

RIGHT
PLEURAL

AORTIC FLOW
PULSES

LV STROKE
VOLUME (ml)
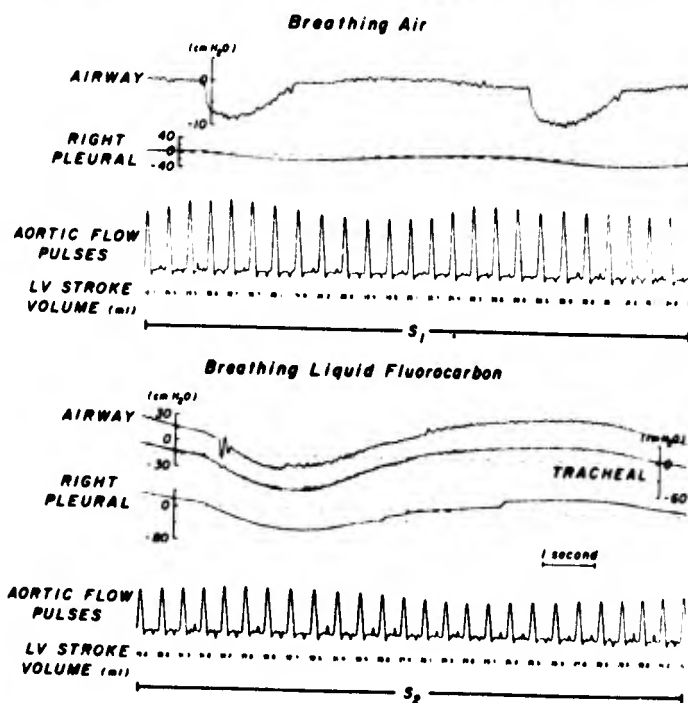
Figure 4. Computer-generated plots of aortic flow pulses and respiratory pressures during air and liquid breathing. See legend of Figure 3 for additional details.

46

Figure 5 is a plot of right (dependent) and left (superior) pleural pressures, and pressures in the esophagus measured at the respective catheter tips during maximum expiration versus the vertical distance of the catheter tip from the midlung level. During both air-breathing and liquid-breathing experiments, the pressure in the superior pleural space was more negative than in the dependent space. However, when breathing air, the vertical gradient in the pleural pressures averaged 0.49 cm H_2O/cm, a value consistent with results from previous studies in air-breathing dogs and chimpanzees measured in this laboratory (2); whereas, during liquid breathing, the gradient was nearly 1.0, a value which would be predicted from hydrostatic principles if the catheter tips were positioned at different levels in a liquid-filled container.

Important to these results, is the fact that this dog developed a chronic pleural effusion shortly after implantation of the flowmeter probe and required frequent aspirations of pleural fluid both before and during the present experiments. All of the biplane roentgenograms obtained during the present study clearly demonstrate remaining fluid in both pleural spaces which could not be completely aspirated through the pleural catheters. Possibly, the pleural pressure gradient of nearly 1.0 resulted from both catheter tips being positioned in two vertical hydraulic spaces separated only by the thin, nearly horizontal anterior and posterior mediastinal membranes. However, a pleural pressure gradient of approximately 1.0 was also found in later studies in dogs that were not known to have an abnormal amount of fluid in their pleural spaces (Section IV).

Note in Figure 5 that when the dog was ventilated with air in the respirator, the pleural pressure at midlung was about 12-13 cm H_2O negative with respect to body surface pressure during expiration, compared to about 3-4 cm H_2O negative relative to body surface pressure when the dog breathed fluorocarbon. Body surface pressure is indicated in the figure by a dashed line with a gradient of 1.0 cm H_2O/cm vertical height. During inspiration the pleural pressures were 3-4 cm H_2O negative relative to body surface pressure when the dog breathed either air or fluorocarbon. The relationships during inspiration were not plotted on this figure, but similar relationships were found in other dogs as shown in Figure 5 of Section VI.

The explanation for the large positive body surface pressure relative to the pleural pressure during expiration when the dog breathed air is as follows: The volume of saline in the respirator had been adjusted to produce equal positive and negative changes in pressure about zero, or atmospheric pressure, at midlung level. Immersion in water with the center of the thorax at atmospheric pressure was expected to produce a minimal change in residual volume of the lung from the value in the air-immersed animal (3,4). However, the fact that body surface pressures relative to pleural pressure at midlung were significantly greater during full-expiration than full-inspiration indicates that the

residual volume of the lung was appreciably less than when the animal breathed air spontaneously.

RELATIONSHIP OF PLEURAL PRESSURES TO VERTICAL HEIGHT
IN THORAX DURING WATER IMMERSION BREATHING AIR
OR BREATHING OXYGENATED LIQUID FLUOROCARBON

(13.5 kg Dog, Right Decubitus Position,
Morphine-Pentobarbital Anesthesia)
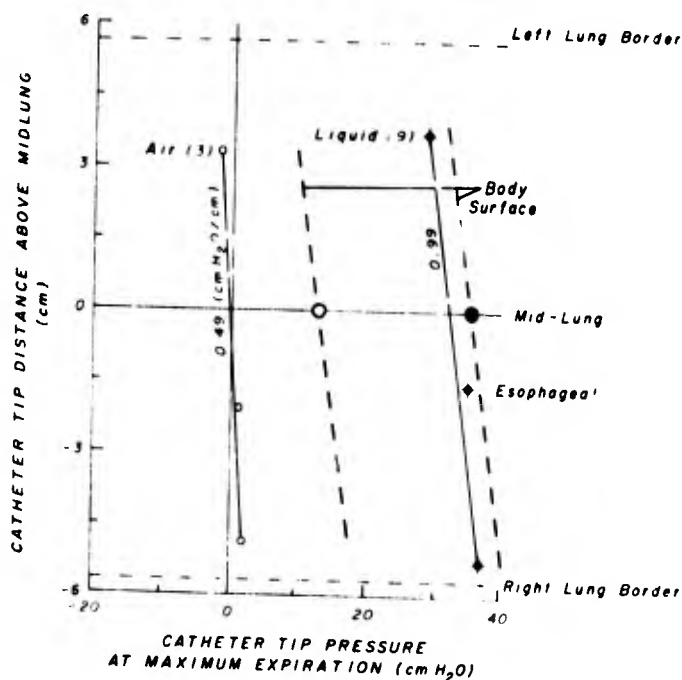
Figure 5. Relationship of pleural and esophageal pressures to vertical height in thorax when breathing first air, then oxygenated FC 80 liquid fluorocarbon in water-immersion respirator. Anesthetized dog in right decubitus position. Position of catheter tips determined from biplane roentgenograms obtained when the respiration pump was in the full expiratory position.

Expiratory reserve volume approximately 1,100 ml gas or liquid. Each determination of pressure was made from the photokymograph by averaging the pressures at maximum expiration pressure for several consecutive respiratory cycles and adjusting this average to catheter-tip level. The number of pressure determinations for aid and liquid respiration are shown in parentheses. Standard errors for air-breathing data were too small to indicate. Note the vertical gradient in pleural fluid pressures of approximately 1.0 cm H_2O/cm when breathing liquid fluorocarbon.

48

The large positive body-surface pressures relative to pleural pressure were necessarily generated as a result of the decreased compliance of the chest wall at the lower than normal residual volume. If the residual volume of the lung had been normal, the difference between body surface and pleural pressure at midlung should have been approximately the same at either extreme of the respiratory cycle and peak-to-peak changes in body surface pressure between full-inspiration and full-expiration should have been less due to the increased compliance of the chest wall at the larger thoracic volume.

Vascular pressure measurements relative to atmospheric pressure and relative to the surface of the body during spontaneous respiration with air, and ventilation with air or liquid fluorocarbon in the water-immersion respirator are summarized in the table below. All pressure measurements shown in the table were referred to midlung level. Pressures relative to the body surface were computed by algebraically subtracting body surface pressure, the pressure in the immersion tank at midchest level, from the vascular pressures measured at corresponding times.

VASCULAR AND BODY-SURFACE PRESSURES
IN WATER-IMMERSION RESPIRATOR WITH AND WITHOUT LIQUID BREATHING
(Dog, 13.5 kg, Morphine-Pentobarbital Anesthesia)

Respiration	BS* Atmos	Pressure, cm H_2O			
		Systemic Arterial		Pulmonary Arterial	
		Atmos	BS	Atmos	BS
Spontaneous					
Exp	0	177/127	177/127	35/15	35/15
Insp	0	165/117	165/117	31/11	31/11
Respirator					
Exp	13	177/124	164/111	38/21	25/8
Insp	-17	148/109	165/126	22/4	39/21
FC80					
Exp	36	156/109	120/73	76/51	40/15
Insp	-56	90/41	146/97	-11/-37	45/19

*BS = body surface. Atmos = atmospheric.

This table can be understood best when supplemented by the data presented in similar form in Tables XIV and XV (See Appendix). Table XIV gives a statistical summary of computer-processed measurements of physiological pressures and other data obtained from studies in Section VI of regional pulmonary blood flow in 7 dogs. None of the 7 had an implanted flowmeter, and all were studied in the left lateral position, but otherwise the experimental arrangement was similar to that used in the present animal. Table XV is a companion table summarizing

pressure measurements when the same 7 animals were exposed to a $+7G_y$ force environment. Although concomitant measurements of left ventricular stroke volume are not available to supplement the 7G pressure measurements, comparison of 7G and 1G pressure data is worthwhile.

The vascular pressures shown in the tables were expressed relative to atmospheric pressure and relative to body surface pressure. However, the pressures can be interpreted more readily if the pressures are also expressed relative to intrathoracic pressure by subtracting the pleural pressure at midlung from the corresponding vascular pressures. This was not done when the tables were prepared, although the pleural pressures at midlung are shown, from which the additional computations can be made. The pleural pressures at midlung were determined from the pleural pressure gradient lines illustrated in Figure 5 of Section VI. All of the data used to plot the pleural pressure graphs in this figure are also included in Tables XIV and XV.

It should be noted that the expiration and inspiration pressures (shown in the Tables) for dogs ventilated with either air or liquid in the water-immersion respirator are maximum and minimum pressures in the respiratory cycle, respectively. When the animals were ventilated with air, the maximum or minimum pressures occurred at the full-expiration or inspiration positions of the respiration pump and hence, at the same time the thorax was minimally or maximally expanded, respectively. The internal and body surface pressures generated by the respiration pump when the animal breathed air reflect mainly chest wall and immersion tank compliance and, therefore, the pressures were in phase with the displacement of the pump. However, when the dogs were ventilated with liquid, the maximum or minimum pressures were determined by the inertia a viscosity of the flowing liquid as well as by the resistance and compliance in the system. Hence, the maximum or minimum pressures occurred before the full expiration or inspiration positions of the respiration pump, and when the pump was stopped the pressures continued to change momentarily, as illustrated in the tracings of Figures 1, 2, and 3 of Section VI.

When the dogs breathed air spontaneously, aortic and pulmonary arterial pressures relative to atmosphere decreased during inspiration without change in the pulse pressures. If the aortic and pulmonary arterial pressures shown in Table XIV are expressed relative to the intrathoracic pressure environment, then the differences between inspiratory and expiratory pressures are not statistically significant. Thus, the inspiratory decrease in these pressures can be attributed to a shift in baseline due to the concomitant decrease in the intrathoracic pressure environment relative to atmosphere.

The relationships between the intrathoracic pressure, the pressure at the body surface, and atmospheric pressure were quite different when the dogs breathed air or liquid in the water-immersion respirator,

50

compared to the relationships during spontaneous respiration in air. Reference to Figure 5 of this section, to Figure 5 of Section VI, and to Table XIV (See Appendix) will clarify these relationships in what follows.

When the dogs were ventilated with air in the respirator, the pleural pressure at midlung was about -0.5 cm H_2O with respect to atmosphere when the pump was in the full-expiratory position, compared to about -18.5 cm H_2O when in the full-inspiratory position. If the vascular pressures are expressed relative to intrathoracic pressure, the respiratory changes in pulmonary arterial and aortic pressures are not statistically significant, although aortic pressures tended to be greater during inspiration.

When the dogs breathed fluorocarbon, the respiratory fluctuations in pulmonary artery pressures relative to intrathoracic pressure were not significantly different, although the pressures were consistently lower during inspiration. Comparison of expiratory and inspiratory pulmonary artery pressures between air- and liquid breathing dogs also shows no significant differences, although the inspiratory pressures in the liquid-breathing dogs were slightly lower than in the air-breathing dogs. Changes in mean left atrial pressure with respiration were in opposite directions, when measurements in air and liquid-breathing animals were compared. In the latter, the mean left atrial pressure increased from about 3.5 cm H_2O during expiration to about 6.5 cm H_2O during inspiration; and in the former, mean left atrial pressure decreased from 12.5 cm H_2O during expiration to 7.5 cm H_2O during inspiration. Mean aortic pressures relative to intrathoracic pressure significantly increased during inspiration, and the inspiratory aortic pulse pressures were about 50% greater than the expiratory pulse pressures.

Similar comments apply to the pressure data (shown in Table XV) for the animals exposed to a 7G force environment and breathing air or fluorocarbon in the respirator. When the animals breathed air, the aortic and pulmonary artery pressures were higher, but the left atrial pressures were nearly identical, comparing measurements relative to intrathoracic pressure at 7G and 1G respectively. In animals exposed to 7G and breathing fluorocarbon, the expiratory and inspiratory aortic and pulmonary arterial pressures were nearly identical with the corresponding measurements at 1G. However, the left atrial pressures were significantly higher during the 7G exposures.

Similar comments also apply to the pressure data in Tables XIV and XV, expressed relative to intrathoracic pressure, for the one dog exposed to 1 and 7G force environments and breathing silicone oil. The aortic pressures in this animal were significantly lower both at 1 and 7G than corresponding pressures in the dogs ventilated with fluorocarbon. Silicone oil is toxic and the experiment had to be terminated after 1 hour of liquid breathing because of progressive hypotension in this dog.

51

The pulmonary arterial pressures decreased during inspiration in the 1G environment but increased by a barely significant amount during inspiration in the 7G environment. Left atrial pressures were not significantly different from corresponding pressures in the fluorocarbon-breathing animals when measurements at 1G are compared, but in the 7G environment left atrial pressures in the silicone-oil-breathing dog were not as elevated compared to the average left atrial pressures in the animals ventilated with fluorocarbon.

Thus, the phasic variations in aortic and pulmonary artery pressures relative to atmosphere in dogs breathing air in the respirator, during exposures to either 1 or 7G force environments, were probably caused by changes in the intrathoracic pressure environment relative to atmosphere. The phasic variations in pulmonary artery pressure in the dogs breathing fluorocarbon during 1 or 7G exposures likewise can be attributed to this effect. However, the inspiratory increase in aortic pressure and aortic pulse pressure in the liquid-breathing dogs, and the respiratory variations in left atrial pressure in either air- or liquid-breathing animals were due to other causes than cyclic changes in intrathoracic pressure relative to atmosphere. Variations in peripheral and pulmonary vascular resistances, and variations in left and right ventricular stroke volumes and their phase relationships, are possible factors.

Mean peripheral vascular resistance can be computed by dividing systemic pressure by cardiac output measured at corresponding times. If the cardiac output measurements in the flowmeter dog are used in the computation, and if mean aortic pressure for this dog is estimated as diastolic pressure increased by one-third of pulse pressure (using the data for this dog shown in Table I), then mean peripheral vascular resistance was $89/3.3=27$ cm H_2O/L/min during expiration, and $113/4.27=27.5$ cm H_2O/L/min during inspiration. For comparison, corresponding values when the dog breathed air in the respirator were $128/3.11=41.2$ cm H_2O/L/min for expiration, and $39/3.43=40.5$ cm H_2O/L/min for inspiration. Thus, computed mean peripheral vascular resistance was nearly the same at either extreme of the respiratory cycle when the dog breathed either air or liquid fluorocarbon in the respirator, although peripheral vascular resistance was about one-third less during fluorocarbon breathing. Hence, the respiratory variations in aortic pressure when the dog breathed liquid in a normal 1G force environment can be attributed to phasic variations in left ventricular stroke volume. Presumably the same was also true for the dogs studied in Section VI during exposures to either 1 or 7G force environments.

Inferences concerning possible phasic changes in right heart output can be made by comparing intrathoracic pressures relative to the body surface at different phases of the respiratory cycle. When the animals breathed fluorocarbon in a 1G environment, the average intrathoracic pressure was about -3 cm H_2O with respect to body surface pressure during inspiration, and about -2 cm H_2O during expiration. In the same dogs exposed to 7G, the corresponding intrathoracic pressures were 0 and -5 cm H_2O. Although the respiratory changes in intrathoracic

52

pressure in the 1G environment were small and not statistically significant, the trend was consistent in the dogs breathing either silicone oil or fluorocarbon during exposures to either 1 or 7G. A decrease of approximately 1 cm H_2O in intrathoracic pressure relative to the body surface should cause a difference of about the same amount in pressure between the extrathoracic vena cava and the right atrium (5). Increased venous return to the right atrium should lead to a greater right heart stroke volume within 1-3 subsequent beats by the Starling mechanism (5,6,7,8). The increase in mean left atrial pressure during inspiration relative to intrathoracic pressure, observed in dogs breathing silicone oil or fluorocarbon during 1 or 7G force environments, may have resulted from augmented flow from the right heart. The greater left atrial transmural pressure thus produced should augment left ventricular stroke volume during inspiration, as observed in the flowmeter dog.

When animals breathed air in the respirator, the intrathoracic pressure was more negative relative to body surface pressure during the expiratory phase, in either 1 and 7G environments, due to the lower-than-normal residual lung volumes in these animals, as noted previously. The increased pressure gradient between the extrathoracic vena cava and right atrium would be expected to increase venous return to the right atrium, which in turn should be followed by increased right heart output during expiration. However, as shown in Tables XIV and XV, left atrial pressure relative to intrathoracic pressure was greatest near full inspiration, and if the flowmeter measurements in the one animal were typical for the others, left ventricular stroke volume was greatest at the start of inspiration. The combined flowmeter and pressure data suggests that respiratory changes in right and left heart outputs were out of phase when the dogs breathed air in the respirator. Out-of-phase changes in right and left heart outputs would imply that during expiration either the greater right than left ventricular output temporarily increased the pulmonary blood volume until the start of inspiration, or the greater venous return to the right heart during expiration resulted in an increased residual volume of the right ventricle. An overdistended right ventricle and a volume-limiting pericardium can produce a decrease in left ventricular output (9) which would persist for a few beats, in this situation, until the large difference in body surface-intrathoracic pressure causing the increased venous return is decreased by the start of inspiration.

One might predict that if the dogs had been ventilated with a normal residual lung volume when breathing air in the respirator, the postulated out-of-phase changes in right and left heart stroke volumes would not have been observed.

Although the mechanisms are speculative, the results of this study indicate that the phasic variations in body surface pressures and concomitant transmitted changes in intrathoracic airway and other internal

53

body pressures required to maintain adequate respiratory gas exchange with liquid fluorocarbon, produce large variations in cardiac output which are reflected by variations in the oxygen contents of mixed venous blood.

References

1. Williams, J. C. P., E. H. Lambert, and J. L. Titus. Use of intra-cardiac A-V nodal potentials in producing complete heart block in dogs. J. Appl. Physiol. 27:740-744 (1969).

2. Wood, E. H., et al. Scintiscanning system for study of regional distribution of blood flow. SAM-TR-70-6, 1970.

3. Jarrett, A. S. Effect of immersion on intrapulmonary pressure. J. Appl. Physiol. 20(6):1261-1266 (1965).

4. Craig, A. B., Jr., and D. E. Ware. Effect of immersion in water on vital capacity and residual volume of the lungs. J. Appl. Physiol. 23(4):423-425 (1967).

5. Opdyke, D. F., et al. Study of simultaneous right and left atrial pressure pulses under normal and experimentally altered conditions. Am. J. Pnysiol. 154:258-272 (1948).

6. Brecher, G. A., and C. A. Hubay. Pulmonary blood flow and venous return during spontaneous respiration. Circ. Res. 3:210-214 (1955).

7. Berglung, E. Ventricular function. VI. Balance of left and right ventricular output: Relation between left and right atrial pressures. Am. J. Physiol. 178:381-386 (1954).

8. Sealy, R. D. Dynamic effect of inspiration on the simultaneous stroke volumes of the right and left ventricles. Am. J. Physiol. 154:273-280 (1948).

9. Shabetai, R., et al. Pulsus paradoxus. J. Clin. Invest. 44(11):1882-1898 (1965).

SECTION IV

Effects of +Gy Acceleration on the Regional Distribution of Pulmonary Blood Flow in Dogs Breathing Organic Liquids in a Whole-Body Water-Immersion Respirator

Abstract

Dogs were supported in the left decubitus position in a whole-body water-immersion respirator which provided control of rate, tidal and residual volumes of ventilation. Successive injections of differentially tagged microspheres ($15\pm5\mu$) were made into the right ventricle at $1G_y$ and during exposures to $7G_y$ when the dogs were being ventilated with room air, and then with an organic liquid (3M fluorocarbon, FC 80, or Dow Corning silicone oil, DC 200, 1.0 cs). The lungs were excised, inflated, dried, embedded en bloc in Styrofoam then cut into 1-cm-thick sections. Blood flow per milliliter of lung tissue was determined for each condition by computer-controlled high-resolution scintiscanning of each section. Pressures in the aorta, pulmonary artery, right and left atria, left pulmonary vein, upper airway and lower trachea, and right and left pleural spaces were recorded. Oxygen saturation of aortic, pulmonary arterial, and left pulmonary venous blood was measured continuously by cuvette oximetry. When at $1G_y$, the fraction of cardiac output traversing the left (dependent) lung was frequently less than for the right. However, fractional flow to the left lung was increased during exposures to $7G_y$ when dogs were breathing air and silicone oil (sp. gr. 1.76), as would be expected.

Introduction

We measured the distribution of pulmonary blood flow in dogs, first breathing air and then breathing either FC 80, liquid fluorocarbon (specific gravity about 1.8 (1) or silicone oil (DC 200) which has a specific gravity of 0.8 (2)). Pulmonary blood flow was measured by injecting radioactive 15-micron-diameter microspheres into the right ventricle, excising and drying the lungs which were then held inflated with air by a steady tracheal pressure of 30 cm H_2O (Figure 1). The dried lungs (left panel) were potted in a polyurethane foam block and sliced transversely on a bandsaw into 20-25 1-cm-thick sections (as shown in the right panel). The complete cephalad surface of each section was scanned to determine the blood flow per cubic centimeter of inflated lung tissue, using a high-resolution computer-controlled scintillation scanner assembly previously developed in this laboratory (3). Up to four injections of differentially tagged microspheres could be made in each dog. The spatial distribution of blood flow was determined for each injection on the basis of the different energy spectra of the respective

isotope tags. Blood flow was determined at 1 and 7G with the dog on its left side, breathing first room air and then an organic liquid.
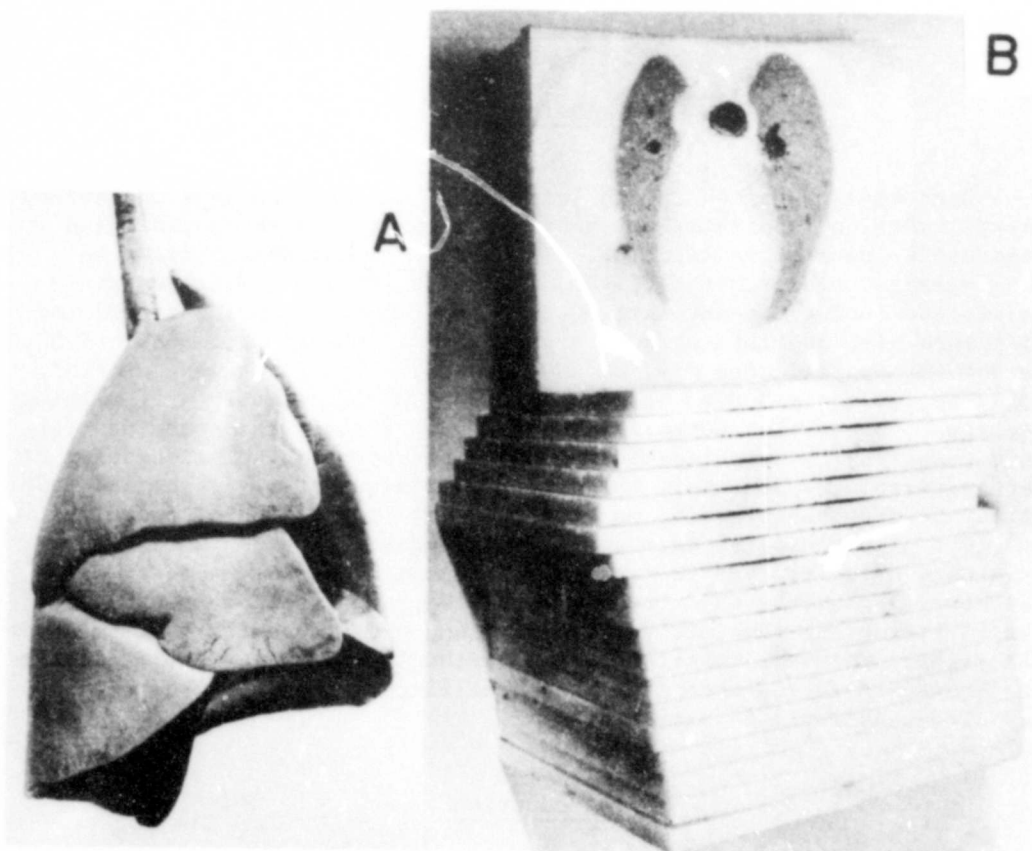
Figure 1A. Photograph of lungs resected en bloc from a dog and dried in air for several days. The lungs were held inflated while drying by a steady air pressure of 30 cm H_2O applied to the trachea.

Figure 1B. Air-dried lungs from a dog were potted in a quick-setting polyurethane foam. After curing for several days in a rectangular mold, the foam block with embedded lungs was cut by bandsaw into 20-25 1-cm-thick sections parallel to the transverse plane of the lung. The entire cephalad surface of each successive section from apices to diaphragmatic surfaces was then scanned by a computer-controlled point-to-point scanning assembly (3). The count and x, y, z coordinates at each point in the scan were stored on magnetic

56

tape, and with appropriate programs, a three-dimensional array of counts in correct anatomical relationship to the inflated lung could be reconstructed for each of the four microsphere injections for display purposes and for computing the spatial distribution of blood flow throughout the entire lung.

Methods

The animals were anesthetized with morphine and pentobarbital and prepared as described in Section II with some modifications. Briefly, saline-filled catheters were introduced into the vascular system without thoracotomy and their tips positioned with fluoroscopic and roentgenographic assistance as follows: Two catheters in the main pulmonary artery for recording pressure and for withdrawal of cuvette oximeter samples; one each in the thoracic aorta (pressure), abdominal aorta (sampling), right ventricle for injection of microspheres, right and left atria, and one in a vein draining the dependent left lung. The tip of the pulmonary vein catheter was advanced as close to the outer margin of the lung as possible without interrupting the flow of the sampled blood. Two saline-filled catheters were introduced into the left and right pleural spaces, also without thoracotomy, and their tips manipulated to the most lateral surfaces of the superior right and dependent lungs. Two saline-filled catheters were positioned in the stomach for aspiration of gas, and in the lower third of the esophagus for recording pressure. A 5/8" or 3/4" (i.d.) pliable endotracheal tube, fashioned of 1/16" wall Tygon, was inserted through a tracheotomy just inferior to the larynx. The trachea was first almost severed transversely, and the tube introduced approximately 11 cm and secured in place by umbilical tape ligatures around the outer circumference of the trachea. A "Y" breathing valve was connected to the endotracheal tube and positioned as close to the tracheotomy as possible to minimize instrument dead space. The esophagus was not ligated. One air-filled catheter fashioned of Tygon tubing was connected to a port with a Luer fitting in the crotch of the "Y" breathing valve to measure tracheal pressure. A second Teflon catheter was passed inside this tubing, through the valve, and advanced until its tip was positioned in either the inferior trachea or a main bronchus. The two concentric catheters were used for pressure recording and sampling during the liquid-breathing portion of the study; at that time both were filled with saline.

The animal was then positioned on its left side in the initially dry water-immersion respirator and the shoulder and pelvic girdles loosely secured by umbilical tape ties looped through cleats in the bottom of the tank. The inspiratory and expiratory sides of the "Y" breathing valve were then connected via 7/8" Tygon tubing to the ports of selector valves passing through the side of the tank.

57

A representative drawing of the complete water-immersion respirator and oxygenator assembly is shown in Figure 2. Figure 3 is a photograph of the actual assembly, and Figure 4 is a photograph of the oxygenator portion.
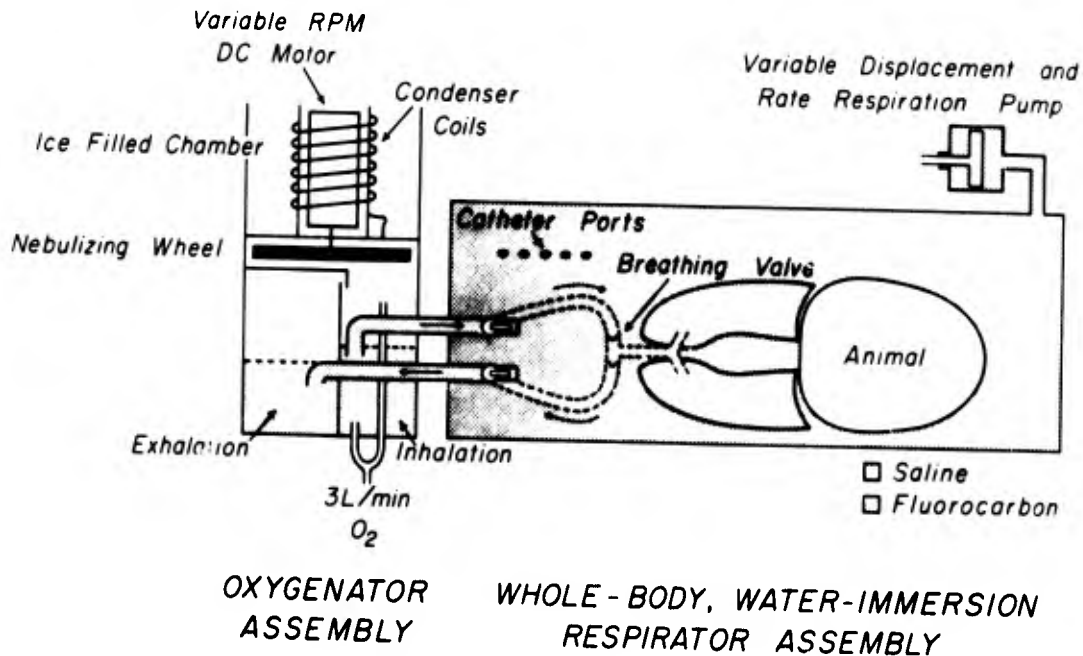
Figure 2. Schematic drawing of water-immersion respirator-oxygenator assembly. The assembly differs from those described in Sections II and III. The oxygenator and breathing compartments were combined into a single unit which was mounted in the cockpit of the centrifuge as an integral part of the respirator. As illustrated, the oxygenator reservoir was divided by a vertical baffle into separate inhalation and exhalation chambers, each capable of holding 5 liters. The liquid was fully oxygenated and carbon dioxide removal completed by continuously circulating fluorocarbon from the exhalation chamber over the nebulizing wheel to drain into the inhalation chamber. Full oxygenation of the fluorocarbon was maintained by bubbling a portion of the 3 L/min oxygen supply through the liquid. Fluorocarbon was continuously in the center of the oxygenator and driven by a shaft extension from the nebulizing wheel. An external valve controlled a shunt-flow of fluorocarbon from inhalation to exhalation chambers, to permit the fluorocarbon to recirculate over the wheel at a rate which could be varied independently of the respiratory rate of the animal. The

level of fluorocarbon in the inhalation chamber was adjust-
ed to the midlung level of the animal by adding or remov-
ing fluorocarbon from the oxygenator and by adjusting the
shunt flow. Liquid levels in each chamber were read on
scales attached to the outside of each chamber. The coils,
packed in crushed ice, condensed fluorocarbon vapor which
otherwise would have been steadily blown off by flow of
oxygen through the chamber. The condensed fluorocarbon was
returned to the inhalation chamber.
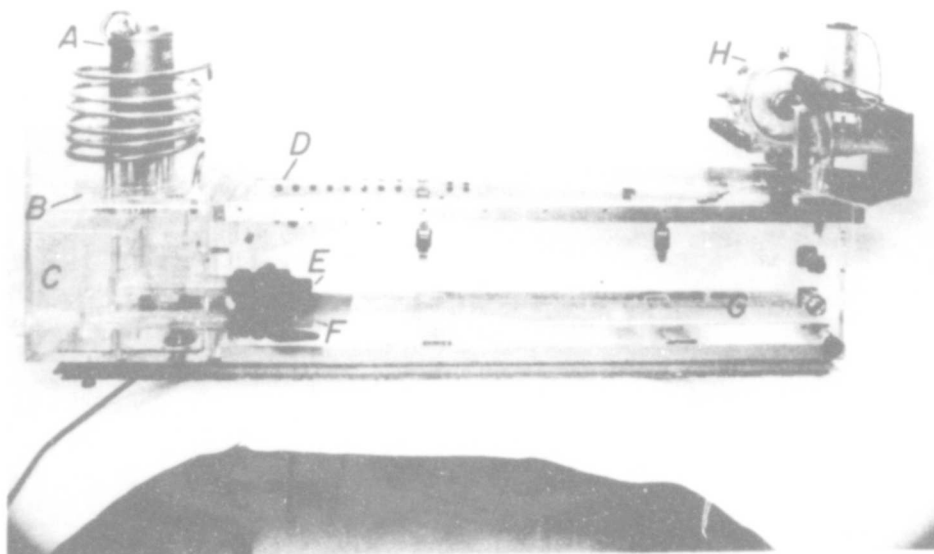
Figure 3. Photograph of the fluorocarbon oxygenator-water-immersion
respirator assembly:
(A) Variable rpm dc motor.
(B) 8-inch finned aluminum nebulizing wheel directs high
velocity spray of fluorocarbon to impact against the
four walls of the chamber. The liquid is nebulized
in a 100 percent oxygen atmosphere. Oxygen diffuses
into and carbon dioxide diffuses out of the liquid
droplets.
(C) Exhalation chamber. The valve which controls shunt
flow of fluorocarbon from inhalation to exhalation
chamber is mounted on outside wall at left end.
(D) Row of catheter ports on far side of respirator.

Selector valves connect separate inhalation and exhalation lines, respectively, to either room air or to oxygenated liquid.

(G) Lucite platform. Elevates animal so that midthoracic level coincides with longitudinal axis (marked by metallic screws) of immersion tank. Water-tight electrical connectors shown on right-end of immersion tank are for ECG leads (top) and thermistor probes (bottom) used to record rectal temperature and temperature of saline within respirator.

(H) Respiration pump. Associated Scotch yoke linkage, pump motor, and linear displacement transducer are shown.
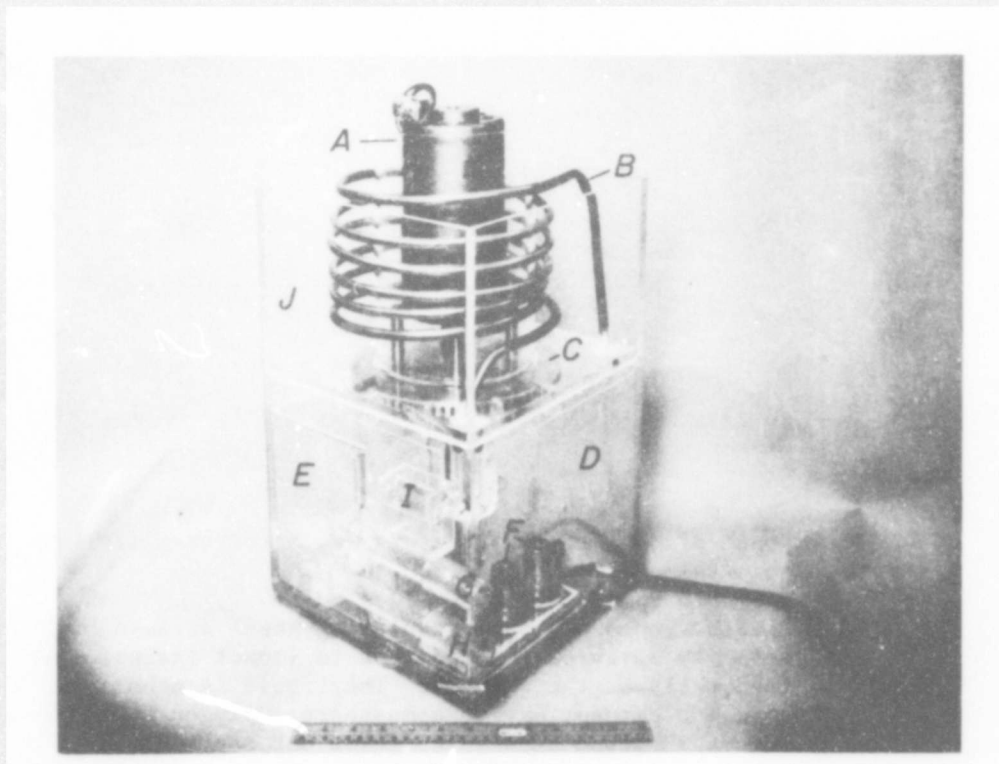
Figure 4

Fluorocarbon spinning disc oxygenator assembly for liquid-breathing studies.

(A) variable rpm dc motor
(B) fluorocarbon condensing coils
(C) atomizing disk
(D) inhalation compartment
(E) exhalation compartment

60

(F) electrical heaters
(G) inhalation line
(H) exhalation line
(I) fluorocarbon trap in oxygen vent port
(J) crushed ice compartment

The assembly (Figure 4) resulted from substantial modifications to the one described in Section II. The modifications were necessary because there were two drawbacks in the original arrangement:

1. Unavoidable spillage of fluorocarbon in the process of connecting and disconnecting the oxygenator from the cockpit assembly. Loss of fluorocarbon made it difficult to maintain an accurate record of the total volume of fluorocarbon in the system from which the volume contained in the animal's lung could be determined.

2. Venous admixture during the period when the oxygenator was disconnected. This was due to the fact that exhaled fluorocarbon was not completely separated from the inhaled fluorocarbon in either the oxygenator reservoir or the breathing compartment.

The new arrangement prevented spillage of fluorocarbon because the oxygenator was mounted in the centrifuge cockpit as an integral part of the respirator and was not disconnected at any time; moreover, venous admixture could not occur because the animal inhaled from and exhaled to separate compartments. The rate of oxygenation of the liquid fluorocarbon was increased in the new oxygenator since only 8 liters of fluorocarbon were needed in the modified system in contrast to 16 liters in the original, and the more powerful electric motor used to drive the nebulizing wheel (1 hp in the modified system versus 1/20 hp in the original) permitted a larger and continuous flow of liquid over the wheel.

The remainder of the assembly was similar to the original. The respiration pump moved saline in and out of the tank in a sinusoidal manner, and either room air or liquid flowed passively in and out of the lungs in response to the alternating positive and negative pressures applied to the body surface by the pump. The exhaled liquid was received in the exhalation compartment. A centrifugal pump, mounted in a central column in the oxygenator and driven by a shaft extension from the nebulizing wheel, pumped a steady flow of liquid from the exhalation chamber upward and over the rapidly spinning nebulizing wheel. The oxygenated liquid drained into the inhalation chamber. The level in this chamber was maintained at midchest level and the temperature of the inhaled liquid was regulated to $37° \pm 1°$ C by electrical heaters. Residual lung volume was adjusted by adding or removing saline from the immersion tank and was measured by subtracting the volume of liquid in the oxygenator and in the inhalation and exhalation lines from the total volume added to the system. The residual lung volume was established early in the

61

experiment, with the dog breathing air, by adding or removing saline to adjust the body surface pressure to balance around zero at the midchest level. The liquid-breathing portion of the study was performed without changing the residual volume.

Techniques for recording pressures, oxygen saturation, and cardiac output were as described in previous sections.

Figure 5 shows a photokymograph recording of the multiple physiological pressures and other variables measured in all dogs to illustrate the conditions under which the microspheres were injected; in this case during an exposure to a force environment of $7G_y$ when breathing air (top panel) and when breathing silicone oil (lower panel). The sinusoidal variations in the pressure traces are due to the sinusoidal alterations in body surface pressure produced by the respiration pump. The pump was stopped in the inspiratory phase of the cycle and the pressures allowed to stabilize for several seconds before the microspheres were injected. During the 7G exposures, the microspheres were injected 120 seconds after the centrifuge reached the 7G plateau.

MULTIPLE PHYSIOLOGICAL VARIABLES RECORDED DURING
EXPOSURE TO 7 G_y IN WATER-IMMERSION RESPIRATOR

(DOG 17 kg, MORPHINE-PENTOBARBITAL ANESTHESIA)

BREATHING AIR

BREATHING SILICONE OIL
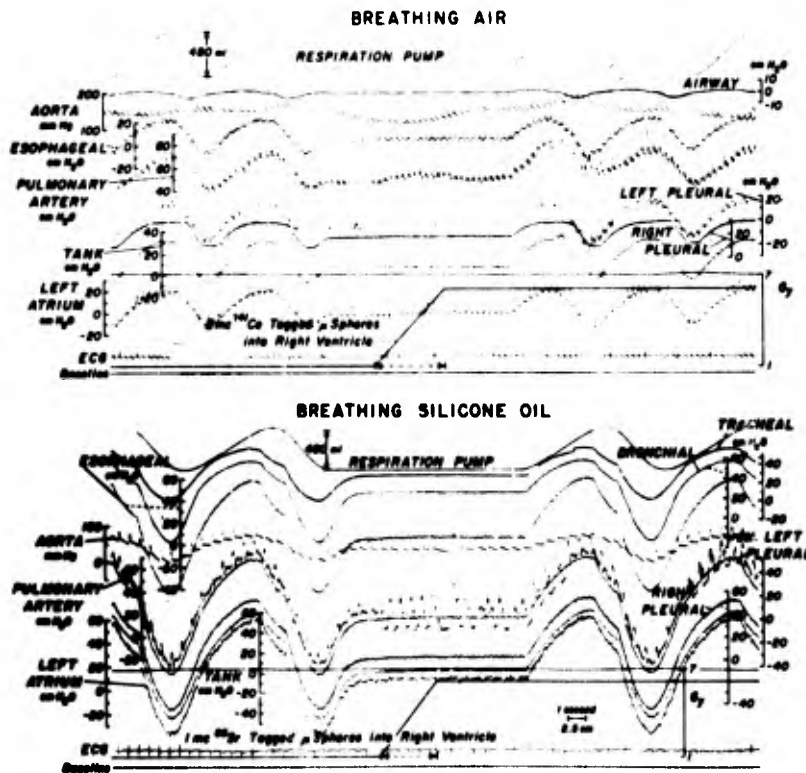
Figure 5

Figure 5. Multiple physiological pressures and other variables in a dog
exposed to +7G$_y$, first breathing air (upper panel) and then
breathing DC 200 silicone oil (lower panel) in water immer-
sion respirator. The anesthetized dog was in the left decub-
itus position. The photokymograph was generated by replay
of the analog magnetic tape which was recorded during the
experiment. For clarity, not all of the variables in the
original recording are shown. The sinusoidal variations in
all of the pressures were produced by the sinusoidal wave-
form of body surface pressure (labeled tank) generated by
the respiration pump. Two minutes after the start of the +7G$_y$
exposure, the respiration pump was stopped in the inspiratory
position and the pressures allowed to stabilize for several
seconds. The radioactive microspheres were then injected
into the right ventricle by a pneumatically driven syringe.
A linear displacement transducer coupled to the syringe bar-
rel recorded the syringe travel for timing purposes. Note
that when the dog breathed air, the body surface and inter-
nal pressures were in phase with the respiration pump. The
peak-to-peak amplitude of the body surface pressures is a
measure of the compliances of the chest wall and immersion
tank in parallel. However, when the dog breathed the consi-
derably more dense and viscous silicone oil, the internal
and body surface pressures lagged the first derivative of
pump displacement due to inertia and viscosity of the res-
pirable liquid. Pressures shown in the photokymograph can-
not be read directly but must be corrected as described in
Section VI of this report.

Figure 6 shows the window settings of the four channels of the
gamma spectrometer used to determine the count rate of each isotope
corrected for the presence of the other three. The numbers were deter-
mined by placing point sources of each isotope at the focal point of
the collimator, one at a time, and recording the normalized count rate
in each channel. For example, when a point of source of ^{51}Cr was counted,
the count rate in the ^{169}Yb channel was 0.14, in the ^{141}Ce channel 0.05,
and in the ^{85}Sr channel, 0.01 of the count rate in the ^{51}Cr channel.
The window settings were found by trial and error as those settings
which would maximize the count rate of each isotope in its own channel
and minimize the count rate in the other channels. The energy fraction
matrix was used in the computer program to solve the four simultaneous
equations necessary to determine the corrected count rate of each iso-
tope at each location in the lung scan.

One millicurie ^{169}Yb was injected when the dog breathed air at +1G$_y$;
3.0 mc ^{141}Ce when breathing air at +7G$_y$, 10 mc 51Cr when breathing liquid
at +1G$_y$; and 1 mc ^{85}Sr when breathing liquid at +7G$_y$. These activities
resulted in approximately equal total counts in the entire lung in each
of the isotope channels at most locations in the scan.

ENERGY FRACTION MATRIX

ISOTOPE	SPECTROMETER CHANNELS IN K.E.V.			
	^{169}Yb 44-58	^{141}Ce 135-154	^{51}Cr 280-326	^{85}Sr 400-650
^{169}Yb	1.00	0.15	0.16	0.03
^{141}Ce	0.04	1.00	0.00	0.03
^{51}Cr	0.14	0.05	1.00	0.01
^{85}Sr	0.16	0.04	0.06	1.00

Figure 6

Results

The three-dimensional array of counts generated by scanning the entire cephalad surface of every lung section successively from the apex to the costrophrenic angles can be displayed in any projection or section of the lung desired in correct anatomical relationship to the topography of the inflated lung.

Figure 7 is a dorsal-ventral projection of the vertical distribution of pulmonary blood flow in one dog; first (in the right panel) when breathing liquid fluorocarbon under the same conditions, right panel. The blood flow is expressed as the fraction of cardiac output per cubic centimeter of inflated lung tissue on the ordinate against vertical height above the midsagittal plane of the inflated lungs on the abscissa. The dependent left border of the lungs is plotted on the left.

COMPARISON OF EFFECT OF INCREASE IN FORCE ENVIRONMENT
ON VERTICAL DISTRIBUTION OF PULMONARY BLOOD FLOW
WHEN BREATHING AIR OR LIQUID FLUOROCARBON (FC 80)
IN WATER-IMMERSION RESPIRATOR-INSPIRATORY POSITION

(Dog 18 kg, Morphine-Pentobarbital Anesthesia, Left Decubitus Position)

Fraction of Total Blood Flow Traversing I Cubic cm of Inflated Lung Parenchyma
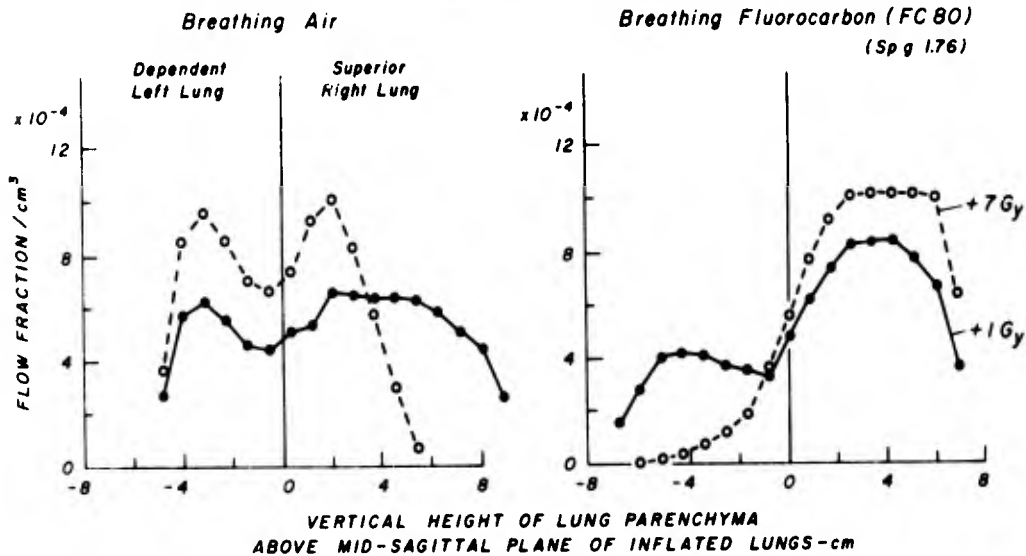
Figure 7. Comparison of effect of increase in the gravitational-inertial
force environment on the vertical distribution of pulmonary
blood flow in anesthetized left decubitus dog, first when
breathing air, and then when breathing FC80 liquid fluoro-
carbon in a water-immersion respirator. Respirator held in
full-inspiratory position during microsphere injections.
$7G_y$ injections were made 120 seconds after start of exposures.
When the dog breathed air, pulmonary blood flow was increased
in the midregions of the lung, but was increased in the supe-
rior right lung when the dog breathed fluorocarbon.

65

During the exposure to 7Gy when this dog was breathing air, blood flow to the most superior portions of the lungs was abolished, while concomitantly, the flow was relatively unchanged in the most dependent region, and was increased in the midthoracic regions of the lung parenchyma.

The results with fluorocarbon breathing were similar in all five dogs. At 1G, blood flow was greater in the superior lung and increased further to the superior and decreased in the dependent lung during the exposures to 7Gy, as would be predicted since the specific gravity of blood (1.0) is less than that of fluorocarbon (1.76).

The average and variability of changes in vertical distribution of pulmonary blood flow produced by an increase in the force environment from 1 to 7Gy in all dogs when breathing air or liquid fluorocarbon are shown as a dorsal-ventral projection in Figure 8.

COMPARISON OF EFFECT OF INCREASE IN FORCE ENVIRONMENT ON VERTICAL DISTRIBUTION OF PULMONARY BLOOD FLOW WHEN BREATHING AIR OR LIQUID FLUOROCARBON IN WATER-IMMERSION RESPIRATOR-INSPIRATORY POSITION

(Morphine Pentobarbital Anesthesia, Left Decubitus Position)

Change In Fraction of Total Blood Flow Traversing:

VERTICAL HEIGHT OF LUNG PARENCHYMA
ABOVE MID-SAGITTAL PLANE OF INFLATED LUNGS-cm
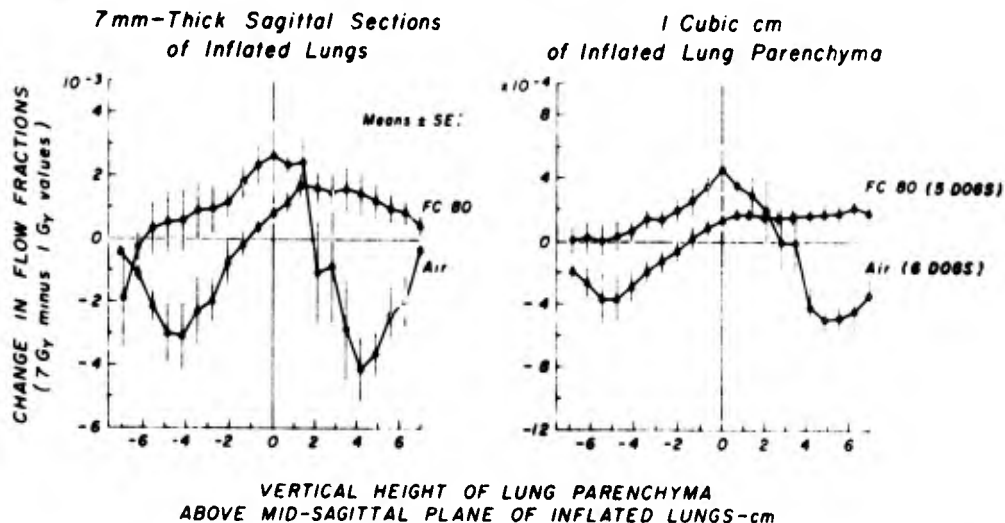
Figure 8. Comparison of effect of increase in the gravitational-inertial force environment on the vertical distribution of pulmonary blood flow in dogs breathing air or liquid fluorocarbon in a water-immersion respirator. Means and standard error of the differences between values determined in anesthetized dogs when respirator held in full inspiratory position during microsphere injections at 1 and 7Gy in left decubitus position. Note that regional pulmonary blood flow, expressed as fraction

66

of the total cardiac output, was increased to the midregions of the lung when breathing air and to the upper lung when breathing the heavier-than-blood liquid fluorocarbon.

In the left panel, the change in blood flow, plotted on the ordinate, is expressed as the fraction of cardiac output traversing successive 7-mm-thick sagittal sections of the lungs, extending from the left lateral dependent border of the lung, on the left, to the right lateral superior border of the right lung, on the right. The average change in flow per cubic cm of lung tissue in each of these cross-sections is shown in the right panel.

The changes produced by an increase in force environment when breathing air were similar to those reported previously in that, as would be expected from hydrostatic considerations based on the much greater specific gravity of blood than that of air-filled alveoli, a striking decrease in flow was observed in superior regions of the lungs. However, contrary to such considerations, no significant change was observed towards the dependent margin of the lungs in spite of the large increase in intravascular pressures present in this region, but rather the maximum increase in flow occurred in the midthoracic regions.

Filling the alveoli with a liquid of greater specific gravity than blood reversed these changes. Flow increased in the superior and decreased in the dependent lung, respectively, during an increase in the force environment.

Since silicone oil, like air, has a specific gravity less than that of blood, it might be expected that an increase in the force environment would have a qualitatively similar effect on the pattern of the vertical distribution of pulmonary blood flow when breathing these two substances. That this is not the case is illustrated by comparison of the changes in vertical distribution of pulmonary blood flow in one dog caused by an increase in force environment from 1 to $7G_y$ when breathing air and silicone oil (Figure 9).

The pattern of the decrease in blood flow to the superior lung was similar in the two instances as might be expected from hydrostatic considerations. However, in the dependent lung the vertical distribution of the change in blood flow per cubic cm of lung parenchyma was strikingly different when breathing air than when breathing silicone oil. In the latter case, flow was increased throughout the dependent lung in accord with hydrostatic considerations. In contrast, during air breathing, flow per cubic centimeter actually decreased in the most dependent two centimeters of lung parenchyma in spite of the fact that intravascular pressures were highest in this region and, if the alveoli and airways remained open, no concomitant increase in alveolar or airway pressure would be expected to counteract the increased intravascular pressures of air breathing.

67

COMPARISON OF EFFECT OF INCREASE IN FORCE ENVIRONMENT ON VERTICAL
DISTRIBUTION OF PULMONARY BLOOD FLOW WHEN BREATHING AIR OR LIQUID
SILICONE OIL IN WATER-IMMERSION RESPIRATOR-INSPIRATORY POSITION

(Morphine Pentobarbital Anesthesia, Left Decubitus Position)

Change In Fraction of Total Blood Flow Traversing:

VERTICAL HEIGHT OF LUNG PARENCHYMA
ABOVE MID-SAGITTAL PLANE OF INFLATED LUNGS-cm
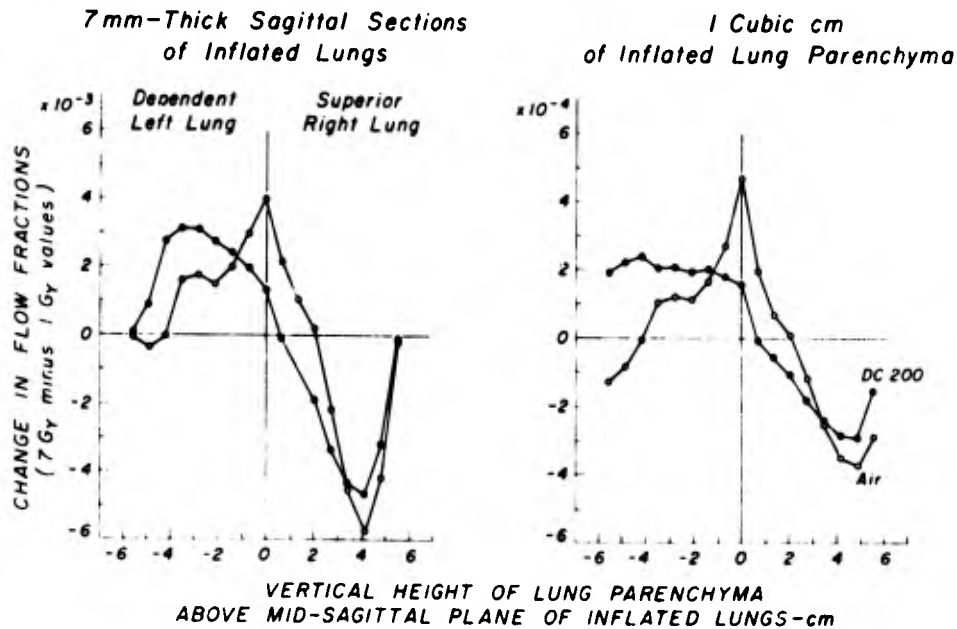
Figure 9. Comparison of effect of increase in gravitational-inertial
force environment on vertical distribution of pulmonary
blood flow in a left decubitus dog, first breathing air and
then DC 200 silicone oil in water-immersion respirator.
Differences between values determined after 120 seconds at
$7G_y$ and values at $1G_y$ are shown. Respirator held in full
inspiratory position during microsphere injections. When
the dog breathed either air or silicone oil (each less dense
than blood), flow decreased in the upper right lung. Flow
increased mainly in the midregions of the lung when the dog
breathed air, but increased in more dependent regions when
the dog was ventilated with silicone oil.

The predominant role of the specific gravity of the liquid being
breathed as a determinant of the vertical distribution of pulmonary
blood flow during liquid breathing can be illustrated by comparing the
changes in vertical distribution of blood flow caused by an increase in
force environment during breathing of a liquid with specific gravity
greater than, and one with less than, that of blood, respectively (Figure
10). As would be predicted from hydrostatic considerations, blood flow
is increased to the upper regions of the lung and decreased in dependent
regions when the alveoli are filled with a liquid, FC80 heavier than

68

blood, and the opposite effect is seen when the alveoli are filled with a liquid less dense than blood, silicone oil.

This figure illustrates that when the alveoli were filled with a liquid with a specific gravity less than that of blood and tissue, the blood flow to the superior lung decreased during an increase in the force environment, similar to the effects when breathing air. However, contrary to the results with air breathing, there was relatively little change in blood flow near the midline of the lung when breathing silicone oil, and flow was increased at all levels dependent to this point.

COMPARISON OF EFFECT OF INCREASE IN FORCE ENVIRONMENT ON VERTICAL DISTRIBUTION OF PULMONARY BLOOD FLOW WHEN BREATHING LIQUIDS OF DIFFERENT SPECIFIC GRAVITY IN WATER-IMMERSION RESPIRATOR-INSPIRATORY POSITION

(Morphine Pentobarbital Anesthesia, Left Decubitus Position)

Change In Fraction of Total Blood Flow Traversing:

7 mm-Thick Sagittal Sections of Inflated Lungs

1 Cubic cm of Inflated Lung Parenchyma

VERTICAL HEIGHT OF LUNG PARENCHYMA ABOVE MID-SAGITTAL PLANE OF INFLATED LUNGS - cm
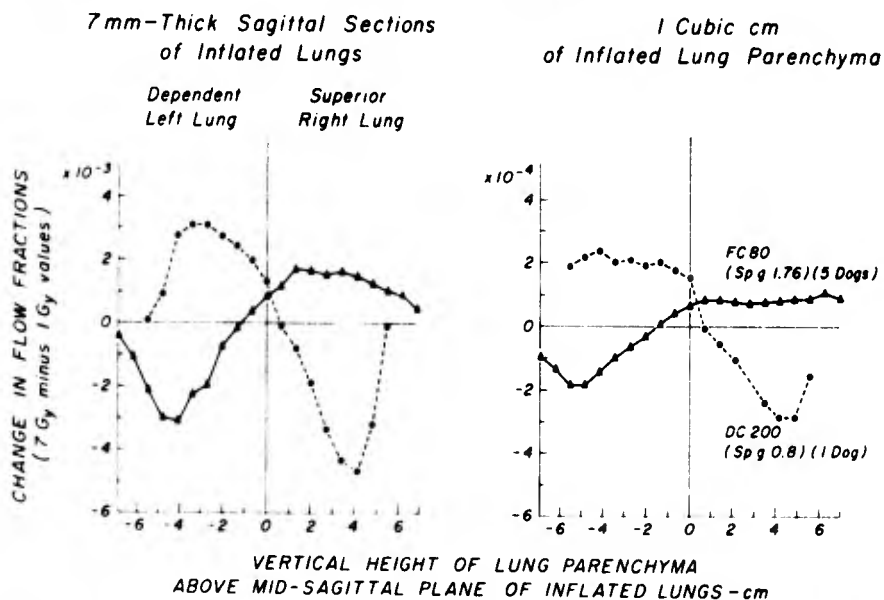
Figure 10. Comparison of effect of increase in the gravitational-inertial force environment on the vertical distribution of pulmonary blood flow in dogs breathing liquids of different specific gravity in a water-immersion respirator. Averages of differences between values determined at end-inspiration in anesthetized dogs when at 1 and $7G_y$ in the left decubitus position. Note the opposite effects of the increased force environment on regional pulmonary blood flow when the dogs were breathing these two liquids. Flow was displaced in the dependent direction when the liquid breathed was less dense than blood, and vice versa when the lungs were filled with the heavier-than-blood fluorocarbon.

69

The mechanisms which prevent an increase or cause an actual decrease in blood flow to the most dependent regions of the lung during an increase in the force environment when breathing air have not been delineated with certainty. A 100% arterial-venous shunt is a consistent finding in the most dependent regions of the lung during exposures to a force environment of 6 to 7G breathing air, and it has been postulated that the associated low oxygen and high carbon dioxide tensions may cause localized vasoconstruction in these regions (4-6). Liquid breathing greatly decreased or eliminated dependent pulmonary arteriovenous shunting during exposures to high force environments and hence the possible effects of localized changes in respiratory gas tensions on vascular resistance (7). Concomitantly, the degree of inertial displacement of the heart and lung parenchyma is greatly reduced during liquid breathing (7). The qualitative differences in the pattern of vertical distribution of blood flow in the lungs between air and liquid breathing may be due in part to the differences in gas tensions in pulmonary capillary blood and tissue as well as to the purely physical factors associated with the large differences in specific gravity and compressibility between air-containing and liquid-containing alveoli and the blood perfusing these structures under the two conditions.

The pleural fluid pressures recorded at or near the superior and dependent surfaces of the lungs when breathing air and liquids of different specific gravity are shown in Figure 11. The average vertical gradient in pleural pressure was slightly but significantly less than 1.0 when breathing air, and slightly but not significantly greater than 1.0 when breathing liquid fluorocarbon. Since the specific gravity of the thoracic contents is certainly greater than 1.0 when breathing fluorocarbon (sp gr 1.76), these results indicate that the specific gravity of the thoracic contents and the magnitude and direction of the force environment are not the sole determinants of the vertical gradient in pleural pressure.

70

Figure 11. Relationship of pleural fluid pressure to vertical height in
the thorax of anesthetized left decubitus dogs breathing first
air, and then either liquid fluorocarbon or liquid silicone
oil in water-immersion respirator. Positions of catheter tips
were determined with the use of biplane thoracic roentgeno-
grams obtained immediately after the microspheres were injec-
ted; respirator held in full inspiratory position. Pleural
and other pressures were stable after the respiration pump
stopped and were determined from photokymograph recordings.
Numbers adjacent to lines connecting data points are verti-
cal gradients in pleural pressure per G acceleration and
have units of specific gravity (cm H_2O/cm/G). Pleural pres-
sure gradients were computed by dividing the difference in
pressure between upper and lower pleural catheter tips by
the vertical distance separating the tips. Thus, the gradi-
ents per G acceleration would have been 1.0 if the catheter
tips had been positioned in a hydrostatic system, 1.76 if
in fluorocarbon, and 0.8 in silicone oil. The average ver-
tical gradient per G acceleration was slightly less than 1.0
when the dogs breathed air and slightly greater than 1.0 when
they breathed fluorocarbon.

The interrelationships of intrathoracic circulatory and pleural
pressures and the vertical distribution of pulmonary blood flow in
relation to the zonal perfusion pressures based on the calculated
differences between mean pulmonary arterial, left atrial, and alveolar
pressures in different regions of the lungs (8) are shown in Figure 12.
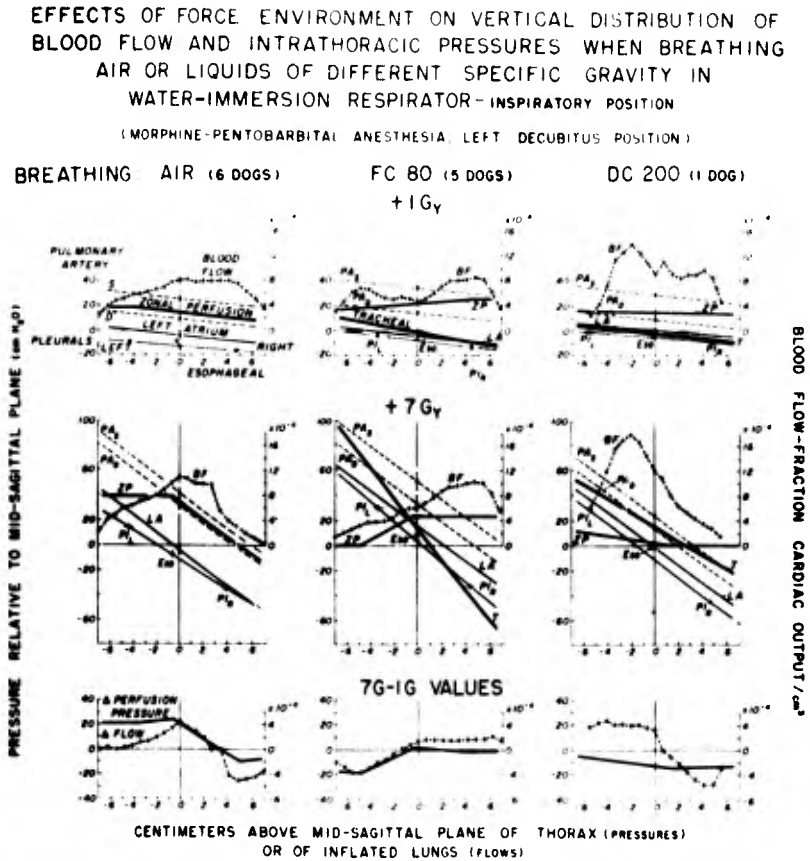
Figure 12. Effects of force environment on vertical distribution of blood
flow and intrathoracic pressures in anesthetized left decubi-
tus dogs breathing air or liquids of different specific grav-
ity in water-immersion respirator. Pressures at 1 and 7G
were obtained from the photokymograph at the interval in the
record where the respiration pump had been stopped prior to
injection of the microspheres (See Figure 5). The lung con-
tained approximately 1,600 ml of respirable liquid at this
time (1,100 ml expiratory reserve volume plus 480 ml inspir-
atory volume). Pulmonary arterial and mean left atrial pres-
sures were referenced to midlung level and estimated in
other regions of the lung, assuming a hydrostatic system.
The interrupted lines passing through the midlung value with
a vertical gradient per G of 1.0 are these estimates. Alveo-
lar pressures were assumed to be atmospheric pressure every-
where in the gas-filled lung. Measurements of tracheal

pressure in the liquid-filled lung were referenced to midlung
level and the solid lines with vertical gradients per G of
either 1.76 or 0.8, as appropriate, were drawn through the
midlung values. Alveolar pressures at different vertical
levels were estimated by these lines, assuming a continuous
system. Zonal perfusion pressures were computed from differ-
ences between mean pulmonary arterial (estimated from systolic
and diastolic values), mean left atrial, and alveolar pres-
sures in different regions of the lung, according to J. B.
West's model of the lung (8).

The regional distribution of pulmonary blood flow and the
changes in this distribution produced by a change in the
inertial force environment appear to be related to the zonal
perfusion pressure and change in this pressure, respectively,
in the dogs that breathed air or liquid fluorocarbon. Re-
gional blood flow does not appear to be related to the zonal
model in the dog ventilated with silicone oil.

The pressure data support the findings of prior studies in this
and other laboratories which indicate that the spatial distribution of
pulmonary blood flow cannot be fully explained by the zonal perfusion
pressure model which relates only differences between pulmonary arterial,
alveolar, pulmonary venous and presumed interstitial pressures in dif-
ferent regions of the lung (9).

References

1. Minnesota Mining and Manufacturing Co. Technical bulletin, "Fluorinert" brand electronic liquids. 3M Co., St. Paul, Minn., 1965.

2. Dow Corning Company, Midland, Mich.

3. Coulam, C. M., W. H. Dunnette, and E. H. Wood. A computer-controlled scintiscanning system and associated computer graphic techniques for study of regional distribution of blood flow. Comput. Biomed. Res. 3:249-273 (1970).

4. Vandenburg, R. A., et al. Regional pulmonary arterial-venous shunting caused by gravitational and inertial forces. J. Appl. Physiol. 25:516-527 (1968).

5. Katori, R., et al. Influence of body position on regional pulmonary arterial-venous shunts in intact dogs. J. Appl. Physiol. 29:288-296 (1970).

6. Reed, J. H., Jr., and E. H. Wood. Effect of body position on vertical distribution of pulmonary blood flow. J. Appl. Physiol. 28:303-311 (1970).

7. Sass, D. J., et al. Effects of $+G_y$ acceleration on blood oxygen saturation and pleural pressure relationships on dogs breathing first air, then liquid fluorocarbon in a whole-body water-immersion respirator. Proceedings of 27th meeting Aerospace Medical Panel, AGARD-NATO, September 15-17, 1970, Garmisch-Partenkirchen, Germany, pp. 7-1 through 7-13.

8. West, J. B., and C. T. Dollery. Distribution of blood flow and the pressure flow relations of the whole lung. J. Appl. Physiol. 20:175-183 (1965).

9. Reed, J. H., Jr. The distribution of pulmonary blood flow (the influence of gravity and increased inertial force environments). Ph.D. dissertation, University of Minnesota, 1967.

Study of Acidemia in Dogs Breathing
Oxygenated FC80 Liquid Fluorocarbon

Introduction

The capability of maintaining arterial P_{CO_2} at normal and below normal levels (16 to 40 mm Hg, depending on respiration rate) in the initial studies with the liquid-breathing system was somewhat surprising, since a major problem in prior liquid-breathing studies has been the accumulation of carbon dioxide in the blood (1-4). Most of the previous studies were performed in animals either totally immersed in and breathing oxygenated fluorocarbon or silicone oil spontaneously (1), or in animals ventilated by simple gravity flow of the respirable liquid in and out of the lungs (2-5). Hypothermia was used in some studies to minimize oxygen demands and carbon dioxide production (1,3), and carbon dioxide buffers were used in others (4,5). The theoretical possibility of controlling blood P_{CO_2} tensions by mechanically assisted ventilation of fluorocarbon liquids had been pointed out (6), and the results of our studies using a water-immersion respirator for accurate control of respiratory variables has confirmed this belief. Neither hypothermia or administration of carbon dioxide buffers was necessary to maintain normal blood gas tensions.

Although blood P_{CO_2} tensions could be maintained at normal or hypocapnic levels for 4 hours or longer in all dogs breathing fluorocarbon we have observed progressive metabolic acidemia from the onset of liquid breathing in almost all of the animals. Figures 1A, B, and C are illustrative. These figures show the results of blood gas and pH measurements in 14 animals breathing first, air or oxygen and then liquid in the respirator. During gaseous respiration, the animals were hyperventilated and thus rendered hypocapnic to minimize spontaneous respiratory movements. The animals were then ventilated with 100% oxygen for 15 to 30 minutes to denitrogenate the blood and other tissues before switching to liquid breathing. A progressive fall in blood pH is evident in the figure from the onset of liquid breathing to values near 7.0 at the end of 4 to 6 hours. The moderate rise in average P_{CO_2} above normal resulted from including in the averages P_{CO_2} tensions in blood sampled immediately after the animals were exposed to force environments of 4 to 7G. Most of these experiments were performed with earlier versions of the respirator in which the oxygenator was disconnected prior to rotation of the centrifuge. While the centrifuge was rotating, the animal breathed from a 4-liter supply of fluorocarbon contained in the breathing compartment. Thus, blood P_{CO_2} levels were higher immediately after the centrifuge stopped rotating than during the 1G control period. Also, a sudden change in the force environment would sometimes partially arouse the anesthetized animal and stimulate spontaneous respiratory movements.

The increased metabolic demands for oxygen and CO_2 removal during these times were not met by the fixed ventilation rate, and a moderate fall in arterial P_{O_2} and rise in P_{CO_2} were measured at the end of the exposure to centripetal acceleration. The inability to explain the progressive fall in blood pH, which was disproportionately greater than the associated moderate rise in P_{CO_2}, prompted the present study.

The purpose of this study was to determine whether or not the acidemia observed in the animals breathing liquid was due to increased production of lactic and pyruvic acid due to breathing fluorocarbon or due to a loss of buffering capacity in the blood, or to both factors. We also broadly examined the blood for electrolytes, red and white cell counts, platelet counts, hemoglobin, hematocrit, serum enzymes, total serum protein and serum electrophoretic pattern, and other blood chemistry variables, looking for abnormalities or clues which might explain the failure of animals to live longer than 30 to 36 hours after breathing fluorocarbon.

FEMORAL ARTERY BLOOD P_{O_2}, pH, AND P_{CO_2}
BEFORE AND AFTER START OF LIQUID BREATHING

(Mean and SE, 13 Dogs Breathing FC 80; 1 Dog, DC 200)
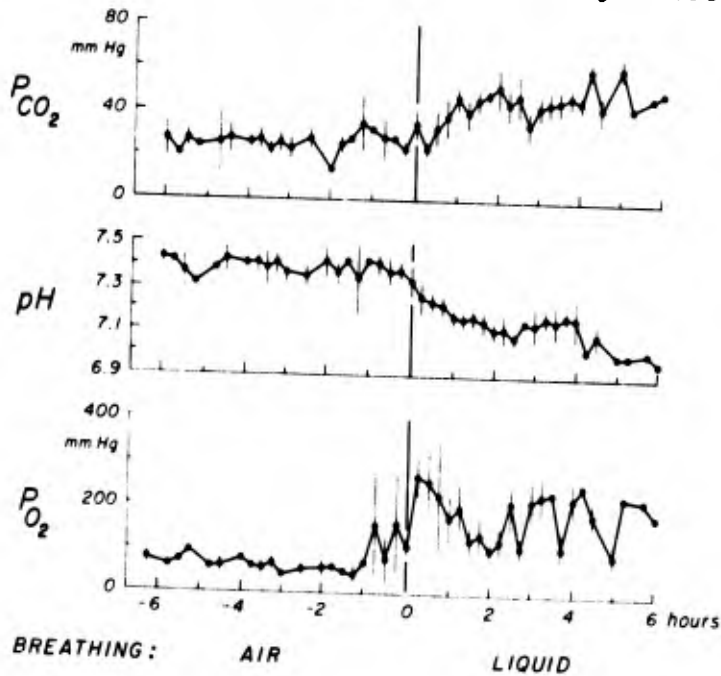
Figure 1A

LEFT PULMONARY VEIN BLOOD P_{O_2}, pH, AND P_{CO_2}
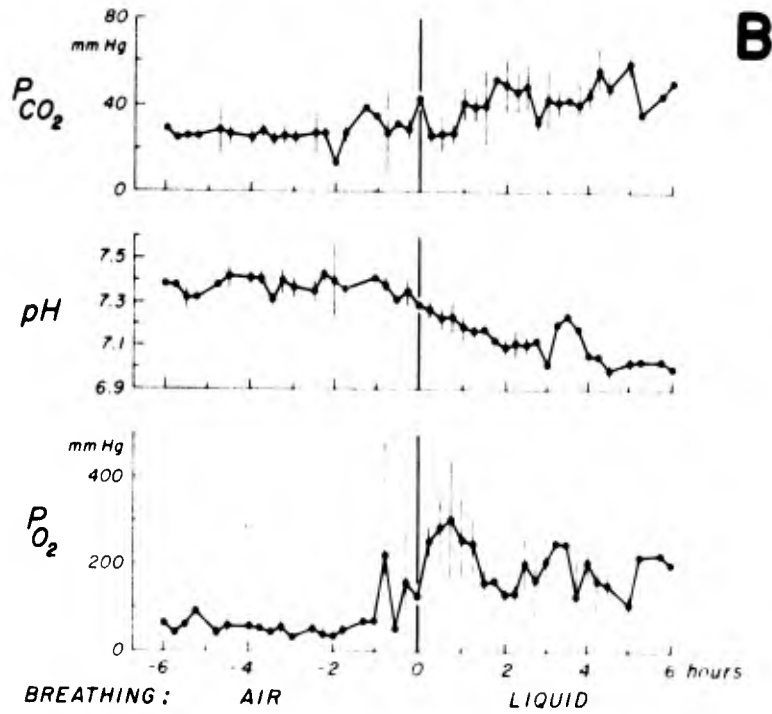
MIXED VENOUS BLOOD P_{O_2}, pH, AND P_{CO_2}

Figures 1B and 1C

77
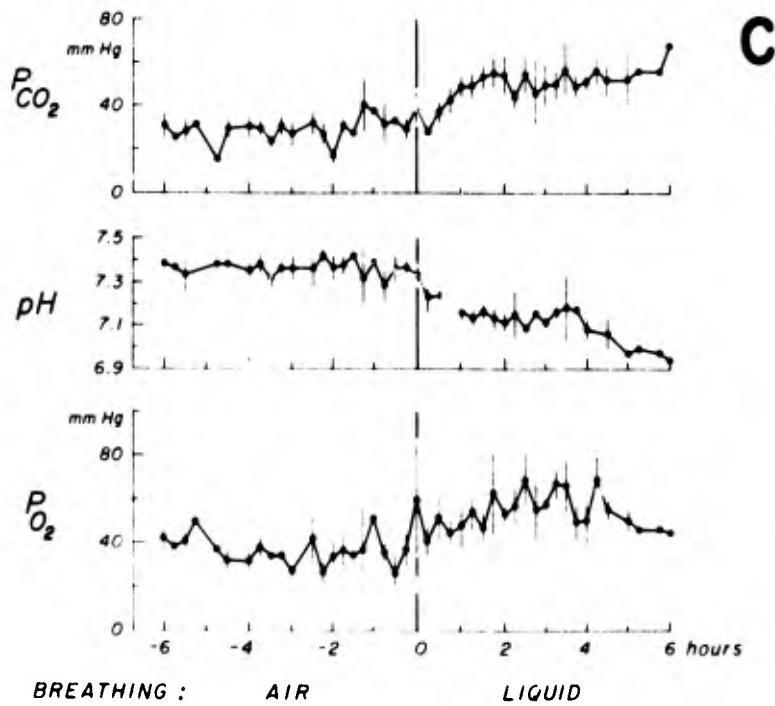
Figures 1A,B, and C. Gas tensions and pH of blood periodically sampled from (A) femoral artery, (B) left pulmonary vein, and (C) mixed venous (pulmonary artery) in 14 dogs breathing first air or oxygen, and then liquid in water-immersion respirator. Measurements were not made every 15 minutes in each of the 14 animals. Each point with vertical bar represents the mean and S.E. of measurements in a variable number of animals (2-14) in that 15-minute interval before or after switching to liquid breathing. A vertical bar is not shown when there was a measurement made only in one animal in a given period. The large variation in blood-oxygen tension 3/4 hour before liquid breathing was due to the fact that not all animals were ventilated with 100% oxygen for the same length of time before switching to liquid breathing, and due to variations in pulmonary A-V shunting among dogs breathing oxygen in the respirator. When breathing air by hyperventilation, each animal was rendered hypocapnic to minimize spontaneous respiratory movements. Minute volume was fixed in each dog at 8-10 350-ml breaths per minute with air or oxygen, and 3-4 480-ml breaths per minute with oxygenated liquid. The variations in average P_{CO_2} and P_{O_2} during liquid ventilation resulted from including in the averages, measurements made immediately after 1-2 minute exposures to centripetal acceleration (+3 to $+7G_y$), along with measurements made during the 1G period. Blood P_{O_2} was decreased and P_{CO_2} increased immediately after these exposures because the greater demands for oxygen supply and CO_2 removal during the exposures were not satisfied by the fixed minute volume. The minute volume had been adjusted to provide satisfactory exchange of alveolar gases during the 1G periods and was left unchanged during exposures to the increased force environments. The acidemia during liquid breathing, or shortly before when the animals were ventilated with 100% oxygen, is out of proportion to the relatively small increase above normal in average femoral artery and mixed venous P_{CO_2}. Since cardiac output in each dog was always within normal limits, a nonrespiratory mechanism is suggested to account for the acidemia.

Methods

Two dogs, 11.0 and 12.5 kg body mass, were anesthetized with morphine and sodium pentobarbital and prepared as described in previous sections except that transseptal catheters were not placed. In dog 16, a prototype P_{CO_2} indwelling electrode was introduced into the supraclavicular artery and manipulated until the tip of the sensor was near the arch of the aorta.

The dogs were then positioned on their left side in a water-immersion liquid-oxygenator assembly which was a modification of the one described in Section IV. The modified assembly is illustrated in the schematic drawing of Figure 2.

ASSEMBLY FOR STUDY OF EFFECTS OF BREATHING LIQUID FLUOROCARBON ON FORCE ENVIRONMENT DEPENDENT REGIONAL DIFFERENCES IN INTRATHORACIC PRESSURES, BLOOD FLOW, AND OXYGENATION
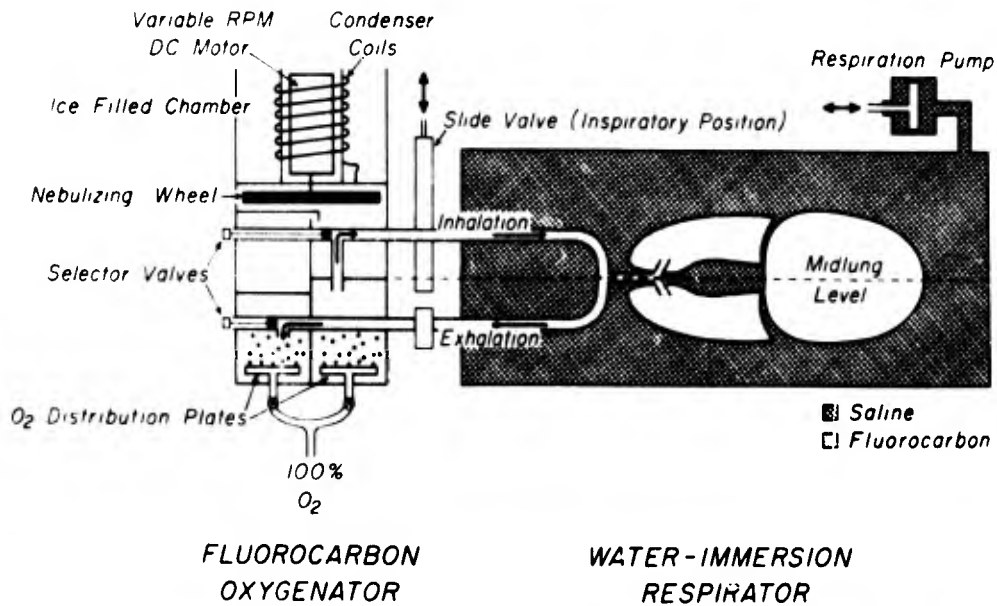
Figure 2. Representative drawing of the water-immersion respirator and fluorocarbon-oxygenator assembly for liquid-breathing studies in dogs. Assembly modified from one described in Figure 2, Section IV. Pneumatically actuated slide valve electrically synchronized to respiration pump directs flow of room air or fluorocarbon, determined by selector valves, through 1" i.d. Lucite inhalation and exhalation lines. Dead space is

minimized by connecting Lucite Y directly to endotracheal
tube. Three sintered stainless steel plates distribute
oxygen flow over a large area near the bottom of the in-
halation and exhalation chambers to partially oxygenate the
fluorocarbon. Complete oxygenation and carbon dioxide re-
moval is accomplished by continuously circulating preoxy-
genated fluorocarbon from the exhalation chamber over the
nebulizing wheel to the inhalation chamber. Fluorocarbon
is circulated by a centrifugal pump (not shown) in the
bottom center of the oxygenator and driven by a shaft exten-
sion from the nebulizing wheel.

A pneumatically actuated slide valve was mounted external to the respira-
tor to open and close the animal's inhalation and exhalation lines in
proper sequence and timing upon electrical command from the respiration
pump. The slide valve replaced the breathing valve originally mounted
within the saline-filled respirator at the outlet of the endotracheal
tube. Also, the inhalation and exhalation lines were brought out at
the end of the respirator in a straight line path to the oxygenator
instead of out the side of the respirator in a "U" shaped path to the
oxygenator as in the original design. The modified valve and inhala-
tion-exhalation line assembly minimized airway pressure losses due to
resistances to flow and due to mass and viscosity of the respirable
liquid. Hence, the peak-to-peak pressures applied to the body surface
of the animal to move the liquid in and out of the lungs in the modified
respirator were one-half the values in the former.

Figure 3 is a photograph of the actual respirator-oxygenator assem-
bly used in the present study.
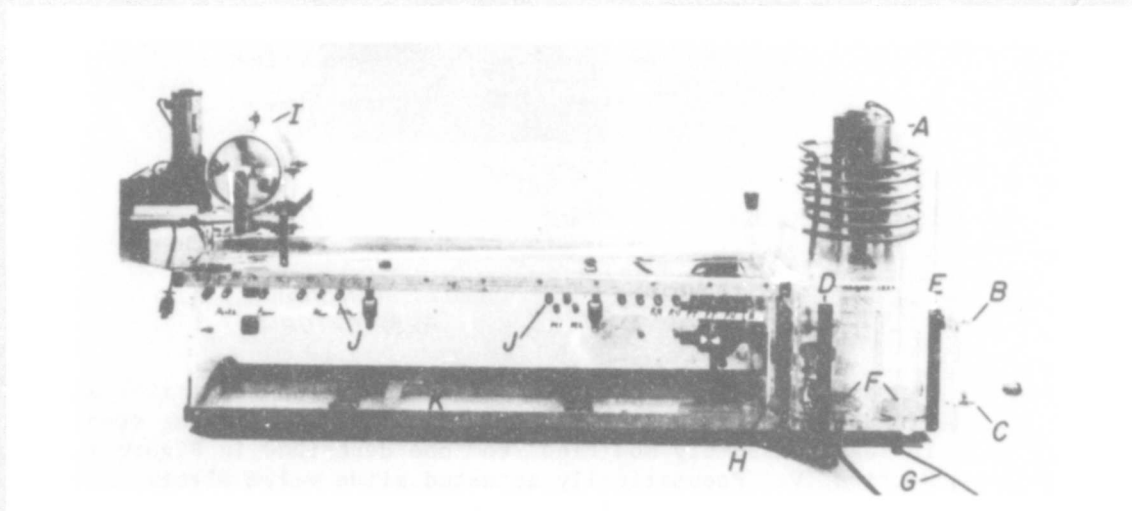
Figure 3. Photograph of water-immersion respirator fluorocarbon-oxygen-
ator assembly. (A) variable rpm dc motor controlled by

separate power supply not shown. (B), (C) selector valves
in inhalation and exhalation lines, respectively. (D), (E)
calibrated scales for determining liquid volume in inhala-
tion and exhalation chambers, respectively. (F) Sintered
stainless steel oxygen distribution plates. (G) Power cord
for electrical heaters (not shown). (H) Slide valve pneu-
matically driven by solenoid valve assembly located on oppo-
site side of photograph. (I) Variable displacement (0-480 ml)
variable rate (0-20/min) respirator pump produces nearly
sinusoidal waveform of body surface pressures within respir-
ator. (J) Catheter ports with gasket assembly for airtight
seal around individual catheters. (K) Cleats for attaching
pelvic and shoulder straps. A Lucite platform (not shown)
positions the animal 4-5 cm above the bottom of the respira-
tor so that midthoracic level is approximately in the hori-
zontal plane through the longitudinal axis of the respirator.

Cardiac output was measured by the indocyanine-green dye technique,
and oxygen saturation was measured by cuvette oximetry in blood contin-
uously sampled from the thoracic aorta and pulmonary artery. These
techniques as well as the photokymograph assemblies, and analog and dig-
ital magnetic tape recording methods have been described in earlier sec-
tions.

Initial calibrations of the dye densitometer, cuvette oximeters,
and strain-gauge pressure manometers were performed with the immersion
tank dry and the dog breathing air spontaneously. Mixed venous blood
samples were then drawn for determinations of electrolytes, glucose,
lactate, pyruvate, hemoglobin, hematocrit, and red-cell, white-cell, and
platelet counts by the Mayo Clinic Biochemistry Laboratory. An arterial
sample was also withdrawn for measurement of blood gases and pH by the
same laboratory as a check on our measurements of the same variables
using the IL 113 blood gas analyzer.

The immersion tank was then filled with physiologic saline at 37°C
and the volume of saline adjusted until the alternating positive and neg-
ative body surface pressures generated by the respiration pump were bal-
anced around zero at midlung level. Tidal volume measured 350 ml by
spirometry. Respiration rate was adjusted until repeated measurements
of the femoral artery P_{CO_2} were within the range of 38 ± 5 mm Hg. Suc-
cinylcholine was administered by continuous drip to prevent spontaneous
respiratory movements. Sodium bicarbonate was given intravenously as
necessary to maintain the femoral artery pH within the range of $7.35 \pm$
0.05.

The first animal developed a large venous-to-arterial shunt pre-
sumably due to dependent pulmonary atelectasis, and was then ventilated
with 100% oxygen for several hours before being switched to liquid
breathing. The second animal fared better and was ventilated with
oxygen for about 1-1/2 hours before liquid breathing

commenced. Arterial and mixed venous blood oxygen saturations were monitored frequently before the animal commenced liquid breathing.

The animal was then swithced to liquid respiration and the rate of the respiration pump adjusted to maintain the femoral artery P_{CO_2} tension within the same range as during gaseous ventilation. Blood oxygen saturation measurements, pressures, cardiac output and other determinations were made periodically during the period of liquid breathing for monitoring purposes. The succinylcholine drip was continued, and sodium bicarbonate was administered as necessary to maintain the femoral artery blood pH within the range of 7.35 ± 0.05. Mixed venous blood samples were periodically withdrawn for repeated clinical laboratory determinations of blood electrolytes and other variables.

After 4-7 hours of liquid breathing, the succinylcholine drip was discontinued and the animal was switched to 100% oxygen respiration. After spontaneous respiratory movements were resumed, the tank was then drained and the animal ventilated with 100% oxygen either by use of an animal-triggered intermittent-positive-pressure respirator or by endotracheal catheter. Femoral artery blood samples were occasionally withdrawn to monitor blood gases and pH in the post liquid-breathing period. Rectal temperature was also monitored and the animal was warmed, as necessary, with electric heating pads.

Anesthesia was maintained throughout the experimental studies in the respirator by supplemental sodium pentobarbital.

Results

The results of the blood gas and pH measurements in each of the two animals are shown in Figures 4A and 4B. The first animal was ventilated with 100% oxygen for 3-1/2 hours prior to liquid breathing and, as shown in Figure 4(A), femoral artery pH promptly decreased shortly after the start of oxygen breathing. Intravenous administration of approximately 40 mEq of sodium bicarbonate reversed the downward shift in pH. Once corrected, the arterial pH remained within the desired range of 7.35 ± 0.05 throughout the 4-hour period of liquid breathing without additional administration of base buffer.

The second animal was ventilated with oxygen for approximately 1-1/2 hours before liquid breathing commenced. Within the first hour of liquid breathing, the pH had decreased below 7.3 and continued to decrease until the downward shift was corrected by administration of sodium bicarbonate 2-1/2 hours after the start of liquid breathing. The pH was returned to the desired range by administration of about 50 mEq of base over a 1-1/2 hour period. However, by the end of the 5th hour of liquid breathing, the pH had again decreased below 7.30.

Approximately 260 ml whole blood had been withdrawn from this animal since the start of the experiment some hours earlier for the determination of electrolytes and other variables by the clinical biochemistry laboratory. This blood was replaced by transfusion of the same amount from a donor dog. The pH remained low after the transfusion, but was returned to the desired range by an additional 22 mEq of sodium bicarbonate.

Since metabolic acidosis was observed in the first animal while breathing 100% oxygen, the decrease in arterial pH could not be attributed to an effect of ventilation with fluorocarbon. After the pH was corrected by administration of sodium bicarbonate, no additional amounts of buffer base were necessary to maintain a normal pH in this animal during the subsequent 4-hour period of liquid breathing.

When the results of previous studies shown in Figures 1A, B, and C are viewed in retrospect, the average pH in the 14 animals may have actually started to decrease during the 15 to 30 minutes of oxygen breathing before the animals were switched to liquid breathing. Metabolic acidosis in these 14 and 2 animals of the present study could have resulted, at least partly, from the loss of hemoglobin in the transport of hydrogen ions by keeping the hemoglobin oxygenated in a high plasma P_{O_2} environment (7).

The results of the clinical laboratory determinations of multiple blood chemistry variables are shown in Table V (See Appendix). Blood lactate and pyruvate levels were normal in both animals. Hence, the metabolic acidosis observed in these animals cannot be attributed to increased production of these acids.

Little significance can be attributed to the minimal changes in other blood chemistry values with the possible exception of the striking decrease in the platelet count after both animals were returned to gaseous ventilation. Since intravascular clots were observed in microscopic sections of the lungs of these two and prior animals, the decrease in blood platelets may have been associated with intravascular clot formation in lungs and elsewhere in the body.

The question remains unanswered as to why these 2 and other animals in these studies have died following liquid breathing. Each of the animals which we attempted to have survive first breathed oxygen and then room air spontaneously after the liquid-breathing studies were concluded. Measurement of oxygen saturation and cardiac output were normal in the immediate post liquid-breathing period. The lung fields were examined periodically by fluoroscopy and, within one hour or so, both lung fields were clear. Arterial and right atrial blood pressures were monitored continuously in several of the prior animals over the subsequent 10 hours with no evidence of cardiovascular disturbances noted. Periodic sampling of arterial blood for pH, P_{CO_2}, and P_{O_2} typically produced normal values

for the first few hours after liquid breathing. Although the cardio-vascular and respiratory systems appeared normal, none of the animals fully regained consciousness or made purposeful movements of skeletal muscles not associated with respiration. Some animals had received succinylcholine, but others had not. Approximately 30 to 36 hours after the start of the liquid breathing, the animals rapidly deteriorated with severe respiratory acidosis until their death.

At autopsy, the lungs in the 2 dogs of this and earlier studies were deeply congested and had a dark red, liver-like appearance and texture. Little grossly normal pulmonary tissue was evident. Micro-scopically, the capillaries were engorged, and intravascular clots were present. Intra-alveolar hemorrhage and edema were observed but neither was a prominent feature. Fluorocarbon could not be expressed from freshly cut sections, and was not visible microscopically.

FEMORAL ARTERY BLOOD GASES

(Dog 16, 11 kg, Morphine-Pentobarbital Anesthesia)

Figure 4A

84
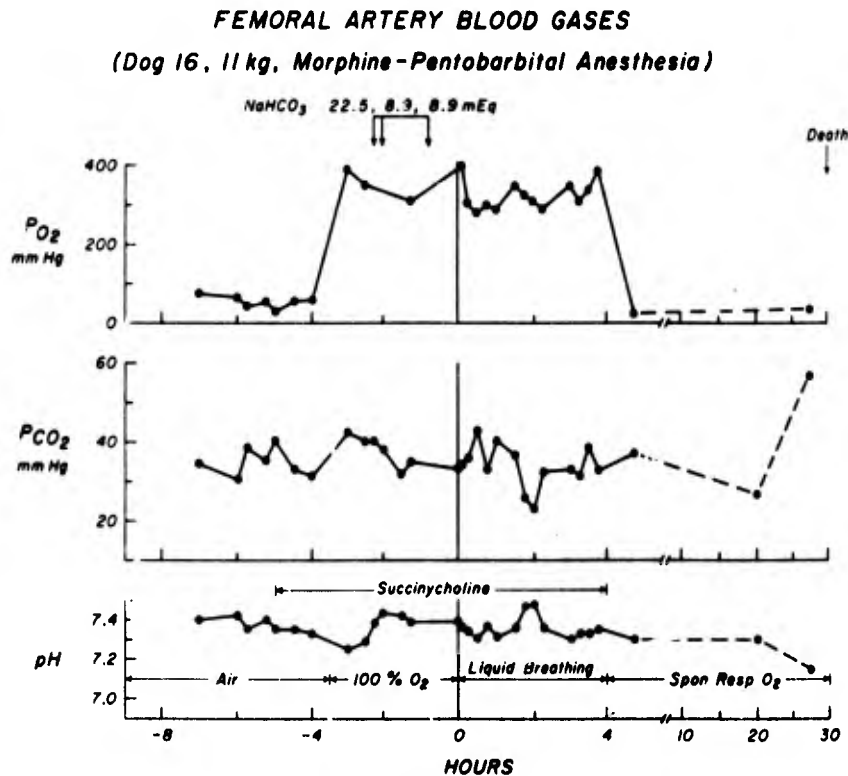
FEMORAL ARTERY BLOOD GASES
(Dog 17, 12.5 kg, Morphine-Pentobarbital Anesthesia)
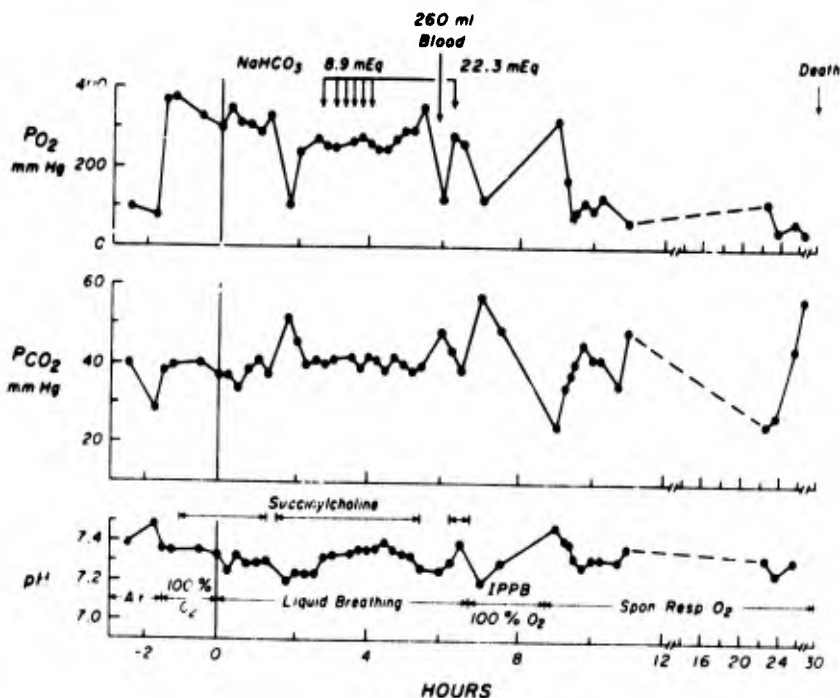
Figure 4B

Figures 4 A,B. Gas tensions and pH of blood sampled periodically from
the femoral artery catheter in 2 dogs breathing first air
or oxygen, and then oxygenated FC 80 liquid fluorocarbon
in a water-immersion respirator. Residual lung volume
about 1,100 ml, tidal volume about 350 ml. Respiration
pump rate 6-7 per minute during gaseous ventilation and
3.5 to 4 per minute during liquid breathing; the rate
was adjusted to maintain P_{CO_2} values within the range
38 ± 5 mm Hg. Succinylcholine was administered by con-
tinuous drip to prevent spontaneous respiratory movements.
Sodium bicarbonate was administered as necessary to main-
tain blood pH within the range 7.35 ± 0.05. In (A) the
decrease in P_{CO_2} below desired range during liquid breath-
ing was due to an increase in rate of the respiration
pump. The rate of ventilation was increased because of
a rising P_{CO_2} reading from an indwelling P_{CO_2} electrode.
When the reading was found to be erroneous, the respira-
tion rate of the pump was decreased and the blood gas
tensions and pH returned to within the desired range.
Note in (B) that when the succinylcholine drip was dis-
continued (unintentionally), P_{CO_2} increased and pH

85

decreased outside desired ranges and, P_{O_2} decreased con-
comitantly. The blood gas tensions and pH returned to
their previous values when the succinylcholine drip was
restarted. Morphine-pentobarbital anesthesia maintained
throughout gaseous and liquid breathing in respirator.

Acute pulmonary congestive atelectasis has been reported in closed-
chest trauma and pulmonary insults of various kinds. Ventilation of
these animals in these studies with either 100% gaseous oxygen or oxy-
genated fluorocarbon for periods of over 30 hours may have contributed
to the demise of the animals by oxygen toxicity (8,9). However, intra-
vascular administration of FC80 fluorocarbon in relatively small quan-
tities (0.1 to 0.25 ml/kg) has been reported to cause death in dogs with-
in a few hours to a few days depending upon the dose, although the mech-
anism is not clearly described (10,11). Intravascular gas emboli and
plugging of the microcirculation elsewhere in the body by clot formation
had been reported (10,11,12,13). Fluorocarbon can enter the circulatory
system of dogs breathing this liquid and be deposited largely in the
brain, fat, muscle and liver in significant quantities (14). Evidently,
surfactant is not washed out of the lungs in very large amounts by the
fluorocarbon (15,16).

The cause of death in the animals of this study is uncertain; however,
oxygen toxicity and passage of fluorocarbon from the lung to the systemic
circulation in toxic quantities were important contributory factors, if
not major causes of death.

To summarize, the results of this study have shown that blood P_{CO_2}
can be maintained within normal limits in dogs ventilated with oxygenated
liquid fluorocarbon for 8 hours or longer in a respirator providing con-
trol of rate and depth of respiration and the residual volume of the lung.
The acidemia observed in animals during ventilation with either 100% oxy-
gen or oxygenated fluorocarbon was not due to increased production of
lactic or pyruvic acid. Since cardiac output and blood P_{CO_2} were within
normal limits, a nonrespiratory mechanism is suggested to account for the
acidemia. Either a loss of buffering capacity of the blood, or increased
production of acid not measured in this study, or both mechanisms, is
suggested.

References

1. Clark, L. C. Jr., and F. Gollan. Survival of mammals breathing organic liquids equilibrated with oxygen at atmospheric pressure. Science 152:1755-1756 (1966).

2. Kylstra, J. A. The feasibility of liquid breathing and artificial gills. In the physiology and medicine of diving and compressed air work (P.B. Bennett and D. H. Elliott, eds.) London: Baillier, pp. 193-212 (1969).

3. Kylstra, J. A., V. Paganelli, and E. H. Lanphier. Pulmonary gas exchange in dogs ventilated with hyperbarically oxygenated liquid. J. Appl. Physiol. 21:177-184 (1966).

4. Modell, J. H., E. J. Newby, and B. C. Ruiz. Long-term survival of dogs after breathing oxygenated fluorocarbon liquid. Fed. Proc. 20(5):1731-1739 (1970).

5. Modell, J. H., et al. Oxygenation by ventilation with fluorocarbon liquid (FC80). Anesthesiology 34(4):312-320 (1971).

6. Gollan, F., et al. Compliance and diffusion during respiration with fluorocarbon fluid. Fed. Proc. 20(5):1725-1730 (1970).

7. Gesell, R. On the chemical regulation of respiration. The regulation of respiration with special reference to the metabolism of the respiratory center and the coordination of the dual function of hemoglobin. Am. J. Physiol. 66:5-49 (1923).

8. Smith, C. W., P. H. Lehan, and J. J. Monks. Cardiopulmonary manifestations with high O_2 tensions at atmospheric pressure. J. Appl. Physiol. 18(5):849-853 (1963).

9. Morgan, T. E. et al. Alterations in pulmonary surface active lipids during exposure to increased oxygen tension. J. Clin. Invest. 44(11):1737-1744 (1965).

10. Nose, Y., et al. Physiological effects of intravascular fluorocarbon liquids. Fed. Proc. 29(5):1789-1804 (1970).

11. Beisang, A. A., et al. Damage assay of kidneys frozen by intra-arterial perfusion with a fluorocarbon. Fed. Proc. 29 (5):1782-1788 (1970).

12. Geyer, R. P. Whole animal perfusion with fluorocarbon dispersions. Fed. Proc. 29(5):1758-1763 (1970).

13. Sloviter, H. A., H. Yamada, and S. Ogoshi. Some effects of intravenously administered dispersed fluorochemicals in animals. Fed. Proc. 29(5):1755-1757 (1970).

14. Holaday, D. A. Distribution of fluorocarbon liquids. Fed. Proc. 29(5):1815-1816 (1970).

15. Modell, J. H., et al. Effect of fluorocarbon liquid on surface properties of pulmonary surfactant. Chest 57(3):263-265 (1970).

16. Ruefer, R. Surfactant and alveolar surface forces after breathing of an inert fluorinated liquid. Fed. Proc. 29(5):1813-1815 (1970).

SECTION VI

Computer Processing of Fnysiological Data

In most of the experiments in the 30 dogs - reported in these separate studies - we routinely recorded pressures via saline-filled catheters which were percutaneously introduced in the thoracic aorta, pulmonary artery, left and right atria, right and left pleural spaces, esophagus, upper trachea, and in either a major bronchus or lower trachea. A description of each of the experiments, including a list of the pressures recorded in each, is given in Tables I and II (See Appendix). Each catheter was connected to a Statham P23d strain-gauge transducer through hydraulically actuated valves which permitted simultaneous flushing of all catheters and switching of all strain gauges to known pressures for calibration. The electrical signal from each strain gauge, as well as signals from the red and infrared cells from each of the three cuvette oximeters, accelerometer, cockpit tilt-angle indicator, respiration pump linear displacement transducer, immersion-tank strain gauge, electrocardiograph amplifier, strain gauges sensing liquid levels in the inhalation and exhalation compartments of the fluorocarbon oxygenator, centrifuge revolution indicator (a microswitch actuated by a cam driven by the centrifuge), syringe travel indicator (for recording the time and volume of injections of indocyanine-green dye, renovist, and microspheres by the remotely controlled, pneumatically actuated power syringe), and other instruments, were transmitted via slip rings to the recording station where all of the variables were recorded on a 45-cm-wide paper photokymograph assembly at 5 cm per second. Most of the variables were also recorded simultaneously on 30-cm-wide paper by a second photokymograph assembly at 25 cm per second. These two assemblies produced the basic record of each experiment.

Figure 1 shows sections taken from the 45-cm-wide photokymograph record in one of the dogs before, during, and after a 1-minute exposure to $+6.9G_y$ when the dog was breathing fluorocarbon in the respirator. Calibration pressures of 0-and 20-cm H_2O were recorded by all gauges except the aortic, and 0 and 100 mm Hg on the aortic gauge, immediately before and after each such experiment. Calibration pressures of 0-, 20-, and 40-cm H_2O were recorded in the beginning section of the record shown. During rotation of the centrifuge, calibration pressures of 0- and 40-cm H_2O were routinely switched into all gauges to record zero baselines and to determine if calibration sensitivities had changed due to the acceleration. These calibrations are shown at the start of the acceleration plateau.

89

ORIGINAL PHOTOKYMOGRAPHIC TRACINGS OF MULTIPLE PHYSIOLOGICAL VARIABLES RECORDED BEFORE, DURING, AND AFTER I-MINUTE EXPOSURE TO +6.9 Gy *(DOG 12.5 kg, BREATHING LIQUID FLUOROCARBON IN WHOLE-BODY WATER IMMERSION RESPIRATOR)*
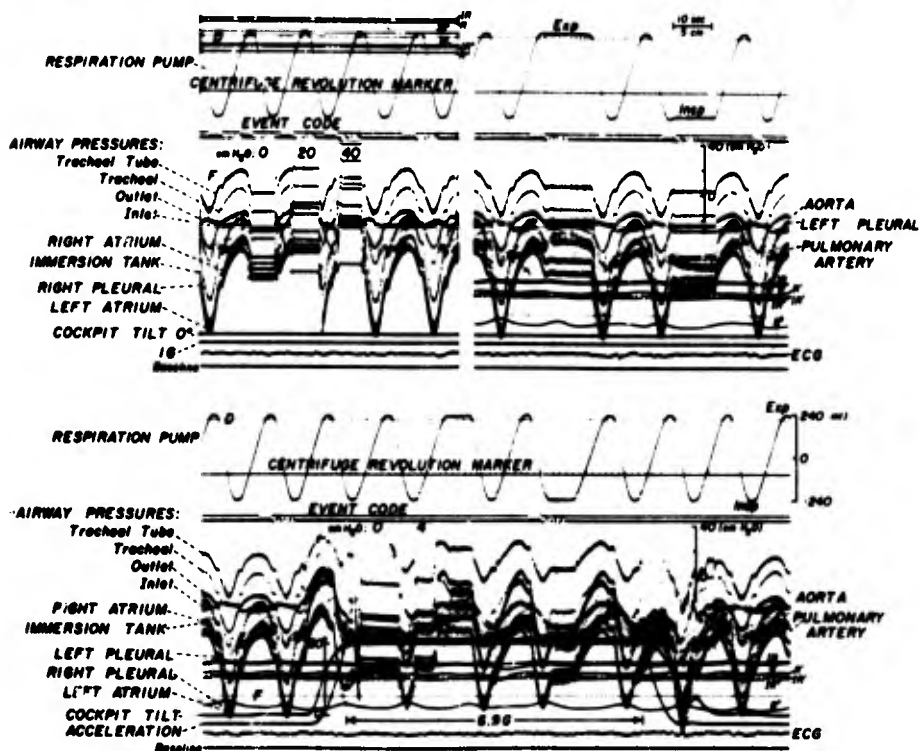
Figure 1. Original photokymographic tracings of 26 physiological variables recorded simultaneously before, during and after a 1 - minute exposure of a dog to 6.9 G_y when breathing liquid fluorocarbon (FC80) in a water-immersion respirator in the left decubitus position. Note that in spite of the fact that 45-cm wide photokymographic paper was used, overlap and consequent difficulty in identifying the multiple galvanometer traces occurred. Manual measurements from these recordings are therefore very difficult. This task is expedited by obtaining parallel recording of 20 of the variables on magnetic tape for subsequent analysis by digital computer. In addition the transmission of red (R) and infrared (IR) light by systemic-arterial pulmonary venous (R', IR') and systemic venous blood (R", IR") being sampled continuously from the aorta, left pulmonary vein, and pulmonary artery via cuvette oximeters are converted on-line by digital computer to oxygen saturation values and second-by-second numerical results displayed on a storage oscilloscope in real time along with other variables, for monitoring purposes in the control room of the centrifuge. This original recording is useful for preliminary visual qualitative analysis of the experimental results,

particularly for detection of possible malfunctions of the multiple transducers and identification of the exact time and sequence of phenomena of particular interest in relation to the event code numbers. These numbers can then be searched for on the digital magnetic tape automatically by the computer and this desired segment of the recording subjected to detailed digital computer analysis. A computer-generated replot of a number of these variables after correction for baseline shift, catheter-tip positions, and minimization of overlap by the computer is shown in Figure 4.

Analysis of paper recordings such as these, by hand, is a laborious task because of the large number of traces, the uncertainty in some cases of identifying the traces when they cross over, and because of the shift in the zero baseline of each pressure trace due to the effects of acceleration on the saline-filled catheter manometer systems. Furthermore, the analyst must construct individual calibration scales for each of the pressure traces since the gauge sensitivities differ, and these scales frequently must be changed to keep the traces within bounds. Once the calibration scales are drawn, the pressures still cannot be read directly because the scale readings must be corrected for shifts in the animal's midlung level (to which the vascular pressures are referred) relative to the zero-pressure reference level, and because we express some of the pressures (the pleurals and esophageal) as pressure at the catheter tip, which means that the hydrostatic head of pressure in each of these catheters must be subtracted from the corresponding pressure measured relative to the zero-pressure reference level. The hydrostatic pressure corrections amount to 1 cm of water per centimeter of vertical height difference between the zero reference level and the tip of the saline-filled catheter. Therefore, this correction can be obtained by measuring the vertical height of the pleural and esophageal catheter tips from the reference plane using the biplane orthogonal roentgenograms obtained during control and acceleration periods (1).

All of the vascular, pleural, esophageal, and airway pressures reported for the first 20 dogs in these studies were hand-measured in this way.

The data reduction problem was enormously simplified by the development of several digital computer programs during the course of these and earlier studies (1,2). All of the pressure data recorded in the seven dogs of the pulmonary blood flow study of Section IV were analyzed by these programs.

1. **Program for on-line digitization of physiological pressures recorded in centrifuge experiments:**

This is an assembly language program used with the CDC 3500 computer

under the MEDLAB monitor; it requires 2,200 words of memory. The program processes the 10-bit data words on each of the 22 channels of the analog-to-digital converter. These channels are utilized as follows:

9 channels- for pressures (viz, aorta, pulmonary artery, left atrium, immersion tank, esophagus, left and right pleural, tracheal and bronchial);

8 channels- reserved for the red and infrared signals for each of four cuvette oximeters, although only three oximeters were used in these experiments;

1 channel- for the respiration pump displacement;

1 channel- for the syringe travel;

1 channel- for the dye densitometer;

1 channel- for the accelerometer;

1 channel- for the BCD event code electrically mixed with the electrocardiogram.

The CDC 3500 computer is a word machine, with each word consisting of 28 bits, including parity bits. With the use of this program, each of the 22 analog-to-digital lines are sampled at a 100-sample-per-second rate by computer clock control, and two 10-bit A-D data values are stored in each computer word. Since core space in the present machine is limited to 2,200 words of memory, instruction words are sometimes overlaid with data words. The data from the A-D converter enters five 222-word buffer areas, and as each buffer is filled, the contents of the buffer are transferred to 7-track IBM compatible tape. Each 4- or 5- minute centrifuge experiment thus results in a tape file consisting of a sequence of 222 words written from the buffers.

Options in this program are selected from a remote terminal numeric keyboard and a storage oscilloscope for message display. Some of the options allow the following:

a. Tape positioning according to file number entered at the keyboard;

b. Display of pressure calibration data immediately after the calibration period. Technical errors in calibration can be detected before the experiment commences and the calibrations can be repeated, if necessary;

c. Printer copy of calibration data for future reference;

d. Tape update. Catheter tip x-y coordinates obtained from
    roentgenograms at a later date can be entered at the key-
    board along with x-ray source-to-film and animal midlung-
    to-film distances necessary for the computation of the true
    vertical height of appropriate catheter tips from the zero-
    reference plane.

hese data are written on the computer disc as they are entered, and
fter all of the updated data are entered, a hard copy is printed to
llow the operator to detect possible dial-in errors. If the catheter
ip and other data necessary for computing pressure corrections are
orrect on the disc, a header record is written on a second, updated
igital tape, followed by a transfer of all of the digital data from
he original tape to this updated tape.

Program for generating an ink-on-paper (Calcomp) plot of the results stored on the updated tape.

This is an assembly language program of 2,050 words designed for
ontrol of rapid incremental plotter (Calcomp), using the MEDLAB moni-
or programming system. The program is used to generate a point-to-
oint plot of the 10 channels of data stored on the updated digital
ape before final processing. Each 222-word record is transferred from
ape to a 222-word buffer in core. The program then calls a subroutine
o unpack the two 10-bit A-D data values contained in each 24-bit com-
uter word, and applies the pressure calibrations and the appropriate
orrections computed from data in the header record. A general purpose
ubroutine for driving the rapid incremental plotter is then called
pon to apply the necessary constants for scaling the corrected pres-
ure and other data into x-y coordinates suitable for the plotting rou-
ine. The latter is a general purpose 800-word plotting subroutine
hat accepts the x-y data from the first subroutine, and drives the
apid incremental plotter.

Figure 3 is a computer-generated plot of the same pressure data
hown in the photokymograph recording illustrated in Figure 2.

93

MULTIPLE PHYSIOLOGICAL VARIABLES RECORDED DURING EXPOSURE TO 7 G$_Y$ IN WATER-IMMERSION RESPIRATOR

(DOG 17 kg, MORPHINE-PENTOBARBITAL ANESTHESIA)
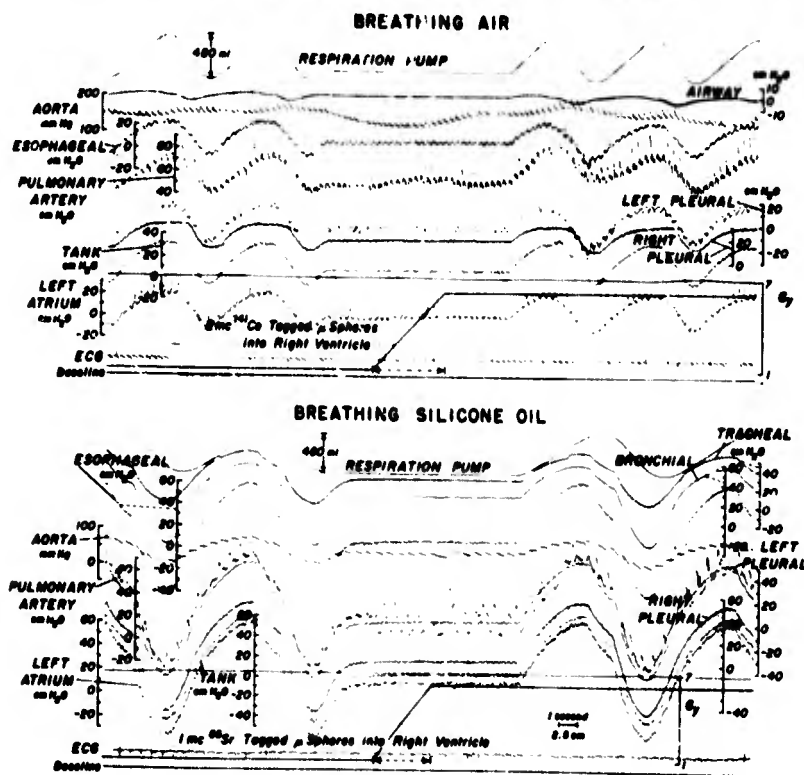
Figure 2. (Reproduced from Figure 5 of Section IV. See legend in Section IV for details).

COMPUTER PROCESSED TRACINGS
OF MULTIPLE PHYSIOLOGICAL VARIABLES
DURING EXPOSURE TO +7 G_y

(Dog, 17 kg, Morphine - Pentobarbital Anesthesia,
Water - Immersion Respirator)
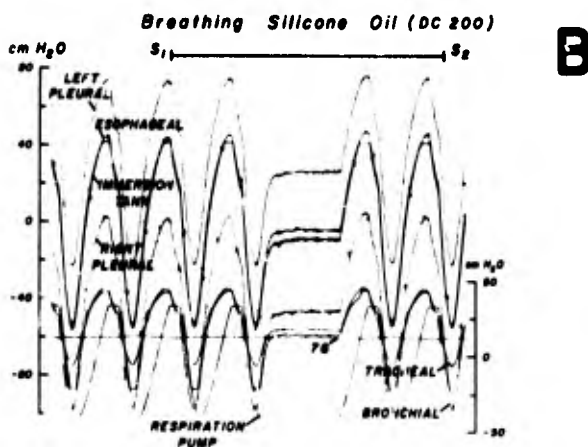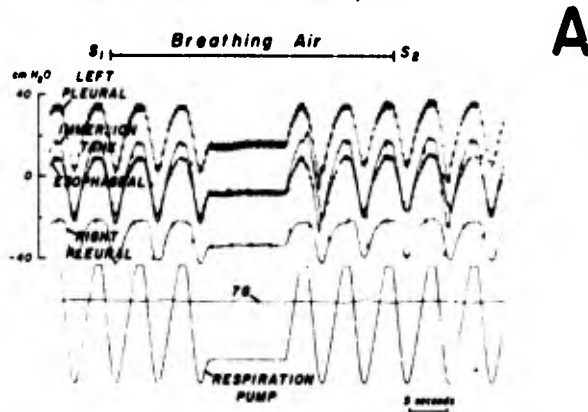
Figures 3A and 3B .

Figures 3A,B. Computer-processed tracings of multiple physiologic variables recorded during exposure of a dog to +7G_y first breathing air (upper panel) and then silicone oil (lower panel) in water-immersion respirator. The horizontal bars (S_1, S_2) mark the periods corresponding to sections from the original photokymograph record illustrated in Figure 2. Unlike the original recording, all pressures can be read directly from the computer-processed tracings without additional corrections because the corrections were applied by the computer as the tracings were processed. Aortic, pulmonary artery and left atrial pressures shown in the original record were not plotted in Figure 2. The vascular pressures are normally plotted on a separate plot with an expanded time scale. These pressures can be read directly also. Note that when the dog breathed air, the sinusoidal alterations in body surface and intrathoracic pressures are in phase with the displacement of the respiration pump, but when the dog breathed silicone oil, the pressures reached their maximum and minimum values before the pump displacement reached its maximum and minimum values, respectively. Furthermore, when the pump was stopped, the pressures continued to change. Note the greater amplitude and different shape of the pressure waveforms in the lower panel compared with corresponding traces in the upper panel. Thus, when the dog was ventilated with air, the pressures generated by the respiration pump were largely due to the compliances of the immersion tank and chest wall in parallel, but when the dog was ventilated with silicone oil, the respiration pump was loaded by the inertial reactance and viscosity of the oil in addition to the compliances mentioned.

Obtaining plots, such as illustrated, is the most time-consuming portion of the computer analysis of the pressure data. To save time, the photokymograph is first examined to select the portion of the record of interest and to eliminate from subsequent analysis, areas in the record containing catheter flushes, noise, etc. An option in the incremental plotter program permits selected portions of the digital tape to be plotted. The time in seconds before or after the nearest BCD event code when the analysis is to start, and similarly when the analysis is to stop, are entered at the keyboard of the peripheral computer station. Considerable time is saved by not plotting unwanted data. The computer-processed records of Figure 2 were obtained with the use of this option.

Unlike the original recording, hand measurement of pressures in the computer plot is relatively easy because the pulmonary artery, left atrium, esophagus, the two pleurals, and the immersion tank pressure traces all have the same baseline and calibration scale which is printed by the computer at the start of each plot. Another two scales are plotted for the aorta and the airway pressures adjacent to the first. Furthermore, each trace can be read directly from the appropriate scale without further corrections, either during the control or during the acceleration portion, because the zero baselines during the acceleration period have been corrected by the computer program to match the baselines for the control period.

Special options, which can be selected at a remote terminal display, permit the following:

a. Any of the 12 traces, except acceleration and event code, can be omitted in the plot;

b. Any portion of the digital tape can be plotted by entering the start and stop numbers of the BCD event codes at the ends of the desired portion;

c. The time scale can be adjusted between 1 and 10 cm per second;

d. A photokymographic recording can be obtained by transfer of the digital data to the digital-to-analog converter. A recording of data processed by the computer with the use of this option is illustrated in Figure 4. Data used to derive this figure were obtained from the same experiment illustrated by the original photokymograph tracings shown in Figure 1.

This computer program is used to examine all or any portion of 12 channels of the updated digital tape prior to final processing. Parity errors on tape, overload of individual A-D channels, and other technical errors in digitizing can be detected and that portion of the tape eliminated from the final processing.

COMPUTER-PROCESSED TRACINGS OF MULTIPLE PHYSIOLOGICAL VARIABLES
RECORDED BEFORE, DURING, AND AFTER I-MINUTE EXPOSURE TO +6.9G_y
(DOG 12.5kg, BREATHING LIQUID FLUOROCARBON IN WHOLE-BODY, WATER-IMMERSION RESPIRATOR)
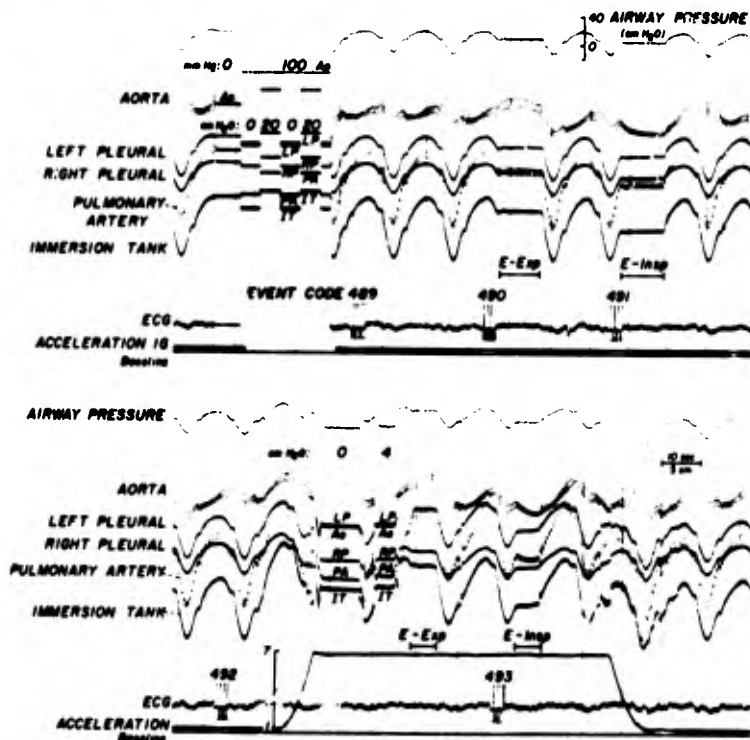
Figure 4. Computer-generated replot of multiple pressures following
correction for baseline shifts and catheter-tip positions
during an exposure to 6.9G. See Figure 1 for additional
details. Note the similarities in contours of the changes
in the thoracic, intra-airway liquid fluorocarbon and cir-
culating pressures caused by the changes in body surface
(immersion tank) pressure generated by the respiration pump
of the respirator. The respiration pump was stopped tem-
porarily in the maximum expiratory (E-exp) and inspiratory
(I-insp) positions so that FC80 and pleural pressures could
be measured under static conditions. Comparison of the
original and computer-processed photokymographic recordings
is an expeditious means of being certain that no malfunctions
have occurred in the multichannel hardware and software com-
ponents of the electronic data processing and digital com-
puter assembly.

3. <u>Program for statistical analysis of physiological pressure measure-
ments:</u>

This is a combination FORTRAN and assembly language program requir-
ing 13,500 words of core, for use with the CDC 3500 MSOS monitor. The

program was designed to analyze physiologic pressures which have a large
sinusoidal component, such as that introduced by the water-immersion
respirator. The program reads successive 15-second blocks of data (1,500
samples from each of 9 pressure channels) from the updated digital tape,
and identifies tne inspiratory and expiratory portions of each respira-
tory cycle. The maximum and minimum data values ave determined for each
pressure channel except the aortic and pulmonary arterial in each res-
piratory cycle. The systolic, mean, and diastolic values are determined
for the aortic and pulmonary arterial pulses which occur nearest the
maximum and minimum values of the left pleural pressure. Appropriate
pressure calibrations and corrections from the tape header record are
applied and the values are printed under expiration and inspiration col-
umn headings. The block of data analyzed is identified in the printout
by the time in seconds of each set of expiration data from the beginning
of the tape file, and the time in seconds of each inspiration and expira-
tion set of values from the nearest event code. The results of the anal-
ysis of each 15-second block of data are read from the updated tape,
processed and printed. After the complete file is analyzed and printed,
the means and standard errors of the means are computed from the values
stored on the disc, and the results of this analysis are printed at the
end of the printout.

An important option in the program enables the operator to select
certain respiratory cycles for analysis. Any 1 through 20 consecutive
cycles can be specified by entering on data cards the number of cycles
to be analyzed and the time in seconds from the event code nearest the
first cycle.

Tables VI and VII (See Appendix) are computer printouts resulting
from the analysis of 9 channels of pressure data recorded on an updated
digital tape. The printout in Table VI is the analysis of 6 consecutive
respiratory cycles immediately preceding the injection of microspheres
into a dog breathing air in the water-immersion respirator during an
exposure to 7Gy, and the printout in Table VII is a similar analysis
of the 7 respiratory cycles before the microsphere injection into the
same dog breathing silicone oil during a similar exposure to centripetal
acceleration. The computer-processed tracings illustrated in Figures
3A and 3I were obtained from approximately the same portions of the
updated tape analyzed in the printouts of Tables VI and VII, respectively.

Computer-processed tracings, such as illustrated in Figure 3, were
routinely obtained prior to the final analysis to determine whether or
not the data in the segment of interest were recorded satisfactorily on
the digital tape. A-D converter overload and other technical errors
are usually apparent in the processed tracings but may easily escape
detection in the printout of the statistical analysis.

The pressure data recorded in the 7 dogs studied in Section IV were
analyzed with these programs. Tables VIII through XIII (See

99

Appendix) summarize the pressures and other data for the individual dogs
under different conditions of respiration and force environment. Tables
XIV and XV (See Appendix) give a statistical summary of the pressure
analysis in the 7 dogs also for these conditions.

The pleural pressure plots shown in Figure 5 were obtained from
the data summarized in Tables XIV and XV.
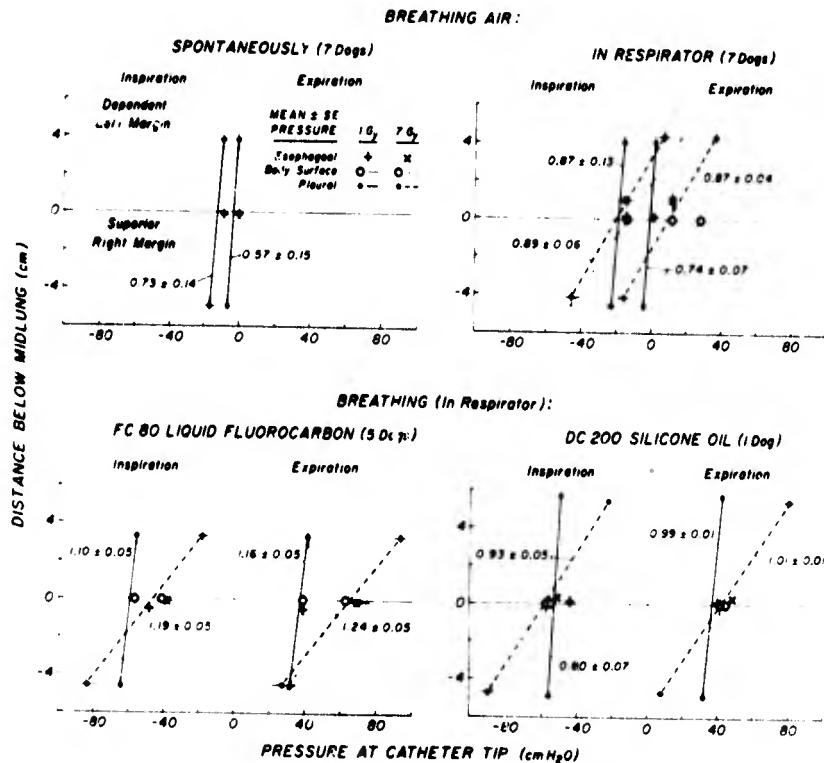
Figure 5. Effect of $+G_y$ acceleration on relationship of pleural and
esophageal pressures to vertical height in thorax of dogs
breathing air, liquid fluorocarbon, and liquid silicone oil
in left decubitus position in water-immersion respirator.
Mean and standard error of pleural, esophageal, and body
surface pressures from computer analysis of 1,065 respiratory
cycles of data recorded in multiple experiments in 7 dogs.
Solid lines connect mean pressures measured simultaneously
in left and right pleural spaces at full inspiration and
full expiration when animals were exposed to normal 1G force
environment. Interrupted lines connect mean values for same
animals exposed to 7Gy. Numbers adjacent to lines are mean
and standard error vertical gradients in pleural pressure
per G acceleration and thus have units of specific gravity
(cm H2O/cm/G). They were obtained by dividing the difference

100

between left and right pleural pressures (cm H_2O) by the product of the vertical distance separating the catheter tips (cm) and the acceleration (G), for individual dogs and then averaging the group. Body surface (immersion tank) pressures were referred to midlung level and predicted elsewhere over the body surface by the faint dashed lines drawn with a vertical gradient of 1.0 through midlung values. Catheter-tip positions were determined from biplane thoracic roentgenograms obtained when respirator was in full expiratory position and approximately 1,100 ml gas or liquid remained in the lungs. Tidal volume with air was approximately 350 ml and with liquid, about 420 ml. Note that when the dogs breathed air, the pleural pressure gradients were less than 1.0, but were greater than 1.0 when liquid fluorocarbon was breathed. Differences between inspiratory and expiratory or between 1 and $7G_y$ gradients are not statistically significant in dogs of the same group. Thus, the data indicate that pleural pressure gradients are strongly influenced but not wholly determined by the weight of the thoracic contents. Note also that there were no significant differences comparing mean gradients determined from the photokymograph measurements during the interval in the record when the respirator pump was stopped at full inspiration (Figure 9, Section IV) and the computer-processed respiration values plotted in Figure 5.

The pressure data summarized in Tables XIV and XV (See Appendix) and the pleural pressure relationships shown in Figure 5 were discussed in Section III. In that section, these data were used to explain the phasic changes in cardiac output observed in animals ventilated with liquids.

To summarize, the development of several digital computer programs for use with the CDC 3500 has made possible much more complete analysis of the moment-to-moment measurements of the numerous physiological pressures routinely recorded when the animals of this study were exposed to either normal or increased force environments. Comparable analysis of these data by hand methods would have required impractically large expenditures of human effort. The computer programs were described and the results of pressure measurements in 7 dogs ventilated with either 1 or 7G force environments are presented.

101

References

1. Wood, E. H., et al. Scintiscanning system for study of regional distribution of blood flow. SAM-TR-70-6, Feb.(1970).

2. Sass, D. J., et al. Digital computer analysis of circulatory and respiratory pressures in water-immersed dogs breathing liquid in force environments of 1 and 7Gy. Aerospace Medical Association Preprint, 1972 Annual Scientific Meeting May 8-11, 1972, Bal Harbour, Fla. pp. 242-243.

Effect of Inflation Levels and Body Position Changes
Upon Regional Pulmonary Parenchymal Movement in Dogs at 1G

Methods and Results

The spatial distribution of inspired air and pulmonary blood flow of man and animals during various respiratory maneuvers, and in various body positions, has been extensively investigated, but there is little or no experimental data on the spatial distribution of the parenchyma under these conditions.

The purpose of this paper is to describe a method of measurement of regional pulmonary parenchymal shifts in dogs during various respiratory maneuvers and body position changes.

In three dogs, 37 to 50 1-mm metal tags were implanted percutaneously in the pulmonary parenchyma in a grid pattern 10 days to 2 weeks prior to the study. This was achieved without significant pneumothorax or hemorrhage in the following manner: the dogs were anesthetized and intubated, saline-filled catheters were inserted percutaneously into their right and left pleural spaces, and pleural fluid pressures were monitored continuously.

A No. 16-gauge needle, 28-cm long (Figure 1) was fitted with a rubber gasket (A) so that, with the trocar (C) in place, the assembly was essentially airtight. The small metal tags were placed in the needle along with two or three 1-mm diameter sugar beads separating the markers; the dog was given several large positive pressure breaths, and the needle was inserted under fluoroscopic control through the appropriate intercostal space into the pulmonary parenchyma up to the mediastinum during the postventilation apneic period. The beads were then extruded at appropriate intervals as the needle was withdrawn. The sugar beads minimized the extrusion of more than one metallic marker at each point. After each insertion, the pleural catheters were aspirated to determine the presence of any blood or air in the pleural space, and upon completion of the procedure, roentgenograms were taken to confirm the presence or absence of pneumo- or hemothorax. This procedure was repeated at each interspace overlying the lung on both sides of the dog until a grid pattern was obtained as shown on the biplane roentgenograms of the chest illustrated in Figure 2. Markers of different shape facilitate identification of individual marker images in the biplane roentgenograms.

The pulmonary tissue response to these metal tags was slight. A photomicrograph of a fixed air-dried lung from a dog 2 weeks after tag insertion is shown in Figure 3. The metal tag was removed prior to microtome sections, and the remaining capsule is composed of compressed alveoli with slight inflammation and fibrous tissue, and is approximately 2 to 3 alveoli thick. To date, in autopsies of 11 dogs with

ASSEMBLY FOR PERCUTANEOUS INSERTION OF METAL TAGS FOR STUDY OF REGIONAL MOVEMENTS OF LUNG PARENCHYMA IN INTACT DOGS
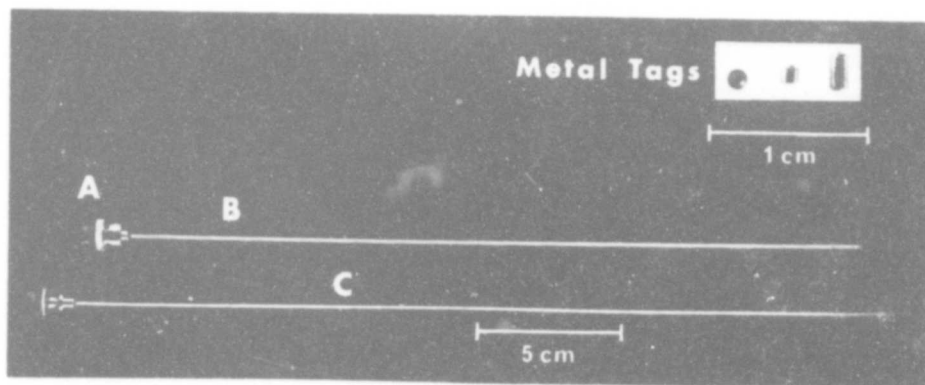
Figure 1. Needle-trocar assembly for tagging pulmonary parenchyma with 1-mm metallic markers of different shape, illustrated in the insert.

ORTHOGONAL ROENTGENOGRAMS OF DOG IN PRONE POSITION
SHOWING LOCATION OF PARENCHYMAL TAGS AT END-INSPIRATION

(Dog 21.5 kg, Morphine - Pentobarbital Anesthesia)
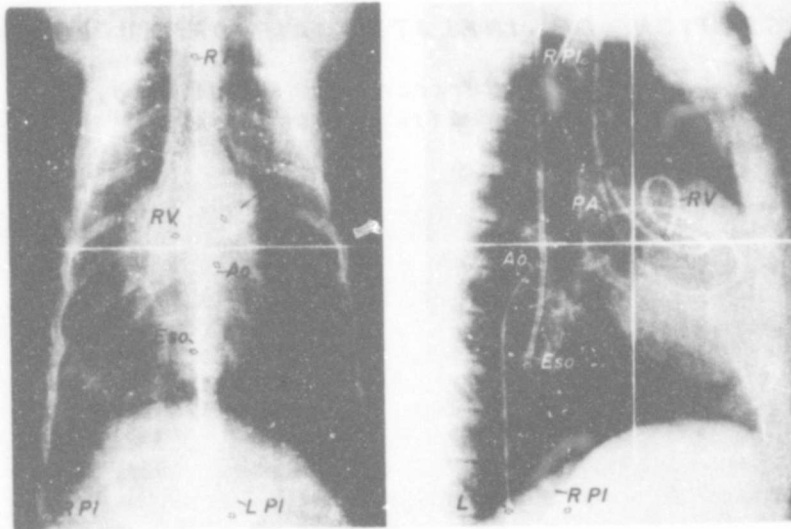
Figure 2. Ventral-dorsal and lateral roentgenograms used to determine
the positions of percutaneously implanted stainless steel
radiopaque tags for measurement of displacements of differ-
ent regions of the lungs and regional lung volumes during
the respiratory cycle, as well as changes in direction and
magnitude of the force environment in dog studied without
thoracotomy. The abbreviations RP1, LP1, RV, RA, Ao, and
Eso indicate the positions of the tips of liquid-filled
catheters connected to strain-gauge manometers for simul-
taneous recordings of pressures from the potential right
and left pleural spaces, the esophagus, right ventricle,
pulmonary artery, and aorta, respectively. The silhouettes
of the steel wire "crosshairs" which intersect at the level
of the sixth thoracic vertebra (left panel) are used as
reference points for measurements of the spatial positions
of metal tags and catheter tips.

percutaneous tag insertion, no pleural adhesions or any other patholo-
gical effects, aside from what is illustrated in this figure, have
been noted.

SECTION OF INFLATED AIR-DRIED LUNG

(Capsule Surrounding Metal Tag, 2 Weeks After Insertion)

| 1 mm | I mm |
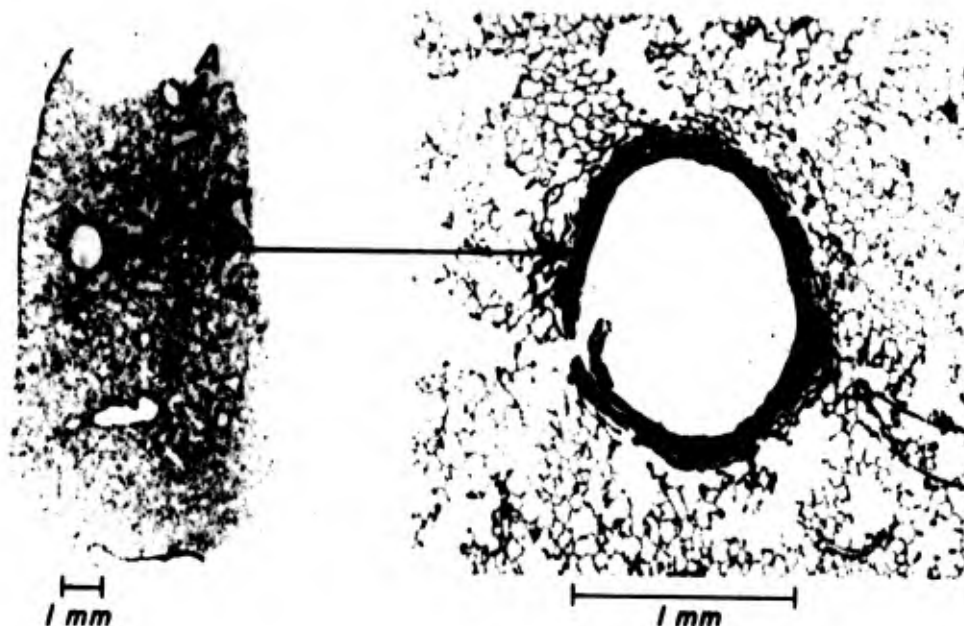
Figure 3. Photomicrograph of a section of inflated air-dried lung from
region where metal tag had been implanted in dog 2 weeks
earlier. Tissue reaction to the tag was slight.

The dogs were studied in a molded half-body supine cast mounted in
a metal cage (shown in Figure 4) 2 weeks after tag insertion. This
facilitated changing the dog's position from prone to head-up or head-
dow , with minimal movement of the limbs, and with minimal neck or chest
displacement. All pleural, esophageal and vascular pressures, and the
parenchymal tag positions were referenced to the spinous process of the
6th thoracic vertebra, which is approximately at the longitudinal and
right-to-left midpoint of the lung. Simultaneous pressure records and
biplane orthogonal roentgenograms were obtained from each dog in the
prone, head-up and head-down positions at functional residual capacity,
at the end of a spontaneous inspiration, and during brief sustained
inflations by 10 and 20 cm H_2O airway pressure.
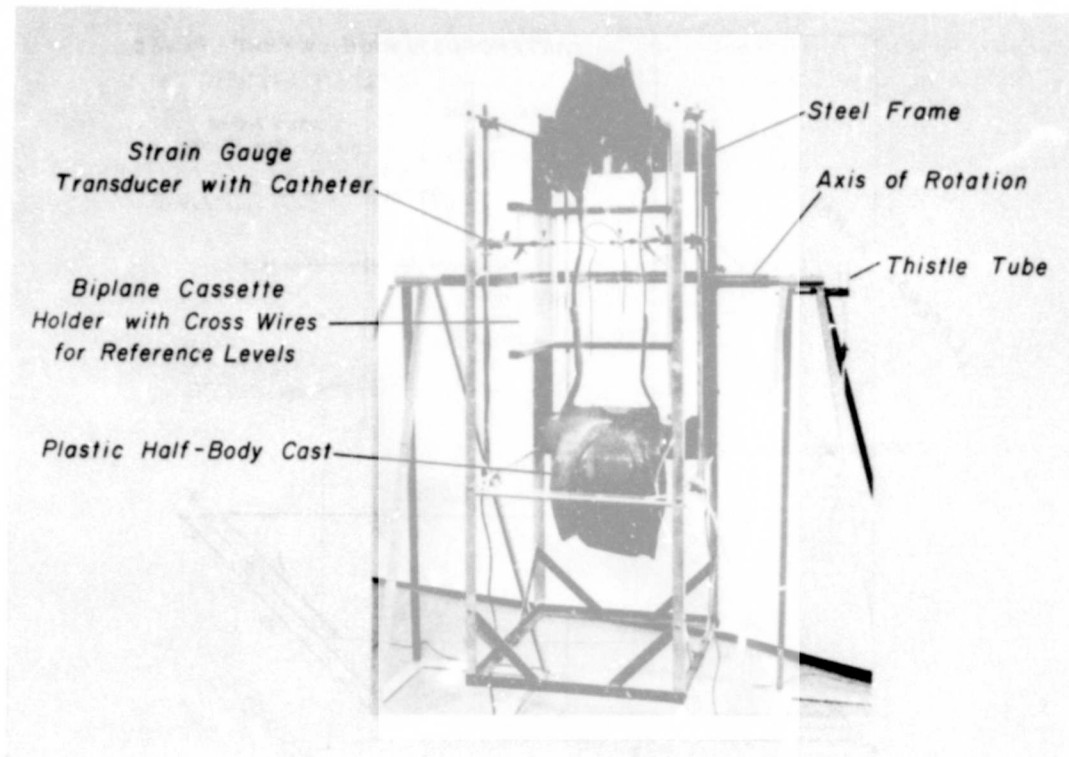
Figure 4. Half-body cast fixed in steel supporting frame used to maintain the dog in the head-up and head-down positions during measurements of pleural pressures and related variables. Method of supporting strain-gauge manometers is illustrated. Cassette holders for biplane roentgenograms with steel-wire crosshairs on their front surface to define zero-pressure reference level from which all transducers were initially calibrated are shown. Dog was secured in half-body cast with band straps around all four extremities and to the steel cage by nylon cords from his eyeteeth to cage top and by similar cords from his ankles to cage bottom. The abdomen was partially supported by a loose binder.

Figure 5 shows the biplane orthogonal x-ray system with the cube representing the dog's chest within the transradiated space. The dimensions of the orthogonal x-ray system (s,q,t,p) and the x',y', and z' coordinates of each tag from the central axes of the two systems must be known in order to correct for the magnification inherent in a divergent x-ray system.
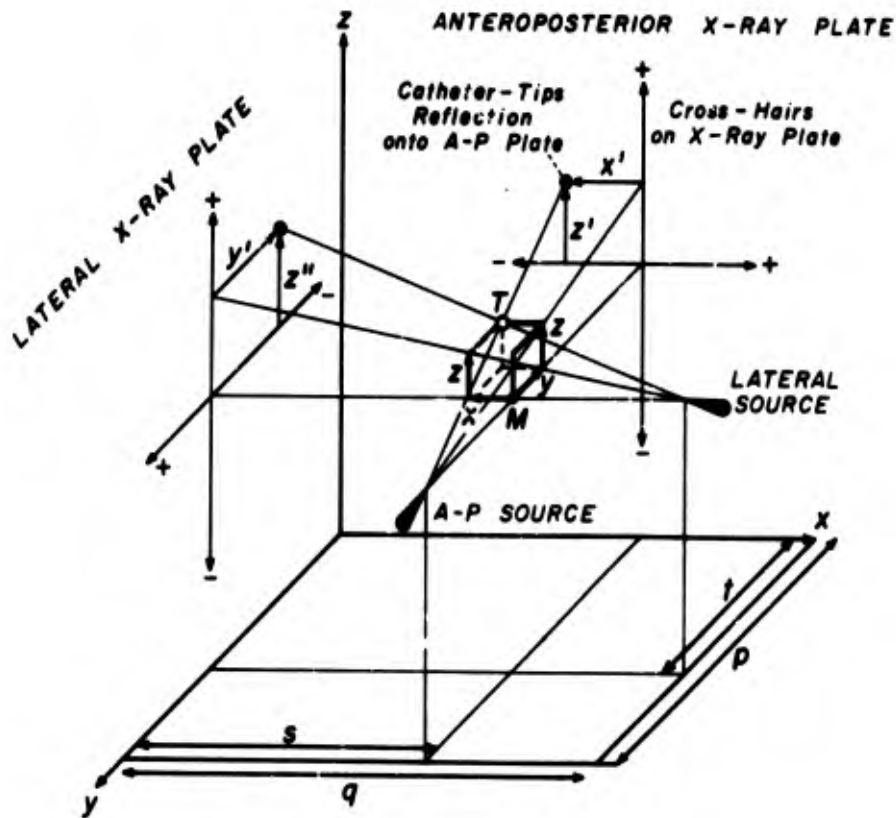
Figure 5. A three-dimensional illustration of measurements which must be obtained from biplane roentgenograms of the thorax to determine spatial coordinates (x,y,z) of metallic tags, in relation to selected anatomic reference point (M). Position of the dog is adjusted so that midpoint of the lungs (level of midpoint of sixth thoracic vertebra) is close to intersection of central axes of respective roentgen beams generated by anteroposterior and lateral roentgen tubes (sources) used to produce biplane roentgenograms of the thorax. Setting reference point (M) of spatial coordinate system at intersection of central axes of two roentgen beams minimizes complexities caused by nonparallel nature of roentgen beams. Position of cassette holders for roentgen films and two pairs of steel wire (crosshairs) mounted on their faces are adjusted so that the intersection of these crosshairs (indicated by + and - signs) coincides with central axes of respective roentgen beams. Tube-to-plate distances (p and q) for anteroposterior and lateral roentgenograms must be known, plus distances (s and t) of reference point M from lateral and anteroposterior x-ray plates, respectively. Distances x' and z', and y' and z', from point of intersection of silhouettes of steel-wire crosshairs, are measured

directly on anteroposterior and lateral chest roentgeno-
grams, respectively. These distances are corrected to true
spatial x,y,z coordinates of each metallic tag.

This magnification correction was facilitated by transferring the
x',y',z' coordinates of each tag from paired orthogonal roentgenograms
into a CDC 3500 digital computer via an electronic plotting table and
an analog-to-digital converter. The accuracy of the x-ray, plotting
table, computer computational and display systems was assessed by the
double-blind determination of distances between beads placed obliquely,
known distances apart, in the space transirradiated by the biplane
orthogonal x-ray system. These results are shown on Figure 6.

COMPARISON OF ACTUAL vs ROENTGENOGRAPHIC
MEASURED DISTANCE BETWEEN RADIOPAOUE
BEADS DISTRIBUTED IN SPACE TRANSRADIATED
BY ORTHOGONAL BIPLANE X-RAY SYSTEMS
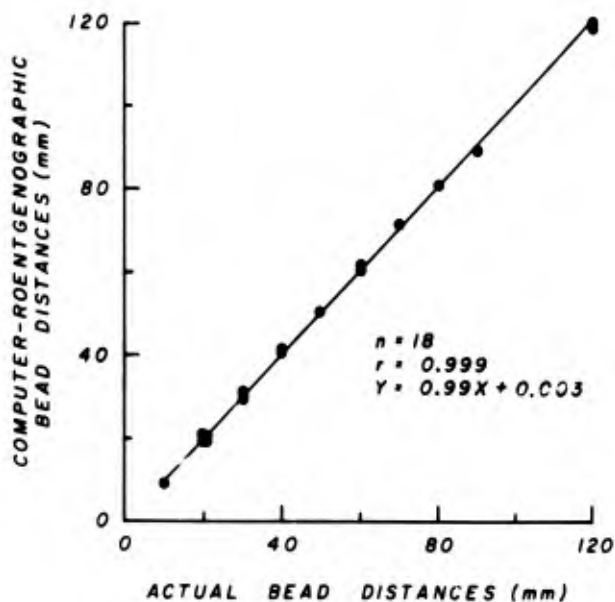
Figure 6. Metallic tags were placed known distances apart along a
straight line passing obliquely through the space trans-
irradiated by the biplane orthogonal system. The actual
versus computer-roentgenographic measurement of the bead
separation is shown.

Using this system, the shift in pulmonary parenchymal tags following changes in body position can be examined, as shown in Figure 7.
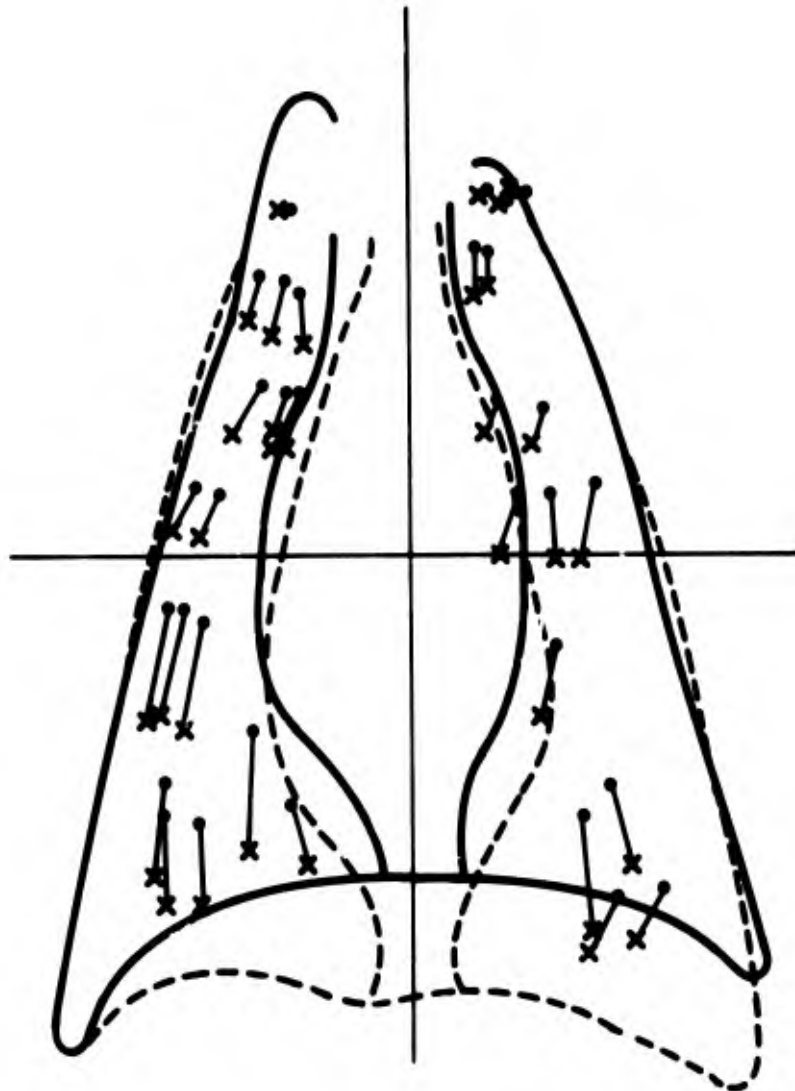
Figure 7. Shift in pulmonary parenchymal tags following a change from prone (•) body position to the head-up (x) body position. Lung at functional residual capacity in both body positions. Solid lines connect corresponding tag positions along their presumed path of movement.

This is the computer-generated plot of lung bead motion during a shift from the prone to the head-up body position with the measurements made at functional residual capacity. The pulmonary parenchymal tag positions at end-inspiration in three dogs in the head-up and head-down positions are shown in Figure 8.

REGIONAL DISPLACEMENT OF LUNG PARENCHYMAL TAGS
AT FRC DURING CHANGE IN BODY POSITION
FROM PRONE TO HEAD-UP AND HEAD-DOWN POSITIONS

(3 Dogs, Morphine-Pentobarbital Anesthesia, 37-40 Tags/Dog)
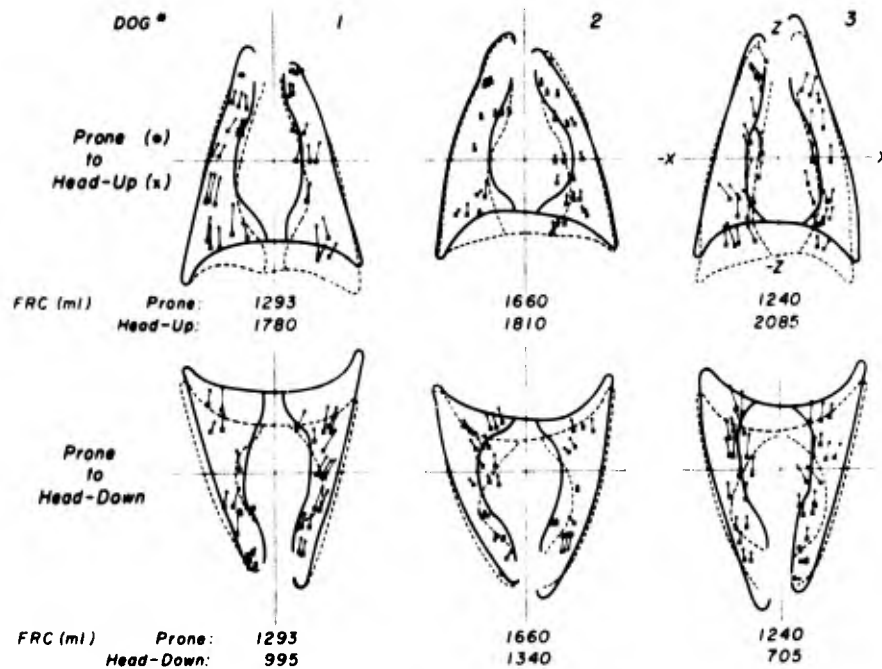
Figure 8. Regional changes in position of lung parenchymal tags at end-expiration during change in body position from prone to head-up position (upper panel) and prone to head-down position (lower panel). Parenchymal shifts in 3 dogs are shown along with individual measurements of functional residual capacity (helium dilution method) in each body position. The influence of the position and shape of the respiratory diaphragm in determining the spatial position of lung parenchyma is evident in this figure.

111

It is apparent that the weight of the abdominal contents and their in-
fluence on diaphragm position greatly influences the spatial distribu-
tion of the pulmonary parenchyma. In all dogs in both head-up and
head-down positions, the parenchymal tags moved downward relative to
T_6 spinous process. The functional residual capacity determined by the
helium dilution method increased in all dogs upon movement from the
prone to head-up position and decreased upon moving from the prone to
head-down position. Note that the parenchymal tag motion closely paral-
lels diaphragm motion and that the position of the chest wall is rela-
tively unchanged. Note also that there is an increased gradient of
movement from the apex to the diaphragm.

We next examined the effect of a spontaneous inspiration upon the
spatial distribution in the head-up, prone, and head-down positions.
The typical changes in position of the parenchymal tags in one dog in
the head-up and head-down positions following inspiration are shown in
Figure 9.

COMPARISON OF REGIONAL DISPLACEMENT OF LUNG PARENCHYMAL TAGS DURING SPONTANEOUS INSPIRATION IN THE HEAD-UP AND HEAD-DOWN POSITIONS

(Dog-21.5 kg, Morphine-Pentobarbital Anesthesia)

Dorsal-Ventral Projections
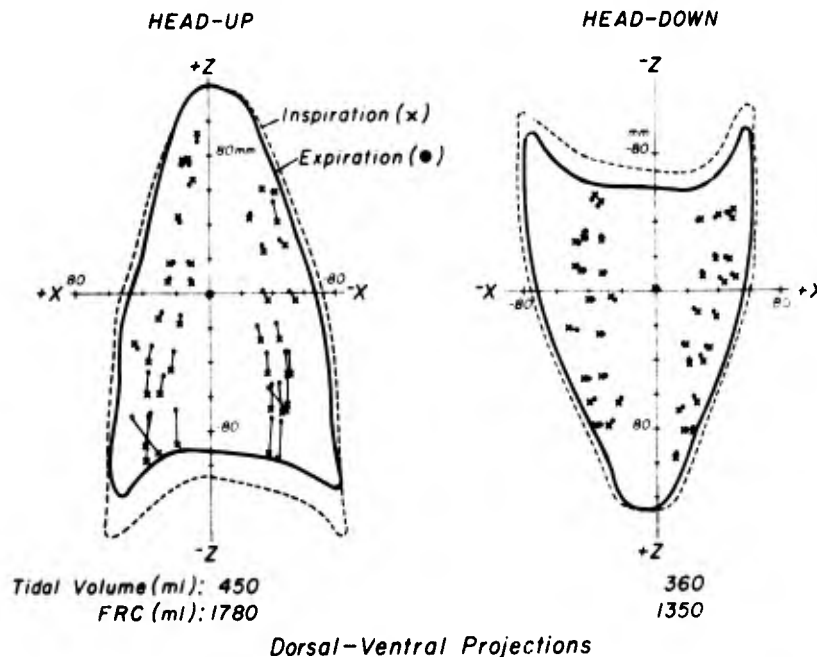
Figure 9. The effect of spontaneous inspiration on the regional dis-
placement of lung parenchymal tags in one dog in the head-
up (left panel) and head-down position (right panel) is
shown. The parenchyma shifts from its positions at expira-
tion (•) to the corresponding position at inspiration (x)
along the paths indicated by the connecting lines. The

112

positions of the diaphragm and abdominal viscera influence movement of the lung parenchyma during respiration.

In general the dog's respiratory tidal volume was decreased in the head-down position but the percent volume change from functional residual capacity was approximately the same in the two positions. There was less caudal displacement of the tags in the head-down than in the head-up positions. This is compensated for to some extent by a more lateral displacement of the parenchymal tags during inspiration in the head-down position. Movement of the parenchymal tags following inspiration in the prone dogs was intermediate between these two patterns.

Finally we examined the pattern of parenchymal tag movement following both spontaneous inspiration and positive-pressure inflation. In all body positions the direction of tag movement following positive-pressure inflation of the lungs or spontaneous inspiration were similar (Figure 10).

COMPARISON OF DISPLACEMENT OF LUNG
PARENCHYMAL TAGS FROM FRC DURING SPONTANEOUS
INSPIRATION AND POSITIVE PRESSURE INFLATION

(Dog-21.5 kg, Morphine—Pentobarbital Anesthesia, Prone Position)

Tidal Volume
(ml)

FRC ●—		
20 cm H$_2$O IPPB o---	480	
Spontaneous Inspiration ✕–	360	
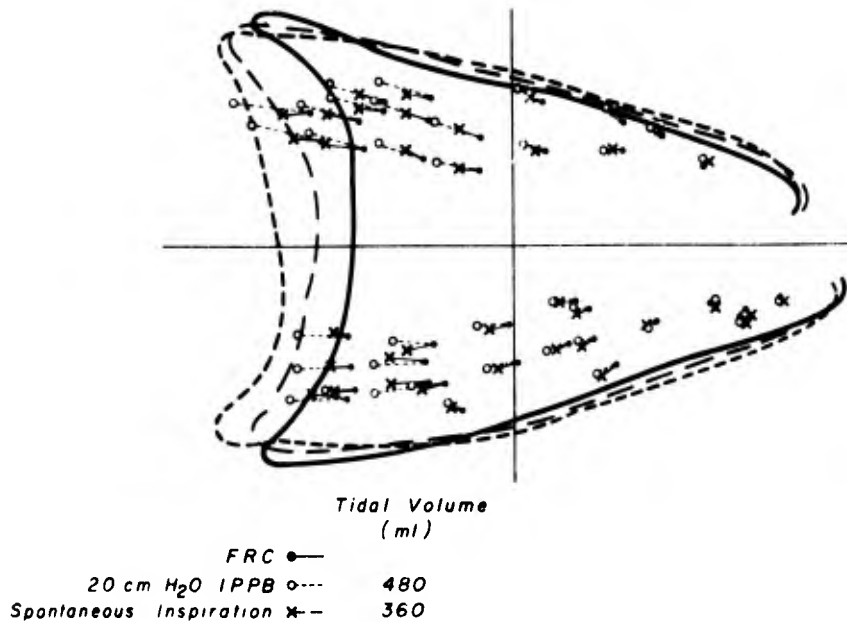
Figure 10. The pattern of parenchymal tag movement during both spontaneous inspiration and 20 cm H$_2$O positive-pressure inflation of the lung are shown in one dog in the prone position.

113

This figure shows parenchymal tag movement in a prone dog during a spontaneous and a 20-cm H_2O positive-pressure inflation of the lungs. Only the magnitude of the bead movement differs and this is proportional to the difference in tidal volume under the two conditions.

Summary

A method for determining regional pulmonary parenchymal movements in the intact animal is described. Preliminary descriptive evidence indicates that the weight of the abdominal viscera significantly influences regional pulmonary displacement, and should be considered in any estimation of the spatial distribution of the pulmonary parenchyma. This method also allows calculations of changes in regional lung volumes which, together with regional pleural pressure determinations, may provide information regarding regional lung compliance in the intact animal. Use of this lung parenchymal tagging procedure for quantitative analysis of changes in regional pulmonary volumes during changes in body position and changes in the magnitude of the gravitational-inertial force environment has been carried out by Greenleaf and co-workers (1).

References

1. Greenleaf, J. F., et al. Effect of changes in the magnitude and direction of the force environment on regional distortion of lung parenchyma in dogs. Physiologist 14:196 (1971).

SECTION VIII

Effect of Changes in the Magnitude and Direction of the Force Environment on Regional Distortion of Lung Parenchyma in Dogs

Methods and Results

The lung is a very mobile and compliant organ that readily conforms to normal changes in shape and volume of the thorax. When an animal is exposed to an increased force environment, inertial forces generated within the lung should produce regional displacements and deformations of the parenchyma depending upon the magnitude and direction of the force environment and the regional mechanical properties of the lung. However in a minimally supported animal, inertial forces may also alter the contour and position of the respiratory diaphragm and displace the mediastinum and chest wall. As demonstrated in the previous section, movement of structures adjacent to the lungs can displace lung parenchyma at some distance away. Hence, in order to study regional changes in position of the lung which are mainly due to inertial forces generated within the lung itself, the animal should be supported in such a way that inertial movements of the chest wall and abdomen are minimized without interfering with movements which are a part of normal respiration. Immersion in water is a practical method of body support which largely satisfies these requirements.

The purpose of the present study was to determine the inertial displacements of the lung in anesthetized dogs exposed to 1 and 7G force environments with the dogs breathing room air in a water-immersion respirator, providing control of respiratory rate, and tidal and residual lung volume. Regional changes in position and volume of the pulmonary parenchyma were determined by first percutaneously implanting 30-40 1-mm metallic markers in the lung parenchyma, and then determining the relative changes in position of the markers using a biplane roentgenographic technique developed in this laboratory by Smith and coworkers (1). Details of the methods are given in Section VII.

The dogs were anesthetized with morphine and sodium pentobarbital, and catheters were percutaneously introduced and positioned in the main pulmonary artery, thoracic aorta, and right and left pleural spaces. The dogs were then placed on their left side in the water-immersion respirator described in Section II and the volume of saline in the tank adjusted until the alternating positive and negative pressures generated over the body surface by the respiration pump balanced around zero at midlung. Residual lung volume under these conditions was about 1,000 ml respiration rate was adjusted to about 8 breaths per minute, and tidal volume to about 350 ml.

Movements of a total of 90-120 markers in three animals were averaged in relation to an x,y, and z rectangular coordinate system with the origin at the midpoint of the body of the sixth thoracic vertebra.

This point is approximately at the center of the thorax as viewed in an anteroposterior thoracic roentgenogram.

The position of each parenchymal tag, and the outlines of the lung borders in relation to the origin of the coordinate axes were fed into a CDC 3500 computer by means of an electronic cursor device. The computer was programmed to divide the lung mathematically into 25 parallelepiped corridors, arranged in a 5 x 5 array. The positions of the tags in each corridor, 3 cm x 4 cm on a side extending from the ventral to the dorsal surface of the lungs, were projected onto the coronal plane of the thorax. The position of the tags in similar corridors, 3 cm x 3 cm on a side extending from the caudad to cephalad surfaces of the lung, were projected onto the transverse plane of the thorax. Since the resultant vector of inertial forces should lie in both planes, these projections portray the distribution and movement of the parenchymal tags in relation to the vertical height in the thorax.

In Figure 1, the average shifts in positions of the beads within each corridor are represented by arrows with the tail of each arrow, representing the position at functional residual capacity, centered within its corridor as it is projected onto the plane of interest.

The standard error of the mean changes in position in the cephalocaudad and right-to-left directions are indicated by the respective lengths of the bars of the crosses at the ends of each line. No cross indicates there was only one sample.

Note the effect of the downward displacement of the diaphragm, during inspiration, in shifting the lung parenchyma. The tags moved caudalward in all regions and lateral-ward in the lateral regions of the lung during inspiration in the normal 1G environment. The cross-sectional projection indicates that during inspiration, the lung parenchyma shifted in the ventral direction from its position at functional residual capacity.

This figure portrays only the changes in position of parenchymal tags located in different regions of the lung. However, the changes in regional volumes of the lung with respiration or due to an increased inertial force environment are also of interest. Regional volumes were calculated by taking pairs of markers falling within each corridor to represent diametrically opposite points on a sphere of parenchyma. The percent change in volume of this sphere between two states of interest was then taken to represent the regional change in volume. Volumes were calculated for all combinations of two markers falling within each corridor for each dog, and the average percent volume change with its standard error was calculated for each corridor.

116

CHANGES IN POSITION OF LUNG PARENCHYMAL TAGS DURING RESPIRATORY CYCLE IN WATER-IMMERSION RESPIRATOR

3 Dogs, Morphine-Pentobarbital Anesthesia, Left Decubitus Position
(+) SE of Inspiratory Change In Y and Z Coordinates
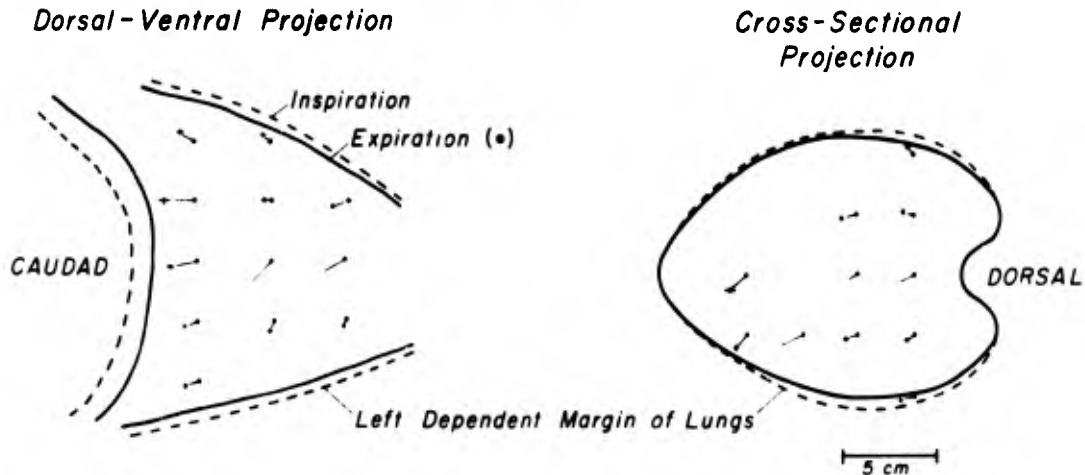
Figure 1. Mean and standard errors of changes in position of lung parenchymal tags during the respiratory cycle of 3 anesthetized dogs in a water-immersion respirator. The tidal volume and respiratory rate were held constant at 480 ml and 12 breaths per minute, respectively.

The regional changes in volume calculated from the changes in position, shown in Figure 1, from functional residual capacity to end-inspiration are shown in Figure 2. The circles with a continuous outline all have the same diameter, representing the control state (in this case end-expiration, i.e., FRC), and are centered in their respective corridor. The circles with dashed outline and varying diameters represent the volume at the second state (end-inspiration) and are centered on the position to which the control element moved. The numbers represent the percent change in volume ± one standard error. The absence of a standard error value indicates that only one pair of markers was found in that corridor.

Note the distribution of percent change in volume is relatively uniform in the dorsal-ventral projection with no discernible regional pattern. The cross-sectional projection indicates a like result.

_17

CHANGES IN POSITION OF LUNG PARENCHYMAL TAGS DURING
RESPIRATORY CYCLE IN WATER-IMMERSION RESPIRATOR

3 Dogs, Morphine-Pentobarbital Anesthesia, Left Decubitus Position
(+) SE of Inspiratory Change In Y and Z Coordinates

Dorsal-Ventral Projection

Cross-Sectional
Projection

Inspiration (+)
Expiration (●)
59±70
70±18
104±6
18
CAUDAD
82±7   20±11
50±7
66±12
Left Dependent Margin of Lungs

40±4
62±12
120±19
3
54±21   DORSAL
56±4
65±12

50±10   Change in Volume (% ± SE)

Position
Area
Exp.   Insp.

5 cm
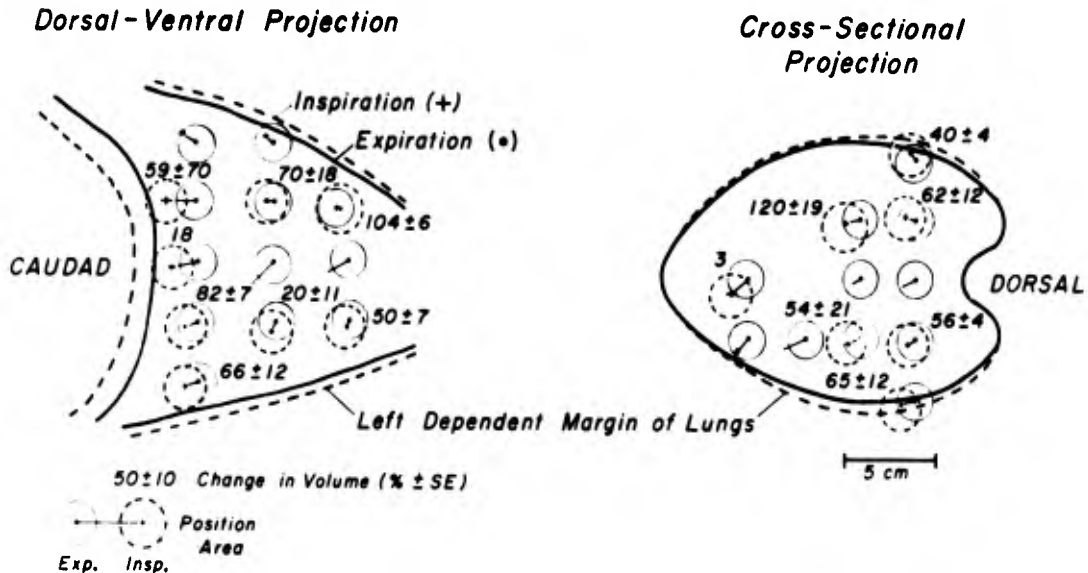
Figure 2. Means and standard errors of changes in position of lung
parenchymal tags, and calculated percentage change in regional
lung volumes during the respiratory cycle of 3 anesthetized
dogs.

In order to discuss the respiratory changes during exposure to
an inertial force environment 7 times normal, we will first indicate
the effect of increased inertial forces on the lung parenchyma when the
animal is at functional residual capacity under these two conditions.

Figure 3 illustrates the average regional change in position and
volume of lung parenchyma at end-expiration during a 1-minute exposure
to a force environment of $7G_y$.

The solid circles and dots represent the 1G control state and the
dashed circles and standard errors the 7G state.

Note the loss of volume in the dependent portion of the lung and
the gain of volume in the superior portions, and the general shift of the
parenchyma in the cephalad direction in the dependent lung and concomi-
tant caudad shift superiorly caused by this increased inertial force
environment.

118

EFFECT OF INCREASED FORCE ENVIRONMENT ON REGIONAL POSITION OF LUNG PARENCHYMAL TAGS AND CALCULATED REGIONAL VOLUMES AT END-EXPIRATION IN WATER-IMMERSION RESPIRATOR

3 Dogs, Morphine-Pentobarbital Anesthesia, Left Decubitus Position
(+) SE of $1G_y$ to $7G_y$ Change in Y and Z Coordinates
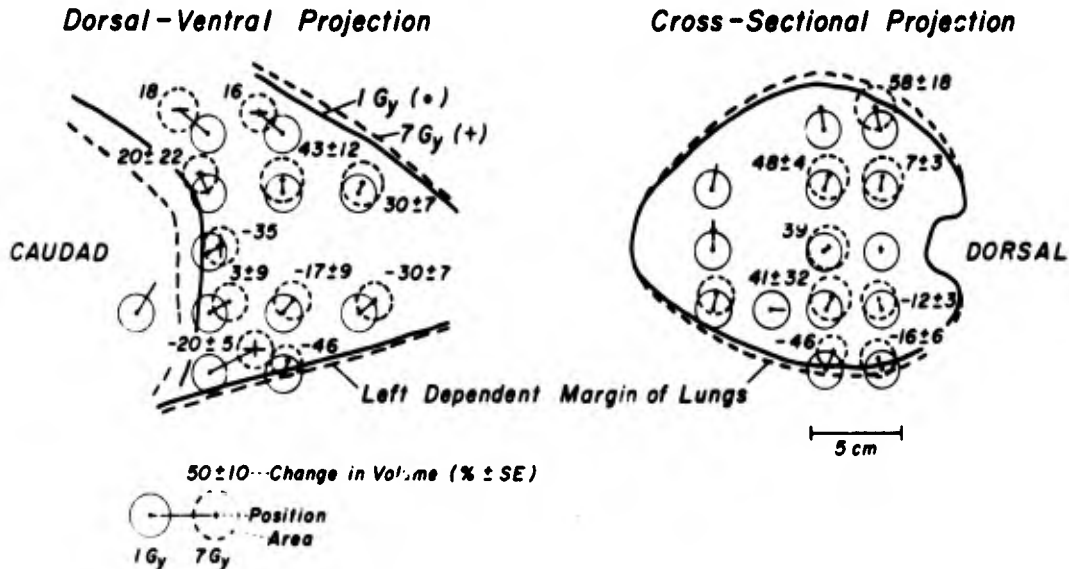
Figure 3. Means and standard errors of changes in position of lung parenchymal tags, and calculated percentage changes in regional lung volumes at end-expiration in 3 anesthetized dogs produced by an increase in the gravitational-inertial force environment from 1 to 7G. See legend of Figure 1 and text for additional details. Note the decrease in dependent regional volumes and the increase in regional volumes in the superior regions of the lung in accord with the results shown in Figure 5.

The cross-sectional projection indicates an almost vertically downward displacement of the parenchyma, again with a loss of volume in the dependent region and an increase in the superior region.

Figure 4 shows the regional change in parenchymal position and volume with inspiration during an inertial force environment 7 times normal. Note the larger change in volume in a region slightly above the midlung and the relatively small or no change in volume in most of the dependent regions.

119

Note as well that the parenchyma tends to shift both caudally and in the dependent direction during inspiration rather than evenly toward the diaphragm and bilaterally as in the 1G case.

CHANGES IN POSITION OF LUNG PARENCHYMAL TAGS AND
CALCULATED REGIONAL VOLUMES IN RESPIRATORY CYCLE
DURING EXPOSURE TO FORCE ENVIRONMENT OF $7G_y$ IN
WATER-IMMERSION RESPIRATOR

3 Dogs, Morphine-Pentobarbital Anesthesia, Left Decubitus Position
(+)SE of Inspiratory Change in Y and Z Coordinates
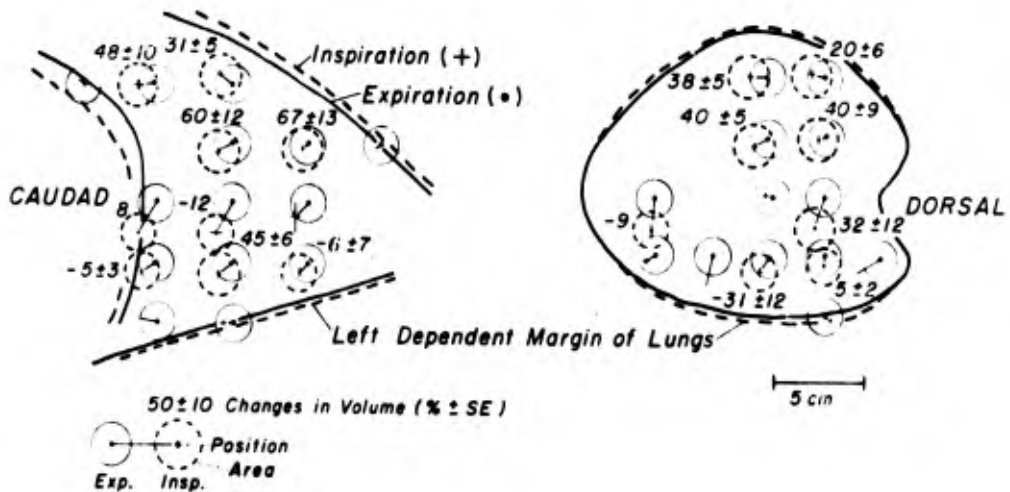
Figure 4. Means and standard errors of respiratory changes in posi-
tion of lung parenchymal tags, and calculated percentage
changes in regional lung volumes of 3 anesthetized dogs dur-
ing exposure to a force environment of $7G_y$. Note that the
largest increase in volume during inspiration (regional ven-
tilation) occurred near the midregions of the thorax where
blood flow is also increased.

To facilitate study of changes in regional volume in relation to
vertical height in the thorax, the lung was divided into 10 sagittal
sections each 1.5 cm thick, and the average change in volume in each
sagittal section was projected onto the coronal plane in order to
obtain a plot of change in regional volume versus vertical height in
the thorax. The regional changes in volume with inspiration in the
normal 1G gravitational force environment are shown in Figure 5.

120

REGIONAL VENTILATION
AT 1G
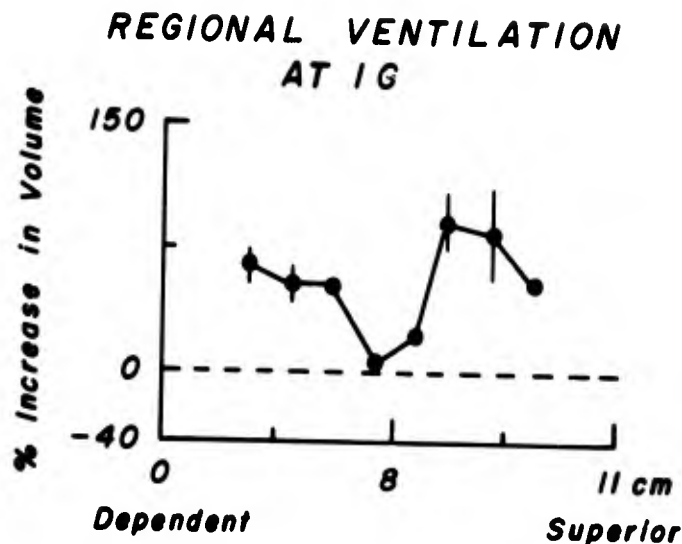
Figure 5. Mean   change in volume during respiration at 1G within 10
1.5-cm-thick sagittal sections for 4 water-plethysmograph-
ventilated dogs. Volumes were calculated for all pairs of
markers representing diameters of spheres having greater
than 1 and less than 10 cm^3. Those falling within each sec-
tion were averaged; the dots are the means, and bars the
standard errors. No standard error indicates only one
sample (i.e., one pair of beads) was found in that section.
Note that the left and right regions (dependent and superior,
respectively) are equally ventilated and that the midregions
were less well ventilated.

Note that the inspiratory changes in regional volumes (regional
ventilation) of the dependent left lung and superior right lung were
not significantly different.

The regional changes at end-expiration caused by an exposure to 7
times the normal gravitational-inertial force environment are shown in
Figure 6.

As would be expected on the basis of the great differences in spe-
cific gravity of the air-containing alveoli and the surrounding elastic
parenchyma and mobile blood, there is a striking increase in regional
volumes in the superior region and a decrease in the dependent region of
the lung. The isovolume region appears to be near midlung or slightly
above.

121

CHANGE IN VOLUME AT FRC
7G-1G
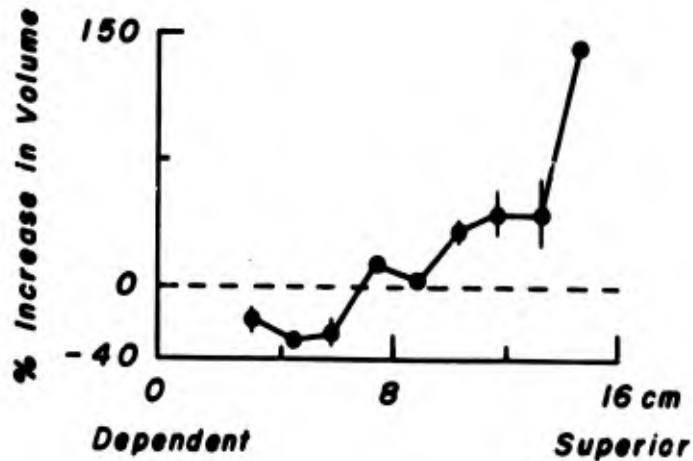
Figure 6. Mean change in FRC in ten 1.5-cm-thick sagittal sections due to increase in acceleration from 1G to 7G in 5 dogs while ventilated with a water plethysmograph. The graphical format is described in the legend of Figure 5. Regional FRC tended to decrease in dependent regions while it increased in superior regions. There was apparently no change in FRC in the midregion of the lung.

Figure 7 indicates that at 7 times the normal gravitational force environment, the change in regional volume during inspiration is greatest at the midregion of the lung. It is particularly noteworthy that this region is at approximately the same vertical height in the thorax, where the regional changes in volume at end-expiration with changes in the force environment are minimal (Figure 4), and at which prior studies have demonstrated the level of pleural and circulatory pressures to be relatively independent of the force environment and where regional blood flow is maximal during exposures to higher force environments.

REGIONAL VENTILATION
AT 7G
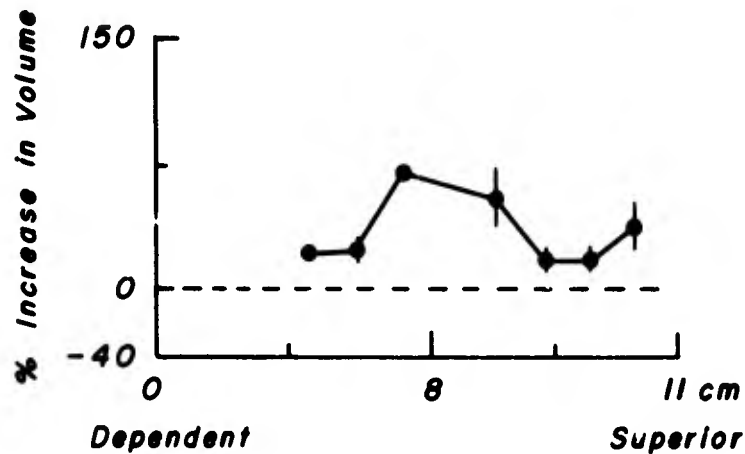
Figure 7. Mean change in volume in ten 1.5-cm-thick sagittal sections
during exposure to 7G in a water plethysmograph. Graphic
format is described in the legend of Figure 5. The percent
change of volume was higher in the midregion of the lung
than in the superior or dependent regions. The area of great-
est ventilation corresponds to the region where FRC was
least changed due to acceleration (Figure 6).

These data indicate that under conditions of increased acceleration
the lung parenchyma tends to shift as though it consisted of bubble-like
buoyant chambers somewhat free to float upward. Calculated changes in
regional volume based on differences in displacement of adjacent lung
parenchymal tags indicated that large increases in regional volume in
superior regions of the lung occur during exposures to an increased
force environment; concomitantly striking decreases occur in regional
volumes in dependent regions.

The calculated changes in regional volume during inspiration indi-
cate that ventilation is shifted into the midregion of the lung during
exposure to high force environments.

References

1. Smith, H. C., et al. Effect of inflation levels and body position
changes upon regional pulmonary parenchymal movement in
dogs at 1G. Physiol. 14:232 (1971).

123

SECTION IX

Gas Embolism Due to Intravenous Injection of FC 80 Fluorocarbon

Gollan and Clark (1) first reported that lethal gas embolism follows the intravenous injection of 1 ml unemulsified FC 75 in dogs. The gas was sampled from the right atrium and found to consist of about 65% nitrogen, 10% oxygen, and 9% carbon dioxide; the undetermined remaining gas was assumed to be fluorocarbon and water vapors. Beisang et al. (2) found gas embolism within about 5 hours after an intravenous injection of FX 80 fluorocarbon in dogs. Both groups of investigators attributed the gas embolism to the evaporation of fluorocarbon within the circulatory system.

However, the development of gas bubbles in the circulation after the intravenous administration of FC 75, FX 80, or FC 80 fluorocarbon liquids in experimental animals has not been a constant finding. Clark and Gollan (3) reported that mice survive the intravenous injection of 2 ml of FX 80. Nose et al. (4) injected 0.1 ml/kg intravenously in two dogs; the dogs died 48 and 60 hours after the injections with extensive hemorrhages and severe edema of the lungs, but gas embolism was not found in either animal. Sloviter et al. (5) injected a 20 kg dog with 2 ml of dispersed FX 80 and measured a rapid increase in right atrial pressure in the dog. They concluded that the elevated pressure was due to multiple platelet microemboli which reached the lungs and caused right heart failure and anoxia. Geyer (6) found that the intravenous injection of 4.0 ml FX 80 per kg body mass was lethal within 1-2 minutes in rats and mice, either anesthetized or unanesthetized. Intravenous gas was not found at autopsy. In this same study, rats were injected intravenously with a stable dispersion of FX 80 and the animals died about 5 hours later with over-distended chests. At autopsy, the lungs were bloated and appeared to have caused the over-distended chest and to have caused death of the animal by suffocation. Other tissues, including the heart, were not affected. Dispersion of other fluorocarbon liquids produced the same effect, and since all of the fluorocarbons which gave rise to the bloated lung syndrome had high vapor pressures, Geyer concluded that bubbles of vapor possibly were arising in vivo and accumulating in the lung. However, little FX 80 vapor was detected in the foam collected from the lungs; Geyer concluded that vapor pressure alone could not explain these effects of FX 80.

Gollan and Clark (1) also found over-distended lungs within 2-4 hours and lasting for about one week after puppies had breathed FC 75. These investigators found virtually no FC 75 in the tissues of mice which had survived the breathing of this liquid. However, Holaday (7) initially estimated that a total of 0.5 ml FX 80 is absorbed in the blood and other body tissues of a 15 kg dog after breathing this liquid for one hour, but in a later study estimated that a total of 450 mg (approx 0.25 ml) of FC 80 is absorbed by a 13.8 kg dog after breathing this liquid for 8 hours, and a total of 1.25 g (approx 0.85 ml) when the

125

Preceding page blank

tissues of the dog are fully saturated with FX 80 (8). In studies in our laboratory, gas embolism was not found at autopsy in any of the 17 dogs that breathed FC 80 for 4 hours or longer and is not mentioned in any studies of animals which had breathed oxygenated fluorocarbon liquids (1,3,7-18).

Studies performed in this laboratory have shown that:

1. Lethal gas embolism occurs within 3/4 to 3 1/2 hours (usually 3/4 to 1 1/4 hours) after the intravenous injection of 0.1 ml FC 80/kg body mass in anesthetized dogs breathing room air, but not in anesthetized dogs breathing oxygenated liquid FC 80 for periods as long as 16 hours;

2. Gas sampled immediately after death from the right ventricle of dogs who died of gas embolism following the intravenous injection of FC 80, was found to consist of FC 80 at its vapor pressure along with oxygen and carbon dioxide at tensions equivalent to their respective tensions in venous blood sampled immediately before death.

3. FC 80 appears in the blood and other body tissues in dogs breathing this liquid. Saturation of the blood with FC 80 is complete within 15 to 30 minutes of liquid breathing. Holaday et al. have reported that the concentration of FC 80 in the blood reaches a plateau in 15 minutes (8).

Figure 1 illustrates some typical changes in arterial blood gas tensions and pH in a dog following a slug injection of 0.1 ml FC 80/kg (FC 80 fluorocarbon) into the right atrium.

BREATHING AIR: BREATHING 100% OXYGEN:

Spontaneous   IPPB   IPPB
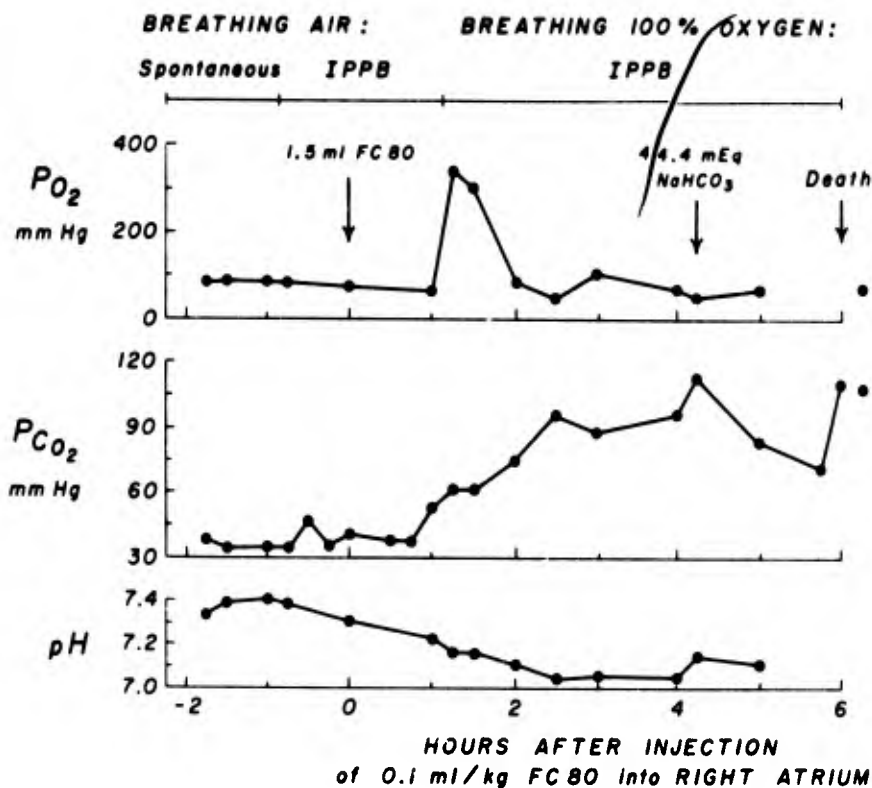
Figure 1. Arterial blood gas tensions and pH in a dog injected with
           1.5 ml unemulsified FC 80 liquid fluorocarbon into the right
           atrium. The dog was prone in a molded fiberglass half-body
           cast and ventilated with intermittent positive pressure
           (IPPB) using a Bird Mark VII respirator. Skeletal muscle
           paralysis was maintained at all times by periodic intravenous
           injections of succinylcholine. Catheters had been intro-
           duced percutaneously and positioned in the pulmonary artery,
           thoracic aorta, and right atrium for recording pressure and
           sampling. (15 kg dog sodium pentobarbital anesthesia).

Approximately one hour after the injection of FC 80, arterial P_{CO_2} in-
creased to 53 mm Hg, pulmonary artery pressure increased to 80/50, and
ventilation of the animal was changed from room air to 100% oxygen.
Arterial blood P_{O_2} increased at first but then returned to values nearly
equal to those measured when the dog was breathing room air. Arterial
P_{CO_2} progressively increased and arterial pH concomitantly decreased
over the next few hours. Both variables were only partially corrected
by intravenous administration of sodium bicarbonate. Pulmonary artery
pressure remained elevated. The dog died 6 hours after the injection
of FC 80 with free gas distending the right atrium and ventricle, with

127

foamed blood in the pulmonary artery, right heart, and venae cavae. There was very little blood and no free gas in the left atrium or ventricle. The lungs were normal to gross and microscopic examination.

Approximately 35 ml of gas was collected into a Haldane gas collection apparatus by needle aspiration of the right ventricle. One ml of this gas was then diluted to 500 ml with room air in a calibrated 1,500 ml plexiglass syringe and the concentration of FC 80 in the diluted gas was determined using a gas chromatograph. Repeated measurements of FC 80 concentration on repeated diluted samples of the gas contained in the Haldane apparatus averaged 0.51 mg FC 80 per liter of gas sampled from the right ventricle. Oxygen and carbon dioxide tensions in this gas were measured with an IL 313 blood gas analyzer.

If a molecular weight of 416 is assumed for FC 80, (which has the formula $C_8F_{16}O$), then the partial pressure exerted by 0.51 gram of FC 80 per liter of gas at 24°C can be computed as:

$$V = NRT$$

$$= \frac{0.51 \; \dfrac{\text{gram FC 80}}{\text{liter}}}{416 \; \dfrac{\text{gram FC 80}}{\text{mole}}} \times 62.4 \; \frac{\text{liter-mm Hg}}{\text{mole-}^\circ K} \times 297^\circ K$$

$$= 22.4 \; \text{mm Hg}$$

This compares favorably with measurements of the vapor pressure of FC 80 supplied by Allied Chemical Corporation, and with vapor pressure data for FC 75 (industrial grade fluorocarbon similar to FC 80) published by the 3M Company (20). See Figure 3.

Thus, the gas sampled from the right ventricle in this dog, immediately after death, had the following composition.

P_{O_2}	= 66 mm Hg
P_{CO_2}	= 108 mm Hg
P_{H_2O}	= 23 mm Hg (at 24°C)
$P_{FC\;80}$	= 22 mm Hg (at 24°C)
*P_{N_2}	= 516 mm Hg
P_{bar}	= 735 mm Hg

(*Estimated: $P_{N_2} = P_{bar} - P_{O_2} - P_{CO_2} - P_{FC\;80}$) (19).

Figure 2 plots the concentration of FC 80 in blood sampled simultaneously from the aorta and pulmonary artery of a dog breathing oxygenated FC 80 liquid fluorocarbon for over 16 hours. One and one-half hours after the start of liquid breathing, 0.1 ml FC 80/kg was injected via a catheter positioned in the left renal artery. The concentration of FC 80 in mixed venous (pulmonary artery) blood reached the plateau value of approximately 850 µg/100 ml within the first 15 to 30 minutes of liquid breathing and changed little following the injection of FC 80 into the

128

renal artery. The concentration in arterial blood (aorta) was consistently equal to or greater than the concentration of FC 80 in simultaneous samples of mixed venous blood. The dog died shortly after the 16th hour of liquid breathing. Gas was not found in the chambers of the heart nor were gas bubbles visible at any site in the circulatory system. Aortic and pulmonary artery pressures were within normal limits until 15 minutes before the animal died.

Platelet counts in blood sampled from the pulmonary artery are also plotted in Figure 2. We attribute no significance to the minor variations in the platelet counts measured during the 23 hours of gaseous and liquid ventilation and include them for reference only.

BLOOD FC 80 CONCENTRATION AND PLATELET COUNTS
DURING LIQUID BREATHING AND FOLLOWING INJECTION
OF FC 80 INTO LEFT RENAL ARTERY

(Dog, 14 kg, Morphine - Pentobarbital Anesthesia)
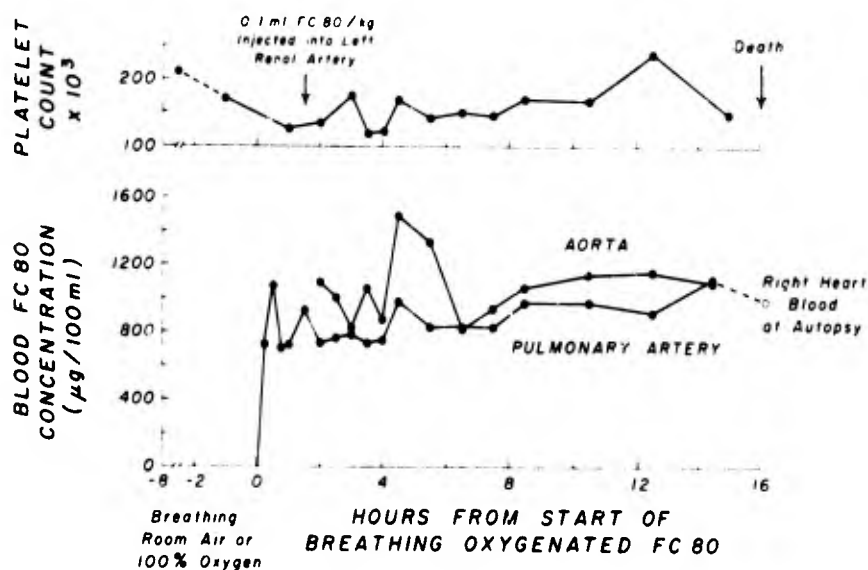
Figure 2. Platelet counts and concentration of FC 80 in blood sampled simultaneously from the aorta and pulmonary artery in dog breathing first air or 100% oxygen, and then oxygenated FC 80 liquid fluorocarbon. Left lateral decubitus dog in water-immersion respirator, fluorocarbon oxygenator assembly described in Section V. Skeletal muscle paralysis was maintained by periodic intravenous injections of succinylcholine. Catheters had been introduced percutaneously and positioned under fluoroscopic guidance into the left renal artery, pulmonary artery, thoracic aorta and right atrium for injection of fluorocarbon, blood sampling, and pressure recording. 0.1 ml FC 80/

129

kg was injected into the left renal artery where indicated
by the arrow. (14 kg dog, sodium pentobarbital anesthesia).

Tissue samples were obtained at autopsy, immediately placed in hex-
ane, and analyzed for FC 80 concentration with the gas chromatograph
according to the method of Holaday (7,8). The results are shown in
Table XVI of the Appendix. Assuming a kidney mass of 50 grams and uni-
form concentration of FC 80 throughout the kidney, approximately 0.50
grams or about 20% of the fluorocarbon injected into the left renal ar-
tery was retained by the left kidney. The concentration of FC 80 in
urine sampled periodically from a catheter in the bladder throughout
the 16 hours of liquid breathing, and at autopsy, was always zero. The
solubility of FC 80 in saline was determined for reference as follows:
10 ml of physiologic saline and 1 ml of FC 80 were agitated vigorously
together in a test tube and two liquids were allowed to stand in con-
tact with each other in the tube overnight at 25°C. Approximately 8 ml
of the saline was then carefully removed with a pipette, and the saline
aliquot was centrifuged at 4,600 rpm for 45 minutes (25°C). The con-
centration of FC 80 in the upper portion of this aliquot of saline was
then determined, and the value shown in Table XVI is the solubility of
FC 80 in saline at 25°C.

The fact that the concentration of FC 80 in the blood reached a
plateau shortly after the start of liquid breathing and changed little
after the injection of FC 80 into the renal artery, indicates that the
blood was saturated with FC 80 during most of the liquid breathing pe-
riod. If the fluorocarbon dissolved in the blood is assumed to exert
the same vapor pressure as pure FC 80 at 37°C, then the estimated ten-
sions of the respiratory gases and vapor tensions of water and fluoro-
carbon in systemic arterial and mixed venous blood when dogs breathe air,
oxygen, or liquid FC 80 are shown in Table XVII of the Appendix. Anal-
yses of the total gas tensions in the blood of animals may explain why
gas embolism occurs after dogs are injected with FC 80 intravenously
while breathing air, and why gas embolism may not occur after the same
dose when dogs are breathing oxygenated FC 80. Thus, when the animal
breathing room air is injected with FC 80, the total vapor pressure of
the respiratory gases, water, and FC 80 in mixed systemic venous blood
is approximately 744 mm Hg. Mean right atrial pressure is typically
only a few mm Hg different from atmospheric and, therefore, the total
gas tension in right atrial blood will exceed the mean absolute pressure
of right atrial blood by about 7 mm Hg (4 mm Hg + mean right atrial
pressure of about 3 mm Hg).

Free gas probably does not evolve in the systemic arteries because
the total gas tension in arterial blood (approx 795 mm Hg) does not ex-
ceed the absolute arterial blood pressure of about 840 mm Hg (740 mm Hg
+ mean arterial pressure of about 100 mm Hg) of a lateral decubitus dog.

Data in the table also suggest why gas embolism does not occur in
dogs breathing FC 80 fluorocarbon. When an animal is ventilated with
oxygenated FC 80 in the water-immersion respirator, the lowest ambient

130

pressure impressed on the animal occurs during inspiration when body surface pressure reaches its minimum value of about 60 mm Hg below atmospheric. Thus, when an animal is injected intravenously with FC 80 while breathing FC 80 in the respirator, the total gas tension in either venous or arterial blood is less than the lowest absolute blood pressure in the circulatory system, and free gas does not evolve. All of our animals were switched at the end of the liquid breathing studies to ventilation with 100% oxygen. Reference to the table shows that the total gas tensions in venous blood is roughly the same when a dog breathes either oxygen gas or oxygenated FC 80, and is appreciably less than the absolute blood pressure in the venous circulation. The total gas tension in arterial blood is greater when the dog breathes 100% oxygen compared with oxygenated FC 80, but still less than absolute arterial blood pressure, assuming a normal arterial pressure. Thus, the animal is protected against gas embolism in arterial and mixed venous blood when the animal breathes either 100% oxygen or oxygenated FC 80, but is not protected from gas embolism appearing in the pulmonary blood when breathing 100% oxygen. We have found that dogs can survive up to 7 hours after the intravenous injection of 0.1 ml FC 80 when the animals breathe 100% oxygen, but survive no longer than 3 1/2 hours after the same dose of FC 80 when they breathe room air.

The lower half of the table shows the total gas tensions which are estimated to occur in dogs breathing air in a 3 ATA environment. As the ambient air pressure is increased, the tendency for gas to evolve from the mixed venous blood is decreased. To determine whether or not a hyperbaric environment can protect dogs from gas embolism due to FC 80 injected into the circulatory system, dogs were injected intravenously with FC 80 and exposed to up to 3 ATA breathing compressed air, and up to 9 ATA breathing 5% oxygen 95% helium. A Bethlehem model 1836 Hp hyperbaric chamber was used in these experiments. All of the dogs died within 6 hours, regardless of the ambient pressure. As illustrated in Table XVII, the total gas tension in the end-pulmonary capillary blood exceeds the total hydrostatic pressure in the pulmonary capillary bed and free gas should evolve at this site. Therefore, neither increase in ambient pressure nor oxygen breathing would be expected to protect animals from gas embolism due to intravenously administered FC 80, since gas may evolve from end-pulmonary capillary blood in either circumstance.

Yet dogs that have breathed oxygenated FC 80 can survive breathing room air spontaneously, ten days or longer at which time FC 80 was still measurable in the blood (8). Possibly in the latter study, the quantity of FC 80 which was absorbed in the circulatory system during liquid breathing did not fully saturate the blood, and thus contributed less than the 55 mm Hg vapor pressure of FC 80 (at 37°C) alone to the total tension of gases dissolved in the blood. The average steady-state concentration in the arterial blood of 17 animals was 0.43 mg/100 ml (S.D.,0.09)(8). In our studies, the solubility of FC 80 in blood was probably at least 0.9 mg/100 ml (Figure 2); the solubility in normal saline (25°C) was about 0.78 mg/100 ml (Table XVI).

Figure 3 plots the vapor pressure versus temperature relationship of a number of fluorocarbon liquids, using data supplied by the manufacturers.

VAPOR PRESSURE – TEMPERATURE RELATIONSHIPS OF FLUOROCARBON LIQUIDS
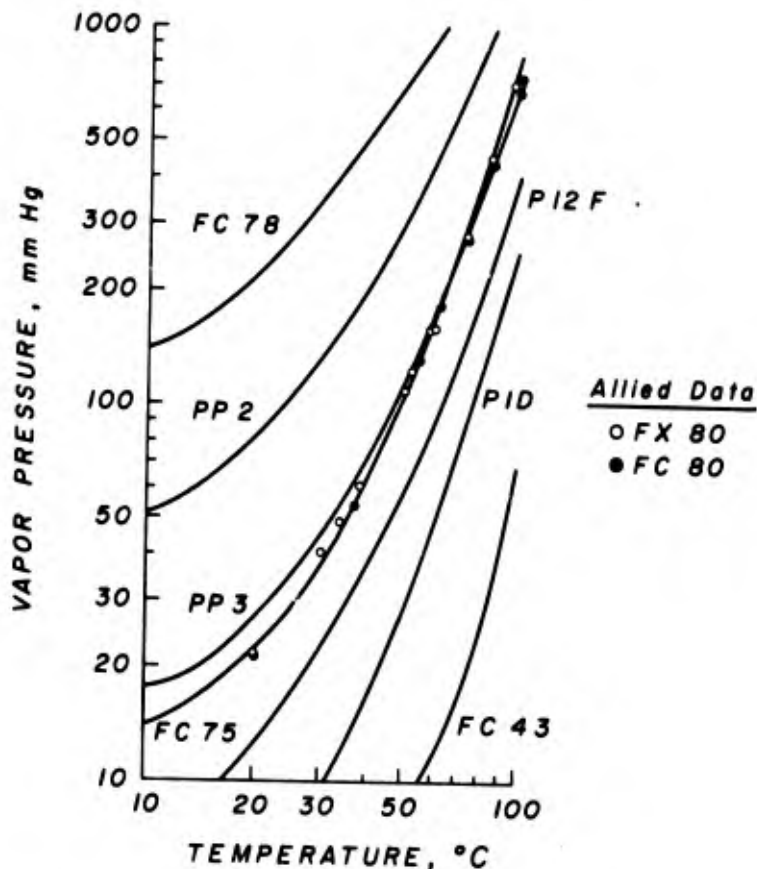
Figure 3. Vapor pressure - temperature relationships of fluorocarbon liquids. The continuous curves were replotted from data supplied by the respective manufacturers: PP2 and PP3, ISC Chemicals Ltd., Avonmouth, Bristol, England; PID and P12F, Allied Chemical Corporation (21), Buffalo, New York; FC 43, FC 75, and FC 78, 3M Company, Saint Paul, Minnesota.

The experimental points are measurements of FX 80 and FC 80 by Allied Chemical Corporation. As shown, FC 75, FC 80, and FX 80, all manufactured by 3M Company, have identical vapor pressure - temperature relationships. Anesthetized dogs breathing room air and injected intravenously with 0.1 ml/kg

of either PP3, FC 80, PP2, or FC 78 die of gas embolism,
whereas dogs injected with similar dose of either P12F, P1D,
or FC 43 do not. One would predict that any other fluoro-
carbon or other inert liquid, which is poorly soluble in
blood and not readily cleared from the circulatory system,
would also produce gas embolism when injected intravenously
in animals breathing air if the vapor pressure of the liquid
at 37°C is approximately 55 mm Hg or greater.

In our studies, intravenous injection of 0.1 ml/kg PP3 or PP2 caused gas
embolism and death in dogs, whereas, injection of comparable amounts of
P12F or P1D did not. Fluorocarbons FX 80, FC 80, and FC 75 all have
essentially the same vapor pressure versus temperature relationship as
shown.

At present, P12F is the best fluorocarbon we have tested for liquid
breathing studies. The safety margin against gas embolism when the blood
contains P12F should be sufficient, yet the vapor pressure should be high
enough to allow evaporation of the liquid from the respiratory passages
after gaseous ventilation is resumed with either air or oxygen.

REFERENCES

1. Gollan F., and R. M. Clark. Experimental pathology after respiration and injection of various fluorocarbon liquids. Exp. Med. Surg. 26:249-262 (1968).

2. Beisang, A. A., et al. Damage assay of kidneys frozen by intra-arterial perfusion with a fluorocarbon. Fed. Proc. 29(5):1782-1788 (1970).

3. Clark, L. C., Jr., and F. Gollan. Survival of mammals breathing organic liquids equilibrated with oxygen at atmospheric pressures. Science 152:1755-1756 (1966).

4. Nose, Y., et al. Physiological effects of intravascular fluorocarbon liquids. Fed. Proc. 29(5):1789-1804 (1970).

5. Sloviter, H. A., et al. Some effects of intravenously administered dispersed fluoro chemicals in animals. Fed. Proc. 29(5):1755-1757 (1970).

6. Geyer, R. P. Whole animal perfusion with fluorocarbon dispersions. Fed. Proc. 29(5):1758-1763 (1970).

7. Holaday, D. A. Distribution of fluorocarbon liquids. Fed. Proc. 29(5):1815-1816 (1970).

8. Holaday, D. A., V. Ferova-Bergerova, and J. J. Modell. Uptake, distribution, and excretion of fluorocarbon FX 80 (Perfluorobutyl Perfluorotetrahydrofuran) during liquid breathing in the dog. Anesthesiology 37(4):387-394 (1972).

9. Lukin, L. Oxygenation of blood during inhalation of a liquid medium. Proc. Soc. Exp. Med. Biol. 121:703-707 (1966).

10. Gollan, F., and L. C. Clark. Prevention of bends by breathing an organic liquid. Trans. Assoc. Am. Physicians LXXX:102-110 (1967).

11. Modell, J. H., et al. Oxygenation by ventilation with fluorocarbon liquid (FX 80). Anesthesiology 34(4):312-320 (1971).

12. Modell, J. H., et al. Long-term survival of dogs after breathing oxygenated fluorocarbon liquid. Fed. Proc. 29(5):1731-1736 (1970).

13. Kylstra, J. A., et al. Hydraulic compression of mice to 166 atmospheres. Science 157:793 (1967).

14. Patel, M. M., et al. Ventilation with synthetic fluids. Surg. Clin. N. A. 51(1):25-36 (1971).

15. Popovic, V. P., and J. E. Baughman. Fifty times longer survival of animals which breathe organic liquid after profound body cooling. Preprints Annual Meeting Aerosp. Med. Assoc. p. 110, 1971.

16. Gollan, F., et al. Compliance and diffusion during respiration with fluorocarbon fluid. Fed. Proc. 29(5):1725-1730 (1970).

17. Boren, H. G. Deposition and removal of carbon particles by fluoro-carbon breathing. Fed. Proc. 29(5):1737-1739 (1970).

18. Patel, M. M., et al. Survival and histopathologic changes in lungs of hamsters following synthetic liquid breathing. Fed. Proc. 29(5):1740-1745 (1970).

19. Comroe, J. H., Jr. Physiology of Respiration Year Book, Chicago, 1965, p. 224.

20. 3M Co. "Fluorinert Brand Electronic Liquids," Data Manual, 1965.

21. Allied Corporation, courtesy of Dr. J. MacKenzie.

APPENDIX

TABLES I through XVII

Preceding page blank

TABLE I

SUMMARY OF EXPERIMENTAL ARRANGEMENT USED IN AIR-BREATHING-AIR-IMMERSION, AND AIR-BREATHING-WATER-IMMERSION STUDIES

Dog No.	Date	Weight (kg)	Special studies	PRESSURES RECORDED — Vascular — AO	PA	LA	RA	LPV	Extra-vascular — ESO	LP1	RP1	IT	Acceleration
-	6 Nov 69	14.0	Test of water-immersion respirator. blood gases measured.	x	--	--	x	--	x	--	--	x	-1Gy
-	11 Nov 69	13.5	Test of water-immersion respirator, blood-gases measured.	x	--	--	x	--	x	--	--	(	-1Gy
1	25 Nov 69	13.0	Test of water-immersion respirator during 6-G centripetal cceleration.	x	x	x	x	x	--	--	--	x	+1, +6Gy
2	3 Dec 69	14.5	Test of water-immersion respirator.	x	x	x	x	x	x	--	--	x	+1Gy
3	5 Dec 69	14.0	Renovist video runs attempted.	x	x	x	x	x	x	--	--	x	+1, +6Gy
4	13 Jan 70	13.5	Double check valve connected to airway with separate inhalation--exhalation lines. Tantalum dust insufflated major airways. Renovist injected in RA for video tape runs.	x	x	x	x	x	x	x	x	x	+1, +6Gy
5	20 Jan 70	11.0	Low and normal residual lung volume, O2 saturation, blood gas, and cardiac output studies. Tantalum dust insufflated major airways for video runs with Renovist injected into RA. First residual lung volume measurements.	x	x	x	x	x	x	x	x	x	+1, +6Gy
6	22 Jan 70	12.5	Low, normal, large residual lung volume O2 saturation, blood gas and cardiac output studies. Renovist injected into RA for video runs.	x	x	x	--	x	x	x	x	x	+1, +6Gy
7	24 Jan 70	13.5	Low, normal, large residual lung volume, O2 saturation, blood gas, and cardiac output studies. Renovist injected into RA for video runs. First ECG recordings.	x	x	x	x	x	x	x	x	x	+1, +6Gy
8	28 Feb 70	14.0	Same	x	x	x	x	x	x	x	x	x	+1, +6Gy

Preceding page blank

TABLE II

SUMMARY OF EXPERIMENTAL ARRANGEMENT USED IN LIQUID-BREATHING STUDIES

Dog No.	Date	Body mass kg.	Description of respirator assembly	Special studies	PRESSURES RECORDED																ACCELERATION
					Airway		Breathing valve		Oxygenator liquid level		Vascular						Extra-vascular				
					Prox	Dist	Inlet	Outlet	Inhale	Exhale	Ao	PA	LA	RA	RV	LTV	LPL	RPL	ESO	IT	
1	31 Mar 70	14.2	Push-pull saline-FC80 pump. Oxygenator off centrifuge with FC80 circulation pump.	Renovist injected into RA with video. 1 G, 6 G O_2 saturation runs ABAI following liquid breathing.	--	--	--	--	--	--	x	x	x	x	x	--	x	x	x	x	+1, +6Gy
-	20 Apr 70	13.0	Unchanged	High, normal, low resid lung volume studies ABWI. FC80 runs at 1 G only.	--	--	--	--	--	--	x	x	x	x	--	x	x	x	x	x	+1, +6Gy
2	21 May 70	10.3	Single respirator pump. Balloon in breathing tank to minimize venous admixture. Oxygenator off centrifuge. FC80 flows passively from oxygenator standpipe at 1 G.	High, normal, low resid lung volume studies, ABWI, and liquid breathing.	--	--	--	--	--	--	x	x	x	x	--	x	x	x	x	x	+1, +6Gy
3	23 June 70	12.0	Unchanged	High, normal, low resid lung volume studies ABWI and FC80. Single endotracheal tube catheter demonstrated partial airway collapse on expiration.	--	--	--	--	--	--	x	x	x	x	--	x	x	x	x	x	+1, +3, +6Gy
-	30 June 70	11.5	Unchanged	Partial collapse of airways studied in dead dog with proximal and distal endotracheal catheters. Tygon endotracheal tube replaced metal used previously.	x	x	x	x	x	x	x	x	--	--	--	--	--	--	x	x	+1Gy
-	2 July 70	-	Single respiration pump. Oxygenator-standpipe reservoir off centrifuge. Passive flow of FC80 to and from oxygenator.	Varied oxygenator liquid level, respiratory rate, and residual volume in study of airway closure.	x	x	x	x	--	--	x	x	--	--	--	--	--	--	x	--	+1Gy
4	8 July 70	13.7	Single respiration pump. Passive flow of FC80 from open reservoir breathing tank. Oxygenator off centrifuge with circulation pump.	Increased compliance of breathing compartment in study of airway closure.	x	x	x	x	--	--	x	x	x	x	--	--	x	x	--	x	+1, +6Gy
5	20 July 70	11.0	Divided breathing compartment open reservoir to minimize venous admixture. Oxygenator off centrifuge.	Two respiration pumps, synchronized in attempt to minimize airway closure during expiratory phase.	x	x	x	x	--	--	x	x	x	x	--	--	x	x	--	x	+1, +6Gy
6	23 July 70	12.3	Unchanged	Stop pump exp and inspir during accel.	x	x	x	x	--	--	x	x	x	x	--	--	x	x	--	x	+1, +4, +7Gy
7	20 Aug 70	13.5	Unchanged	E-M flowmeter implanted root of aorta stroke volume vs phase of respiration studied.	x	x	x	x	--	--	x	x	--	x	x	--	x	x	x	x	-1, -4, -7Gy
8	14 Jan 71	15.5	Cockpit-mounted oxygenator.	Renovist-videometry runs. Parenchymal lung tags. Test of disc vs bubble oxygenation.	x	x	x	x	x	x	x	x	x	x	--	--	x	x	x	x	+1, +7Gy
9	17 Feb 71	17.5	Externally mounted Starr-Edwards valves replaced breathing valve.	Renovist's cardio-green, microsphere injections at 7 G ABWI, 1 & 7 G LB parenchymal tags, ext thor scan.	x	x	--	--	--	x	x	x	x	--	x	x	x	x	x	x	+1, +7Gy
10	24 Mar 71	17.0	Replaced Starr-Edwards valves with orig breathing valve for silicone oil expt.	Microspheres 1, 7 G ABWI 1, 7 G LB. Parenchymal tags	x	x	--	--	x	x	x	x	x	x	x	--	x	x	x	x	+1, +7Gy
11	30 Mar 71	13.0	Unchanged	Microspheres 1, 7G ABWI 1, 7G LB. Parenchymal tags. Renovist-videometry runs. External thoracic scans.	x	x	--	--	--	--	x	x	x	x	--	--	x	x	x	x	+1, +7Gy
12	3 June 71	14.5	Unchanged	Microspheres 1 G ABWI only. Parenchymal tags. External thoracic scan.	x	x	--	--	--	--	x	x	x	x	--	--	x	x	x	x	+1Gy
13	7 June 71	15.0	Unchanged	Microspheres 1, 7 G ABWI 1, 7 G LB. External thoracic scan.	x	x	--	--	x	x	x	x	x	x	x	--	x	x	x	x	+1, +7Gy
14	8 June 71	13.3	Unchanged	Millar cath-tip gauge ILPA microspheres 1, 7 G ABWI and 1, 7 G LB. External thoracic scan.	x	x	--	--	--	--	x	x	x	x	--	--	x	x	x	x	+1, +7Gy
15	10 June 71	13.5	Unchanged	Microspheres 7 G ABWI, 1 G, 7 G LB. Parenchymal tags External thoracic scan.	x	x	--	--	--	--	x	x	x	x	--	--	x	x	x	x	+1, +7Gy
16	2 Dec 71	11.0	Externally mounted, pneumatically actuated slide valve porting large bore inhalation and exhalation lines.	Indwelling PCO_2 electrode supraclavicular artery. Blood gas - blood chemistry determinations at constant PCO_2 = 40mm Hg. Biplane video, motion of parenchymal tags	x	x	--	--	--	--	x	x	--	x	--	--	x	x	x	x	$+1G_y$
17	7 Dec 71	12.5	Unchanged	Blood gas - blood chemistry determinations at constant PCO_2 = 40mm Hg.	x	x	--	--	--	--	x	x	--	x	--	--	x	x	x	x	$+1G_y$

ABAI Air-Breathing, Air-Immersion

ABWI Air-Breathing, Water-Immersion

Preceding page blank

TABLE II

No. of Experiments	Symbol	+1Gy Immersed in Air				No. of Experiments	Vertical Gradient ($cm\ H_2O/cm/C$)	+6Gy Immersed in Air				Vertical Gradient ($cm\ H_2O/cm/G$)
		T_L(2) (cm)	LPl(1) ($cm\ H_2O$)	Y_R(2) (cm)	RPl(1) ($cm\ H_2O$)			T_L(2) (cm)	LPl(1) ($cm\ H_2O$)	Y_R(2) (cm)	RPl(1) ($cm\ H_2O$)	
7	○	-4.0	-1.0	4.7	-7.8	1	0.78	-3.7	+19	5.2	-16.0	0.65
4	▽	-4.4	0	4.1	-7.8	1	0.92	-3.2	+20	4.2	-11.0	0.74
1	□	-4.9	1.7	3.9	-4.5	1	0.71	-4.2	+26	3.3	-7.0	0.73
6	△	-3.4	-2.2	4.8	-4.0	3	0.22	-2.6	+11	4.7	-11.3	0.51
8	○	-3.3	-1.0	5.8	-7.8	3	0.75	-3.1	+22	5.1	-16.0	0.77
Mean (±SE)	-	-4.0 (±0.7)	-0.4 (±1.3)	4.7 (±0.7)	-6.1 (±1.6)	-	0.68 (±0.13)	-3.4 (±0.5)	19.6 (±4.9)	4.5 (±0.7)	-12.3 (±3.4)	0.68 (±.05)

No. of Experiments	Symbol	+1Gy Immersed in Water				No. of Experiments	Vertical Gradient ($cm\ H_2O/cm/C$)	+6Gy Immersed in Water				Vertical Gradient ($cm\ H_2O/cm/G$)
		T_L(2) (cm)	LPl(1) ($cm\ H_2O$)	Y_R(2) (cm)	RPl(1) ($cm\ H_2O$)			T_L(2) (cm)	LPl(1) ($cm\ H_2O$)	Y_R(2) (cm)	RPl(1) ($cm\ H_2O$)	
4	○	-4.5	+1	4.0	-6.5	2	0.88	-4.9	20.5	3.9	-10.5	0.59
5	▽	-5.5	0	5.5	-7.2	3	0.65	-5.8	25.0	5.8	-26.0	0.73
6	□	(3)	-	-	-	1	-	-	-	-	-	-
4	△	-3.8	-1	3.9	-3.5	2	0.32	-4.9	31.0	3.5	-5.5	0.72
6	○	-3.5	+5	5.6	-4.0	4	0.99	-4.0	34.2	5.5	-16.0	0.88
Mean (±SE)	-	-4.3 (±0.8)	1.25 (±2.3)	4.8 (±0.8)	-5.3 (±1.6)	-	0.71 (±0.17)	-4.9 (±0.4)	27.7 (±2.7)	4.7 (±0.5)	-14.5 (±3.8)	0.73 (±0.07)

(1) LPl and RPl-left and right pleural pressures at the catheter tip.

(2) T_L and Y_R-vertical height of left and right catheter tip, from midthoracic plane.

(3) Pleural catheters accidentally withdrawn from pleural space.

Preceding page blank

TABLE IV

OXYGEN SATURATION AND PHYSIOLOGICAL SHUNT DATA SUMMARY OF 14 LIQUID-BREATHING EXPERIMENTS (Means ± S.E.)

Condition	AIR BREATHING – AIR IMMERSION					AIR BREATHING – WATER IMMERSION					100% O₂ WATER IMMERSION					FC80 LIQUID BREATHING, WATER IMMERSION				
	O₂ Saturation %			Venous-Arterial Shunt %		O₂ Saturation %			Venous-Arterial Shunt %		O₂ Saturation %			Venous-Arterial Shunt %		O₂ Saturation %			Venous-Arterial Shunt %	
	FA	PV	PA	Syst	Pulm	FA	PV	PA	Syst	Pulm	FA	PV	PA	Syst	Pulm	FA	PV	PA	Syst	Pulm
+1 Gy control	91.2* ±2.0* (13)	91.2 ±2.3 (10)	56.6 ±3.2 (13)	16.2 ±3.8 (14)	17.2 ±5.1 (12)	95.3 ±0.6 (13)	88.6 ±1.4 (11)	61.1 ±2.2 (12)	7.9 ±1.6 (13)	23.7 ±3.1 (12)	99.0 ±0.6 (10)	95.2 ±2.9 (9)	69.1 ±4.0 (10)	1.6 ±0.8 (11)	9.4 ±5.3 (10)	97.9 ±1.0 (13)	99.0 ±0.5 (10)	71.6 ±2.7 (13)	2.3 ±1.0 (13)	1.4 ±0.8 (10)
+3Gy	--	--	--	--	--	86.8	69.5	52.5	23.0	61.3	--	--	--	--	--	--	--	--	--	1.8
+6Gy	75.0	--	60.0	--	--	86.0 ±4.1 (4)	75.2 ±4.2 (3)	61.5 ±3.8 (4)	16.6 ±0.8 (2)	66.2	--	--	--	--	--	96.5 ±2.8 (2)	99.7	72.2 ±10.4 (2)	13.6 ±2.8 (2)	1.8
20 seconds +6Gy	--	--	--	50.4 ±13.6 (2)	72.8	78.0 ±1.3 (2)	62.1 ±4.3 (2)	57.9 ±2.7 (2)	47.6 ±1.8 (4)	71.2 ±14.6 (4)	85.0	87.0	79.5	68.6	53.8	97.4 ±1.2 (5)	95.2 ±0.9 (5)	72.2 ±2.8 (5)	8.4 ±2.7 (5)	3.6 ±1.3 (5)
+7Gy	81.0	68.0	57.0	--	--	80.3 ±3.0 (8)	67.3 ±4.9 (6)	60.8 ±2.6 (7)	44.9 ±9.5 (8)	72.4 ±11.9 (5)	91.7 ±6.2 (3)	85.8 ±9.6 (2)	63.2 ±3.4 (3)	24.0 ±19.1 (2)	32.0 ±18.1 (2)	96.0 ±1.3 (8)	95.9 ±2.1 (4)	72.9 ±.0 (8)	11.1 ±4.8 (6)	16.3 ±7.5 (4)
+3Gy	--	--	--	--	--	84.5	65.0	49.0	27.0	67.4	--	--	--	--	--	--	--	--	--	--
+6Gy	72.0	--	52.0	--	--	82.2 ±4.4 (4)	70.0 ±4.6 (3)	57.0 ±4.4 (4)	27.7 ±16.1 (2)	74.4	--	--	--	--	--	94.0 ±5.0 (2)	99.5	68.7 ±9.0 (2)	23.2 ±9.6 (2)	3.3
60 seconds +6Gy	--	--	--	46.7 ±13.2 (2)	--	73.5 ±1.4 (2)	55.5 ±6.3 (2)	50.6 ±2.3 (2)	49.6 ±2.0 (4)	72.7 ±13.1 (4)	64.5	63.5	57.5	82.3	78.2	95.4 ±2.0 (5)	97.1 ±1.4 (5)	69.0 ±4.3 (5)	9.2 ±2.9 (5)	7.5 ±4.0 (5)
+7Gy	30.5	52.0	--	--	--	76.7 ±3.3 (8)	62.9 ±5.3 (6)	54.5 ±3.1 (7)	46.1 ±9.4 (8)	71.7 ±8.0 (5)	61.3 ±14.7 (3)	79.3 ±8.8 (2)	57.7 ±4.2 (3)	31.7 ±18.3 (2)	44.8 ±14.6 (2)	91.3 ±1.7 (8)	90.1 ±3.9 (4)	67.6 ±3.2 (8)	22.9 ±6.9 (8)	32.6 ±14.5 (4)
120 seconds +6Gy	--	--	--	--	--	--	--	--	--	--	--	--	--	--	--	88.0	91.5	62.5	27.1	17.1
+7Gy	--	--	--	--	--	74.3 ±5.7 (3)	52.0	50.5 ±7.8 (2)	43.1 ±9.2 (3)	30.8	96.0	--	63.0	--	--	88.4 ±2.6 (5)	89.0 ±6.8 (3)	64.0 ±3.5 (5)	27.0 ±6.6 (5)	29.5 ±18.2 (3)

Small shunts; i.e., <20% are probably not significant.
( ) Number of dogs included in the mean. The value used for each dog in computing the mean is itself the mean value for all runs on that dog.

Preceding page blank

TABLE V

MIXED VENOUS BLOOD CHEMISTRY DETERMINATIONS IN DOGS VENTILATED WITH FC80 FLUOROCARBON

Experimental Conditions	Time	Sodium mEq/L plasma (140-154)*	Potassium mEq/L plasma (3.55-4.39)*	Chloride mEq/L plasma (100-119)*	Calcium mg/100ml (8.9-10.1)	Phosphorus mg/100ml (2.5-4.5)	True Blood Sugar mg/100ml (65-90)	Blood Urea mg/100ml (10-60)	Hemoglobin gm/100ml (11.0-18.0)*	Hematocrit Percent (44)*	Red blood cell Conc. per mm x 10^6 (4.5-9.0)*	White blood cell Conc. per mm (4400-9500)*	Platelets per mm (250,000-450,000)	Bilirubin (indirect) mg/100ml (0-0.9)	Lactate mM/L (0.93-1.65)	Pyruvate mM/L (0.08-0.16)	LDH units/L (0-127)	SGOT units/L (0-24)	Total Protein gm/100ml (6.0-7.7)	Albumin gm/100ml serum (3.3-4.3)	Alpha 1 Globulin gm/100ml serum (0.1-0.4)	Alpha 2 Globulin gm/100ml serum (0.3-0.8)	Beta Globulin gm/100ml serum (0.4-1.1)	Gamma Globulin gm/100ml serum (0.4-1.4)
Breathing air, immersed in water, 6 1/2 hours before start of liquid breathing	1615	144	3.7	117	-	-	63	22	15.3	42	4.33	12,000	120,000	-	-	-	-	-	-	-	-	-	-	-
Breathing oxygen, immersed in water, 2-3 hours before start of liquid breathing	2040	135	3.7	118	8.1	5.05	79	25	13.1	32	3.29	13,000	72,000	0.2	0.34	0.08	-	-	4.16	2.16	0.32	0.48	0.46	0.25
Breathing FC80 for 1 1/2 hours	2235	144	4.1	120	-	-	78	26	7.5	20	2.54	13,300	-	-	0.42	0.07	-	-	-	-	-	-	0.07	-
Breathing FC80 for 4 hours	2450	140	3.8	116	8.1	4.13	78	23	9.9	36	4.15	12,700	104,000	0.2	0.70	0.07	-	-	4.06	2.07	0.35	0.56	0.07	0.25
Breathing oxygen immediately after liquid breathing	2222	-	-	-	-	-	-	-	10.6	28	3.2	6,200	26,000	-	-	-	17	63	-	-	-	-	-	-
Breathing air, immersed in water, 1 1/2 hours before start of liquid breathing	1600	143	3.4	116	8.3	6.22	73	28	16.9	46	4.59	3,000	120,000	0.1	0.92	0.09	-	-	5.72	2.70	0.70	0.60	1.35	0.37
Breathing oxygen, immersed in water, 1/2 hour before start of liquid breathing	1650	140	5.0	113	-	-	66	27	17.0	56	4.18	11,600	77,500	-	0.73	0.09	-	-	-	-	-	-	-	-
Breathing FC80 for 1 1/2 hours	1835	144	4.1	120	-	-	66	23	15.6	48	3.67	12,500	97,500	0.3	0.51	0.05	-	-	4.78	2.58	0.26	0.36	0.36	0.33
Breathing FC80 for 5 1/4 hours	2036	142	3.3	117	8.3	-	72	21	16.3	50	3.85	6,900	95,000	0.3	0.53	0.05	-	-	-	-	-	-	-	-
Breathing oxygen immediately after liquid breathing	2140	-	-	-	-	-	-	-	16.0	46	3.93	7,700	117,500	-	-	-	160	92	-	-	-	-	-	-
Breathing oxygen for 12 1/2 hours after liquid breathing	1015	-	-	-	-	-	-	-	17.3	57	5.73	4,700	3,000	-	-	-	-	-	-	-	-	-	-	-

Dog 16 11.0 kg, 3-4 December 1971
Dog 17 12.5 kg, 7-8 December 1971

* Range of normal values for the dog. Source: Respiration and Circulation (P. L. Altman and B. S. Bittner, eds) FASEB April 1971. All other ranges shown in ( ) are Mayo Clinic Laboratory normal limits in humans (dog data not available).

147   Preceding page blank

TABLE VI

RUN... 37   TIME...7103 24 1919   ACTG... 7.11

	LPL	RPL	INT	AO	PA	LA	DSA	RESP	ESO
ZERO...	342	379	511	120	369	173	206	550	313
PLEVEL...	476	409	653	450	473	318	397	523	495
CATNTP...	-9	7	1	1	1	1	1	1	1
GCATNTP..	-22	56	19	10	15	19	-2	-2	18

	LPL	RPL	DSA	RESP	ESO
YP...	39	55	49	7	56
GYP...	22	49	9	7	56
VP...	-49	79	9	9	14
GVP...	-34	85	9	9	23

	LPL	RPL	DSA	RESP	ESO
V...	-91	95	9	9	12
GV...	-70	73	9	9	20

TT	ML	BML	P	PP	S	SP
3	19	24	990	990	100	100

--- TT-ZERO

INSPIRATION... 72.13 SECONDS AFTER CODE 111

	MEAN	MIN		MEAN	MIN	MAX
LPL	8.3	2.0	LA	-23.9	-27.3	
RPL	-35.0	-39.0	DSA	-7.2	-7.3	
INT	-16.5	-22.0	AO	150.3	142.5	160.0
ESO	-15.0	-20.3	PA	40.8	33.5	45.5
RSP	14.4	30.1		VERTICAL GRADIENT	.980

EXPIRATION COMPLETED AT 337.17 SECONDS FROM START OF RUN

EXPIRATION... 74.79 SECONDS AFTER CODE 111

	MEAN	MAX		MEAN	MAX	PIN
LPL	31.3	34.2	LA	-8.0	7.3	
RPL	-25.1	-23.6	DSA	-7.3	-7.3	
INT	14.2	16.7	AO	149.1	154.5	146.4
ESO	-4.6	0.9	PA	72.1	89.5	69.1
RSP	-1.7	-6.9		VERTICAL GRADIENT	.806

INSPIRATION... 77.66 SECONDS AFTER CODE 111

	MEAN	MIN		MEAN	MIN	MAX
LPL	8.1	2.1	LA	-23.4	-33.1	
RPL	-34.7	-36.0	DSA	-7.5	-7.5	
INT	-15.0	-22.3	AO	147.6	142.4	159.0
ESO	-15.5	-20.6	PA	40.2	35.4	45.6
RSP	12.4	30.0		VERTICAL GRADIENT	.559

EXPIRATION COMPLETED AT 343.49 SECONDS FROM START OF RUN

EXPIRATION... 81.07 SECONDS AFTER CODE 111

	MEAN	MAX		MEAN	MAX	PIN
LPL	29.0	33.0	LA	-1.7	6.5	
RPL	-24.4	-23.0	DSA	-7.5	-7.6	
INT	11.0	17.0	AO	148.1	159.4	142.4
ESO	3.4	6.9	PA	73.5	89.1	63.0
RSP	10.9	-4.7		VERTICAL GRADIENT	.804

INSPIRATION... 83.01 SECONDS AFTER CODE 111

	MEAN	MIN		MEAN	MIN	MAX
LPL	8.3	2.0	LA	-23.5	-27.1	
RPL	-34.1	-37.1	DSA	-7.3	-7.6	
INT	-15.4	-22.6	AO	145.3	137.6	157.3
ESO	-15.4	-19.9	PA	41.0	37.4	46.8
RSP	13.1	30.1		VERTICAL GRADIENT	.949

EXPIRATION COMPLETED AT 348.22 SECONDS FROM START OF RUN

EXPIRATION... 85.80 SECONDS AFTER CODE 111

	MEAN	MAX		MEAN	MAX	PIN
LPL	32.3	34.7	LA	-9.1	6.5	
RPL	-24.6	-23.6	DSA	-7.6	-7.6	
INT	15.0	17.0	AO	144.5	155.6	141.2
ESO	5.7	7.4	PA	73.5	89.5	62.3
RSP	-1.0	-7.6		VERTICAL GRADIENT	.812

INSPIRATION... 88.37 SECONDS AFTER CODE 111

	MEAN	MIN		MEAN	MIN	MAX
LPL	8.0	2.1	LA	-22.7	-31.5	
RPL	-34.1	-37.9	DSA	-7.6	-7.8	
INT	-15.3	-22.7	AO	147.9	139.1	159.2
ESO	-15.0	-20.2	PA	43.5	37.1	48.5
RSP	15.3	31.6		VERTICAL GRADIENT	.757

EXPIRATION COMPLETED AT 353.86 SECONDS FROM START OF RUN

EXPIRATION... 91.44 SECONDS AFTER CODE 111

	MEAN	MAX		MEAN	MAX	PIN
LPL	32.3	34.4	LA	-8.0	6.9	
RPL	-24.7	-24.2	DSA	-7.4	-7.0	
INT	14.0	16.7	AO	153.6	163.9	149.7
ESO	5.7	7.0	PA	73.7	89.5	64.8
RSP	1.3	-7.6		VERTICAL GRADIENT	.816

INSPIRATION... 94.91 SECONDS AFTER CODE 111

	MEAN	MIN		MEAN	MIN	MAX
LPL	8.1	2.0	LA	-23.6	-27.1	
RPL	-35.5	-38.8	DSA	-7.9	-8.0	
INT	-15.5	-22.4	AO	152.1	147.1	160.9
ESO	-15.3	-20.3	PA	42.7	37.2	46.2
RSP	12.4	29.4		VERTICAL GRADIENT	.597

EXPIRATION COMPLETED AT 359.70 SECONDS FROM START OF RUN

EXPIRATION... 96.78 SECONDS AFTER CODE 111

	MEAN	MAX		MEAN	MAX	PIN
LPL	33.2	36.2	LA	-8.1	8.1	
RPL	-23.9	-22.6	DSA	-7.9	-7.0	
INT	16.1	18.2	AO	155.3	164.4	151.7
ESO	6.9	8.4	PA	74.1	89.5	63.0
RSP	-0.2	-6.1		VERTICAL GRADIENT	.816

INSPIRATION... 99.44 SECONDS AFTER CODE 111

	MEAN	MIN		MEAN	MIN	MAX
LPL	7.2	3.0	LA	-24.6	-30.8	
RPL	-34.6	-37.6	DSA	-7.9	-8.2	
INT	-16.3	-22.4	AO	145.5	136.4	156.4
ESO	-16.4	-19.2	PA	41.6	37.8	43.4
RSP	13.9	29.4		VERTICAL GRADIENT	.565

EXPIRATION COMPLETED AT 363.98 SECONDS FROM START OF RUN

EXPIRATION... 101.48 SECONDS AFTER CODE 111

	MEAN	MAX		MEAN	MAX	PIN
LPL	32.6	40.1	LA	-13.2	7.9	
RPL	-36.3	-24.1	DSA	-7.7	8.6	
INT	-11.5	-9.1	AO	137.5	145.3	138.9
ESO	-8.1	2.2	PA	46.7	71.4	37.7
RSP	6.4	6.4		VERTICAL GRADIENT	.893

MIN/ LPL /MAX	MIN/ RPL /MAX	MIN/ INT /MAX	MIN/ ESO /MAX	MIN/ RSP /MAX	MIN/ LA /MAX	MIN/ DSA /MAX
2.0 34.2	-39.6 -23.6	-22.0 16.7	-20.3 6.5	30.1 -6.9	-27.3 7.3	-7.3 -7.3
2.1 33.9	-38.1 -23.9	-22.3 17.0	-20.6 6.5	30.0 -4.7	-33.1 6.5	-7.5 -7.6
2.0 34.7	-37.2 -23.6	-22.6 17.4	-19.9 7.4	31.6 -7.6	-27.1 6.5	-7.6 -7.6
2.1 34.4	-37.9 -24.2	-22.7 16.7	-20.2 7.0	31.6 -7.6	-31.5 6.9	-7.8 -7.0
2.0 36.2	-38.8 -22.6	-22.4 18.2	-20.3 8.4	29.4 -6.1	-27.1 8.1	-8.0 -7.0
3.0 40.1	-37.6 -24.1	-22.4 -9.1	-19.2 2.2	29.4 -6.4	-30.8 7.9	-8.2 8.6

MIN/ INSP-AO /MAX	MAX/ EXP-AO /MIN	MEAN/ AO /MEAN	MIN/ INSP-PA /MAX	MAX/ EXP-PA /MIN	MEAN/ PA /MEAN
142.1 167.0	154.5 146.4	150.3 147.1	33.5 45.5	89.1 69.1	40.2 72.1
142.4 159.4	155.6 141.2	147.6 146.1	35.4 45.6	89.5 63.0	41.0 73.5
137.6 157.3	155.6 141.2	145.3 144.5	37.1 45.8	89.5 62.3	41.0 73.5
139.2 159.2	163.9 149.7	147.9 144.9	37.2 48.5	89.5 64.8	43.5 73.7
147.1 160.9	164.4 151.7	152.1 155.3	37.8 46.2	89.5 63.0	42.7 73.7
136.4 156.4		145.5 137.9	37.8 43.4	71.4 37.7	41.6 46.7

	INSPIRATION			EXPIRATION		
	MEAN(MIN)	STANDARD ERROR	MEAN(MAX) STANDARD ERROR		MEAN(MAX)	STANDARD ERROR	MEAN(MIN) STANDARD ERROR
LPL	2.22	1.9887E-01		LPL	35.56	7.929VE-01	
RPL	-38.07	3.2626E-01		RPL	-23.69	1.0841E-01	
INT	-22.44| 1.4735E-01		INT	13.43	3.7774E 00	
ESO	-20.09| 2.0134E-01		ESO	0.33	8.7981E-01	
RSP	30.37	3.6353E-01		RSP	-6.42	7.2159E 00	
LA	-29.16| 1.0445E 00		LA	7.19	2.8766E-01	
DSA	-7.76	1.5007E-01		DSA	-7.80	2.7119E 00	
AO	140.46	1.0061E 00	158.00 6.0590E-01	AO	150.18	3.6404E 00	143.04 3.0849E 00
PA	36.40	4.0986E-01	46.34 7.7960E-01	PA	46.46	2.9762E 00	90.00 4.5924E 00

	MEAN(MEAN)	STANDARD ERROR		MEAN(MEAN)	STANDARD ERROR
AO	149.18	1.0413E-01	AO	149.18	2.5749E 00
PA	41.05	5.9043E-01	PA	69.02	4.4646E 00

VERTICAL GRADIENT FOR MEAN (MIN)... .96   VERTICAL GRADIENT FOR MEAN (MAX)... .82

TABLE VII

RUN... 41   TIME...7103 24 2144   ACTB... 7.14

	LPL	RPL	INT	AO	PA	LA	DSA	RESP	ESO
ZERO...	349	331	521	131	336	371	279	383	317
PLEVL...	475		662		497	469	449	446	457
CATHTP...	-4	0	1	1	1			1	1
QCATHTP..	-20	47	11	0	11	11	10	0	11

	LPL	RPL	DSA	RESP	ESO
YP...	39	48	20		61
QYP...	43	47	23	5	60
SYP...	-55	74	12	-20	10
OYP...	-42	76	12	-28	17

	LPL	RPL	DSA	RESP	ESO
V...	-42	64	10	-18	14
QV...	-36	63	10	-18	15

TV	ML	QML	P	PP	B	SP
0	39	10	900	990	100	100

151

Preceding page blank

—— TV-ZERO

INSPIRATION... 84.89 SECONDS AFTER CODE 152

EXPIRATION... 74.23 SECONDS AFTER CODE 152

INSPIRATION... 83.19 SECONDS AFTER CODE 152

EXPIRATION... 87.70 SECONDS AFTER CODE 152

INSPIRATION... 91.41 SECONDS AFTER CODE 152

EXPIRATION... 96.06 SECONDS AFTER CODE 152

INSPIRATION... 99.52 SECONDS AFTER CODE 152

EXPIRATION... 104.28 SECONDS AFTER CODE 152

INSPIRATION... 107.64 SECONDS AFTER CODE 152

EXPIRATION... 112.14 SECONDS AFTER CODE 152

INSPIRATION... 115.71 SECONDS AFTER CODE 152

EXPIRATION... 120.49 SECONDS AFTER CODE 152

INSPIRATION... 123.81 SECONDS AFTER CODE 152

EXPIRATION... 128.39 SECONDS AFTER CODE 152

VERTICAL GRADIENT FOR MEAN (MIN)... .00   VERTICAL GRADIENT FOR MEAN (MAX)... 1.00

TABLES VI AND VII, LEGENDS

The upper quarters of Tables VI and VII identify the data analyzed and display all data entered at the keyboard of the peripheral station which was used to update the digital tape originally recorded at the time of the experiment; A-D converter values for pressure calibrations recorded prior to each of the ten to fifteen 2-5 minute experiments in each animal and the computed corrections applied to each pressure trace. For example, Table VI (a) is the analysis of a 7.01 G experiment which commenced at 1915 hours, March 24, 1971, with digitized pressure and other data recorded after the 37th file mark on tape. Rows labeled zero and P level are A-D converter values for 0 and 20 cm H_2O calibration pressures, respectively, for all pressures except the aortic; and 0 and 100 mm Hg, respectively, for the aortic.

DSA and RSP refer to bronchial and tracheal pressures, respectively. IMT is the abbreviation for immersion tank (or body surface), and other abbreviations should be obvious. CATHTP are pressure corrections in cm H_2O (mm Hg for the aortic) which were algebraically subtracted from each of the appropriate calibrated pressures recorded during the 1G control period to refer to vascular and airway pressures to midlung level and to adjust pleural and esophageal pressures to their catheter tip position. GCATHTP corrections were subtracted from pressures which were recorded during exposures of the animal to greater than 1G force environments. These pressure corrections were computed from the remaining data in the header record. Xp, Yp are catheter-tip coordinates (in mm) from the reference axes in biplane films obtained during the 1G control period, and Y is the computed vertical height (in mm) corrected for x-ray magnification, of the catheter tip above the reference plane (zero pressure reference) at 1G. ML is the position of the animal's midlung above the reference crosshair in the A-P x-ray obtained at 1G. The GXP, GYP, GY and GML are corresponding measurements in biplane films obtained during exposures to other than 1G. TT is the vertical position of the water level in the thistle tubes above the reference crosshair determined in the A-P film obtained during exposures to increased force environments. The water-filled thistle tubes are mounted on each side of the animal's thorax, and are used to record zero baseline pressures on all manometers during exposures to centripetal acceleration.

All measurements obtained from images in the biplane films were corrected for x-ray magnification computed from source to film (P,PP) and reference axis to film (S,SP) distances in millimeters.

The interrupted line labeled TT-zero indicates that the subsequent analysis is of data recorded after the pressure in the thistle tubes was recorded (zero pressure baseline) at the start of the acceleration

153

Preceding page blank

plateau (see Figure 1). In what follows in the printout, the inspiratory and expiratory portions of each respiratory cycle are analyzed separately and each cycle is identified by the time from the nearest BCD event code (simultaneously recorded on both photokymographs, analog and digital tape), and the time from the start of the tape record. The particular respiratory cycles analyzed in these two print-outs had been previously selected after first examining the original photokymograph and computer-processed tracings. The identifying data necessary to select these cycles for analysis were entered on data cards in the MSOS program.

The last third of the printouts lists the minimum and maximum values found by the program for each respiratory cycle analyzed and a statistical summary of this data is shown at the end.

TABLE VIII

COMPUTER-PROCESSED MEASUREMENTS OF MULTIPLE PHYSIOLOGICAL PRESSURES AND OTHER VARIABLES IN DOGS BREATHING ORGANIC LIQUIDS

SUMMARY FOR INDIVIDUAL DOGS AND MEANS FOR THE GROUP

$\pm 1G_Y$ BREATHING AIR, IMMERSED IN AIR (Means $\pm$ S.E.)

DOG (1) NUMBER		T_L (2) (cm)	LPL (3) (cm H2O)	T_R (2) (cm)	RPL (3) (cm H2O)	T_E (2) (cm)	ESO (3) (cm H2O)	VERTICAL(4) GRADIENT (cm H2O/CM/G)	AORTA (mm Hg) SYSTOLIC	MEAN	DIASTOLIC	PULMONARY ARTERY (cm H2O) SYSTOLIC	MEAN	DIASTOLIC	LA (cm H2O) DIASTOLIC	MEAN
9	EXPIR (40)	-3.1	-2.7±0.5 -10.8±1.31	5.1	-4.4±.21 -13.9±1.91	0.20	-0.78±0.39 -3.00±1.92	0.26 0.35	144.1±8.4 140.6±4.8	124.7±6.6 112.8±0.1	112.3±6.5 106.1±4.6	37.9±1.7 24.0±1.2	26.2±1.0 17.4±1.7	24.9±1.2 15.1±0.0	10.0±6.1 -2.7±1.3
10	EXPIR (S11 O11) INSP (2) (14)	-5.5	3.1±0.51 -7.94±0.98	5.3	-4.94±.04 -14.76±1.54	0.1	-0.5±.87 -10.2±.23	0.75 0.6	173.3±10.0 156.0±3.6	156.5±7.6 163.8±2.0	167.6±4.8 133.1±0.7	54.0±3.9 31.3±4.4	41.5±2.8 25.4±1.5	34.3±3.2 20.1±0.3	5.1±0.9 -11.4±2.1
11	EXPIR (1) INSP (4)	-3.3	-3.29 -13.98	3.6	-4.05 -22.14	0.2	-0.15 -17.32	0.11 1.14	137.9 138.5	113.7 113.3	93.9 91.5				10.8 -9.6
12	EXPIR (2) INSP (20)	-4.3	-1.82±6.54 -9.21±0.6	5.2	-10.14±0.61 -15.44±0.89	-0.3	1.1±5.04 -8.1±0.33	7.6 0.6	163.3±6.4 159.2±6.2	152.4±0.8 134.6±2.2	165.8±0.3 141.6±0	32.0±0.3 24.6±1.2	25.5±0.7 20.0±0.3	21.3±0.8 16.3±0.4	22.0±1.1 15.9±0.6
13	EXPIR (1) INSP (10)	-5.1	0.67 -13.13	6.5	-10.48 -26.35	0.3	-2.82 -16.72	0.9 1.14	125.3 117.4	113.5 105.2	108.2 96.5	50.4 42.3	40.1 32.3	34.1 17.2	1.3 -15.3
14	EXPIR (1) INSP (3)	-1.8	-1.39 -2.26	4.0	-4.22 -4.78	0.1	-0.05 -0.31	0.65 0.4	184.2 117.0	106.3 101.6	97.2 87.8	(6)	(6)	(6)	9.5 3.6
15															

| Mean ± SE 6 dogs 91 resp cycles analyzed | -3.94±.56 | -0.91±.95 -9.55±1.74 | 4.95±.62 | -6.3±1.25 -16.26±3.03 | 0.10±.09 | -0.3±0.53 -8.9±2.68 | 0.5±.13 0.7±.14 | 165.5±7.8 136.3±7.5 | 127.3±3.8 119.5±6.9 | 117.5±5.6 104.±6.2 | 43.6±5.3 30.6±4.2 | 33.9±6.1 23.9±3.2 | 26.9±3.3 17.2±1.1 | 6.±2.9 -5.2±3.5 |

(1) Top number in ( ) indicates number of experiments, bottom number in ( ) indicates total number of respiratory cycles analyzed.

(2) T_L, T_R, T_E vertical distances of left pleural, right pleural, and esophageal catheter tips, respectively, measured at the catheter tip.

(3) LPL, RPL left and right pleural pressure, and esophageal pressure; (LPL - RPL) ÷ [(T_R-T_L) (acceleration in G units)].

(4) Vertical gradient of pleural pressure (LPL - RPL) ÷ [(T_R-T_L) above horizontal plane through animal's midling.

(5) Immersion tank pressure (body surface pressure) at midling level.

(6) Pulmonary pressure recorded with Millar catheter-tip manometer in this dog, and the pressures were not analyzed by the computer.

-155

TABLE IX

COMPUTER-PROCESSED MEASUREMENTS OF MULTIPLE PHYSIOLOGICAL PRESSURES AND OTHER VARIABLES IN DOGS BREATHING ORGANIC LIQUIDS.

SUMMARY FOR INDIVIDUAL DOGS AND MEANS FOR THE GROUP

$+1G_Y$ BREATHING AIR, IMMERSED IN WATER

DOG NUMBER	$Y_L^{(2)}$ (cm)	$LPL^{(3)}$ (cm H2O)	$Y_R^{(2)}$ (cm)	$RPL^{(3)}$ (cm H2O)	$Y_E^{(2)}$ (cm)	$ESO^{(3)}$ (cm H2O)	VERTICAL$^{(4)}$ GRADIENT (cm H2O/CM/G)	BODY$^{(5)}$ SURFACE (cm H2O)	AORTA (cm Hg) SYSTOLIC	MEAN	DIASTOLIC	PULMONARY ARTERY (cm H2O) DIASTOLIC	SYSTOLIC	MEAN	LA (cm H2O) DIASTOLIC	MEAN
9 (3)(44)	-4.	-0.13±.79 / -14.48±.38	4.6	-5.69±.46 / -18.59±.52	-0.1±0	1.45±.77 / -14.62±1.12	0.57±.03 / 0.47±0.06	14.67±1.79 / -15.92±0.70	163.3± 4.0 / 135.1± 3.1	123.1±3.6 / 112.7±2.7	104.3±3.5 / 94.4±2.5	29.0±6.6 / 15.0±10.1	19.1±7.2 / 3.9±9.0	11.7±7.5 / -5.4±8.1	—
10 (S11-O11)(2)(30)	-5.4±0.2	4.1±.09 / -11.11±.49	5.05±.05	-3.39±0.59 / -16.72±1.87	-0.35±.05	2.65±0.6 / -11.92±.09	0.72±.06 / 0.33±.12	9.6±0.23 / -11.88±0.74	156.7± 2.6 / 153.4± 2.3	140.4±5.8 / 138.6±6.0	131.5±7.8 / 127.8±6.8	34.4±2.9 / 29.3±3.5	40.8±4.7 / 23.0±5.8	30.0±3.6 / 18.3±4.1	5.5±0.5 / -13.3±1.3
11 (3)(31)	-4.28±.02	4.04±.92 / -12.91±1.11	3.02±.02	-2.75±.92 / -20.37±1.31	-0.36±.14	3.65±.72 / -11.39±.84	0.93±.06 / 1.02±.12	12.81±4.93 / -13.67±2.63	146.5± 7.6 / 141.9± 7.2	124.3±6.3 / 118.0±5.7	108.3±6.3 / 95.5±5.7	33.7±3.9 / 12.6±2.2	24.3±2.5 / 9.1±1.6	20.6±2.9 / 2.6±0.9	5.1±1.3 / -10.7±1.5
12 (3)(32)	-6.9	1.98±0.71 / -9.01±0.10	5.3	5.11±0.29 / -17.74±0.24	-0.7	0.93±1.51 / -7.67±1.13	0.70±0.05 / 0.50±.01	7.60±.05 / -4.65±1.92	130.4± 0.5 / 145.2± 0.8	137.4±1.7 / 131.9±1.9	127.7±2.4 / 121.3±3.1	44.0±1.7 / 21.9±1.9	35.2±1.4 / 18.9±1.4	27.0±0.7 / 15.1±0.9	29.2±0.7 / 10.7±0.7
13 (6)(57)	-4.9±0.2	2.05±.95 / -18.73±1.43	6.13±.03	-8.03±.95 / -29.21±1.27	0.1	-4.56±1.08 / -20.13±1.39	0.72±.02 / 0.9±.04	10.50±0.38 / -1.55±0.61	122.8± 6.7 / 115.6± 6.4	104.5±5.7 / 95.1±6.0	95.5±5.9 / 78.9±6.0	39.8±6.1 / 20.0±3.5	30.0±4.7 / 17.2±3.3	27.6±4.5 / 13.9±3.2	3.7±1.2 / -19.7±0.9
14 (3)(35)	-2.7	0.53±0.67 / -18.71±0.77	4.2	-2.56±.64 / -23.84±.15	-0.2	1.60±0.36 / -15.23±0.59	0.47±0.08 / 0.74±0.11	13.34±0.12 / -14.30±1.04	135.0±13.6 / 124.1±12.9	104.4±12.7 / 94.4±12.6	83.2±10.7 / 74.6±12.5	(6)	(6)	(6)	9.9±1.5 / -18.0±2.3
15 (7)(85)	-2.31±.01	4.8±.44 / -20.9±0.56	3.89±.01	-0.76±.40 / -30.12±.54	0.7	5.11±0.95 / -19.05±1.28	0.9±.07 / 1.49±.14	12.53±0.95 / -20.72±1.63	105.4± 2.7 / 91.4± 2.0	90.6± 2.1 / 76.4± 2.7	60.0± 2.1 / 61.0± 4.3	37.0±2.9 / 8.9±0.8	29.5±1.6 / 5.9±0.4	24.7±.9 / 2.2±.5	15.5±0.8 / -14.5±0.9
Mean ± SE 31 Exp in 7 dogs 376 Resp cycles analyzed	-4.07±.44	2.5±.72 / -15.14±1.68	4.60±.38	4.01±.90 / -22.37±2.07	0.14±.17	1.84±.91 / -14.29±1.66	0.74±.07 / 0.97±.13	11.5±1.08 / -14.4±1.68	136.9± 6.6 / 129.6± 8.0	117.8±7.0 / 109.6±6.4	104.7±7.6 / 93.6±9.2	39.7±3.6 / 17.9±3.0	29.8±3.1 / 12.8±3.2	23.6±2.7 / 7.9±3.6	11.9±3.8 / -11.0±4.5

(1) Top number in ( ) indicates number of experiments, bottom number in ( ) indicates total number of respiratory cycles analyzed.
(2) Y_L, Y_R, vertical distances of left pleural, right pleural, and esophageal catheter tips, respectively, above horizontal plane through animal's midlung.
(3) LPL, RPL-left and right pleural pressure, and esophageal pressure, measured at the catheter tip.
(4) Vertical gradient of pleural pressures,(LPL - RPL)÷[(Y_R-Y_L)] (acceleration in G units)].
(5) Immersion tank pressure (body surface pressure) at midlung level.
(6) Pulmonary pressure recorded with Millar catheter-tip manometer in this dog, and the pressures were not analyzed by the computer.

Preceding page blank

TABLE X

COMPUTER-PROCESSED MEASUREMENTS OF MULTIPLE PHYSIOLOGICAL PRESSURES AND OTHER VARIANTS IN DOGS BREATHING ORGANIC LIQUIDS

SUMMARY FOR INDIVIDUAL DOGS AND MEANS FOR THE GROUP

$+7G_y$ BREATHING AIR, INCREASE IN WATER

DOG	(1) NUMBER	$Y_L^{(2)}$ (cm)	LPL(3) (cm H_2O)	$Y_R^{(2)}$ (cm)	RPL(3) (cm H_2O)	$Y_E^{(2)}$ (cm)	ESO(3) (cm H_2O)	VERTICAL GRADIENT(4) (cm H_2O/cm,G)	BODY SURFACE(5) (cm H_2O)	AORTA (mm Hg) SYSTOLIC	DIASTOLIC	MEAN	PULMONARY ARTERY (cm H_2O) SYSTOLIC	DIASTOLIC	MEAN	La (cm H_2O) MEAN
9	(4) (20)	-3.5	40.69±.88 15.46±1.53	4.95±.05	-11.8±5.44 -38.26±2.94	0.5	11.21±3.67 -11.29±.99	0.79±.05 0.91±.07	35.50±.40 .02±.29	169.5±5.6 162.6±9.8	136.3± 7.5 123.6± 9.4	151.3± 7.5 140.7±10.6	63.5±1.5 34.7±2.0	46.9± 1.9 26.6± 1.5	53.9± 1.6 30.9± 1.7	--
10	S11. 011) (1) (6)	-5.6	37.57 4.34	4.5	-18.20 -40.57	-0.8	13.34 -17.47	0.78 0.63	18.31 -29.61	164.0 134.1	145.9 139.8	154.4 146.1	86.7 50.4	65.6 36.8	74.5 43.8	11.9 -25.1
11	(3) (17)	-3.3	37.25±2.9 16.95±.81	2.2	-3.3±2.77 -34.71±.70	-1.6	15.60±1.95 -5.83±.55	0.7±.08 0.9±.02	37.14±3.73 -16.51±1.19	147.6±7.5 157.3±0.7	141.8± 4.4 119.6± 1.2	154.1± 6.3 134.4± 5.1	73.4±7.8 34.4±5.4	61.6± 6.8 13.4± 4.7	53.1± 4.8 25.2± 4.7	21.4±1.0 -11.5±1.6
12	(1) (2)	-4.9	45.33 20.41	5.3	-23.24 -49.48	-3.7	22.47 1.63	0.95 0.97	32.68 -4.54	174.4 162.1	148.5 133.3	159.7 145.8	79.4 37.8	58.9 14.5	67.1 28.7	52.0 15.4
13	(5) (25)	-4.86±.08	30.43±.63 -7.92±.87	6.16±.04	-26.97±1.7 -74.93±5.69	-.44±0.6	1.37±1.17 -36.04±.63	0.73±.02 0.83±.07	23.34±1.73 -23.65±1.39	131.4±12.3 112.0±2.3	104.7 ±9.1 79.7 ±8.6	110.5 ±9.2 93.1±10.7	57.9±15.1 39.0±10.0	52.1±13.0 36.5± 9.6	53.6±14.1 37.7± 9.7	12.0±0.5 -25.5±0.4
14	(3) (25)	-3.4	31.41±1.89 1.82±1.81	3.8	-15.28±3.43 -37.22±4.55	-0.7	11.18±2.72 -16.30±4.07	0.92±.03 0.7±.03	29.20±5.8 -13.23±2.16	161.1±12.3 140.7±15.0	115.0±14.2 90.4±14.5	132.7±11.5 114.5±15.1	(6)	(6)	(6)	21.1±9.1 -15.4±1.6
15	(3) (26)	-3.5	34.91±2.41 .6±1.38	2.2	-7.21±.73 -44.44±.07	-0.8	14.16±.50 -15.82±.25	1.04±.07 1.12±.03	22.13±.47 -16.21±.36	122.4±1.5 106.2±2.3	97.7 ±3.3 70.5±3.0	109.0 ±2.3 90.9 ±2.6	61.5 ±3.3 28.9±3.6	45.6± 2.0 20.1± 4.1	51.8± .8 24.0±3.5	24.2±2.2 -15.2±1.7
Mean ± SE 20 Exp in 7 dogs (119 Resp cycles analyzed)		-4.40±.35	36.85±1.97 7.4±3.91	4.16±.57	-15.15±3.19 -43.64±5.22	-1.04±.48	12.34±2.40 -16.54±4.44	.87±.04 .94±.06	27.6±2.67 -13.51±3.26	156.9±8.9 143.2±9.0	127.6±8.1 105.9±10.0	139.4 ±8.4 123.7 ±9.1	70.8± 4.8 37.2± 3.2	51.8± 3.7 26.6± 4.3	59.0 ±3.9 31.7± 3.1	23.7±2.0 -12.6±4.1

(1) Top number in ( ) indicates number of experiments, bottom number in ( ) indicates total number of respiratory cycles analyzed.

(2) Y_L, Y_R, Y_E vertical distances of left pleural, right pleural, and esophageal catheter tips, respectively, above horizontal plane through animal's midlung.

(3) LPL, RPL left and right pleural pressure, and esophageal pressures, measured at the catheter tip.

(4) Vertical gradient of pleural pressures-(LPL - RPL)÷(Y_R-Y_L) (acceleration in G unit;a)].

(5) Immersion tank pressure (body surface pressure) at midlung level.

(6) Pulmonary pressure recorded with Millar catheter-tip manometer in this dog, and the pressures were not analyzed by the computer.

TABLE XI

COMPUTER-PROCESSED MEASUREMENTS OF MULTIPLE PHYSIOLOGICAL PRESSURES AND OTHER VARIABLES IN DOGS BREATHING ORGANIC LIQUIDS

SUMMARY FOR INDIVIDUAL DOGS AND MEANS FOR THE GROUP

$+N_{O_2}$, BREATHING 100% OXYGEN, IMMERSED IN WATER

DOG	(1) NUMBER	T_L (2) (cm)	LPL (3) (cm H$_2$O)	T_R (2) (cm)	RPL (3) (cm H$_2$O)	T_E (2) (cm)	ESO (3) (cm H$_2$O)	VERTICAL GRADIENT (4) (cm H$_2$O/CM/VC)	BODY SURFACE (5) (cm H$_2$O)	AORTA (mm Hg) SYSTOLIC	AORTA MEAN	AORTA DIASTOLIC	PULMONARY ARTERY (cm H$_2$O) SYSTOLIC	PULMONARY ARTERY MEAN	PULMONARY ARTERY DIASTOLIC	LEFT ATRIUM (cm H$_2$O) MEAN
9	(1) (20)	-5.6	3.80 / -10.85	4.6	-3.36 / -18.11	-0.5	-1.53 / -11.92	0.72 / 0.73	11.10 / -15.56	157.7 / 148.0	161.5 / 132.7	129.6 / 120.4	55.0 / 29.9	43.2 / 23.9	34.3 / 19.2	7.1 / -13.7
10	(Sil Oil) (1) (20)	-3.3	0.43 / -14.72	5.1	-3.58 / -18.28	0.6	0.10 / -13.98	0.48 / 0.42	11.50 / -15.56	140.7 / 130.9	119.0 / 109.8	101.8 / 90.2	36.6 / 15.2	28.5 / 13.2	23.0 / 9.6	-- / --
11	-- / --	--	--	--	--	--	--	--	--	--	--	--	--	--	--	--
12	-- / --	--	--	--	--	--	--	--	--	--	--	--	--	--	--	--
13	(1) (15)	-4.7	-0.22 / -22.04	6.1	-9.37 / -23.24	0	-1.29 / -22.11	.85 / .96	12.73 / -19.50	126.5 / 103.4	104.6 / 87.4	92.9 / 74.5	15.8 / 2.1	12.5 / 1.0	11.5 / -0.1	2.3 / -23.4
14	(3) (45)	-2.67±.09	-0.14±.10 / -19.54±.76	4.27±12	-1.84±.86 / -27.60±2.27	-0.10±.26	1.77±.14 / -15.24±.57	0.25 / 1.17	11.51±.45 / -16.74±.78	125.6±5.9 / 102.5±9.2	102.7±6.2 / 83.6±6.8	92.8±6.7 / 66.7±5.9	(6)	(6)	(6)	7.24±1.4 / -16.9±0.5
15	-- / --	--	--	--	--	--	--	--	--	--	--	--	--	--	--	--
Mean ± SE 6 Exp in 4 Exp 95 Resp Cycles Analyzed		-4.02±.62	0.96±0.96 / -16.99±2.64	5.03±.39	-4.34±1.65 / -24.33±3.72	0.0±.32	0.53±0.71 / -15.81±2.21	0.57±.13 / 0.82±.16	11.71±0.35 / -16.85±0.93	137.2±7.8 / 121.2±11.1	116.8±9.0 / 103.4±11.3	104.2±8.7 / 86.6±11.5	35.8±11.3 / 15.7±8.0	28.1±6.9 / 12.7±4.6	22.9±6.6 / 9.9±5.6	5.5±1.6 / -16.0±2.9
16	(2) (13)	-3.6	31.34±.64 / .94±1.08	3.8	15.61±1.47 / -38.97±.90	-0.7	12.8±.5 / -15.26±.7	0.93±.04 / 0.74±.04	26.76±.22 / -11.26±1.93	156.6±3.5 / 147.1±5.4	125.0±1.3 / 113.6±2.5	107.0±1.2 / 58.6±.6	(6)	(6)	(6)	21.2±1.0 / -16.0±0.2

$+N_{O_2}$ = BATHING 100% OXYGEN, IMMERSED IN WATER

(1) Top number in ( ) indicates number of experiments, bottom number in ( ) indicates total number of respiratory cycles analyzed.

(2) T_L, T_R, T_E = vertical distances of left pleural, right pleural, and esophageal catheter tips, respectively, midling.

(3) LPL, RPL = left and right pleural pressure, and esophageal pressure, (LPL, RPL) ÷ the catheter tip.

(4) Vertical gradient of pleural pressure, (LPL - RPL) ÷ [(T_R-T_L)] (acceleration in G = ts)].

(5) Immersion tank pressure (body surface pressure) at midling level.

(6) Pulmonary pressure recorded with Millar catheter-tip manometer in this dog, and the pressures were not analyzed by the computer.

161

Preceding page blank

TABLE XII

COMPUTER-PROCESSED MEASUREMENTS OF MULTIPLE PHYSIOLOGICAL PRESSURES AND OTHER VARIABLES IN DOGS BREATHING ORGANIC LIQUIDS

SUMMARY FOR INDIVIDUAL DOGS AND MEANS FOR THE GROUP

‡IC_T BREATHING FC80 LIQUID FLUOROCARBON, IMMERSED IN WATER

DOG NUMBER (1)	V_L (2) (cm)	LPL (3) (cm H₂O)	T_R (2) (cm)	RPL (3) (cm H₂O)	V_E (2) (cm)	ESO (3) (cm H₂O)	VERTICAL GRADIENT (4) (cm H₂O/CM/G)	BODY SURFACE (5) (cm H₂O)	TRACHEAL (cm H₂O)	BRONCHIAL (cm H₂O)	AORTA (cm Hg) SYSTOLIC	AORTA MEAN	AORTA DIASTOLIC	PULMONARY ARTERY (cm H₂O) SYSTOLIC	PA MEAN	PA DIASTOLIC	LA (cm H₂O) MEAN
(9) (110)	-3.3	42.5±2.19 / -56.7±2.05	5.1	32.8±2.65 / -63.8±2.05	0.6	37.78±2.01 / -46.95±1.20	1.10±.16 / 0.93±.10	40.60±1.75 / -34.33±2.15	25.17±.99 / -23.84±.89	34.03±4.46 / -33.30±6.88	159.6±4.5 / 116.4±4.8	137.3±4.2 / 91.7±5.0	120.0±3.9 / 53.4±5.5	77.3±2.3 / -26.1±2.7	67.6±2.2 / -33.7±2.6	60.9±2.3 / -41.3±3.4	--
(11) (3b)	-3.63±.13	44.0±.37 / -59.51±.60	3.33±.02	36.5±.22 / -66.9±.40	.70	35.42±.59 / -40.64±1.65	1.01±.10 / 1.07±.07	26.76±15.08 / -65.24±3.17	27.60±1.57 / -32.63±1.77	20.88±6.91 / -69.57±0.62	144.4±3.8 / 88.9±5.0	123.2±3.7 / 63.0±5.2	105.7±4.6 / 39.9±6.8	68.0±1.2 / -36.1±4.6	60.3±.7 / -42.5±2.3	58.3±0.7 / -45.3±0.9	46.7±1.0 / -60.±0.8
12	--	--	\- No liquid breathing studies in this dog \-														--
(13) (22)	-5.2	41.57±4.54 / -51.42±3.73	5.3	27.9±.07 / -64.81±.40	0	76.55±4.52 / -52.30±1.30	1.24±.08 / 1.22±.07	63.75±3.71 / -47.99±1.76	16.45±3.84 / -20.26±1.37	17.65±2.25 / -38.00±4.25	140.6±4.0 / 82.5±12.0	120.5±4.5 / 61.3±10.1	107.0±3.1 / 44.8±9.4	89.6±7.9 / -13.4±.4	76.6±5.0 / -19.3±7.0	71.6±.6 / -25.0±5.3	41.4±.4 / -12.±.1
(14) (63)	-2.3	40.69±3.63 / -52.6±1.53	4.5	32.19±2.99 / -59.9±2.06	0.40	40.96±3.12 / -50.66±1.81	1.26±.13 / 1.10±.21	45.47±3.66 / -55.71±2.81	17.87±1.59 / -20.32±1.78	13.12±2.97 / -40.14±1.61	136.4±2.0 / 71.5±4.2	112.1±1.9 / 49.7±4.4	102.9±3.1 / 33.6±6.9	(6)	(6)	(6)	25.6±2.6 / -44.2±2.5
(15) (44)	-2.10±.15	35.47±3.35 / -59.02±1.50	4.20±.13	27.90±3.56 / -66.70±1.87	.39±.07	37.96±3.31 / -54.34±1.18	1.21±.05 / 1.21±.07	36.4±4.10 / -59.56±2.95	11.75±1.66 / -24.03±1.26	7.85±4.57 / -40.34±3.38	116.2±5.3 / 67.4±4.4	101.0±4.5 / 47.5±2.5	85.5±3.7 / 29.9±1.4	73.9±4.1 / -27.6±2.7	60.7±3.9 / -33.5±2.0	52.7±3.5 / -36.1±1.9	42.3±3.7 / -55.7±1.7
Mean±SE (230 Cycles)	-3.34±.56	40.36±1.66 / -55.86±1.65	4.58±.42	31.63±1.63 / -64.45±1.27	.52±.08	38.53±0.76 / -48.93±2.65	1.16±.05 / 1.11±.05	38.64±3.33 / -56.56±2.66	19.73±2.88 / -24.22±2.26	18.71±4.41 / -40.27±2.65	139.4±7.0 / 85.3±8.7	118.8±6.0 / 60.6±6.0	110.8±8.0 / 40.3±4.1	77.2±4.6 / -25.8±4.7	66.3±3.8 / -32.5±.9	60.9±4.0 / -38.2±.9	39.±3.9 / -53.1±3.4

‡IC_T BREATHING DC200 SILICONE OIL, IMMERSED IN WATER

DOG NUMBER (1)	V_L (2) (cm)	LPL (3) (cm H₂O)	T_R (2) (cm)	RPL (3) (cm H₂O)	V_E (2) (cm)	ESO (3) (cm H₂O)	VERTICAL GRADIENT (4)	BODY SURFACE (5)	TRACHEAL	BRONCHIAL	AORTA SYSTOLIC	AORTA MEAN	AORTA DIASTOLIC	PA SYSTOLIC	PA MEAN	PA DIASTOLIC	LA MEAN
(10) (28)	-5.7	42.3±.60 / -7.37±1.33	4.9	31.8±.63 / -55.96±2.05	-0.10±0	39.62±.90 / -44.0±.51	0.99±.01 / 0.60±.07	41.23±1.18 / -57.78±.34	28.69±1.46 / -26.59±3.23	42.09±1.51 / -40.92±0.50	88.1±3.2 / 35.2±3.8	69.1±3.0 / 11.6±4.0	61.6±2.1 / -4.8±3.7	68.7±1.2 / -33.2±1.3	60.1±.2 / -35.3±0.6	55.7±1.1 / -39.1±0.4	41.2±.4 / -47.3±.5

(1) Top number in ( ) indicates number of experiments, bottom number in ( ) indicates total number of respiratory cycles analyzed.
(2) V_L, T_R, T_L=vertical distances of left pleural, right pleural, and esophageal catheter tips, respectively.
(3) LPL, RPL=left and right pleural pressure, and esophageal pressures, measured at the catheter tip.
(4) Vertical gradient of pleural pressures (LPL - RPL)=U(T_R-T_L) (acceleration in G units).
(5) Immersion tank pressure (body surface pressure) at midlung level.
(6) Pulmonary pressure recorded with Millar catheter-tip manometer in this dog, and the pressures were not analyzed by the computer.

TABLE XIII

COMPUTER-PROCESSED MEASUREMENTS OF MULTIPLE PHYSIOLOGICAL PRESSURES AND OTHER VARIABLES IN DOGS BREATHING ORGANIC LIQUIDS

SUMMARY FOR INDIVIDUAL DOGS AND MEANS FOR THE GROUP

+7G_y BREATHING FC80 LIQUID FLUOROCARBON, IMMERSED IN WATER

DOG	N[1] NUMBER	Y_L[2] (cm)	LPL[3] (cm H_2O)	T_R[2] (cm)	RPL[3] (cm H_2O)	Y_E[2] (cm)	ESO[3] (cm H_2O)	VERTICAL[4] GRADIENT (cm H_2O/CM/G)	BODY[5] SURFACE (cm H_2O)	TRACHEAL (cm H_2O)	BRONCHIAL (cm H_2O)	AORTA (mm Hg) SYSTOLIC	AORTA (mm Hg) MEAN	DIASTOLIC	PULMONARY ARTERY (cm H_2O) SYSTOLIC	MEAN	DIASTOLIC	LA (cm H_2O) MEAN
9	(4) (16)	-3.6	83.6± 3.66 -28.91± 2.06	5.0	10.67± .77 -93.90± 2.63	0.9	47.49±3.95 -51.35±2.33	1.21±.01 1.04±.04	47.46± 2.20 -51.96± 2.50	36.46± 3.26 -16.60± 5.08	28.31± 1.12 -47.94± 1.44	170.0±11.2 117.5±10.1	148.8± 9.4 85.5± 8.6	132.4± 8.5 59.8± 8.1	94.9±18.5 -19.6± 5.0	84.4± 3.6 -25.2± 4.1	78.4± 3.8 -31.7± 2.0	— —
11	(2) (7)	-3.3	85.53± 2.24 -23.25± 6.41	2.9	26.55±3.22 -83.07±2.39	0.2	39.92±1.85 -44.99±2.63	1.33±.03 1.34±.05	47.17± 2.66 -51.92± 3.52	33.03±15.11 -21.46±15.62	8.81±23.7 -39.67± 2.02	152.0±11.3 92.3±20.0	133.8±12.9 73.1±21.6	122.0±15.2 58.1±23.1	83.2± 2.9 -26.1± 5.5	74.2± 2.9 -31.5± 5.5	69.3± 0.8 -36.6± 5.2	62.4±3.5 -48.5±2.7
12			No liquid breathing studies on this dog															—
13	(2) (6)	-5.7	102.82± 3.77 -8.56±10.16	6.0	9.35±2.61 -105.51±4.29	-0.5	66.26±1.70 -44.17±4.97	1.13±.02 1.17±.02	56.72±12.53 -63.04± 9.54	13.04± 7.08 -19.30±13.88	37.40± 5.62 -18.44±12.03	160.1±10.2 90.0±16.1	140.1± 7.7 67.9±15.7	131.9± 7.7 52.0±14.2	116.8±18.5 10.9±15.0	109.8±13.3 3.9±12.7	101.7±14.0 -2.5±11.0	79.9±0.9 -23.5±0.5
14	(3) (20)	-1.8	101.25± 1.08 -14.30± .97	3.9	53.33± .89 -64.13± .40	0.2	90.60±1.32 -23.60± .67	1.39±.20 1.24±.01	87.18± 3.06 -28.65± 1.12	25.04± 2.04 -8.72± .62	39.67± 3.37 -6.48± 2.97	164.0± 2.5 88.5± 3.1	141.4± 4.1 66.5± 2.6	133.2± 2.9 52.9± 2.4	(6)	(6)	(6)	77.5±1.2 -18.2±0.7
15	(9) (32)	-2.21±.12	91.75± 5.05 -15.97± 2.32	4.81±.04	35.63±4.94 -71.76±2.63	0.23±.05	80.71±4.13 -22.28±1.18	1.13±.01 1.15±.02	74.64± 5.18 -33.27± 3.32	17.56± 3.30 -18.02± 3.08	26.65± 8.91 -18.70± 3.10	130.2± 7.4 88.6± 5.2	134.8± 6.7 70.3± 4.0	121.9± 5.6 52.6± 3.1	118.4± 5.0 7.1± 3.7	105.0± 4.6 0.5± 2.6	97.6± 4.5 -4.9± 1.9	87.3±5.0 -23.3±3.1
(81 Cycles)		-3.32±.68	92.95± 3.96 -18.20± 3.36	4.52±.32	27.11±8.21 -83.06±7.43	0.12±.24	68.99±7.60 -38.08±5.91	1.24±.05 1.15±.05	62.64± 7.31 -41.19± 4.75	23.03± 4.44 -16.96± 2.21	28.20± 5.45 -26.29± 7.59	139.8± 3.9 95.4± 5.6	139.8± 2.7 72.7± 3.4	128.3± 2.6 55.1± 1.6	103.3± 8.5 -6.7± 9.2	93.8± 4.6 -13.0± 9.0	86.9± 7.7 -19.1± 8.8	76.5±2.2 -29.6±4.6

+7G_y BREATHING DC200 SILICONE OIL, IMMERSED IN WATER

DOG	N[1] NUMBER	Y_L[2] (cm)	LPL[3] (cm H_2O)	T_R[2] (cm)	RPL[3] (cm H_2O)	Y_E[2] (cm)	ESO[3] (cm H_2O)	VERTICAL[4] GRADIENT	BODY[5] SURFACE	TRACHEAL	BRONCHIAL	AORTA SYSTOLIC	AORTA MEAN	DIASTOLIC	PA SYSTOLIC	MEAN	DIASTOLIC	LA MEAN
10	(2) (8)	-5.6	80.6± 2.93 -22.62± .30	6.7	7.83±2.30 -89.46±5.62	-0.3	46.33±1.65 -51.33±1.31	1.01±.01 0.93±.05	46.20± 3.00 -54.99± 3.80	42.65± 3.50 -16.16± 9.77	40.59± 5.00 -31.35± 1.36	91.3± 2.7 48.6± 2.0	72.4± 2.6 16.6± 4.5	66.9± 1.3 -1.9± 6.0	84.6± 0.3 -15.6± 2.7	76.6± 0.2 -19.5± 0.8	71.0± 0.1 -24.6± 1.3	51.3±2.2 -50.0±5.9

(1) Top number... ( ) indicates number of experiments, bottom number in ( ) indicates total number of respiratory cycles analyzed.
(2) Y_L, Y_R, Y_E = vertical distance of left pleural, right pleural, and esophageal catheter tips, respectively, above horizontal plane through animal's midlung.
(3) LPL, RPL = left and right pleural pressures, and esophageal pressure, measured at the catheter tip.
(4) Vertical gradient of pleural pressures (Y_R - Y_L)/(P_R - P_L) (acceleration in G units)).
(5) Immersion tank pressure (body surface pressure) at midlung level.
(6) Pulmonary pressure recorded with Miller catheter-tip manometer in this dog, and the pressures were not analyzed by the computer.

Preceding page blank

VASCULAR PRESSURES RELATIVE TO ATMOSPHERE AN...

RESPIRATION		Body Surface ('Immersion Tank)		Systemic Arterial		Pulm...
				Atmosphere	Body Surface	Atmosphere
SPONTANEOUS <u>AIR</u> 9 Experiments in 6 dogs 91 Respiratory cycles analyzed	Expiration	0	Systolic Mean Diastolic	197.9 +10.6 173.8 ∓12.0 159.8 ∓13.1	197.9 173.8 159.8	43.8 +5.3 33.8 ∓4.1 28.6 ∓3.3
	Inspiration	0		188.1 +10.2 161.2 ∓9.4 148.8 ∓12.5	188.1 161.2 148.8	30.6 +4.2 23.9 ∓3.2 17.2 ∓1.1
RESPIRATOR <u>AIR</u> 31 Experiments in 7 dogs 376 Respiratory cycles analyzed	Expiration	11.56 +1.08		186.2 +9.0 160.2 ∓9.5 142.4 ∓10.3	174.6 148.6 130.8	39.7 +3.6 29.8 ∓3.1 23.6 ∓2.7
	Inspiration	-14.41 +1.88		176.3 +10.9 149.1 ∓11.4 127.6 ∓12.5	190.7 163.5 142.9	17.9 +3.0 12.8 ∓3.2 7.9 ∓3.8
<u>100% OXYGEN</u> 6 Experiments in 4 dogs 95 Respiratory cycles analyzed	Expiration	11.71 +0.35		179.8 +10.6 158.8 ∓12.2 141.8 ∓11.8	168.1 147.1 130.1	35.8 +11.3 28.1 ∓8.9 22.9 ∓6.6
	Inspiration	-16.85 +0.93		164.8 +15.1 140.6 ∓15.4 120.5 ∓15.6	181.7 157.5 137.4	15.7 +8.0 12.7 ∓6.6 9.5 ∓5.6
<u>FC80</u> 31 Experiments in 5 dogs 250 Respiratory cycles analyzed	Expiration	38.64 +3.33		189.6 +9.5 161.6 ∓8.2 148.0 ∓10.9	151.0 123.0 109.4	77.2 +4.6 66.3 ∓3.8 60.9 ∓4.0
	Inspiration	-56.56 +2.86		116.0 +11.8 82.7 ∓8.2 54.8 ∓5.6	172.6 139.3 111.4	-25.8 +4.7 -32.3 ∓4.9 -38.2 ∓4.9
<u>DC200</u> 4 Experiments in 1 dog 28 Respiratory cycles analyzed	Expiration	41.23 +1.18		119.8 +4.4 94.0 ∓4.1 83.8 ∓2.9	78.6 52.8 42.6	68.7 +1.2 60.1 ∓1.2 55.7 ∓1.1
	Inspiration	-57.78 +0.34		47.9 +5.2 15.8 ∓5.4 -6.5 ∓5.0	105.7 73.6 51.3	-32.2 +1.3 -35.3 ∓0.6 -39.1 ∓0.4

Preceding page blank

TABLE XIV

PUTER PROCESSED MEASUREMENTS OF MULTIPLE PHYSIOLOGICAL PRESSURES DURING +1Gy FORCE ENVIRONMENT IN WATER-IMMERSION RESPIRATOR, WITH AND WITHOUT LIQUID BREATHI

TO ATMOSPHERE AND BODY SURFACE cm H2C   (Means ± S.E.M.)   PLEURAL, ESOPHAGEAL, AND AIRWAY PRESSURES RELATIVE TO ATMOSH

Pulmonary Arterial		Left Atrium		Y_L (cm)	LP1 (cm H2O)	Y_R (cm)	RP1 (cm H2O)	Y_E (cm)	ES (cm
Atmosphere	Body Surface	Atmosphere	Body Surface						
43.8 +5.3	43.8								
33.8 ∓4.1	33.8	9.8 +2.9	9.8	-3.85 +0.56	-0.91 +0.98	4.95 +.42	-6.38 +1.25	0.1 +0.09	-0.54
28.6 ∓3.3	28.6								
30.6 +4.2	30.6								
23.9 ∓3.2	23.9	-5.0 +3.5	-5.0	—	-9.55 +1.74	—	-16.24 +3.03	—	-8.95
17.2 ∓1.1	17.2								
39.7 +3.6	28.1								
29.8 ∓3.1	18.2	11.9 +3.8	0.3	-4.07 +0.44	2.50 +0.72	4.60 +0.38	-4.01 +0.90	-0.14 +0.17	1.84
23.6 ∓2.7	12.0								
17.9 +3.0	32.3								
12.8 ∓3.2	27.2	-11.0 +4.5	3.1	—	-15.14 +1.68	—	-22.37 +2.07	—	-14.29
7.9 ∓3.8	22.3								
55.8 +11.3	24.1								
28.1 ∓8.9	16.4	5.5 +1.6	-6.1	-4.02 +0.62	0.96 +0.96	5.03 +0.39	-4.54 +1.65	0.00 +0.32	-0.53
22.9 ∓6.6	11.2								
15.7 +8.0	32.6								
12.7 ∓6.6	29.6	-18.0 +2.9	-1.2	—	-16.99 +2.64	—	-24.33 +3.72	—	-15.81
9.5 +5.6	26.4								
77.2 +4.6	38.6								
66.3 ∓3.8	27.7	39.8 +3.9	1.2	-3.34 +0.54	40.86 +1.46	4.58 +0.42	31.48 +1.63	0.52 +0.08	38.53
60.9 ∓4.0	22.3								
-25.8 +4.7	30.8								
-32.3 ∓4.9	24.3	-53.1 +3.4	3.5	—	-55.86 +1.65	—	-64.45 +1.27	—	-48.93
-38.2 ∓4.9	18.4								
58.7 +1.2	27.5								
60.1 ∓1.2	18.9	41.2 +0.4	0.0	-5.7	42.34 +0.60	4.9	31.88 +0.63	-0.10	39.62
55.7 ∓1.1	14.5								
-32.2 +1.3	25.6								
-35.3 ∓0.6	22.5	-47.1 +2.5	10.7	—	-49.67 +1.35	—	-55.98 +2.08	—	-44.00
-39.1 ∓0.4	18.7								

Y_L, Y_R, Y_E vertical distance of left and right pleural and esophageal catheters, respectively, at cathe

LP1, RP1, Eso and left, right pleural and esophageal pressures, respectively.

OPHAGEAL, AND AIRWAY PRESSURES RELATIVE TO ATMOSPHERE (Means ± S.E.M.)

Y_R (cm)	RPl (cm H$_2$O)	Y_E (cm)	ESO (cm H$_2$O)	VERTICAL GRADIENT (cm H$_2$O/cm/G)	TRACHEAL (cm H$_2$O)	BRONCHIAL (cm H$_2$O)	PLEURAL PRESSURE AT MIDLUNG Atmos.	BS
95 ±.42	-6.38 ±1.25	0.1 ±0.09	-0.54 ±0.53	0.57 ±.15	0	0	-3.5	-3.5
—	-16.24 ±3.03	—	-8.95 ±2.68	0.73 ±.14	0	0	-12.5	-12.5
60 ±0.38	-4.01 ±0.90	-0.14 ±0.17	1.84 ±0.91	0.74 ±0.07	0	0	-0.5	-12.0
—	-21.37 ±2.07	—	-14.29 ±1.66	0.87 ±0.13	0	0	-18.5	-4.1
03 ±0.39	-4.54 ±1.65	0.00 ±0.32	-0.53 ±0.71	0.57 ±0.13	0	0	—	—
—	-24.33 ±3.72	—	-15.81 ±2.21	0.82 ±0.16	0	0	—	—
58 ±0.42	31.48 ±1.63	0.52 ±0.08	38.53 ±0.76	1.16 ±0.05	19.73 ±2.88	18.71 ±4.4?	36.5	-2.1
—	-64.45 ±1.27	—	-48.93 ±2.45	1.10 ±0.05	-24.22 ±2.26	-40.27 ±2.6?	-59.5	-2.9
	31.88 ±0.63	-0.10	39.62 ±0.90	0.99 ±0.01	28.69 ±1.46	42.09 ±1.5?	36.5	-4.7
—	-55.98 ±2.08	—	-44.00 ±0.51	0.60 ±0.07	-26.59 ±3.23	-40.92 ±0.0?	-53.0	-4.8

and esophageal catheters, respectively, at catheter tip from midthoracic plane.

pressures, respectively.

A

SUMMARY OF COMPUTER-PROCESSED MEASUREMENT OF MULTIPLE PHYSIOLOGICAL PRESSURES DURING + 7G

		Body Surface (Immersion Tank) (cm H_2O)	Systemic Arterial		Pulmonary Arterial		Lef
RESPIRATION			Atmosphere (cm H_2O)	Body Surface (cm H_2O)	Atmosphere (cm H_2O)	Body Surface (cm H_2O)	Atmosphere (cm H_2O)
SPONTANEOUS AIR	EXPIRATION INSPIRATION	No studies at 7G$_y$ breathing air spontaneously			—	—	—
RESPIRATOR AIR 2C Experiments in 7 dogs 119 Respiration cycles analyzed	EXPIRATION	28.04 +2.67	(1) 216.1 +12.1 (2) 189.6 +11.4 (3) 173.5 +11.0	188.1 161.6 145.5	7C.8 +4.8 59.0 +3.9 51.8 +3.7	42.8 31.0 23.8	23.8 +6.0
	INSPIRATION	-13.81 +3.26	194.8 +12.2 168.2 +12.4 148.1 +13.6	208.6 182.0 161.9	37.2 +3.2 31.7 +3.1 24.0 +4.3	51.0 43.5 38.4	-12.9 +6.1
100% OXYGEN 2 Experiments in 1 dog 13 Respiration cycles analyzed	EXPIRATION	26.76 +0.22	213.0 +4.8 174.1 +1.8 145.5 +1.6	186.2 147.3 118.7	(4)	(4)	21.2 +1.0
	INSPIRATION	-11.28 +1.93	200.1 +7.3 154.2 +3.8 120.5 +0.8	211.4 165.5 131.8	(4)	(4)	-16.4 +0.2
FC80 22 Experiments in 5 dogs 81 Respirator cycles analyzed	EXPIRATION	62.64 +7.91	217.3 +5.3 190.1 +5.3 174.5 +3.5	154.7 127.5 111.9	103.3 +8.6 93.6 +8.5 86.9 +7.7	40.7 31.0 24.3	76.8 +5.2
	INSPIRATION	-41.19 +4.75	129.7 +7.6 98.9 +4.6 74.9 +2.2	170.9 140.1 116.1	-6.7 +9.2 -13.0 +9.0 -19.1 +8.8	34.5 28.2 22.1	-29.6 +6.6
DC200 2 Experiments in 1 dog 8 Respirator cycles analyzed	EXPIRATION	44.20 +3.60	124.2 +3.7 98.5 +3.5 88.3 +1.8	80.0 54.3 44.1	84.6 +0.5 76.6 +0.2 71.0 +0.1	40.4 32.4 26.8	51.5 +2.2
	INSPIRATION	-54.99 +0.30	66.4 +2.7 22.8 +6.1 -2.6 +8.2	121.4 77.8 52.4	-15.8 +2.7 -19.9 +0.8 -24.6 +1.3	39.2 35.1 30.4	-50.0 +3.9

(1) Systolic, (2) Mean, (3) Diastolic, and (4) Pulmonary artery pressure measured with Millar catheter-tip manometer in this dog, and the pressures were not analyzed by the computer.

169

Preceding page blank

B

TABLE XV

MEASUREMENT OF MULTIPLE PHYSIOLOGICAL PRESSURES DURING + $7G_y$ FORCE ENVIRONMENT IN WATER-IMMERSION RESPIRATOR, WITH AND WITHOUT LIQUID BREATHING

...ATIVE TO ATMOSPHERE AND BODY SURFACE (Means ± S.E.)										
	Pulmonary Arterial		Left Atrium		Y_L (cm)	LP1 (cm H_2O)	Y_R (cm)	PP1 (cm H_2O)		
...y Surface (cm H_2O)	Atmosphere (cm H_2O)	Body Surface (cm H_2O)	Atmosphere (cm H_2O)	Body Surface (cm H_2O)						PLEURAL, ESOPHAGEAL, AND AIRWAY PRESSURES
...aneously	—	—	—	—	—	—	—	—		
.1 / .6 / .5	70.8 ±4.8 / 59.0 ±3.9 / 51.8 ±3.7	42.8 / 31.0 / 23.8	23.8 ±6.0	4.2	-4.4 ±0.35	35.85 ±1.97	4.16 ±0.57	-5.15 ±3.19	-1.
.6 / .0 / .9	37.2 ±3.2 / 31.7 ±3.1 / 24.0 ±4.3	51.0 / 43.5 / 36.4	-12.9 ±6.1	0.9	—	7.42 ±3.91	—	-45.67 ±5.22	
.2 / .3 / .7	(4)	(4)	21.2 ±1.0	-5.6	-3.40	31.34 ±0.64	3.80	-15.61 ±1.47	-0.
.4 / .5 / .8	(4)	(4)	-16.4 ±0.2	-5.1	—	0.94 ±1.08	—	-38.97 ±0.90	
.7 / .5 / .9	103.3 ±8.6 / 93.6 ±8.5 / 86.9 ±7.7	40.7 / 31.0 / 24.3	76.8 ±5.2	14.2	-3.32 ±0.68	92.95 ±3.96	4.52 ±0.52	27.11 ±8.21	0.1
.9 / .1 / .1	-6.7 ±9.2 / -13.0 ±9.0 / -19.1 ±8.8	34.5 / 28.2 / 22.1	-29.6 ±6.6	11.6	—	-18.20 ±3.56	—	-83.68 ±7.43	
.0 / .3 / .1	84.6 ±0.5 / 76.6 ±0.2 / 71.0 ±0.1	40.4 / 32.4 / 26.8	51.5 ±2.2	7.3	-5.4	80.49 ±2.93	4.7	7.83 ±2.30	-0.
.4 / .8 / .4	-15.8 ±2.7 / -19.9 ±0.8 / -24.6 ±1.3	39.2 / 35.1 / 30.4	-50.0 ±3.9	5.0	—	-22.43 ±0.03	—	-89.48 ±3.62	

...ured with Millar catheter-tip manometer in
...re not analyzed by the computer.

Y_E, Y_L, Y_R vertical distance of esophageal, left, and right pleural catheters, r...

ESO, LP1, PR1 - Esophageal, left, and right pleural pressures, respectively.

HOUT LIQUID BREATHING

AL, AND AIRWAY PRESSURES RELATIVE TO ATMOSPHERE (Means ± S.E.)

	PPl (cm H_2O)	Y_E (cm)	ESO (cm H_2O)	VERTICAL GRADIENT (cm H_2O/cm/G)	TRACHEAL (cm H_2O)	BRONCHIAL (cm H_2O)	PLEURAL PRESSURE AT MILLUNG (cm H_2O) Atmos	BS
	—	—	—	—	—	—	—	—
37	-5.15 ±3.19	-1.04 ±0.49	12.36 ±2.40	0.87 ±0.04	0	0	10.0	-18.0
	-45.67 ±5.22	—	-14.59 ±4.46	0.89 ±0.06	0	0	-20.0	-6.2
	-15.61 ±1.47	-0.70	12.89 ±0.75	0.93 ±0.04	0	0	—	—
	-38.97 ±0.90	—	-15.26 ±0.07	0.79 ±0.04	0	0	—	—
52	27.11 ±8.21	0.12 ±0.24	68.99 ±7.60	1.24 ±0.05	23.03 ±	28.20 ±5.45	62.5	-0.1
	-33.68 ±7.43	—	-38.08 ±5.91	1.19 ±0.05	-16.98 ±2.21	-26.29 ±7.59	-46.0	-4.8
	7.83 ±2.30	-0.30	48.33 ±1.65	1.01 ±0.01	42.69 ±3.90	40.59 ±5.60	43.5	-0.7
	-89.48 ±3.62	—	-51.33 ±1.31	0.93 ±0.05	-14.16 ±9.77	-31.85 ±1.56	-58.5	-3.5

right pleural catheters, respectively, from midthoracic plane.

essures, respectively.

TABLE XVI

Concentration of FC 80 in tissues and body fluids immediately after a 14 kg dog had breathed FC 80 for 16 hours. 1.4 ml FC 80 was injected into left renal artery 1 1/2 hours after start of liquid breathing.

Source	FC 80 Concentration mg/100 g tissue mg/100 ml fluid
Brain (left parietal lobe, white and gray matter)	14.40
Right kidney (cortex and medulla)	4.70
Left kidney (cortex and medulla)	966.20
Spleen	3.70
Liver	3.20
Bile	3.38
Urine	0
Heart Blood (right ventricle)	0.986
Saline (25°C)	0.785

Preceding page blank

TABLE XVII

ESTIMATED GAS TENSIONS (mm Hg) IN THE BLOOD OF ANIMALS INJECTED INTRAVENOUSLY WITH FC80 LIQUID FLUOROCARBON UNDER DIFFERENT CONDITIONS OF VENTILATION AND AMBIENT PRESSURE*

Average Barometric Pressure (PBA) (740 mm Hg at Rochester, Minnesota)

Breathing:	Arterial Blood			End-Pulmonary Capillary Blood			Mixed Venous (Pulmonary Artery) Blood		
	Air	O_2	FC 80	Air	O_2	FC 80	Air	O_2	FC 80
P_{O_2}	97	620	400	101	653	430	40	55	50
P_{CO_2}	40	40	40	40	40	40	46	46	46
P_{H_2O}	47	47	47	47	47	47	47	47	47
P_{N_2}	556	0	0	552	0	0	556	0	0
$P_{FC\,80}$	55	55	55	55	55	55	55	55	55
Total Blood Gas	795	762	542	795	795	572	744	203	198
Tension (P_T) (PBA-PT)	+55	+22	-198	+55	+55	-168	+4	-537	-542

Breathing Compressed Air (Ambient Pressure (P_A) 1480 mm Hg)

	Arterial Blood	End-Pulmonary Capillary Blood	Mixed Venous (Pulmonary Artery) Blood
P_{O_2}	203	215	45
P_{CO_2}	40	40	46
P_{H_2O}	47	47	47
P_{N_2}	1190	1178	1190
$P_{FC\,80}$	55	55	55
Total Blood Gas	1535	1535	1383
Tension (P_T) (PA-PT)	+55	+55	-97

*After Comroe (18), P224

Preceding page blank